

ISSN 2413-5577

№ 2

Апрель – Июнь

2023

Экологическая безопасность прибрежной и шельфовой зон моря



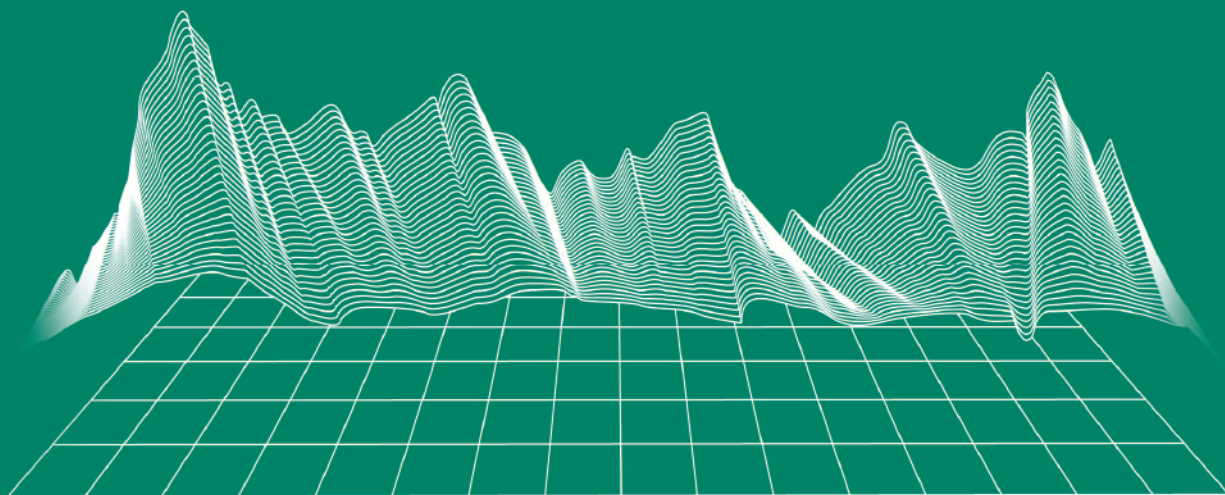
Ecological Safety of Coastal
and Shelf Zones of Sea

No. 2

April – June

2023

ecological-safety.ru



ISSN 2413-5577

No. 2, 2023

April – June

Publication frequency:

Quarterly

16+

ECOLOGICAL SAFETY OF COASTAL AND SHELF ZONES OF SEA

Scientific and theoretical peer reviewed journal

FOUNDER AND PUBLISHER:

Federal State Budget Scientific Institution

Federal Research Centre

“Marine Hydrophysical Institute of RAS”

The Journal publishes original research results, review articles (at the editorial board's request) and brief reports.

The Journal aims at publication of results of original scientific research concerning the state and interaction of geospheres (atmosphere, lithosphere, hydrosphere, and biosphere) within coastal and shelf areas of seas and oceans, methods and means of study thereof, ecological state of these areas under anthropogenic load as well as environmental protection issues.

The Journal's editorial board sees its mission as scientific, educational and regulatory work to preserve the ecological balance and restore the resource potential of coastal and shelf areas believing that despite the geographical limitations of the areas under study, the processes taking place within them have a significant impact on the waters of the seas and oceans and economic activity.

The Journal publishes original research materials, results of research performed by national and foreign scientific institutions in the coastal and shelf zones of seas and oceans, review articles (at the editorial board's request) and brief reports on the following major topics:

- Scientific basis for complex use of shelf natural resources
- Marine environment state and variability
- Coastal area state and variability; coast protection structures
- Monitoring and estimates of possible effects of anthropogenic activities
- Development and implementation of new marine environment control and monitoring technologies

The outcome of the research is information on the status, variability and possible effects of anthropogenic activities in the coastal and shelf marine areas, as well as the means to perform calculations and to provide information for making decisions on the implementation of activities in the coastal zone.

e-mail: ecology-safety@mhi-ras.ru

website: <http://ecological-safety.ru>

Founder, Publisher and Editorial Office address:

2, Kapitanskaya St.,
Sevastopol, 299011, Russia

Phone, fax: + 7 (8692) 54-57-16

EDITORIAL BOARD

- Yuri N. Goryachkin** – Editor-in-Chief, Chief Research Associate of FSBSI FRC MHI, Dr.Sci. (Geogr.), Scopus ID: 6507545681, ResearcherID: I-3062-2015, ORCID 0000-0002-2807-201X (Sevastopol, Russia)
- Vitaly I. Ryabushko** – Deputy Editor-in-Chief, Head of Department of FSBSI FRC A. O. Kovalevsky Institute of Biology of the Southern Seas of RAS, Chief Research Associate, Dr.Sci. (Biol.), ResearcherID: H-4163-2014, ORCID ID: 0000-0001-5052-2024 (Sevastopol, Russia)
- Elena E. Sovga** – Deputy Editor-in-Chief, Leading Research Associate of FSBSI FRC MHI, Dr.Sci. (Geogr.), Scopus ID: 7801406819, ResearcherID: A-9774-2018 (Sevastopol, Russia)
- Vladimir V. Fomin** – Deputy Editor-in-Chief, Head of Department of FSBSI FRC MHI, Dr.Sci. (Phys.-Math.), ResearcherID: H-8185-2015, ORCID ID: 0000-0002-9070-4460 (Sevastopol, Russia)
- Tatyana V. Khmara** – Executive Editor, Junior Research Associate of FSBSI FRC MHI, Scopus ID: 6506060413, ResearcherID: C-2358-2016 (Sevastopol, Russia)
- Vladimir N. Belokopytov** – Leading Research Associate, Head of Department of FSBSI FRC MHI, Dr.Sci. (Geogr.), Scopus ID: 6602809060, ORCID ID: 0000-0003-4699-9588 (Sevastopol, Russia)
- Sergey V. Berdnikov** – Chairman of FSBSI FRC Southern Scientific Centre of RAS, Dr.Sci. (Geogr.), ORCID ID: 0000-0002-3095-5532 (Rostov-on-Don, Russia)
- Valery G. Bondur** – Director of FSBSI Institute for Scientific Research of Aerospace Monitoring “AEROCOSMOS”, vice-president of RAS, academician of RAS, Dr.Sci. (Tech.), ORCID ID: 0000-0002-2049-6176 (Moscow, Russia)
- Temir A. Britayev** – Chief Research Associate, IEE RAS, Dr.Sci. (Biol.), ORCID ID: 0000-0003-4707-3496, ResearcherID: D-6202-2014, Scopus Author ID: 6603206198 (Moscow, Russia)
- Elena F. Vasechkina** – Deputy Director of FSBSI FRC MHI, Dr.Sci. (Geogr.), ResearcherID: P-2178-2017 (Sevastopol, Russia)
- Isaac Gertman** – Head of Department of Israel Oceanographic and Limnological Research Institute, Head of Israel Marine Data Center, Ph.D. (Geogr.), ORCID ID: 0000-0002-6953-6722 (Haifa, Israel)
- Sergey G. Demyshev** – Head of Department of FSBSI FRC MHI, Chief Research Associate, Dr.Sci. (Phys.-Math.), ResearcherID C-1729-2016, ORCID ID: 0000-0002-5405-2282 (Sevastopol, Russia)
- Nikolay A. Diansky** – Chief Research Associate of Lomonosov Moscow State University, associate professor, Dr.Sci. (Phys.-Math.), ResearcherID: R-8307-2018, ORCID ID: 0000-0002-6785-1956 (Moscow, Russia)
- Vladimir A. Dulov** – Head of Laboratory of FSBSI FRC MHI, professor, Dr.Sci. (Phys.-Math.), ResearcherID: F-8868-2014, ORCID ID: 0000-0002-0038-7255 (Sevastopol, Russia)
- Victor N. Egorov** – Scientific Supervisor of FSBSI FRC A. O. Kovalevsky Institute of Biology of the Southern Seas of RAS, academician of RAS, professor, Dr.Sci. (Biol.), ORCID ID: 0000-0002-4233-3212 (Sevastopol, Russia)
- Vladimir V. Efimov** – Head of Department of FSBSI FRC MHI, Dr.Sci. (Phys.-Math.), ResearcherID: P-2063-2017 (Sevastopol, Russia)
- Vladimir B. Zalesny** – Leading Research Associate of FSBSI Institute of Numerical Mathematics of RAS, professor, Dr.Sci. (Phys.-Math.), ORCID ID: 0000-0003-3829-3374 (Moscow, Russia)
- Andrey G. Zatspein** – Head of Laboratory of P.P. Shirshov Institute of Oceanology of RAS, Chief Research Associate, Dr.Sci. (Phys.-Math.), ORCID ID: 0000-0002-5527-5234 (Moscow, Russia)
- Vasily V. Knysh** – Leading Research Associate of FSBSI FRC MHI, professor, Dr.Sci. (Phys.-Math.), ResearcherID: B-3603-2018 (Sevastopol, Russia)
- Sergey K. Kononov** – Director of FSBSI FRC MHI, corresponding member of RAS, Dr.Sci. (Geogr.), ORCID ID: 0000-0002-5200-8448 (Sevastopol, Russia)
- Gennady K. Korotaev** – Scientific Supervisor of FSBSI FRC MHI, corresponding member of RAS, professor, Dr.Sci. (Phys.-Math.), ResearcherID: K-3408-2017 (Sevastopol, Russia)
- Alexander S. Kuznetsov** – Leading Research Associate, Head of Department of FSBSI FRC MHI, Ph.D. (Tech.), ORCID ID: 0000-0002-5690-5349 (Sevastopol, Russia)
- Michael E. Lee** – Head of Department of FSBSI FRC MHI, Dr.Sci. (Phys.-Math.), professor, ORCID ID: 0000-0002-2292-1877 (Sevastopol, Russia)
- Pavel R. Makarevich** – Chief Research Associate, MMBI KSC RAS, Dr.Sci. (Biol.), ORCID ID: 0000-0002-7581-862X, ResearcherID: F-8521-2016, Scopus Author ID: 6603137602 (Murmansk, Russia)
- Ludmila V. Malakhova** – Leading Research Associate of A. O. Kovalevsky Institute of Biology of the Southern Seas of RAS, Ph.D. (Biol.), ResearcherID: E-9401-2016, ORCID: 0000-0001-8810-7264 (Sevastopol, Russia)
- Gennady G. Matishov** – Deputy Academician – Secretary of Earth Sciences Department of RAS, Head of Section of Oceanology, Physics of Atmosphere and Geography, Scientific Supervisor of FSBSI FRC Southern Scientific Centre of RAS, Scientific Supervisor of FSBSI Murmansk Marine Biological Institute KSC of RAS, academician of RAS, Dr.Sci. (Geogr.), professor, ORCID ID: 0000-0003-4430-5220 (Rostov-on-Don, Russia)
- Sergey V. Motyzhev** – Chief Research Associate of Sevastopol State University, Dr.Sci. (Tech.), ResearcherID: G-2784-2014, ORCID ID: 000 0-0002-8438-2602 (Sevastopol, Russia)
- Alexander V. Prazukin** – Leading Research Associate of FSBSI FRC A. O. Kovalevsky Institute of Biology of the Southern Seas of RAS, Dr.Sci. (Biol.), ResearcherID: H-2051-2016, ORCID ID: 0000-0001-9766-6041 (Sevastopol, Russia)
- Anatoly S. Samodurov** – Head of Department of FSBSI FRC MHI, Dr.Sci. (Phys.-Math.), ResearcherID: V-8642-2017 (Sevastopol, Russia)
- Dimitar I. Trukhchev** – Institute of Metal Science, equipment, and technologies “Academician A. Balevski” with Center for Hydro- and Aerodynamics at the Bulgarian Academy of Sciences, Dr.Sci. (Phys.-Math.), professor (Varna, Bulgaria)
- Naum B. Shapiro** – Research Associate of FSBSI FRC MHI, Dr.Sci. (Phys.-Math.), ResearcherID: A-8585-2017 (Sevastopol, Russia)

РЕДАКЦИОННАЯ КОЛЛЕГИЯ

- Горячкин Юрий Николаевич** – главный редактор, главный научный сотрудник ФГБУН ФИЦ МГИ, д. г. н., Scopus Author ID: 6507545681, ResearcherID: I-3062-2015, ORCID ID: 0000-0002-2807-201X (Севастополь, Россия)
- Рябушко Виталий Иванович** – заместитель главного редактора, заведующий отделом ФГБУН ФИЦ «ИнБИОМ им. А.О. Ковалевского РАН», главный научный сотрудник, д. б. н., ResearcherID: H-4163-2014, ORCID ID: 0000-0001-5052-2024 (Севастополь, Россия)
- Совга Елена Евгеньевна** – заместитель главного редактора, ведущий научный сотрудник ФГБУН ФИЦ МГИ, д. г. н., Scopus Author ID: 7801406819, ResearcherID: A-9774-2018 (Севастополь, Россия)
- Фомин Владимир Владимирович** – заместитель главного редактора, заведующий отделом ФГБУН ФИЦ МГИ, д. ф.-м. н., ResearcherID: H-8185-2015, ORCID ID: 0000-0002-9070-4460 (Севастополь, Россия)
- Хмара Татьяна Викторовна** – ответственный секретарь, научный сотрудник ФГБУН ФИЦ МГИ, Scopus Author ID: 6506060413, ResearcherID: C-2358-2016 (Севастополь, Россия)
- Белокопытов Владимир Николаевич** – ведущий научный сотрудник, заведующий отделом ФГБУН ФИЦ МГИ, д. г. н., Scopus Author ID: 6602809060, ORCID ID: 0000-0003-4699-9588 (Севастополь, Россия)
- Бердников Сергей Владимирович** – председатель ФГБУН ФИЦ ЮНЦ РАН, д. г. н., ORCID ID: 0000-0002-3095-5532 (Ростов-на-Дону, Россия)
- Бондур Валерий Григорьевич** – директор ФГБНУ НИИ «АЭРОКОСМОС», вице-президент РАН, академик РАН, д. т. н., ORCID ID: 0000-0002-2049-6176 (Москва, Россия)
- Бритаев Темир Аланович** – главный научный сотрудник ФГБУН ИПЭЭ, д. б. н., ORCID ID: 0000-0003-4707-3496, ResearcherID: D-6202-2014, Scopus Author ID: 6603206198 (Москва, Россия)
- Васечкина Елена Федоровна** – заместитель директора ФГБУН ФИЦ МГИ, д. г. н., ResearcherID: P-2178-2017 (Севастополь, Россия)
- Гертман Исаак** – глава департамента Израильского океанографического и лимнологического исследовательского центра, руководитель Израильского морского центра данных, к. г. н., ORCID ID: 0000-0002-6953-6722 (Хайфа, Израиль)
- Демьшев Сергей Германович** – заведующий отделом ФГБУН ФИЦ МГИ, главный научный сотрудник, д. ф.-м. н., ResearcherID: C-1729-2016, ORCID ID: 0000-0002-5405-2282 (Севастополь, Россия)
- Дианский Николай Ардалянович** – главный научный сотрудник МГУ им. М. В. Ломоносова, доцент, д. ф.-м. н., ResearcherID: R-8307-2018, ORCID ID: 0000-0002-6785-1956 (Москва, Россия)
- Дулов Владимир Александрович** – заведующий лабораторией ФГБУН ФИЦ МГИ, профессор, д. ф.-м. н., ResearcherID: F-8868-2014, ORCID ID: 0000-0002-0038-7255 (Севастополь, Россия)
- Егоров Виктор Николаевич** – научный руководитель ФГБУН ФИЦ ИнБИОМ им. А.О. Ковалевского РАН, академик РАН, профессор, д. б. н., ORCID ID: 0000-0002-4233-3212 (Севастополь, Россия)
- Ефимов Владимир Васильевич** – заведующий отделом ФГБУН ФИЦ МГИ, д. ф.-м. н., ResearcherID: P-2063-2017 (Севастополь, Россия)
- Залесный Владимир Борисович** – ведущий научный сотрудник ФГБУН ИВМ РАН, профессор, д. ф.-м. н., ORCID ID: 0000-0003-3829-3374 (Москва, Россия)
- Зацепин Андрей Георгиевич** – руководитель лаборатории ФГБУН ИО им. П.П. Ширшова РАН, главный научный сотрудник, д. ф.-м. н., ORCID ID: 0000-0002-5527-5234 (Москва, Россия)
- Кныш Василий Васильевич** – ведущий научный сотрудник ФГБУН ФИЦ МГИ, профессор, д. ф.-м. н., Researcher ID: B-3603-2018 (Севастополь, Россия)
- Коновалов Сергей Карпович** – директор ФГБУН ФИЦ МГИ, член-корреспондент РАН, д. г. н., ORCID ID: 0000-0002-5200-8448 (Севастополь, Россия)
- Коротасев Геннадий Константинович** – научный руководитель ФГБУН ФИЦ МГИ, член-корреспондент РАН, профессор, д. ф.-м. н., ResearcherID: K-3408-2017 (Севастополь, Россия)
- Кузнецов Александр Сергеевич** – ведущий научный сотрудник, заведующий отделом ФГБУН ФИЦ МГИ, к. т. н., ORCID ID: 0000-0002-5690-5349 (Севастополь, Россия)
- Ли Михаил Ен Гон** – заведующий отделом ФГБУН ФИЦ МГИ, профессор, д. ф.-м. н., ORCID ID: 0000-0002-2292-1877 (Севастополь, Россия)
- Макаревич Павел Робертович** – главный научный сотрудник ММБИ КНЦ РАН, д. б. н., ORCID ID: 0000-0002-7581-862X, ResearcherID: F-8521-2016, Scopus Author ID: 6603137602 (Мурманск, Россия)
- Малахова Людмила Васильевна** – ведущий научный сотрудник ФГБУН ФИЦ ИнБИОМ им. А.О. Ковалевского РАН, к. б. н., ResearcherID: E-9401-2016, ORCID ID: 0000-0001-8810-7264 (Севастополь, Россия)
- Матишов Геннадий Григорьевич** – заместитель академика-секретаря Отделения наук о Земле РАН – руководитель Секции океанологии, физики атмосферы и географии, научный руководитель ФГБУН ФИЦ ЮНЦ РАН, научный руководитель ФГБУН ММБИ КНЦ РАН, академик РАН, д. г. н., профессор, ORCID ID: 0000-0003-4430-5220 (Ростов-на-Дону, Россия)
- Мотыжев Сергей Владимирович** – главный научный сотрудник СевГУ, д. т. н., ResearcherID: G-2784-2014, ORCID ID: 0000-0002-8438-2602 (Севастополь, Россия)
- Празукин Александр Васильевич** – ведущий научный сотрудник ФГБУН ФИЦ ИнБИОМ им. А.О. Ковалевского РАН, д. б. н., Researcher ID: H-2051-2016, ORCID ID: 0000-0001-9766-6041 (Севастополь, Россия)
- Самодуров Анатолий Сергеевич** – заведующий отделом ФГБУН ФИЦ МГИ, д. ф.-м. н., ResearcherID: V-8642-2017 (Севастополь, Россия)
- Трухчев Димитър Иванов** – старший научный сотрудник Института океанологии БАН, профессор, д. ф.-м. н. (Варна, Болгария)
- Шапиро Наум Борисович** – ведущий научный сотрудник ФГБУН ФИЦ МГИ, д. ф.-м. н., ResearcherID: A-8585-2017 (Севастополь, Россия)

CONTENTS

No. 2. 2023

April – June, 2023

<i>Kuznetsov A. S.</i> Spectral Characteristics of Wind Variability in the Coastal Zone of the South Coast of Crimea 1997–2006.....	6
<i>Dyakov N. N., Malchenko Yu. A., Lipchenko A. E.</i> Hydrological and Hydrochemical Regime of Hypersaline Koyashskoye Lake (Kerch Peninsula).....	21
<i>Lomakin P. D., Ryabtsev Yu. N.</i> Study of Wastewater Distribution near the Heracleon Peninsula (Crimea) in the Upwelling Situation Based on Expedition Data and Numerical Modelling.....	49
<i>Kochergin V. S., Kochergin S. V.</i> Variational Identification of the Initial Field of Chlorophyll A Concentration in the Transport Model according to Remote Sensing Data	61
<i>Gurova Yu. S., Yakushev E. V., Berezina A. V., Novikov M. O., Gurov K. I., Orekhova N. A.</i> Numerical Modelling of RedOx Condition Dynamics at the Water-Sediment Interface in Sevastopol Bay	71
<i>Slepchuk K. A., Khmara T. V.</i> Winter Peak of Phytoplankton Bloom in Sevastopol Bay according to Numerical Modelling	91
<i>Bufetova M. V., Egorov V. N.</i> Lead Contamination of Water and Sediments of Taganrog Bay and the Open Part of the Sea of Azov in 1991–2020	105
<i>Soloveva O. V., Tikhonova E. A.</i> The First Data on the Hydrocarbon Composition of Water, Bottom Sediments of the North Crimean Canal and Soils Adjacent to Agricultural Land	120
<i>Serebryany A. N., Denisov D. M., Khimchenko E. E.</i> Autonomous Internal Wave Measurer based on Temperature Transmitters for Shelf Studies.....	134

СОДЕРЖАНИЕ

№ 2. 2023

Апрель – Июнь, 2023

<i>Кузнецов А. С.</i> Спектральные характеристики изменчивости ветра в прибрежной зоне Южного берега Крыма в 1997–2006 годах.....	6
<i>Дьяков Н. Н., Мальченко Ю. А., Липченко А. Е.</i> Гидролого-гидрохимический режим гиперсоленого озера Кояшского (Керченский полуостров).....	21
<i>Ломакин П. Д., Рябцев Ю. Н.</i> Исследование распространения сточных вод у Гераклеийского полуострова (Крым) в ситуации апвеллинга на основе экспедиционных данных и численного моделирования	49
<i>Кочергин В. С., Кочергин С. В.</i> Вариационная идентификация начального поля концентрации хлорофилла <i>a</i> в модели переноса по данным дистанционного зондирования.....	61
<i>Гурова Ю. С., Якушев Е. В., Березина А. В., Новиков М. О., Гуров К. И., Орехова Н. А.</i> Численное моделирование динамики окислительно-восстановительных условий на границе вода – донные отложения в Севастопольской бухте.....	71
<i>Слепчук К. А., Хмара Т. В.</i> Зимний пик цветения фитопланктона в Севастопольской бухте по результатам численного моделирования	91
<i>Буфетова М. В., Егоров В. Н.</i> Загрязнение свинцом воды и донных отложений Таганрогского залива и открытой части Азовского моря в 1991–2020 годах	105
<i>Соловьева О. В., Тихонова Е. А.</i> Первые данные об углеводородном составе воды, донных отложений Северо-Крымского канала и почв прилегающих сельскохозяйственных угодий.....	120
<i>Серебряный А. Н., Денисов Д. М., Химченко Е. Е.</i> Автономный измеритель внутренних волн на базе измерительных преобразователей температуры для исследований на шельфе	134

Spectral Characteristics of Wind Variability in the Coastal Zone of the South Coast of Crimea 1997–2006

A. S. Kuznetsov

*Marine Hydrophysical Institute of RAS, Sevastopol, Russia
e-mail: kaskasev@mail.ru*

Abstract

The paper studies the spectral characteristics of the coastal wind field variability near the South coast of Crimea in the zone of horizontal inhomogeneities of the land surface underlying the atmosphere and sea to specify the role of the coastal wind variability in the formation of coastal water circulation features. Reliable knowledge of these features is necessary for ecological standardization of the anthropogenic impact on marine ecosystems as part of ecological and economic processes management in the coastal sea zone. Archived data were used from standard meteorological observations of wind variability over a 10-year period of instrumental monitoring (1997–2006) at the Black Sea hydrophysical sub-satellite testing area of Marine Hydrophysical Institute near Cape Kikineiz onshore and offshore and at the hydrometeorological station near Cape Nikita (Yalta). The advanced information technology of processing and quality control of vector data was used to ensure the unity of multi-year measurements, which allowed increasing the accuracy of measured wind characteristics. The peculiarities of spectral characteristics of the coastal wind field variability in daily, mesoscale and seasonal ranges were found out. The obtained *in situ* results were compared with the known results of numerical modelling using modern models of regional atmospheric circulation with high spatial and temporal resolution. The scientific novelty of the work is in obtaining representative empirical knowledge during the analysis of materials on the peculiarities of wind condition variability near the coast in zones with horizontal heterogeneities of the properties of the land surface underlying the atmosphere and comparing these results with the existing model developments. Such integrated studies provide reliable knowledge of the circulation patterns of coastal waters off the South coast of Crimea given the effects of local winds.

Keywords: South coast of Crimea, coastal zone, marine ecosystem, monitoring, meteorological parameters, wind conditions, distribution histogram, spectral density

Acknowledgements: The work was performed under state assignment of Marine Hydrophysical Institute of RAS on topic FNNN-2021-0005 “Complex interdisciplinary research of oceanologic processes, which determine functioning and evolution of the Black and Azov Sea coastal ecosystems”.

For citation: Kuznetsov, A.S., 2023. Spectral Characteristics of Wind Variability in the Coastal Zone of the South Coast of Crimea 1997–2006. *Ecological Safety of Coastal and Shelf Zones of Sea*, (2), pp. 6–20. doi:10.22449/2413-5577-2022-2-6-20

© Kuznetsov A. S., 2023



This work is licensed under a Creative Commons Attribution-Non Commercial 4.0 International (CC BY-NC 4.0) License

Спектральные характеристики изменчивости ветра в прибрежной зоне Южного берега Крыма в 1997–2006 годах

А. С. Кузнецов

*Морской гидрофизический институт РАН, Севастополь, Россия
e-mail: kaskasev@mail.ru*

Аннотация

Целью работы является исследование спектральных характеристик изменчивости поля прибрежного ветра у Южного берега Крыма в зоне горизонтальных неоднородностей подстилающей атмосферу поверхности суши и моря для уточнения роли изменчивости прибрежного ветра в формировании особенностей циркуляции прибрежных вод. Достоверные знания об этих особенностях необходимы для экологического нормирования антропогенного воздействия на морские экосистемы в рамках управления эколого-экономическими процессами в прибрежной зоне моря. Используются архивные данные стандартных метеорологических наблюдений изменчивости ветра за 10-летний период инструментального мониторинга (1997–2006 гг.) на Черноморском гидрофизическом подспутниковом полигоне Морского гидрофизического института у м. Кикинеиз на суше и в море, а также на гидрометеорологической станции у м. Никита (г. Ялта). Для обеспечения единства многолетних измерений использована перспективная информационная технология обработки и контроля качества векторных данных, которая позволила повысить точность измеряемых характеристик ветра. Выявлены особенности спектральных характеристик изменчивости поля прибрежного ветра в суточном, мезомасштабном и сезонном диапазонах. Полученные натурные результаты сопоставлены с известными результатами численного моделирования с использованием современных моделей региональной атмосферной циркуляции с высоким пространственным и временным разрешением. Научная новизна работы заключается в получении репрезентативных эмпирических знаний при анализе материалов об особенностях изменчивости ветровых условий у побережья в зонах с горизонтальными неоднородностями свойств подстилающей атмосферу земной поверхности и сопоставлений этих результатов с существующими модельными разработками. Такие комплексные исследования позволяют получить достоверные знания о закономерностях циркуляции прибрежных вод у Южного берега Крыма с учетом воздействия местных ветров.

Ключевые слова: Южный берег Крыма, прибрежная зона, морская экосистема, мониторинг, метеопараметры, ветровые условия, гистограмма распределения, спектральная плотность

Благодарности: работа выполнена в рамках государственного задания ФГБУН ФИЦ МГИ по теме FNNN-2021-0005 «Комплексные междисциплинарные исследования океанологических процессов, определяющих функционирование и эволюцию экосистем прибрежных зон Черного и Азовского морей».

Для цитирования: *Кузнецов А. С.* Спектральные характеристики изменчивости ветра в прибрежной зоне Южного берега Крыма в 1997–2006 годах // Экологическая безопасность прибрежной и шельфовой зон моря. 2023. № 2. С. 6–20. EDN XYCHJS. doi:10.29039/2413-5577-2023-2-6-20

Introduction

Currently, the development of natural, economic and recreational complexes near the South coast of Crimea is due to the intensive development of its land area and the coastal zone of the Black Sea. Based on estimates of the level of anthropogenic pressure on the coastal zones and ecotones of the Black Sea coast of Crimea, it was noted in [1] that the coastal ecosystems of the Black Sea tend to degrade under the influence of anthropogenic pollution entering the marine environment, which requires adoption of legal restrictive measures. According to [1, 2], an ecotone is a zone at the interface between two media, where boundary effects are manifested in a special mode of geochemical processes that create the possibility of the existence of specific biocenoses and ecosystems in the boundary zones. Near the Southern coast of Crimea (SCC), such zones are the coastal ecotone of the land and the coastal marine ecotone, which exist at the boundary of land and sea.

The water area of the marine ecotone is the coastal extremity of the shelf zone and includes an adjacent shallow strip of the open part of the sea, bays and gulfs. The existence zone of the coastal ecotone of the sea near Cape Kikineiz of the SCC occupies a coastal strip limited by depths of 50–70 m at a distance of up to 1 km from the coast. To establish the degree of damage caused to the coastal ecosystem by pollution of this water area, reliable data on the intensity of processes in the coastal frontal zones and sections are required [1, 2]. The circulation of waters in the shallow coastal area of the shelf near the SCC has its own regularities [3, 4] and differs from the dynamics of waters in the adjacent shelf-slope part of the sea, as well as from the Rim Current [5]. The specific features of coastal water circulation are determined by the geographic location and structure of the unique natural landscape of the SCC, the shape of the coastline and bottom relief, and the intensification and stability of water circulation are associated with oceanological and meteorological disturbances.

At the current level of the Black Sea pollution flux [6] entering the marine environment, it is necessary to apply ecological regulation of anthropogenic impacts on marine ecosystems in the framework of managing ecological and economic processes in the coastal zone of the sea [7]. In order to determine scientifically based limiting norms of the pollution fluxes entering marine environment, along with the estimates of their level and the capabilities of the ecosystem assimilation capacity, reliable knowledge about the features of coastal water circulation is required. Based on the results of long-term field studies of the coastal currents near the SCC, presented in [3, 4], the regularities of the cyclonic circulation of the stationary alongshore current and the features of its variability in the gravitational-inertial, subinertial and seasonal ranges were revealed. Experimental identification of the factors causing such an intensification of currents is an urgent task.

It is known that the intensity of the wind circulation in the sea depends on the wind conditions of the atmospheric surface layer. Near the coast in the zone of the surface underlying the atmosphere (land and sea), the characteristics of the air flow (wind) are variable over a wide range. From the analysis of the published

results of research on wind characteristics near the SCC, the following should be noted. According to the instrumental measurements, the wind variability near the coast is formed as a result of contribution of a large-scale wind field, which is transformed when the wind flows around the Main Range of the Crimean Mountains, and a superposition of local formations of thermal and orographic origin^{1), 2), 3), 4)} [8]. At the same time, the practical value of the results of modelling studies obtained at Marine Hydrophysical Institute (MHI) according to the data of a regional retrospective analysis (reanalysis) based on various numerical models of atmospheric circulation, presented in a series of works [9–15], should be especially noted.

The main elements of the large-scale cyclonic circulation of the Black Sea waters are the Rim Current jet and two macrocyclonic gyres in the eastern and western parts of the sea [5, 16]. The seasonal variability of the large-scale circulation of the Black Sea waters is largely determined by the action of the driving stress of the wind, and the wind field vorticity is the main characteristic that determines the generation of wind circulation in the sea [9]. On seasonal time scales of variability, vorticity of the field of the driving wind velocity modulus on the Black Sea surface includes background vorticity associated with the general large-scale atmospheric circulation and a regional component. Regional vorticity associated with orography and contrast between the characteristics of the underlying surface of the sea and land dramatically affects the formation of the total wind field of the surface layer of the atmosphere [13], which, as a result, is the dominant factor in the formation of variability of hydrophysical fields of the Black Sea [11]. Based on the results of a review of materials from early *in situ*^{1)–4)} [8] and theoretical studies [9–15], brief information is given below, which is necessary for further discussion of the results of studies of spectral characteristics of the surface wind field variability in the zone of the land and sea surface underlying the atmosphere.

The hydrometeorological regime of the SCC and adjacent water areas is mainly determined by macrocirculation processes of the Mediterranean climatic region, features of coastline configuration, and geomorphological structure of the Crimean Peninsula [8, 9]. Atmospheric processes occurring over the Black Sea are distinguished by a wide variety of forms, which are largely due to the features of baric conditions and orographic features of the SCC.

¹⁾ Lapin, M.N., 1954. [*The Black Sea Pilot*]. Leningrad: Izd-vo Gidrograficheskogo Upravleniya Voenno-Morskikh Sil, 506 p. (in Russian).

²⁾ Potapov, N.S., 1956. [Breeze Circulation on the South coast of Crimea]. In: Shuleykin, V.V., ed., 1956. *Trudy Morskogo Gidrofizicheskogo Instituta*. Moscow: Izd-vo AN SSSR. Vol. 8, pp. 98–108 (in Russian).

³⁾ Chernyakova, A.P., 1965. Typical Wind Fields of the Black Sea. In: MGMO ChAM, 1965. [*Collection of Works of the Basin Hydrometeorological Observatory of the Black and Azov Seas*]. Leningrad: Gidrometeoizdat. Iss. 3, pp. 78–121 (in Russian).

⁴⁾ Zats, V.I., Lukyanenko, O.Ya. and Yatsevich, G.V., 1966. [*Hydrometeorological Regime of the Southern Coast of Crimea*]. Leningrad: Gidrometeoizdat, 120 p. (in Russian).

During the year, barico-circulation features of atmospheric processes over the Black Sea have well-defined seasonal differences. In this case, the regional vorticity of the wind field is the main factor in the formation of the seasonal course of the vorticity of the wind velocity field, which varies from cyclonic in winter to anticyclonic in summer [8, 9]. As it is known, wind conditions on land and near the coast are significantly different from wind conditions in open areas of the sea [8]. Geomorphological and orographic subregional features of the SCC region change the nature of regional atmospheric circulation and contribute to the emergence of its local manifestations¹⁾⁻⁴⁾ [8–10, 12–15].

The purpose of this work is to study spectral characteristics of multiscale variability of the coastal wind on the basis of the archival data obtained over a 10-year period of instrumental monitoring from 1997 to 2006 near Cape Kikineiz at the Black Sea hydrophysical sub-satellite testing area (BSHSTA) of MHI, as well as the data from the meteorological station at Cape Nikita. The scientific novelty of the work lies in obtaining reliable empirical knowledge based on the analysis of archival materials on variability of characteristics of the coastal wind in zones with horizontal inhomogeneities of the properties of the earth's surface underlying the atmosphere and comparison of these characteristics with existing theoretical developments. These materials are necessary for further studies of variability of the spectral characteristics of the coastal wind field near the SCC and revealing their relationship with the features of coastal water circulation [4].

Materials and methods

This paper presents the results of processing and analysis of the archival data of standard meteorological observations of wind variability performed on a contractual basis in 1997–2006 near Cape Kikineiz and at Cape Nikita (Fig. 1). The means for monitoring the hydrometeorological situation at BSHSTA of MHI provided contact monitoring of the wind field characteristics at the polygon near Cape Kikineiz in the zone of the land's surface underlying the atmosphere and the coastal zone of the sea. The wind characteristics were measured at the coastal hydrometeorological station of Katsiveli village (Fig. 1) with coordinates 44.38° N and 33.98° E, at a height of ~ 40 m and at a distance of ~ 150 m from the water's edge. The measurements of the wind characteristics near Cape Nikita (Fig. 1) were carried out at the Nikitsky Sad meteorological station, located at a distance of ~ 25 km to the northeast of Cape Kikineiz, with coordinates of 44.51° N and 34.24° E, at a height of ~ 200 m and at a distance of ~ 550 m from the water's edge. The wind characteristics of the atmospheric surface layer were measured in the Goluboy Gulf (Fig. 1) at the marine hydrometeorological station of the stationary oceanographic platform [3] with coordinates 44.39° N and 33.98° E, at an altitude of 18 m above sea level and at a distance of ~ 450 m from the coast. The measurements on the platform at sea are presented for the 7-year observation period 1997–2003 during the seasons of the greatest development of the breeze from May to October.



Fig. 2. Schematic map of the studied area near the South coast of Crimea. The circles are for onshore weather stations, the star is for those in the Goluboy Gulf. Line I denotes the ridge orientation near Cape Kikineiz, line II – near Cape Nikita

The south coast of the Crimean Peninsula from Cape Sarych to Cape Ai-Todor is protected by the Main Range of the Crimean Mountains, blocking direct access to northern winds²⁾. The southern cliffs of the mountain range, as well as the adjacent coastline near the village of Katsiveli, are oriented from the west-southwest to the east-northeast (straight line I in Fig. 1). The land area between the cliffs and the coast reaches a width of 4 km, and the heights of the mountains are in the range of 1000–1200 m. From Cape Ai-Todor to Cape Nikita, the coastal strip of the SCC is protected by a mountain range from the northeast²⁾, where the slopes of the mountains towards the sea are oriented from the southwest to the northeast (straight line II in Fig. 1). At Cape Nikita, the land strip between the mountain range and the coastline reaches a width of 8 km, with the height of the adjacent mountain range ~ 1200 m.

The instrumental measurements of the wind field characteristics were made by M-63M anemorumbographs. The wind meters operated in the standard averaging mode with 8-term registration of measurements in one day. Every 3 hours, the instantaneous successive values of the modulus of the velocity and direction of the wind vector averaged over a 10-minute time interval were recorded. The totality of the initial chronological sequences for the 10-year period of research amounted to 29,216 pairs of components of 3-hour readings of the coastal wind vector characteristics.

According to the passport data, the primary measuring transducers of the anemograph have typical metrological characteristics with a sensitivity (the least significant digit of the meter) for the wind velocity channel no more than 0.1 m/s and the wind direction channel no more than 3°. The measurement technology made it possible to exclude the contribution of faulty values and significant methodological measurement errors, and further application of the procedure for analyzing the results of statistical processing of the set of vector data for monitoring wind characteristics made it possible to increase the averaged data accuracy. To ensure the uniformity of long-term measurements, the materials underwent data quality control in the prescribed manner and, on their basis, vector-averaged 9-hour and average daily values of the wind velocity and direction modulus were calculated. The results of statistical processing of vector-averaged data, taking into account the analysis of the actual values of the current histograms of distribution of the modulus of the wind velocity vector and direction, ensured an increase in the accuracy of measurements of wind components to the limiting levels of random errors [17]. At certain averaging intervals, the limiting random mean-square errors in measuring the modulus of the wind vector velocity and direction are reduced to 0.1–0.2 m/s and to 5°, respectively.

On the basis of a set of initial data of instrumental measurements, 3652 pairs of mean hourly values of the wind vector components were formed. The *in situ* data are further used in full in statistical and spectral analysis. It should be noted that in the course of modelling studies in [10, 13, 15], to identify the contribution of the breeze against the background of synoptic disturbances, a special method of digital filtering of the processed data, the “method of difference composites”, was used under the assumption that the fields of breeze and synoptic circulation are additive. The spectral analysis of the vector characteristics of the air flow (wind) in this work was carried out within the framework of a linear (filter) estimation of the energy spectrum of oscillations, similar to the method of analyzing a set of vector data in [3, 4] through periodogram smoothing using a fast Fourier transform procedure. The features of the method of spectral analysis of vector characteristics are presented in the works^{5), 6)}. On the basis of these materials, a software information product used in this work was developed. The choice of vector data filtering parameters made it possible to reliably investigate the energy contribution and spectral features of the distribution of the total energy density of oscillations with multiscale variability of the coastal wind field. Estimations of breeze characteristics were also obtained under the assumption that the fields of the breeze and synoptic circulation are additive.

⁵⁾ Konyaev, K.V., 1981. [*Spectral Analysis of Random Oceanological Fields*]. Leningrad: Gidrometeoizdat, 207 p. (in Russian).

⁶⁾ Blatov, A.S., Bulgakov, N.P., Ivanov, V.A., Kosarev, V.N. and Tuzhilkin, V.S., 1984. *Variability of Hydrophysical Fields of the Black Sea*. Leningrad: Gidrometeoizdat, 240 p. (in Russian).

Discussion and results

In the zone of narrowing of the continental slope between the southern tip of the Crimean Peninsula and the Anatolian coast, the water area of the Black Sea is divided along the meridian 34° E passing through the territory of BSHSTA of MHI (33.984° E) to the eastern and western parts [12], where macrocyclonic circulations of currents (“Knipovich spectacles”) are formed [16]. The transitional zone between the gyres, adjacent to the territory of BSHSTA of MHI, is both functionally and territorially associated with the connecting “bridge of Knipovich spectacles”.

The Crimean Mountains, horizontal inhomogeneities of the underlying surface, and thermal land-sea contrasts cause disturbances in the lower part of the atmospheric boundary layer, contributing to the generation and development of a wide range of mesoscale processes near the SCC. One of the empirical problems considered in this paper is the study of the variability features of such mesoscale disturbances based on the spectral analysis of *in situ* data. Taking into account the previously accumulated knowledge obtained on the basis of numerical modeling of the atmospheric circulation over the Black Sea, it is possible to reasonably identify the variability features of the coastal wind characteristics.

The structure of atmospheric fields in the zone of the coastal ecotone of land and sea near the SCC is most variable in the spring-summer and summer-autumn seasons (May–October) [10, 14, 15]. At this time of the year, the daily variability of atmospheric fields is clearly expressed due to the maximum intensification of breeze circulation, which is the result of temperature contrasts between the sea and land associated with daily and seasonal cycles. The daytime breeze (sea breeze) is a gravitational flow of air propagating towards the land, and the night breeze (continental breeze) has the opposite direction. Instrumental studies of breeze circulation near the village of Katsiveli have been carried out since 1949²⁾ by a complex of upper-air observations, including drifter balloon-pilot studies. Subsequently, a representative method for studying breeze circulation was numerical simulation using regional atmospheric circulation models with high spatial and temporal resolution [9, 13–15]. The set of *in situ* data on the variability of coastal wind characteristics analyzed in this paper makes it possible to resume contact field studies of the breeze circulation features near the SCC at a new technological level in order to subsequently assess the role of local winds in the formation of coastal water circulation features.

A significant increase in wind velocities in the sea, compared to its velocities on land near Cape Kikineiz, has been instrumentally recorded since 1983. Fig. 2 shows the multi-year average full energy spectra of coastal wind oscillations near the SCC for 1997–2003, calculated from 9-hour vector-averaged data in the range of wind field variability periods from 18 hours to 2 days. The spectra in Fig. 2, *a* are calculated according to the data of the marine meteorological point in the Goluboy Gulf, the onshore meteorological point near Cape Kikineiz and the onshore meteorological station near Cape Nikita during the period of intensification of breeze circulation (May–October) and demonstrate a significant energy contribution of wind oscillations over a period of 24 h (1 day).

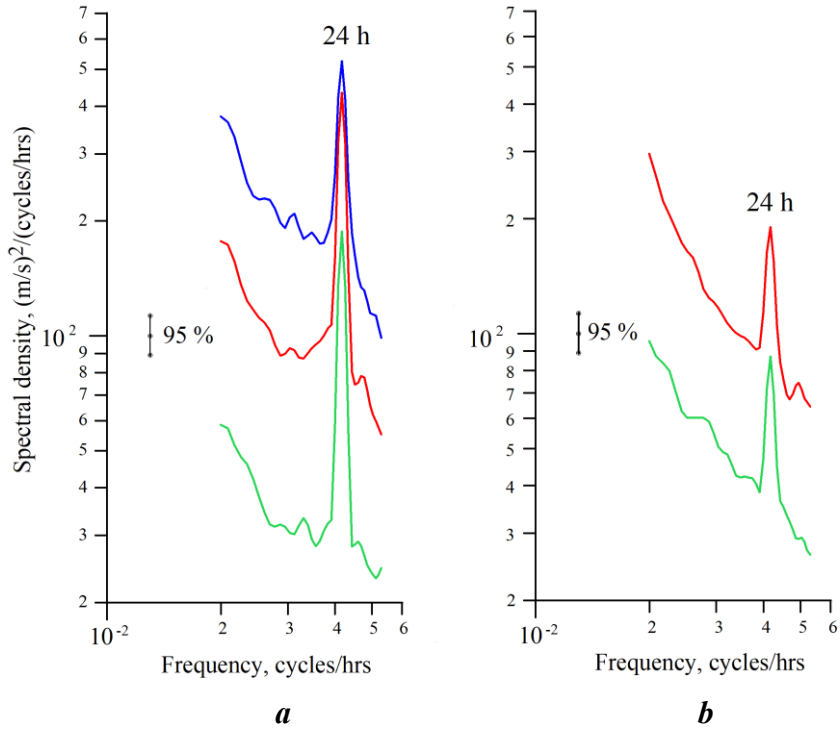


Fig. 2. Full energy spectra of wind oscillations near the South coast of Crimea in the period range of 18 h – 2 days: *a* – at intensification of breeze circulation and daily variability of the coastal wind field (May – October) according to data from the marine meteorological point in the Goluboy Gulf, the onshore meteorological point near Cape Kikineiz and the onshore meteorological station near Cape Nikita (blue, red and green lines, respectively); *b* – at weaker daily variability of the coastal wind field (November – April) according to the data of the onshore meteorological point near Cape Kikineiz and the onshore meteorological station at Cape Nikita (red and green lines, respectively) at the 95 % confidence interval

The spectral maxima significantly exceed the limits of the 95% confidence interval and are credible. The long-term average spectra calculated from the data of the onshore meteorological point near Cape Kikineiz and the onshore meteorological station near Cape Nikita in November–April (Fig. 2, *b*) demonstrate a decrease in the energy contribution of wind oscillations over a period of 24 h compared with the spectra in Fig. 2, *a*. Wind characteristics were not measured in November–April at the meteorological point in the Goluboy Gulf near Cape Kikineiz.

As it is known, the daytime breeze carries the sea air in the atmospheric surface layer towards the coast, while the night breeze is directed from the coast towards the sea. As a result, a single quasi-cyclic process is formed with an oscillation period of 1 day, where the velocities of the daytime breeze near the Crimean Mountains can reach 8 m/s, and the night breeze near Crimea can reach 5 m/s [10] with a characteristic total breeze velocity of about 4–5 m/s [15]. Based on the presented complete energy spectra, the corresponding long-term average values of the daily coastal wind oscillation velocities were calculated for each of the observation points. In May–October, the average annual velocities of daily wind fluctuations in the sea near Cape Kikineiz were 9.7 m/s, on the shore near Cape Kikineiz – 10.4 m/s, and on the coast near Cape Nikita – 8.0 m/s. In November–April, the average multi-year velocities of daily wind fluctuations on the shore near Cape Kikineiz were 4.2 m/s, and on the shore near Cape Nikita – 3.1 m/s.

In the seasons of breeze circulation intensification (Fig. 2, *a*), the average multi-annual daily wind variability rates near Cape Kikineiz between the sea and land differed slightly, and on land between Cape Kikineiz and Cape Nikita had a difference of ~ 2 m/s. During the seasons of decreasing intensity of diurnal wind fluctuations (Fig. 2, *b*), the differences on land between Cape Kikineiz and Cape Nikita were ~ 1 m/s. The indicated average annual seasonal breeze velocities obtained from the *in situ* data near Cape Nikita almost coincide with the velocities calculated from the data of the regional reanalysis of atmospheric circulation for the Black Sea region based on the mesoscale model [10]. The daily wind variability velocities found on land near Cape Kikineiz during the period of weakening of the breeze circulation of the wind (November–April) also coincide with the model estimates.

However, in the spring-summer and summer-autumn seasons (May–October), with the intensification of breeze circulation, the average multi-year velocities of wind oscillations with a daily period near Cape Kikineiz both on land and sea exceed the corresponding model estimates of the characteristic breeze velocity [15] almost twofold. In this regard, it should be noted that in work ²⁾, instrumental observations revealed a daily contribution of the local nighttime thermal wind of the slopes, when the released air periodically flows down from the Crimean Mountains. In [13], based on the results of modelling mesoscale features of atmospheric circulation in the coastal part of the SCC, it was shown that night breeze velocities can reach 10 m/s, which is associated with the appearance of a katabatic wind that occurs at night and propagates down the slope of the adjacent mountains near the village of Katsiveli [14]. The revealed mean annual wind velocities with a diurnal period significantly exceed the typical breeze velocities, which is

due to the additional daily contribution of the local thermal wind and orography. The night katabatic wind makes a certain contribution to the daily fluctuations of the total wind in the village of Katsiveli. Occasionally, reaching hurricane force, it creates a situation of natural disaster, tearing off roofs from houses and buildings, breaking and uprooting perennial trees.

According to the rectilinear coastline scheme [15], the direction of the breeze is almost perpendicular to the coastline. The Crimean Mountains with heights near the SCC in the range of 1000–1200 m significantly change the structure of the breeze circulation. The sea breeze propagation height in Crimea is 500–1000 m [13], while it was noted in work ²⁾ that the upper limit of the sea breeze can reach 1600 m. In such cases, only the upper part of the flow penetrates onto land beyond the Main Range of the Crimean Mountains. In the case when high mountains block the propagation of breeze further on land ²⁾ [10, 15], an area of strong alongshore breeze air flows is formed near the SCC [15]. During the day, the breeze circulation periodically changes in terms of velocity and direction. With the development of both daytime and nighttime breezes, the action of the Coriolis force leads to the rotation of the velocity field vector during the day [10]. During the daily cycle, the development of the breeze is accompanied by a gradual change in its direction in a clockwise direction. Such diurnal dynamics of the local wind introduces additional distortions in *in situ* studies of the characteristics of the coastal wind field near the SCC in the range of mesoscale, synoptic and seasonal variability, which must be taken into account when processing and analyzing *in situ* data.

High Crimean Mountains significantly change the structure of the regional wind field near the coast ^{2)–4)} [8, 9, 13, 15] and form the alongshore structure of the coastal wind near the SCC, including the breeze component, both on land and in the near, relatively narrow coastal strip of the sea [14]. Fig. 3 shows the frequency distribution histograms of the alongshore wind directions near the SCC.

The mountains near the SCC significantly complicate the situation, creating a complex superposition of breeze and mountain-valley winds in the land-sea junction zone. In order to suppress the contribution of intense daily fluctuations caused by local winds (breezes, mountain-valley and katabatic winds) in the implementations, the procedure of daily vector averaging of the initial data was performed. The asterisk in Fig. 3 shows the maximum value of the probability density of the contribution of local winds from the mountains (from 345°), calculated from the initial data of the sea and coastal meteorological points near Cape Kikineiz before their daily averaging. At Cape Nikita, the intensive contribution of local winds from the mountains was not identified in the initial realizations. In Fig. 3, two main almost collinear directions are distinguished, along which the alongshore circulation of the coastal wind near the SCC is oriented.

To analyze the large-scale variability of the wind field near the SCC, we used the average daily and average monthly vector-averaged values of the coastal wind velocity and direction modulus, formed over a 10-year period of *in situ* observations. Fig. 4 shows the long-term average full energy spectra of wind oscillations near the SCC for 1997–2006 in the variability range of 24–512 days.

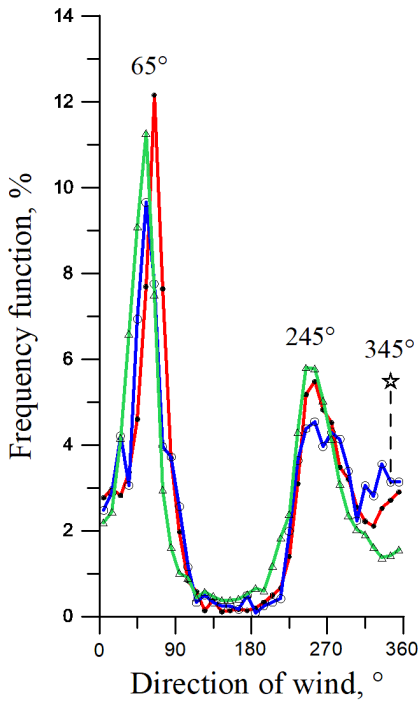


Fig. 3. Histograms of the frequency distribution of alongshore wind directions near the South coast of Crimea based on daily vector-averaged multi-year data from the Goluboy Gulf marine meteorological station, the onshore meteorological station at Cape Kikineiz and the onshore meteorological station at Cape Nikita (blue, red and green lines, respectively). Kikineiz and the onshore meteorological station near Nikita (blue, red and green lines, respectively). The star shows the maximum probability density value of diurnal slope wind contribution from land in the raw, not averaged data of the offshore and onshore meteorological points at Cape Kikineiz

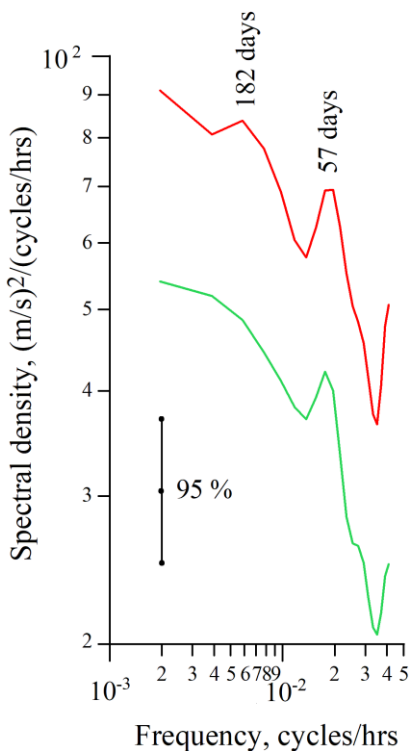


Fig. 4. The 1997–2006 long-term average full energy spectra of wind variability near the South coast of Crimea in the range of periods 24–512 days based on the data from the onshore meteorological point at Cape Kikineiz and onshore meteorological station Nikita (red and green lines, respectively) at 95 % confidence interval

The spectra in Fig. 4 demonstrate the reliable energy contribution of coastal wind fluctuations over a period of about two months (57 days) at the measurement points on land. The nature of the wind intense variability at the indicated points is almost identical, however, the values of the mean annual velocities of coastal wind oscillations near Cape Kikineiz are almost 1.5 times higher. Previously, the results of long-term studies of the coastal current variability near Cape Kikineiz [3] were published, where seasonal fluctuations of currents on the annual period, the second and third annual harmonics were reliably identified, as well as current fluctuations with a period of about two months, identified in the set of long-term average energy spectra of coastal current variability near the SCC (Fig. 2 in [3, p. 161]). Further spectral analysis of the *in situ* data presented in this paper made it possible to reliably separate the seasonal fluctuations of the coastal wind field on annual and semi-annual periods at a 90 % confidence interval.

This paper presents preliminary results of a study of the spectral characteristics of the coastal wind variability near the SCC, obtained from the analysis of archival *in situ* data. Further development of instrumental synchronous studies of the field of coastal wind and currents at BSHSTA of MHI near the SCC will allow to obtain new representative *in situ* data within the framework of the problem under study.

Conclusion

New scientific results were obtained on the basis of processing and analysis of archival data of standard meteorological observations of wind variability for a 10-year period of instrumental monitoring performed in 1997–2006 at the Black Sea hydrophysical sub-satellite testing area of the Marine Hydrophysical Institute near Cape Kikineiz on land and in the sea, as well as at the hydrometeorological station near Cape Nikita of the SCC. To ensure the uniformity of long-term measurements, a promising information technology for processing and quality control of vector data was used, which made it possible to improve the accuracy of measured wind characteristics.

On the basis of archival data of a full-scale experiment, the mean long-term full energy spectra of coastal wind field oscillations for the diurnal range of variability were studied. The seasonal variability of the intensity of diurnal wind fluctuations, associated with intra-annual changes in the contribution of breeze and local mountain-valley winds in the boundary zone of land and sea, was reliably revealed. Intense fluctuations of the coastal wind were revealed for periods of about 57 days, and the seasonal fluctuations of the coastal wind field near the SCC were reliably separated for annual and semi-annual periods.

The experience of working with the data from contact monitoring of wind characteristics allows us to continue instrumental *in situ* studies in this direction at the modern technological level. Representative estimates of the variability of coastal wind conditions and their contribution to the formation of the coastal water circulation structure are required to obtain new empirical knowledge in the framework of this problem that has not been sufficiently studied so far. A comprehensive analysis of current variability data and time-synchronous data of local wind

characteristics makes it possible to obtain new scientific knowledge about cause-and-effect relationships and the contribution of wind variability of the near-water layer of the atmosphere to the formation of a quasi-stationary structure, regime and multi-scale variability of coastal water circulation off the coast, which remains one of the priority tasks of the Marine Hydrophysical Institute of the Russian Academy of Sciences.

REFERENCES

1. Belyaev, V.I., Doroguntsov, S.I., Sovga, E.E. and Nikolaenko, T.S., 2001. Estimation of Degree of Anthropogenic Loads on Coastal Zones and Ecotons of the Black Sea Coast of Ukraine. *Morskoy Gidrofizicheskiy Zhurnal*, (1), pp. 55–63 (in Russian).
2. Lebedev, V., Aizatulin, T. and Khailov, K., 1989. *The Living Ocean*. Moscow: Progress Publishers, 327 p.
3. Kuznetsov, A.S., 2022. Mean Long-Term Seasonal Variability of the Coastal Current at the Crimea Southern Coast in 2002–2020. *Physical Oceanography*, 29(2), pp. 139–151. doi:10.22449/1573-160X-2022-2-139-151
4. Kuznetsov, A.S. and Ivashchenko, I.K., 2023. Features of Forming the Alongcoastal Circulation of the Coastal Ecotone Waters nearby the Southern Coast of Crimea. *Physical Oceanography*, 30(2), pp. 171–185. doi:10.29039/1573-160X-2023-2-171-185
5. Ivanov, V.A. and Belokopytov, V.N., 2013. *Oceanography of the Black Sea*. Sevastopol: ECOSI-Gidrofizika, 210 p.
6. Pokazeev, K., Sovga, E. and Caplina, T., 2021. *Pollution on the Black Sea. Observation about the Ocean's Pollution*. Cham, Switzerland: Springer Nature Switzerland AG, 213 p. <https://doi.org/10.1007/978-3-030-61895-7>
7. Timchenko, I.E. and Igumnova, E.M., 2011. Control over the Ecological-Economic Processes in the Integral Model of the Coastal Zone of the Sea. *Physical Oceanography*, 21(1), pp. 45–62. doi:10.1007/s11110-011-9103-9
8. Koveshnikov, L.A., Ivanov, V.A., Boguslavsky, S.G., Kazakov, S.I. and Kaminsky, S.T., 2001. Problems of Heat and Dynamic Interaction in a Sea – Atmosphere – Land System of the Black Sea Region. In: MHI, 2001. *Ekologicheskaya Bezopasnost' Pribrezhnoy i Shel'fovoy Zon i Kompleksnoe Ispol'zovanie Resursov Shel'fa* [Ecological Safety of Coastal and Shelf Zones and Comprehensive Use of Shelf Resources]. Sevastopol: MHI. Iss. 3, pp. 9–52 (in Russian).
9. Efimov, V.V., Shokurov, M.V. and Barabanov, V.S., 2002. Physical Mechanisms of Wind Circulation Forcing over the Inland Seas. *Izvestiya, Atmospheric and Oceanic Physics*, 38(2), pp. 217–227.
10. Efimov, V.V. and Barabanov, V.S., 2009. Breeze Circulation in the Black-Sea Region. *Physical Oceanography*, 19(5), pp. 289–300. <https://doi.org/10.1007/s11110-010-9054-6>
11. Knysh, V.V., Korotaev, G.K., Moiseenko, V.A., Kubryakov, A.I., Belokopytov, V.N., Inyushina, N.V., 2011. Seasonal and Interannual Variability of Black Sea Hydrophysical Fields Reconstructed from 1971–1993 Reanalysis Data. *Izvestiya, Atmospheric and Oceanic Physics*, 47(3), pp. 399–411. <https://doi.org/10.1134/S000143381103008X>
12. Efimov, V.V. and Anisimov, A.E., 2011. Climatic Parameters of Wind-Field Variability in the Black Sea Region: Numerical Reanalysis of Regional Atmospheric Circulation. *Izvestiya, Atmospheric and Oceanic Physics*, 47(3), pp. 350–361. <https://doi.org/10.1134/S0001433811030030>

13. Efimov, V.V., Barabanov, V.S. and Krupin, A.V., 2012. Simulation of Mesoscale Features of Atmospheric Circulation in the Crimean Black Sea Region. *Morskoy Gidrofizicheskiy Zhurnal*, (1), pp. 64–74 (in Russian).
14. Efimov, V.V., Barabanov, V.S. and Iarovaya, D.A., 2014. [Mesoscale Processes in the Atmosphere of the Black Sea Region]. In: V. A. Ivanov and V. A. Dulov, eds., 2014. *Monitoring of the Coastal Zone in the Black Sea Experimental Sub-Satellite Testing Area*. Sevastopol: ECOSI-Gidrofizika, pp. 250–271 (in Russian).
15. Efimov, V.V. and Krupin, A.V., 2016. Breeze Circulation in the Black Sea Region. *Russian Meteorology and Hydrology*, 41(4), pp. 240–246. <https://doi.org/10.3103/S1068373916040026>
16. Bulgakov, S.N., Korotaev, G.K. and Whitehead, J.A., 1996. The Role of Buoyancy Fluxes in the Formation of a Large-Scale Circulation and Stratification of Sea Water. Part I: The Theory. *Izvestiya, Atmospheric and Oceanic Physics*, 32(4), pp. 548–556 (in Russian).
17. Kuznetsov, A.S., 2018. System of Assessment of the Vector Data Quality and Opportunity of Antenna Measurements of Currents. *Ecological Safety of Coastal and Shelf Zones of Sea*, (1), pp. 50–57. doi:10.22449/2413-5577-2018-1-50-57 (in Russian).

Submitted 17.04.2023; accepted after review 30.04.2023;
revised 03.05.2023; published 26.06.2023

About the author:

Alexander S. Kuznetsov, Leading Research Associate, Head of the Shelf Hydrophysics Department, Marine Hydrophysical Institute of RAS (2 Kapitanskaya St., Sevastopol, 299011, Russian Federation), Ph.D. (Tech.Sci.), **AuthorID: 860912**, **SPIN-code: 1838-7191**; **ORCID ID: 0000-0002-5690-5349**; **Scopus Author ID: 57198997777**, kaskasev@mail.ru

The author has read and approved the final manuscript.

Hydrological and Hydrochemical Regime of Hypersaline Koyashskoye Lake (Kerch Peninsula)

N. N. Dyakov *, Yu. A. Malchenko, A. E. Lipchenko

*Sevastopol Branch of the Federal State Budgetary Institution
“N.N. Zubov State Oceanographic Institute”, Sevastopol, Russia*

** e-mail: dyakoff@mail.ru*

Abstract

A landscape feature of Crimea and the Kerch Peninsula is the presence of a large number of hypersaline lakes and bays, many of which are valuable reserves of therapeutic muds. The article summarizes the results of the hydrological and hydrochemical field studies conducted by the Sevastopol Branch of State Oceanographic Institute in 2015–2022 in the area of hypersaline Koyashskoye Lake located within Natural Reserve Opuksky. Hydrological studies of the lake included the determination of its morphometric characteristics and calculation of the main components of the water balance. Hydrochemical studies included the analysis of samples of brine and bottom sediments. The mineralization of the lake water was measured using different methods. Besides, the following indicators were identified in the samples: dissolved oxygen content and biochemical oxygen demand for five days, pH and total alkalinity, nutrient and pollutant (anionactive surfactants, petroleum, heavy metals) contents. The microelement composition of brine and pollution of bottom sediments were assessed. It was determined that the lake water balance input is formed mainly from atmospheric precipitation and filtration of the Black Sea water through the bay-bar. The major water balance output is evaporation. During an *in situ* experiment using a ground evaporator GGI-3000 and automatic weather station, evaporation for hypersaline waters was estimated and a formula for its calculation was determined. It was found that high concentrations of inorganic forms of phosphorus and nitrogen characterize the waters of Koyashskoye Lake. In summertime, oxygen concentrations can fall to hypoxic values. The bottom sediments of the lake were polluted with zinc, the concentration of which exceeded the maximum permissible concentration.

Keywords: Koyashskoye Lake, natural reserve Opuksky, water balance, thermohaline structure, hydrochemical regime, pollution

Acknowledgement: The work was performed on the topic of state assignment 3.1.2 of the Central Scientific and Technical Center of Roshydromet “Development of methodological recommendations for taking into account climate information in the formation of sectoral plans for adaptation to climate change”. The authors are grateful to the staff of the Sevastopol branch (SB) of SOI for their help: A. A. Polozok for calculating the area of the lake, O. V. Levitskaya for editing the text, A. A. Belogudov for arranging the drawings, S. A. Zhilyaev for sampling, S. A. Bobrov and V. Yu. Erkushov for hydrochemical analyses.

© Dyakov N. N., Malchenko Yu. A., Lipchenko A. E., 2023



This work is licensed under a Creative Commons Attribution-Non Commercial 4.0 International (CC BY-NC 4.0) License

For citation: Dyakov, N.N., Malchenko, Yu.A. and Lipchenko, A.E., 2023. Hydrological and hydrochemical regime of hypersaline Koyashskoye Lake (Kerch Peninsula). *Ecological Safety of Coastal and Shelf Zones of Sea*, (2), pp. 21–48. doi:10.29039/2413-5577-2023-2-21-48

Гидролого-гидрохимический режим гиперсоленого озера Кояшского (Керченский полуостров)

Н. Н. Дьяков*, Ю. А. Мальченко, А. Е. Липченко

ФГБУ «Государственный океанографический институт им. Н.Н. Зубова»,
Севастополь, Россия
*e-mail: dyakoff@mail.ru

Аннотация

Ландшафтной особенностью Крыма и Керченского полуострова является наличие большого числа гиперсоленых озер и заливов, многие из которых представляют собой ценные резерваты лечебных грязей. Цель статьи – обобщить результаты гидролого-гидрохимических экспедиционных исследований Севастопольского отделения ФГБУ «ГОИН» за 2015–2022 гг. в районе гиперсоленого озера Кояшского, расположенного в пределах природного заповедника «Опукский». Гидрологические исследования озера включали определение его морфометрических характеристик и расчеты основных компонент водного баланса. Гидрохимические исследования состояли из анализа проб рапы и донных отложений. Минерализацию вод озера измеряли различными методами. Кроме того, в отобранных пробах определяли следующие показатели: содержание растворенного кислорода и биохимическое потребление кислорода за пять суток, водородный показатель и общую щелочность, содержание биогенных элементов и загрязняющих веществ (анионных поверхностно-активных веществ, нефтепродуктов, тяжелых металлов). Оценивали микроэлементный состав рапы и загрязнение донных отложений. Определено, что приходная часть водного баланса озера формируется преимущественно за счет атмосферных осадков и фильтрации вод Черного моря через пересыпь. Основной расходной частью водного баланса является испарение. В ходе натурального эксперимента с помощью наземного испарителя ГГИ-3000 и автоматической метеостанции получены оценки испарения для гиперсоленых вод и определена формула для его расчета. Выявлено, что воды озера Кояшского характеризуются высокими значениями концентраций неорганических форм фосфора и азота. В летний период возможно понижение концентрации кислорода вплоть до гипоксических значений. Донные отложения озера были загрязнены цинком, концентрация которого превышала предельно допустимую концентрацию.

Ключевые слова: озеро Кояшское, природный заповедник Опукский, водный баланс, термохалинная структура, гидрохимический режим, Крымский полуостров, соленые озера

Благодарности: работа выполнена по теме государственного задания 3.1.2 ЦНТП Росгидромета «Разработка методических рекомендаций по учету климатической информации при формировании отраслевых планов адаптации к изменению климата». Авторы благодарят сотрудников Севастопольского отделения (СО) ФГБУ «ГОИН» за помощь: А. А. Полозок – в расчете площадей озера, О. В. Левицкую – в редактировании текста, А. А. Белогудова – за оформление рисунков, С. А. Жилева – за отбор проб, С. А. Боброву и В. Ю. Еркушова – за проведение гидрохимических анализов.

Для цитирования: Дьяков Н. Н., Мальченко Ю. А., Липченко А. Е. Гидролого-гидрохимический режим озера Кояшского // Экологическая безопасность прибрежной и шельфовой зон моря. 2023. № 2. С. 21–48. EDN VDSWWQ. doi:10.29039/2413-5577-2023-2-21-48

Introduction

A landscape feature of Crimea is the presence of a large number of saline waterbodies with a specific composition of water and bottom sediments [1]. In accordance with work¹⁾, salt (saline, hypersaline) lakes are commonly referred to as the lakes in which water salt content exceeds the salinity of ocean waters, i.e., more than 35 ‰. There are about 300 saline lakes on the territory of Crimea²⁾, of which 48 are large ones, 26 of which with an area of more than 1 km².

According to the origin of the basins and shallows, feeding conditions and hydrological regime, the saline lakes of Crimea can be divided into two types – waterbodies in the basins of marine and continental origin.

By geographical location and presence of balneological resources, the hypersaline lakes of Crimea are usually divided into four main groups: Perekop, Yevpatoria, Kerch, and Tarkhankut [1]. Some authors²⁾ identify additionally the Chersonesus and Sivash Area groups of lakes [2].

The hypersaline lakes of the Kerch group are most numerous, diverse in their origin, and promising for economic use (Fig. 1).

On the Kerch Peninsula, some small shallow lakes of continental origin – Marfovskoye, Kirkoyashskoye, Maryevskoye (Shimakhanskoye, Borisovo, Solenoye), Achi, Karach-Kol, Parpach-Kol, etc. – are located. The hypersaline lakes of marine (estuary) origin of the Kerch group include lakes separated by bay-bars in the coastal zone of the Black Sea – Adzhigol, Kachik, Uzunlarskoye and Koyashskoye; two more lakes (Aktashskoye and Chokraskoye) are located near the coast of the Sea of Azov; and four saline waterbodies (Yanyshskoe, Balchi-Kol, Tobechikskoye and Churubashskoye) border with the Kerch Strait.

Koyashskoye (Opukskoye, Elkinskoye, Elkenskoye) Lake, which is a part of the *Opuksky Nature Reserve* (ONR) State Budgetary Institution, is located at the foot of the Parpach Ridge on the eastern outskirts of the southwestern plain of the Kerch Peninsula and forms a closed lagoon [3]. The complete separation of the lake from the Black Sea by a narrow sandy spit took place relatively recently, less than 2 thousand years ago. Earlier, in ancient times, the seaport of the settlement of Kimmerikon was located on the shore of the lake [4]. The lake is the mouth of a flooded gully, which is separated from the Black Sea by a narrow embankment about 30–80 m wide [1]. In accordance with [5, 6], the dimensions of entire Koyashskoye

¹⁾ Grokhovsky, L.M., 1972. [*Lake Salt Deposits, their Studies and Commercial Evaluation*]. Moscow: Nedra, 168 p. (in Russian).

²⁾ Aizenberg, M.M., ed., 1964. [*Surface Water Resources of the USSR. Main Hydrological Characteristics. Vol. 6. Ukraine and Moldavia. Iss. 4. Crimea*]. Leningrad: Gidrometeoizdat, 243 p. (in Russian).

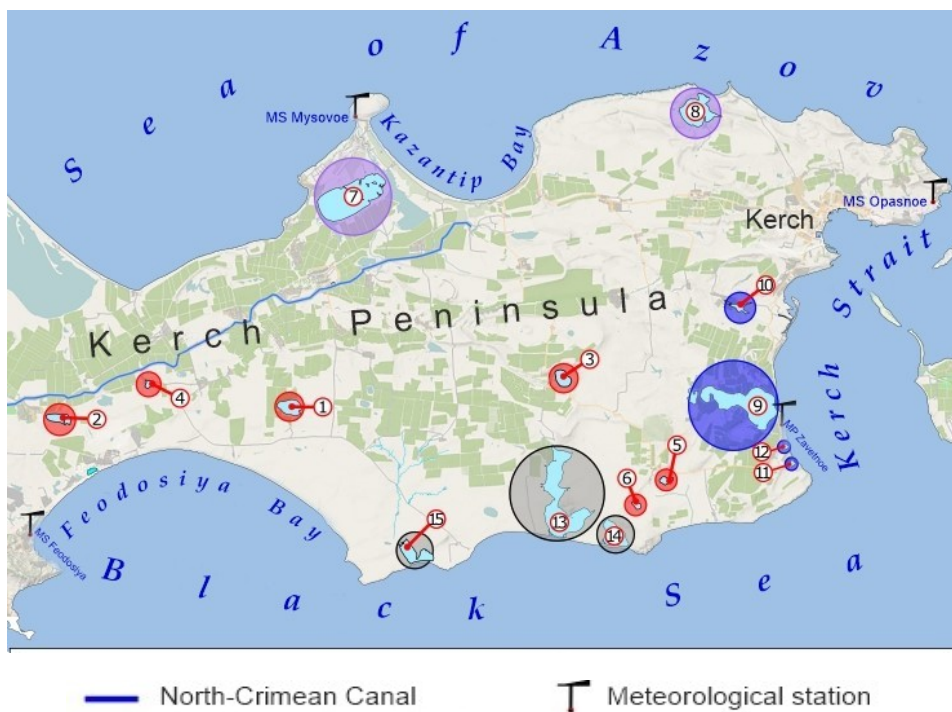


Fig. 1. Major hypersaline lakes of the Kerch group: lakes of continental origin (“kols”) (red colour); lakes of marine (liman) origin of the Sea of Azov basin (violet colour); of the Kerch Strait basin (blue colour); and of the Black Sea basin (grey colour). 1 – Karach-Kol, 2 – Achi, 3 – Marfovskoye, 4 – Parpach-Kol, 6 – Kirkoyashskoye, 7 – Aktashskoe, 8 – Chokraskoye, 9 – Tobechikskoye, 10 – Churubashskoye, 11 – BalchiKol, 12 – Yanyshskoye, 13 – Uzunlarskoye, 14 – Koyashskoye, 15 – Kachik

lake at the maximum filling are as follows³⁾: length – 3.9 km, average width – 1.4 km, maximum width – 3 km, area ~5.4 km², depth – from 0.3 to 0.8 m (Table 1). The waterbody is elongated from northwest to southeast and has an oval shape (Fig. 2). Koyashskoye Lake consists of a number of bays (lagoons) separated by sand spits (arrows). There are some passages in the spits through which water is exchanged among waterbodies. In the southwestern part of Koyashskoye Lake, the system of spits (sand spits) separates two bays (lakes). The largest of the lakes, called Maloye Elkinskoye, has an area of 0.83 km², the greatest length of 1.53 km, and an average width of 0.54 km. From the northeast, Maloye Elkinskoye Lake is separated from Koyashskoye Lake by a nameless spit, which we propose to call

³⁾ Lisovsky, A.A., ed., 2011. [Surface Water Bodies of Crimea. Management and Use of Water Resources: Reference Book]. Simferopol: KRP “Izd. Krymchpedgiz”, 242 p. (in Russian).

the Klyukina Spit in honor of A.A. Klyukin, a famous researcher of the Crimea and one of the creators of the ONR. The Klyukina Spit has a length of 1.1 km (Table 2).

The width of the Klyukina Spit under conditions of maximum lake filling (without any extinct areas) is 40–70 m, in the root parts it increases to 100–160 m. In the body of the spit, a ravine has been located for a long time with an average width of 400–480 m, through which water is exchanged between Maloye Elkinskoye Lake and Koyashskoye Lake proper (Fig. 3, *b*). From one to three small islands can periodically appear in the ravine. The width of the ravine

Table 1. Morphometric characteristics of Koyashskoye Lake

Waterbody	Maximum length, km	Width, km		Area, km ²	Depth, m	
		mean	maximum		mean	maximum
Koyashskoye Lake (without bays)	3.70	1.20	2.00	4.45	0.5	0.8
Maloye Elkinskoye Lake	1.53	0.54	0.78	0.83	0.2	0.3
South-western bay	0.73	0.19	0.39	0.14	0.1	0.2
South-eastern bay	0.15	0.07	0.12	0.01	0.1	0.2
Koyashskoye Lake	3.90	1.40	3.00	5.43	0.3	0.8

Table 2. Morphometric characteristics of spits and bay-bars of Koyashskoye Lake

Accumulation form	Maximum length, km	Width, km		Area, km ²
		mean	maximum	
Klyukina Spit	1.10	0.060	0.16	0.070
Zapadnaya Spit	0.72	0.010	0.02	0.010
Vostochnaya Spit	0.10	0.006	0.01	0.001
Bay-bar at the sea boundary	3.30	0.110	0.15	0.350

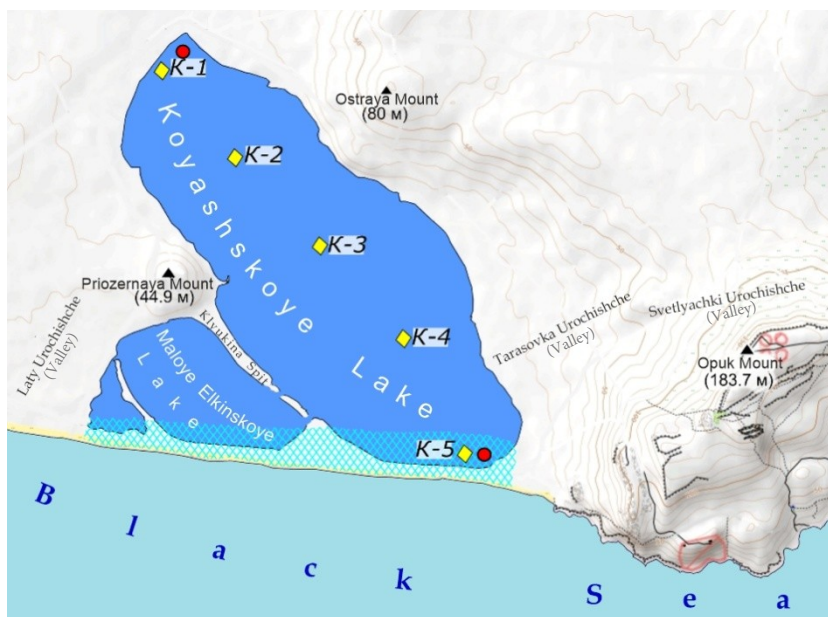


Fig. 2. Schematic map of hypersaline Koyashskoye Lake: red dots are for brine sampling points; diamonds are for mud sampling points; blue cross-hatched area is for the sea water filtration zone (Urochishche – isolated terrain feature)

and the number of islands in it depend on the interannual and seasonal variations of the components of the water balance of Koyashskoye Lake. Over the past 40 years, the spit ravine has increased, and, as a rule, two islands have been observed. The intensity of water exchange through the ravine in the body of the Klyukina Spit is determined by the levels of brine in Koyashskoye Lake and Maloye Elkinskoye Bay (Lake), as well as the speed and direction of the wind.

Based on lithological data [7], the bottom soils of Maloye Elkinskoye Bay (Lake) are composed of silts (muds) about 70 cm deep, below which there is a layer of shell detritus with silty joining material. The Klyukina Spit is composed mainly of shell detritus with shell valves, but at depths of 8–17 cm and below 49 cm there is a layer of silt. The thickness of the accumulated shell material in the body of the Klyukina Spit is small $\sim 0.308 \cdot 10^{-3} \text{ km}^3$ [7]. Maloye Elkinskoye Lake rarely dries up even during the dry period due to the filtration of sea water through the bay-bar. Thus, water is always present in it.

To the west of Maloye Elkinskoye Lake, the Zapadnaya Spit, 720 m long and 10–20 m wide, separates one more small south-western waterbody (bay), dry for most of the year (Fig. 3, c). Water exchange between the south-western waterbody and Maloye Elkinskoye Lake is possible through a narrow ravine (1–3 m) in the northern root part of the Zapadnaya Spit. The south-western waterbody (bay) is filled with water mainly owing to the filtration of the Black Sea water

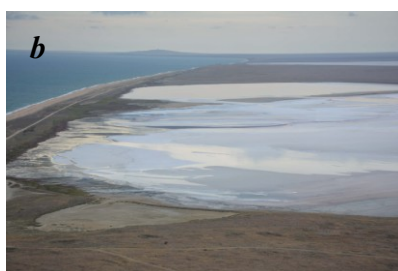
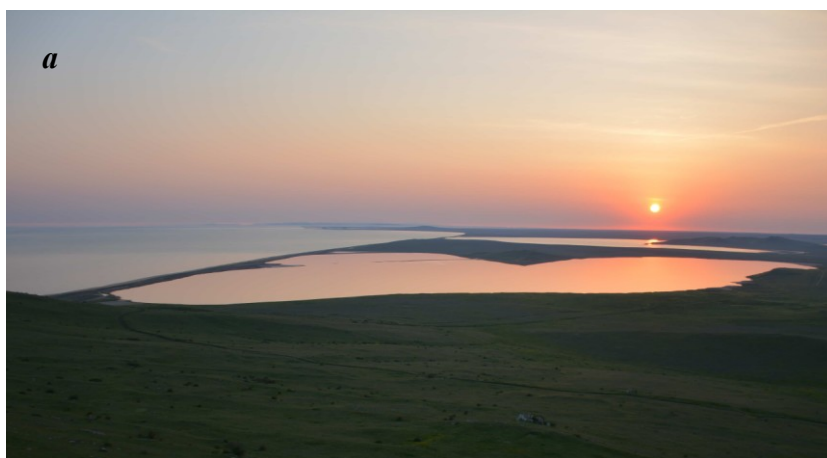


Fig. 3. Koyashskoy Lake (a view from the Mount Opuk) on 25 April 2019 (*a*); in the foreground: south-eastern waterbody and Vostochnaya Spit, in the middle: Koyashskoye Lake, in the background: Klyukina Spit and Maloye Elkinskoye Lake on 17 September 2019 (*b*); Zapadnaya Spit and south-western waterbody on 27 April 2014, through a passage in the spit, water comes on a small scale from Maloye Elkinskoye Lake (*c*)

through the bay-bar, as well as the inflow of water (brine) in a limited volume through a narrow passage from Maloye Elkinskoye Lake. In the west, in the rear part of the bay-bar, the south-western waterbody is sided by a small low (ditch), in which sea water accumulates due to storm overwash and filtration of the Black Sea waters and then enters the waterbody.

On the opposite section of the bay-bar of Koyashskoye Lake there is another small bay – the south-eastern waterbody with an area of 0.01 km², a length of 150 m and an average width of 70 m (Table 1, Fig. 3, *b*). The waterbody is separated from Koyashskoye Lake by a small spit called “Vostochnaya”, 100 m long and 6–10 m wide. Water exchange of the south-eastern waterbody with Koyashskoye Lake takes place through a 25-meter passage in the spit. As a rule, during the research, the south-eastern waterbody was dried up or filled with a small amount of water (brine).

The bay-bar of Koyashskoye Lake, together with Maloye Elkinskoye Lake and the south-western waterbody, is ~3.3 km long and is composed of sand, shells, and detritus from psephytic to silty sizes [7]. The shell is dominated by modern Black Sea pelecypoda and rapana. The underwater coastal slope of the beach is bold, without a bar. During periods of storms, a strip of beach 20–25 m wide usually undergoes wind and wave action. According to [7, 8], during extreme storms, waves can overflow the bay-bar, reaching the water area of Koyashskoye Lake, and throw shells (*Rapana venosa*, *Cardium edule*) and detritus into the rear part of the bay-bar. During the 2016–2022 field studies, we recorded no facts of the Black Sea water inflow through the lake bay-bar during extreme storm waves. Near the lake, there were no strips of household garbage, plastic, usually carried out by waves, and the shell was represented by single specimens of *Rapana* only, most likely brought there by gulls. According to [8], the bay-bar of Koyashskoye Lake is a typical coastal bar after a two-stage period of formation. Favourable conditions for the formation of bars are created during a slowdown in the sea level rise rate, and the transformation of an underwater bar into an island bar and then into an off-shore one occurs with a subsequent lowering of the sea level.

3 km south of the bay-bar of Koyashskoye Lake, the so-called Ship Rocks (Parus, Elken-Kaya, Elchan-Kaya, Karaviya) protrude from under the water 10.0 to 23.4 m above sea level. Ship Rocks are the remains of eroded layers of Meotic shell and detritus limestone and are inclined in different directions at angles of 30–85 degrees. They top a horseshoe-shaped bank bounded by a 10 m isobath. The depth of the bank near the rocks is 5 m, 500 m from them – 9 m, and at a distance of 1000 m – 12 to 14 m [9].

To the east of the lake, Mount Opuk is located, 183.7 m high, which is one of the highest on the Kerch Peninsula. Near the Black Sea coast, this mount ends the Parabolic Ridge, which is a continuation of the Parpach Ridge [9]. On the northern shore of Koyashskoye Lake, Mount Ostraya is located, with the heights of 80.0–88.9 m. The coast in the northern part of the lake is steep for 500–650 m, with the heights of cliffs up to 5–10 m. On the western shore of Koyashskoye Lake, there is a rounded mountain Priozernaya with the height of 44.9 m and diameter of about 600 m.

Bottom sediments are layered black-gray silts up to 1.5 m thick (with salt interlayers). Almost in all periods of field studies of the Sevastopol Branch of State Oceanographic Institute on Koyashskoye Lake, a pink color of salt was observed, which is associated with high content of beta-carotene and the presence of a large number of cysts *Dunaliella* [3]. Koyashskoye Lake muds have the following granulometric characteristics: coarse silts (median value 6.3 μm , maximum particle size 45 μm) are located near the sandy coastal bay-bar; thinner silts (median value 5.1 μm , maximum particle size 30 μm) are found in the areas of the lake, which are remote from the shore. According to their mineral and salt composition, the Koyashskoye Lake muds are comparable to the muds of the Dead Sea [6]. The balance reserves of therapeutic muds are 1720.0 thousand m^3 in category C1 [1]. Currently, brine and muds are not exploited and can be a reserve for use by the Crimean health resorts.

Materials and methods

In 2015–2022, in the area of Koyashskoye Lake, the Sevastopol Branch of State Oceanographic Institute totally conducted 30 expeditions, performed 638 hydrochemical determinations in the brine of the lake:

Year	2015	2016	2017	2018	2019	2020	2021	2022
Number of expeditions	1	3	6	3	6	6	3	2
Number of hydrochemical determinations	11	34	94	52	142	150	89	66

At the final stage of studies in 2020–2021, sampling and analysis of bottom sediments (muds) from the bottom of the lake was carried out in order to study their chemical composition and pollution level in order to assess their safety and potential suitability for use in balneological purposes. Fig. 2 shows a map of Koyashskoye Lake with plotted sampling points, including a network of stations for determining the trace element composition described in work³⁾.

The areas of water (brine) and extinct areas were measured, as well as changes in the lake bay-bar. In order to perform morphometric and water balance studies, the information obtained from artificial earth satellites Landsat 4–5 with a resolution of 15–30 m and Sentinel-2 (with a resolution of 10 m per pixel for the visible range) was used from open sources. To interpret the images (distinguishing water bodies within the land and the land-sea boundary), the method of combining space images in different spectral ranges was used in accordance with [10, 11]. When analyzing the state of salt lakes and estuaries, watered soils (silt – mud) in the drained area are displayed in pink, which allows them to be clearly separated from the water surface of the waterbody, which is displayed in shades of blue [10]. Additionally, for greater accuracy of interpretation, UAV surveys made by the specialists of the Sevastopol Branch of State Oceanographic Institute, and photographic documentation of the state of the surface of lakes during regular expeditions were used where possible.

Water balance studies included the determination of the formula for the water balance of Koyashskoye Lake and estimates of the main balance components. Calculations were made concerning the amount of atmospheric precipitation falling on the lake surface, for which the specified morphometric data (see Table 1) and the results of measurements of atmospheric precipitation at the nearest marine hydrometeorological station (MS) Feodosiya were used.

Most of the empirical formulas proposed for calculating evaporation from a water surface are based on Dalton's law, i.e., the intensity of evaporation is proportional to the difference in the partial pressure of water vapour over this surface and the wind speed function:

$$E = C(e_0 - e_2)f(V_2),$$

where E – layer of evaporated water (mm); $f(V_2)$ – some function of the wind speed at a height of 2 m above the waterbody surface; C – empirical coefficient; e_0 – saturation air water vapour pressure above the surface of a waterbody

at water temperature (hPa); e_2 – actual air water vapour pressure at a height of 2 m above the waterbody surface (hPa).

The formulas of this type are widely represented by the empirical formulas of V.S. Samoilenko⁴⁾, Braslavsky – Vikulina [12], State Hydrographical Institute⁵⁾, Braslavsky – Nurgaliev, and Shulyakovskiy⁶⁾. According to work⁵⁾, control calculations of evaporation performed with the help of the formulas proposed by various authors for 35 evaporation basins showed that the Braslavsky–Vikulina formula had the smallest standard error (12.5 %), that is why it was recommended as a calculated one in work⁵⁾:

$$E = 0.14n (e_0 - e_2) (1 + 0.72V_2), \quad (1)$$

where n – number of days in a month.

In 2020–2022, in the warm period (April – November), we conducted an experiment to calculate the evaporation of water from hypersaline lakes and bays of Crimea (Koyashskoye Lake, Yuzhny Sivash Bay). The actual intensity of evaporation of brines was determined using a ground evaporator GGI-3000; simultaneously with a 15 min discreteness, hydrometeorological parameters were recorded using an automatic weather station and a high-precision electronic thermometer LTA (the water temperature in the surface layer of the evaporator was measured). The performed full-scale experiment made it possible to obtain the relationship equation between the measured and calculated evaporation values. Preliminarily, the best agreement between the calculated and experimental data was obtained by applying formula (1), while the saturation pressure of air water vapour above the water surface in the evaporator was calculated taking into account Raoult's law for dissolved substances, as according to work²⁾, the volume of evaporation from the surface of the brine of a hypersaline lake is 30–40 % less than from the surface of a fresh waterbody. Formula (1) was used to estimate the monthly volumes of evaporation of the brine from Koyashskoye Lake in 2006–2022, taking into account changes in the surface water area of the lake in different months.

Hydrochemical studies of hypersaline Koyashskoye Lake included analysis of samples of brine and bottom sediments. Samples were studied according to the appropriate analysis methods. Immediately after sampling, the temperature, density, and pH of the water were determined, as well as the fixation of dissolved oxygen, the titrimetric analysis of which was performed in a mobile laboratory. Samples for petroleum were preserved with carbon tetrachloride, samples for anionactive surfactants were preserved with chloroform. Samples for biogenic elements were frozen without preservation, and samples for heavy metals were preserved with nitric acid. Bottom sediments were cooled to 5–6 °C and delivered

⁴⁾ Samoilenko, V.S., 1952. [Modern Theory of Oceanic Evaporation and its Practical Application]. *Trudy GOIN*, 21, pp. 3–31 (in Russian).

⁵⁾ Kuznetsov V.I., Golubev V.S. and Fedorova T.G., 1969. [*Guidelines for Calculation of Evaporation from Water Body Surface*]. Leningrad: Gidrometeoizdat, 84 p. (in Russian).

⁶⁾ Vinnikov, S.D. and Proskuryakov, B.V., 1988. [*Hydrophysics (Physics of Land Waters)*]. Leningrad: Gidrometeoizdat, 248 p. (in Russian).

to the laboratory of the State Autonomous Institution of the Republic of Crimea “Center for Laboratory Analysis and Technical Measurements” within a day to determine their contamination with petroleum and heavy metals (chromium, zinc, cadmium, copper, nickel, lead, cobalt, mercury, arsenic, strontium, and iron). Further, the following indicators were determined in the certified Laboratory of Marine Chemistry of the Sevastopol Branch of State Oceanographic Institute:

- water salinity (mineralization) and chlorine content by various methods;
- total alkalinity;
- content of biogenic elements: nitrates, nitrites, phosphates, silicates, total nitrogen, and total phosphorus;
- content of pollutants: anionactive surfactants, petroleum, heavy metals.

In the study of salinity (mineralization) of lake waters, various physical and chemical methods of determination were used, such as densitometry (measurement of water density), refractometry, argentometric titration, gravimetry and electrical conductivity. The last two methods were used in the work at the final stage of studies in 2019–2022. Different methods of salinity measurements were compared, error estimates were obtained, and the most accurate method for determining salinity of hypersaline Koyashskoye Lake was determined.

Results and discussion

Water balance. Fig. 4 shows the results of calculations of the surface water area of Koyashskoye Lake. It can be seen that the lake surface area water is characterized by significant interannual and seasonal variations – from maximum values in February–April to minimum values in August–October.

The equation of Koyashskoye Lake water balance can be written as follows:

$$\Delta B = V_f + V_u + V_{prec} + V_{sr} - V_{evap},$$

where ΔB – changes in the water level (brine) in the lake; V_f – Black Sea water entering the waterbody by filtration through the bay-bar; V_u – discharge of underground sources; V_{prec} – precipitation; V_{sr} – drainage basin slope runoff; V_{evap} – evaporation.

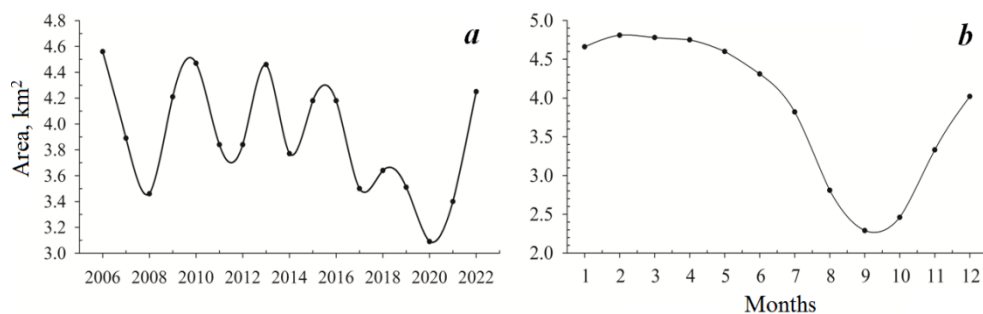


Fig. 4. Interannual (a) and seasonal (b) variations of the surface water area of Koyashskoye Lake

The climate aridity in the area of Koyashskoye Lake determines the poverty of the territory in fresh surface and groundwater [13]. Groundwater outlets into the hypersaline lakes of the Kerch group are rare and small in debit [5], so they can be neglected²⁾.

Most likely, slope runoff in Koyashskoye Lake is also insignificant. The main watercourse runs along an unnamed gully ~2 km long, which flows into Koyashskoye Lake to the north-west of Mount Ostraya. For the entire cycle of our studies, the flow into the lake along this gully was absent or insignificant. On the mountain range, there is one permanent spring, which collects water from the epicarstic horizon in an artificial gallery, and about twenty dry wells. All of them drain into a 50-meter stratum of Meotic limestone with high reservoir properties [13]. Condensation water can act as an additional source of nourishment. According to calculations [14], condensation on the Opuk mountain range can reach 23 % of the annual precipitation norm with a condensation runoff module of $2.38 \text{ L}\cdot\text{s}^{-1}\cdot\text{km}^2$ per year.

The main inflow of fresh water into Koyashskoye Lake is carried out due to atmospheric precipitation. In the long-term variations of the amount of atmospheric precipitation in the area of the Kerch Peninsula, with their significant inter-annual variability, it is possible to single out periods of increased moisture at the end of the 20th century and a decrease in precipitation in the 1950–1980s, as well as in recent years (2006–2020). Over the entire period of measurements at meteorological station Feodosiya, a significant trend towards an increase in annual and seasonal (except summer) precipitation was revealed, but for the WMO last climatic period (1991–2020) and after the regime shift of 1976–1977 (1978–2020) significantly less precipitation fell (Tables 3, 4), especially in spring and autumn seasons, for which significant trends in the decrease in precipitation were revealed in Feodosiya: minus 19.7 mm/10 years and minus 24.0 mm/10 years, respectively.

Climate aridization of the Kerch Peninsula is stipulated by the regional features of global climate change in the Northern Hemisphere. From the 1990s to the present, in the area of Koyashskoye Lake, there have been significant trends in the increase in average annual and average monthly air temperatures. In general, over the long-term period, the average annual values of air temperatures at MS Feodosiya (the station with the longest series of observations in the lake area) have a significant warming trend with a linear trend slope of $1.1 \text{ }^\circ\text{C}/100 \text{ years}$.

The seasonal distribution of precipitation in the coastal zone of the Kerch Peninsula is typical for territories with a transitional type of climate (from marine to continental) in the temperate zone with a maximum of precipitation in summer and winter and a minimum in spring and autumn. In 2006–2022, the winter maximum amount of precipitation falling on the surface of the lake was 528 thousand m^3 , or 33 % of the total precipitation per annum (1623 thousand m^3). It is stipulated by the highest frequency of precipitation and is associated with the fact that during this season the Kerch Peninsula is influenced by an area of high pressure in the northeast of the mainland and cyclonic intrusions from the west and southwest leading to an increase in cloudiness and precipitation. The summer,

Table 3. Long-term annual average amount of atmosphere precipitations (AP) and linear trend characteristics (mm/10 years) of annual average precipitation amounts at meteorological station Feodosiya

Period	AP, mm	Trend, mm/10 years	R^2	$ t $	P_0	D_0
<i>Long-term observational series</i>						
1870–2020	415	<u>12.0</u>	0.421	5.190	< 0.001	1.68
<i>Period after the last regime shift in 1976–1977</i>						
1978–2020	473	–8.1	0.096	1.722	0.100	1.56
<i>Last WMO period</i>						
1991–2020	476	–40.6	0.096	1.722	0.100	1.56

Note: The numbers in bold are trend slope coefficients significant at no less than 95 level; the underlined numbers are trends significant at 99 level; D_0 – Durbin–Watson test.

Table 4. Linear trend slope coefficient (mm/10 years) for seasonal amounts of atmosphere precipitations according to the meteorological station Feodosiya's data

Seasons	Long-term observational series (1870–2020)	Period after the last regime shift in 1976–1977	Last WMO period (1991–2020)
Winter	<u>2.1</u>	–2.5	–0.1
Spring	2.5	–6.4	–19.7
Summer	2.2	1.0	–7.0
Autumn	2.6	–2.0	–24.0

Note: The numbers in bold are trend slope coefficients significant at no less than 95 level; the underlined numbers are trends significant at 99 level.

secondary, maximum of precipitation of 439 thousand m^3 (27 % of the total precipitation per annum) is usually associated with the development of convective activity. In the summer months, the air masses coming from the sea area are most saturated with water vapour, and this period of the year is marked by the maximum partial pressure. In spring and autumn, when pressure gradients weaken, local circulation develops. The breezes observed during this period, bring no precipitation. In these seasons, the minimum values of precipitation volumes entering Koyashskoye Lake are noted – 239 thousand m^3 (15 %) in autumn and 417 thousand m^3 (25 %) in the spring season. Fig. 5 shows long-term seasonal variations of the amount of precipitation (thousand m^3 /month), according to observations at meteorological station Feodosiya in 2006–2022.

Evaporation from the lake surface is the main output of its water balance. The long-term average evaporation for the period under study is 3152 thousand m^3 , i. e., almost twice the amount of precipitation. The largest amount of water evaporates in the warm season (May–September) – 2466 thousand m^3 (78.2 %) (Fig. 5).

Despite the increase in air temperature in recent decades and the precipitation reduction, studies carried out by the Sevastopol Branch of State Oceanographic Institute, showed that Koyashskoye Lake was one of the few hypersaline lakes of the Kerch Peninsula, which had hardly ever dried up completely. Thus, in the summer seasons of 2017 and 2020, almost all the salt lakes of the Kerch Peninsula dried up, with the exception of Koyashskoye and Aktashskoye Lakes.

In addition to atmospheric precipitation, the lake is fed due to the filtration of the Black Sea waters (as a result, far less salty water is brought by streams through the bay-bar into the lake). Moreover, the employees of the Sevastopol Branch of State Oceanographic Institute discovered for the first time that in cases of intense filtration (on 03.09.2017), the salinity in the areas of the lake close to the bay-bar can decrease to 19.7–20.9‰, i.e., it becomes close to the Black Sea water salinity. It should be noted that the ratio of the length of the bay-bar

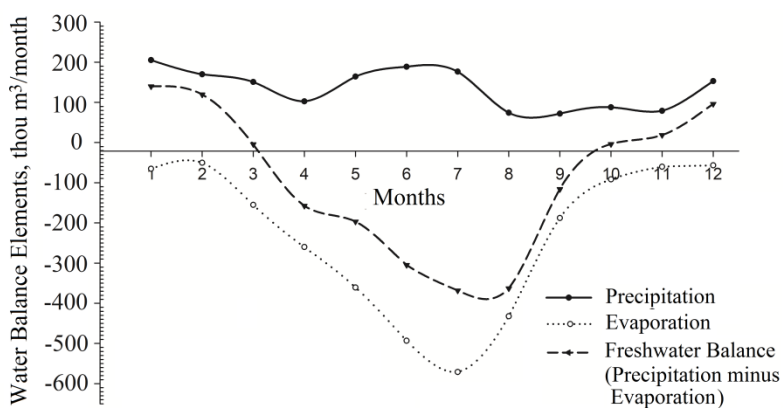


Fig. 5. Seasonal variations of water balance elements of Koyashskoye Lake

to the total length of the coastline of Koyashskoye Lake is the maximum one (0.39) compared with the similar indicator for other large estuary lakes of the Kerch Peninsula – Uzunlarskoye (0.06), Tobechnikskoye (0.09), and Chokrakskoye (0.11). In previous studies, it was indicated that in some years (2000, 2001, 2007) salt precipitation occurred over a significant area [10]. At the same time, stripes and spots coloured from pink to reddish-brown often occupied a significant area of the precipitated salt. For the period of work in 2015–2022, the area of salt precipitation (saline land) was 2.8–3.8 km², and that of dried silts (extinct areas) was 0.2–0.5 km². The minimum surface water areas of Koyashskoye Lake, 0.70–0.81 km², were recorded in September 2019 and October 2014; the maximum filling of the lake with water (with the surface water area of 5.0 km²) was recorded in January 2017.

In general, the smallest surface water area was observed in late summer and early autumn, which was stipulated by intense evaporation, a decrease in precipitation, and filtration through the bay-bar due to a decrease in wave activity at this time of the year. The measurements performed by us in summertime, showed that the depth of the lake in summer did not exceed 0.1–0.4 m.

Hydrochemical regime. Currently, the hydrochemical regime indicators of Koyashskoye Lake are studied insufficiently. The most complete study of the macrocomponent composition of Koyashskoye Lake was carried out in the 1960s⁷⁾. According to data of work⁷⁾, when brine density was 1.224 g/cm³ and total salt content was 26.54 wt. %, the main components were NaCl, MgSO₄, and MgCl₂ – 20.06, 2.44, and 3.86 wt. %, respectively. The content of other salts was significantly below 0.1 wt. %.

The main feature of the lake is the high value of the metamorphosis coefficient (MC), the value of the ratio of the magnesium sulfate and magnesium chloride concentration, proposed by N.S. Kurnakov⁷⁾ to assess the degree of transformation of the waters of estuary lakes. As a comparison, the MC value of the Black Sea waters is 0.67. Close MC values are observed in the waters of Sivash Bay, as well as in the lakes that have retained a genetic connection with the sea (Chokrakskoye and Tobechnikskoye) or are used to evaporate sea water during salt mining (Saks-koye). In other hypersaline lakes of Crimea, which have partially or completely lost their connection with the parent basin, the MC values are much lower. For example, the MC value is 0.25 for the nearby Uzunlarskoye Lake. The high MC value, which is close to that in the sea water, indirectly confirms the significant filtration of the Black Sea waters through the bay-bar and the absence of significant freshwater runoff, which enriches the waterbody with magnesium sulfate.

Salinity, mineralization. The conducted studies show that the salinity of waters and their mineralization little depend on the measurement method used in almost the entire range of values. Only when the values of the indicator are close to salt load, there is a decrease in salinity in relation to the value measured by the gravimetric method (dry residue). The results closest to the true value of salinity and

⁷⁾ Ponizovskii, A.M., 1965. [*Salt Resources of the Crimea*]. Simferopol: Izd-vo “Krym”, 162 p. (in Russian).

mineralization are obtained by the argentometric titration method, which is quite understandable given the proximity of the MC to the values of the Black Sea water.

In a number of samples, we recorded cases of a decrease in salinity to the sea water values or close to them. At the same time, the mineralization value of the lake waters, as a rule, did not depend on the method of determination used within the error of the densitometric determination of density in highly diluted solutions (Table 5).

In general, the concentration of salts in the waters of Koyashskoye Lake can vary over a very wide range, from 19.7 to 238.0 g/dm³. As mentioned above, the cases of detection of extremely low salinity values are associated with the filtration of sea waters. At the same time, diluting waters do not mix immediately due to the high density, but form quasi-stable flows, which, in the absence of wind mixing, can exist for quite a long time. As a rule, abnormally low water salinity was observed in the spring or autumn seasons, when the lake basin was almost completely filled with water, and the freshened areas were invisible during visual inspection. With strong brine evaporation before the salt is loaded, some part of it precipitates, which leads to an apparent conclusion about the MC change. When the water cools and sea water flows in, the salt ratio regains its original value.

Comparison of the results of mineralization measurements performed by various methods with the results obtained by the densitometric method is shown in Fig. 6. It can be seen that the densitometric method gives results comparable with the argentometric method in almost the entire range of measured values. Small deviations are observed only in high salinity values. A similar conclusion can be made with regard to other methods used to measure the indicator, which confirms the above assumption about the genetic proximity of the waters of Koyashskoye Lake and the Black Sea.

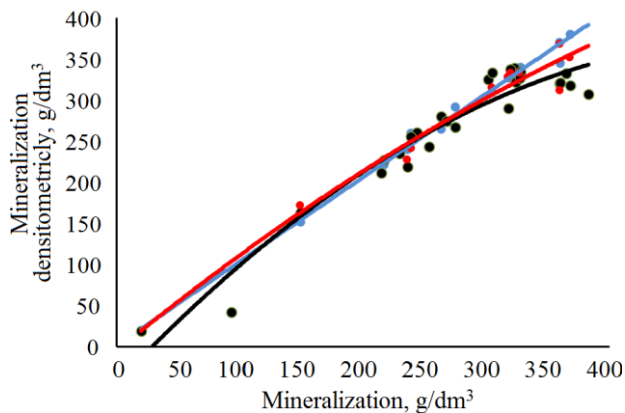


Fig. 6. Comparison of mineralization values obtained by the densitometric method with those obtained by other detection methods: gravimetric method M(Gr) (black line); argentometric method M(Ag) (blue line); electrical conductivity method M(C) (red line) in samples taken by SB SOI for 2015–2022

Table 5. Physical and chemical indicators of Koyashskoye Lake waters according to the data from SB SOI surveys for 2015–2022

Sample number	Date	<i>T</i>	Indicators of brine salt composition							
			ρ	M(Ds)	n^{20}	M(Rf)	Cl	<i>S</i>	M(Ag)	M(Gr)
1	09.10.2015	13.0	1.150	215	N/D	N/D	118	184	212	N/D
2	13.04.2016	15.2	1.167	244	N/D	N/D	145	221	261	N/D
3	23.06.2016	37.2	1.209	323	N/D	N/D	189	278	339	N/D
4	14.08.2016	36.0	N/D	N/D	N/D	N/D	12	21	21	N/D
5	09.03.2017	14.8	1.175	254	N/D	N/D	136	208	244	N/D
6	26.04.2017	18.0	1.067	93	N/D	N/D	24	41	43	N/D
7	01.06.2017	26.1	1.201	302	N/D	N/D	181	268	326	N/D
8	17.07.2017	35.4	1.236	365	N/D	N/D	185	273	332	N/D
9	03.09.2017	31.0	1.010	20	N/D	N/D	11	20	20	N/D
10	13.10.2017	22.5	1.188	275	1.378	292	149	226	267	N/D
11	18.04.2018	23.0	1.178	263	1.374	265	156	236	280	N/D
12	01.06.2018	25.6	1.217	328	1.384	340	186	274	335	N/D
13	21.08.2018	25.5	1.252	383	1.392	406	171	255	307	N/D
14	06.02.2019	8.8	1.154	217	1.368	222	126	196	227	N/D
15	23.04.2019	19.0	1.158	230	1.370	235	131	203	236	N/D
16	31.05.2019	29.5	1.178	268	1.376	275	153	233	275	N/D
17	20.06.2019	37.0	1.216	324	1.383	332	179	266	322	N/D
18	17.09.2019	26.8	1.103	149	1.358	152	91	147	163	172
19	17.10.2019	15.0	1.245	368	1.389	380	177	261	318	352
20	15.01.2020	10.2	1.210	305	1.380	310	186	272	334	315
21	09.04.2020	18.5	1.216	320	1.383	330	188	275	338	333

Sample number	Date	T	Indicators of brine salt composition							
			ρ	M(Ds)	n^{20}	M(Rf)	Cl	S	M(Ag)	M(Gr)
22	22.04.2020	17.6	1.215	318	1.382	327	162	242	290	328
23	29.05.2020	17.8	1.221	327	1.383	327	182	268	327	333
24	18.07.2020	36.0	1.235	360	1.388	371	178	265	321	368
25	28.10.2020	16.0	1.241	360	1.384	345	179	264	321	312
26	21.06.2021	31.5	1.160	239	1.374	260	142	219	255	241
27	06.08.2021	32.0	1.158	236	1.371	240	122	189	219	228
28	14.11.2021	13.0	1.222	330	1.382	327	188	275	338	355
29	16.02.2022	12.0	1.142	205	1.366	206	119	186	214	214
30	03.09.2022	27.0	1.169	252	N/D	N/D	179	265	321	341

Note: T – water temperature ($^{\circ}\text{C}$); ρ – brine density (g/cm^3); M(Ds) – mineralization (g/cm^3) by density; M(Rf) – mineralization (g/cm^3) by refraction; Cl – chlorid ion concentration (g/dm^3) by argentometry; S – salinity ($\%$) by argentometry; M(Ag) – mineralization (g/cm^3) by argentometry; M(Gr) – mineralization (g/cm^3) by gravimetry; N/D – determination was not performed.

The results of studies of the hydrochemical regime indicators of the Koyashskoye Lake waters (brine) are presented in Table 6.

Dissolved oxygen. The concentration of dissolved oxygen in the lake waters varies from hypoxic values ($1.1 \text{ mg}/\text{dm}^3$, 15 % of sat.) to $8.9 \text{ mg}/\text{dm}^3$ (379 % of sat.), but in general, the concentration of dissolved oxygen was close to saturation at a given temperature and salinity throughout the year.

Normal aeration is maintained due to the absorption of atmospheric oxygen and photosynthesis occurring in the surface layers in colonies of protozoan algae (*Dunaliella*, etc.). Considering that most of the year the surface of the lake is covered with a salt crust, it should be assumed that the penetration of oxygen into the deeper water layers is carried out exclusively due to diffusion, which cannot be recognized as an effective mechanism under conditions of concentrated high-density brines. In the bottom area, the formation of hypoxic zones is possible, in which putrefactive decomposition of dead biomass occurs. As a result, hydrogen sulfide and sulfides can accumulate in the water column.

The periodic development of hypoxia in the lake water column also determines the large range of fluctuations in *pH values*, which is 1.92 pH units (6.92–8.84 pH units). Low pH values correspond to high values of total alkalinity, which in this type

Table 6. Hydrochemical indicators of quality of Koyashskoye Lake waters according to the data of SB SOI in 2015–2022

Sample number	pH	Alk, mmol/dm ³	BOD ₅ , mgO ₂ /dm ³	Content										
				of dissolved oxygen		of nutrients*, µg/dm ³								
				mg/dm ³	% sat.	PO ₄	P _{tot}	SiO ₃ ²⁻	NO ₂	NO ₃	NH ₄	N _{tot}		
1	7.95	5.517	N/D	N/D	N/D	698	N/D	N/D	N/D	N/D	N/D	N/D	N/D	N/D
2	8.25	3.556	N/D	N/D	N/D	60	302	N/D	N/D	N/D	N/D	N/D	N/D	N/D
3	7.80	3.960	N/D	N/D	N/D	82	428	N/D	N/D	N/D	N/D	N/D	N/D	N/D
4	8.60	2.629	N/D	N/D	N/D	64	82	N/D	N/D	N/D	N/D	N/D	N/D	N/D
5	7.75	4.016	N/D	N/D	N/D	53	716	N/D	N/D	N/D	N/D	N/D	N/D	N/D
6	8.84	6.014	7.3	2.00	27	312	464	N/D	N/D	N/D	N/D	N/D	N/D	N/D
7	8.07	2.695	14.4	1.68	90	244	320	N/D	N/D	N/D	N/D	N/D	N/D	N/D
8	7.19	3.038	92.6	0.74	46	138	626	N/D	N/D	N/D	N/D	N/D	N/D	N/D

Continued

Sample number	pH	Alk, mmol/dm ³	BOD ₅ , mgO ₂ /dm ³	Content										
				of dissolved oxygen		of nutrients*, µg/dm ³								
				mg/dm ³	% sat.	PO ₄	P _{tot}	SiO ₃ ²⁻	NO ₂	NO ₃	NH ₄	N _{tot}		
9	8.65	1.693	5.9	7.55	113	29	572	N/D	N/D	N/D	N/D	N/D	N/D	N/D
10	7.66	8.657	9.9	0.95	41	533	1181	N/D	N/D	N/D	N/D	N/D	N/D	N/D
11	8.11	6.065	26.9	8.91	379	147	423	N/D	N/D	N/D	N/D	N/D	N/D	N/D
12	8.33	8.715	95.4	1.12	15	202	712	N/D	N/D	N/D	N/D	N/D	N/D	N/D
13	6.92	22.35	97.6	N/D	N/D	1656	2779	N/D	N/D	N/D	N/D	N/D	N/D	N/D
14	8.04	9.522	15.1	2.77	83	44	182	N/D	N/D	N/D	N/D	N/D	N/D	N/D
15	8.09	1.462	8.3	2.68	97	65	232	1823	46	92	890	10450		
16	8.08	4.308	34.6	6.38	93	196	386	709	70	87	1577	4951		
17	7.80	4.768	53.9	N/D	N/D	55	588	1271	9	57	1333	19282		
18	8.01	25.200	13.5	2.85	80	619	828	1914	21	11	1826	10769		
19	7.56	29.500	13.9	1.85	91	46	6771	448	53	128	14	565		

Sample number	pH	Alk, mmol/dm ³	BOD ₅ , mgO ₂ /dm ³	Content									
				of dissolved oxygen		of nutrients*, µg/dm ³							
				mg/dm ³	% sat.	PO ₄	P _{tot}	SiO ₃ ²⁻	NO ₂	NO ₃	NH ₄	N _{tot}	
20	7.93	7.117	62.9	0.42	19	448	965	1058	73	139	1631	3374	
21	7.64	7.407	18.4	1.62	89	215	691	2371	58	66	1681	6981	
22	7.67	7.198	20.6	2.20	111	211	634	654	55	202	1418	8097	
23	7.76	10.747	19.7	6.01	302	109	324	554	80	29	1904	11784	
24	7.07	25.734	21.5	2.58	175	765	2189	1247	107	447	3277	6681	
25	7.48	30.539	23.3	0.26	13	292	865	834	53	201	1657	14610	
26	8.25	2.005	34.5	4.93	226	233	288	662	44	43	883	7320	
27	7.11	5.787	110.3	N/D	N/D	582	356	765	163	18	478	4394	
28	7.73	5.001	119.6	2.46	86	292	869	679	104	7	121	9500	
29	7.80	5.147	2.4	2.38	68	243	475	1511	96	9	498	5598	
30	7.32	8.968	63.9	1.92	107	476	901	972	90	6	275	11700	

* The concentration is given on element basis.

Note: Alk – alkalinity; N/D – determination was not performed.

of samples is determined not only by bicarbonate alkalinity, but also by hydrosulfide alkalinity. When considering these mechanisms, it is necessary to take into account the fact that, despite the high saturation of water with oxygen, its concentration remains low, which creates favourable conditions for the occurrence of anaerobic processes and the production of hydrogen sulfide, which determines the production of low pH and high total alkalinity values.

The decrease in the concentration of dissolved oxygen is largely determined by the increase in its consumption. In all analyzed samples, an increased value of BOD₅ was observed, which many times exceeded the MPC of natural waters (2.1 mgO₂/dm³). The highest BOD₅ values are observed in summertime and are determined by the excess production of salt-tolerant algae and bacteria. During this period, the lake becomes a eutrophic waterbody, and large reserves of biogenic elements remain in its waters.

The concentration of *biogenic elements* in the waters of Koyashskoye Lake is mainly related to its water content. As can be seen from the data in Table 6, the highest total phosphorus concentrations were observed from July to October. At the same time, the concentrations of mineral forms of phosphorus were minimal. In the rest of the year, the concentrations of total and mineral phosphorus had similar values. This nature of the seasonal distribution of phosphorus forms indicates the activation of the processes of assimilation of phosphorus phosphate in the hot season. Most of it passes into the composition of living matter in the form of organophosphorus compounds and is in suspension. Further, organic forms from dead forms of plankton and their metabolic products are partially removed to bottom sediments and partially mineralized, thus replenishing the loss of the element. The analysis of the obtained data shows that, unlike sea and fresh surface waters, the maximum productivity of which occurs in spring and early summer, the microflora of hypersaline lakes, in particular Koyashskoye Lake, has a maximum level of production in the hottest season.

A similar conclusion can be made concerning other biogenic elements. Thus, a decrease in the concentration of dissolved forms of *silicates* as a rule, was observed in summer, when the consumption of the element necessary for building the protective cover of some organisms and cell membranes reached its maximum.

The concentration of *nitrite nitrogen* in almost all analyzed samples exceeded the MPC and varied within 7–447 µg/dm³. Significantly higher concentrations were also observed for *ammonium nitrogen*, but no excess of the MPC (2,900 µg/dm³) was recorded in most of the analyzed samples. The one and only sample taken on 18.07.2020, showed that the concentration of ammonium nitrogen was 1.1 of the MPC. High concentrations (565–19,282 µg/dm³) in Koyashskoye Lake are also characteristic of *total nitrogen*.

The totality of the listed features of the dynamics of various forms of nitrogen indicates the difference in the mechanisms of nitrogen assimilation and transformation in hypersaline lakes. In slightly saline and fresh waters, part of the nitrogen that enters with surface and underground runoff in the form of nitrates, is released

into the atmosphere in the form of gaseous products during microbiological denitrification. In hypersaline lakes, this mechanism is difficult due to the lack of specific microflora, which creates favorable conditions for the accumulation of nitrites and the production of ammonium salts and amines, which partially pass into bottom sediments, which are a source of secondary pollution. At the same time, depending on the degree of filling of the lake basin, the concentration of nitrogen compounds in the lowest oxidation state can vary by two or more orders of magnitude.

The state of contamination of the waters of Koyashskoye and other lakes with organic xenobiotics was studied in separate samples. The work was not systematic due to methodological difficulties in the analysis of samples with high salinity. Anionactive surfactants and petroleum were determined in the samples. Despite the dilution of the samples, most of them formed a stable emulsion, which did not make it possible to detect organic pollutants. Three determinations of anionactive surfactants were performed, the results of which showed that their concentration varied within 77–1200 $\mu\text{g}/\text{dm}^3$ at MPC = 100 $\mu\text{g}/\text{dm}^3$ for fishery waters. The petroleum concentration in a single sample taken on June 1, 2018, was 0.06 mg/dm^3 (1.2 of the MPC). Given the low man-caused load on the lake located within the specially protected natural area, it can be stated that its waters are slightly polluted. Elevated concentrations of anionactive surfactants can be stipulated by natural surfactants formed as a result of saponification of fatty acids.

Currently, the trace element composition of the Koyashskoye Lake waters and the pollution of its waters with salts of heavy metals are studied insufficiently. In [1], they refer to a survey conducted in the 1970s in order to identify reserves of therapeutic muds²⁾. There was no possibility to find more recent data, so in the future we will rely on the available data. The study mentioned above was carried out on a network of four stations on a section along the axis of the lake (see Fig. 1). Comparative results of this study and our data are presented in Table 7.

The comparison of two series of determination performed in work [1] and those performed by the Sevastopol Branch of State Oceanographic Institute shows that at present, the concentrations of all elements can be higher than the MPC. Particularly high excess of the standard is observed for copper and lead. At the same time, the concentrations of all elements are highly dynamic, and their value often changes by an order of magnitude.

Pollution of bottom sediments. On December 11, 2020, we carried out the study of pollution of bottom sediments, which can potentially be used as therapeutic muds. Samples were taken at a point of constant monitoring, analysis was carried out in an accredited laboratory of the State Autonomous Institution of the Republic of Crimea “Center for Laboratory Analysis and Technical Measurements”. In the Russian Federation, MPC values for pollutants in bottom sediments have not officially been established, therefore, the *Neue Niederlandische Liste* was used concerning indicative values for rationing the quality of bottom sediment⁸⁾.

⁸⁾ Warmer, H. and van Dokkum, R., 2002. *Water Pollution Control in the Netherlands. Policy and Practice 2001*. Lelystad: RIZA, 77 p.

Table 7. Microelement content ($\mu\text{g}/\text{dm}^3$) of Koyashskoye Lake waters according to the data from work [1] and from monitoring by SB SOI, Clarke values of elements in the ocean [15, 16] and maximum permissible concentration (MPC) ⁹⁾

Parameter	Microelement								
	Zn	Cu	Ni	Pb	Sr	Cr	Co	Fe	Mn
<i>C</i> at point:									
K-1	< 0.05	3.07	< 0.1	< 0.02	< 0.50	< 0.02	< 0.02	N/D	N/D
K-3	< 0.05	2.45	< 0.1	< 0.02	24.17	< 0.02	0.53	N/D	N/D
K-4	55.80	1.17	< 0.1	< 0.02	27.57	< 0.02	0.27	N/D	N/D
K-5	2.50	0.76	< 0.1	< 0.02	25.83	< 0.02	< 0.02	N/D	N/D
14	N/D	20.30	N/D	6.00	N/D	0.60	N/D	N/D	1.5
15	N/D	154.80	N/D	212.60	N/D	17.30	N/D	N/D	280.0
17	N/D	96.10	N/D	335.10	N/D	17.00	N/D	N/D	480.9
20	N/D	83.00	N/D	34.00	N/D	5.20	N/D	305.50	277.0
21	N/D	6.00	N/D	22.00	N/D	32.80	N/D	91.30	115.3
22	N/D	32.00	N/D	37.00	N/D	13.50	N/D	47.38	137.0
25	N/D	46.40	N/D	217.00	N/D	6.60	N/D	150.80	200.4
26	N/D	10.50	N/D	131.30	N/D	112.20	N/D	2567.90	129.6
27	N/D	64.60	N/D	49.30	N/D	313.30	N/D	997.10	391.5
28	N/D	53.10	N/D	38.10	N/D	238.30	N/D	1379.20	196.0
29	N/D	49.90	N/D	135.10	N/D	11.90	N/D	57.20	5.9

⁹⁾ Ministry of Agriculture of the Russian Federation, 2016. *On the Approval of Water Quality Standards for Water Bodies of Fishing Importance, Including Standards for the Maximum Permissible Concentrations of Harmful Substances in the Waters of Water-Based Fishing Objects.* Order No. 552 of the Ministry of Agriculture of the Russian Federation of 13.12.2016 (in Russian).

Parameter	Microelement								
	Zn	Cu	Ni	Pb	Sr	Cr	Co	Fe	Mn
Clarke*	4.90	0.50	1.7	0.03	200.00	0.20	0.05	20.00	0.2
MPC*	50.00	5.00	10.0	10.00	4140.0	20.00	5.00	50.00	50.0

* Values of MPC of elements and of their Clarkes in the Earth's crust.

Note: N/D – determination was not performed; values exceeding MPC are given in bold.

Indicators of pollution of bottom sediments are presented in Table 8. High level of pollution of bottom sediments with the elements, for which the MPC standard is established according to document ⁸⁾, was observed for zinc only. For other elements, the concentration did not exceed the rated value. The same can be said about petroleum, the concentration of which was below the accepted MPC value. Attention is also drawn to the ratio of the obtained values of the concentration of elements to the accepted values of their Clarkes. Thus, the concentration of zinc and strontium exceeded the accepted Clarke value by two and three times, respectively. On the other hand, for iron, the technophilicity of which is characterized by rather high values, the ratio to Clarke was less than 0.5. Such a low concentration of iron is probably due to specific features of the surrounding landscape, since almost the entire territory of the peninsula is included in the so-called Kerch iron-ore basin. In particular, the Kyz-Aulskoye and Novoselovskoye deposits are known in this area. The depth of formation of ores is 25–100 m,

Table 8. Pollutant concentration (mg/kg) in the surface layer of bottom sediments of Koyashskoye Lake (at K-1 point)

Parameter	OP	Cr	Zn	Cd	Cu	Ni	Pb	Co	Hg	As	Sr	Fe
Concentration	< 50	< 5	174	< 1	< 20	< 50	< 10	< 5	0.005	< 1	1114	19480
MPC	50	–	140	0.80	35	35	85	N/D	0.300	29	N/D	N/D
Clarke	–	83	83	0.13	47	58	16	18	0.08	1.7	340	46500

Note: N/D – determination was not performed; values exceeding MPC are given in bold.

and water process of these areas, which are a part of the drainage basin of lakes, leads to an increase in the iron content in bottom sediments. In particular, the iron content in bottom sediments of the Uzunlarskoye Lake exceeded 50,000 mg/kg during the expeditions of the Sevastopol Branch of State Oceanographic Institute. Such a significant difference in the composition of bottom sediments of closely located lakes can be explained by the small amount of surface slope runoff into Koyashskoye Lake.

Conclusion

Based on the above, the following conclusions can be made:

1. The surface water area of Koyashskoye Lake is characterized by significant interannual and seasonal variations – from maximum values in February–April to minimum values in August–October. The aridity of the climate in the Koyashskoye Lake area determines the poorness of the territory in fresh surface and underground waters. The slope runoff of Koyashskoye Lake is minor.

2. Atmospheric precipitation provides the main inflow of fresh water into Koyashskoye Lake. The seasonal distribution of precipitation in the coastal zone of the Kerch Peninsula is typical for territories with a transitional type of climate (from marine to continental) in the temperate zone with a maximum of precipitation in summer and winter and a minimum in spring and autumn. In 2006–2022, the winter maximum amount of precipitation falling on the surface of the lake was 528 thousand m³, or 33 % of the total precipitation per annum (1623 thousand m³). The summer, secondary, maximum of precipitation of 439 thousand m³ (27 % of the total precipitation per annum) is usually associated with the development of convective activity.

3. In addition to atmospheric precipitation, of all other input components, the lake is fed to a greater extent due to the filtration of the Black Sea waters (as a result, far less salty water enters Koyashskoye Lake through the bay-bar separating the lake from the sea). In cases of intense filtration (on September 3, 2017), the salinity in the areas of the lake close to the bay-bar can decrease to 19.7–20.9 ‰, i. e., it becomes close to the Black Sea water salinity.

4. Comparison of changes in the surface water area of the lake, obtained as a result of the analysis of satellite images for 2006–2022, with the calculated main components of the Koyashskoye Lake water balance (evaporation, precipitation, freshwater balance) showed that the main contribution to the formation of the balance in the warm period of the year was made by evaporation. During the cold period of the year, the water balance of the lake is determined mainly by precipitation and filtration of the Black Sea waters through the bay-bar.

5. In most of the analyzed chemical samples, the waters of Koyashskoye Lake were characterized by good oxygen saturation. Nevertheless, in summertime, oxygen concentrations can fall to hypoxic values. The main reason here is the high value of BOD₅, which in all samples exceeded the maximum permissible concentration established for sea waters.

6. The brine of the lake is characterized by high concentrations of inorganic forms of phosphorus and nitrogen. At the same time, under conditions of hypoxia, a sufficiently large amount of reduced forms of nitrogen (nitrite and ammonium) is formed in the waters, and the concentration of nitrate nitrogen decreases.

7. The bottom sediments of Lake Koyashskoye are polluted with zinc, the concentration of which exceeded the established maximum permissible concentration and Clarke standards. At the same time, the concentration of iron, which exceeded the Clarke in Uzunlarskoye Lake, amounted to only 0.5 of the Clarke value in the waters of Koyashskoye Lake. This indicates a small amount of surface slope water runoff entering the waterbody and good filtration of the Black Sea waters through the bay-bar.

REFERENCES

1. Pasinkov, A.A., Sotskova, L.M. and Shepherd, V.I., 2014. Environmental Problems of Conservation and Sustainable Use Balneological Resources of Salt Lakes of the Crimea. *Scientific Notes of Taurida V.I.Vernadsky National University. Series: Geography*, 27(2), pp. 97–117 (in Russian).
2. Anufrieva, E., Holynska, M. and Shadrin, N., 2014. Current Invasions of Asian Cyclopoid Species (Copepoda: Cyclopidae) in Crimea, with Taxonomical and Zoogeographical Remarks on the Hypersaline and Freshwater Fauna. *Annales Zoologici*, 64(1), pp. 109–130. doi:10.3161/000345414X680636
3. Shadrin, N.V., Drobetskaya, I.V., Chubchikova, I.N. and Terentyeva, N.V., 2008. Carotenoids in Red Salt of the Hypersaline Koyashskoye Lake (Crimea Black Sea): Preliminary Communication. *Morskoy Ehkologicheskij Zhurnal = Marine Ecological Journal*, 7(4), pp. 85–87 (in Russian).
4. Golenko, V.K., 2007. [*Ancient Kimmerikon and its Surroundings*]. Simferopol: Sonat, 408 p. (in Russian).
5. Kayukova, E.P., 2016. Investigation of Hydromineral Resources of the Eastern Crimea. In: E. M. Nesterov, V. A. Snytko and S. I. Makhova, eds., 2016. [*Geology, Geoecology, Evolution Geography: Proceedings of the International Workshop*]. Saint Petersburg: Izd-vo RGPU im. A. I. Gerzena, pp. 60–64 (in Russian).
6. Kotova, I.K., Kayukova, E.P., Mordukhai-Boltovskaya, L.V., Platonova, N.V. and Kotov, S.R., 2015. Pattern of the Composition Formation of Oozy Mud from the Dead Sea and Salt Lakes of Crimea. *Vestnik of St. Petersburg State University. Series 7. Geology, Geography*, (2), pp. 85–106 (in Russian).
7. Kapralov, A.A., 2006. Variety of Vegetable Associations and their Dynamics on the Spit of Koyashskoye Lake. In: SNBG, 2006. *Collection of Works of the State Nikitsky Botanical Gardens*. Yalta: SNBG. Iss. 126, pp. 121–132 (in Russian).
8. Yastreb, V.P., 2009. Development and Modern Condition of Water Reservoirs on the Azov and Black Sea Coast in Holocene. In: MHI, 2009. *Ekologicheskaya Bezopasnost' Pribrezhnoy i Shel'fovoy Zon i Kompleksnoe Ispol'zovanie Resursov Shel'fa* [Ecological Safety of Coastal and Shelf Zones and Comprehensive Use of Shelf Resources]. Sevastopol: ECOSI-Gidrofizika. Iss. 20, pp. 145–152 (in Russian).
9. Klyukin, A.A., 2006. Nature and Variety of Factors of Environment of Territory of the Opuk Nature Reserve. In: SNBG, 2006. *Collection of Works of the State Nikitsky Botanical Gardens*. Yalta: SNBG. Iss. 126, pp. 8–22 (in Russian).
10. Kharitonova, L.V., Yastreb, V.P., Khmara, T.V. and Nikolskiy, N.V., 2012. Study of Water Regime of the Kerch Group Lakes-Lagoons Using Sattelite Data. In: O. A. Petrenko, 2012. *Current Fishery and Environmental Problems of the Azov-Black Sea Region: Materials of VII International Conference. Kerch, 20-23 June 2012*. Kerch: YugNIRO Publishers'. Vol. 1, pp. 201–206 (in Russian).

11. Borovskaya, R.V. and Smirnov, S.S., 2020. Technology of Water Surface Area Calculation Using Data Received from Artificial Satellite of Sentinel-2 Series, its Implementation for Determination of the Surface Areas of the Crimean Saline Lakes. *Monitoring Systems of Environment*, 40, pp. 36–43. doi:10.33075/2220-5861-2020-2-36-43
12. Shereshevsky, A.I. and Synytska, L.K., 2006. [Modern Assessment of Calculated Evaporation from Water Surface of Dnipro Water Reservoirs to Calculate it while Working Out Hydro Power Plant Operating Modes]. In: UHMI, 2006. *Nauchnye Trudy UkrNIGMI* [Scientific Works of UHMI]. Kiev: UHMI. Vol. 255, pp. 213–228 (in Ukrainian).
13. Klimchouk, A.B., Amelichev, G.N., Vakhrushev, B., Timokhina, E.I., Naumenko, V.G., 2014. Hypogene Karst Phenomena in the Opuk Massif in the Kerch Peninsula. *Speleology and Karstology*, (12), pp. 57–68 (in Russian).
14. Vakhrushev, B.A. and Vakhrushev, I.B., 2006. Reservation Objects of Mountain Opuk and its Territories. In: SNBG, 2006. *Collection of Works of the State Nikitsky Botanical Gardens*. Yalta: SNBG. Iss. 126, pp. 23–33 (in Russian).
15. Perelman, A.I., 1982. [*Geochemistry of Natural Waters*]. Moscow: Nauka, 154 p. (in Russian).
16. Kist, A.A., 1987. [*Phenomenology of Biogeochemistry and Bioinorganic Chemistry*]. Tashkent: Fan, 236 p. (in Russian).

Submitted 9.04.2023; accepted after review 30.04.2023;
revised 03.05.2023; published 26.06.2023

About the authors:

Nikolay N. Dyakov, Director of Sevastopol Branch of N. N. Zubov's State Oceanographic Institute (61 Sovetskaya St., Sevastopol, 299011, Russian Federation), Ph.D. (Geogr.), **ORCID ID: 0000-0003-2622-7695**, dyakoff@mail.ru

Yuri A. Malchenko, Senior Research Associate, Sevastopol Branch of N. N. Zubov's State Oceanographic Institute (61 Sovetskaya St., Sevastopol, 299011, Russian Federation), **ORCID ID: 0000-0002-7422-2824**, mvr121@yandex.ru

Alexander A. Lipchenko, Senior Research Associate, Sevastopol Branch of N. N. Zubov's State Oceanographic Institute (61 Sovetskaya St., Sevastopol, 299011, Russian Federation), **ORCID ID: 0000-0002-7840-7009**, lipch2015@yandex.ru

Contribution of the authors:

Nikolay N. Dyakov – formulation and research task statement, preparation of the article text

Yuri A. Malchenko – processing and analysis of hydrochemical data, preparation of information on the hydrochemical regime

Alexander A. Lipchenko – water balance calculations

All the authors have read and approved the final manuscript.

Study of Wastewater Distribution near the Heracleean Peninsula (Crimea) in the Upwelling Situation Based on Expedition Data and Numerical Modelling

P. D. Lomakin *, Yu. N. Ryabtsev

Marine Hydrophysical Institute of RAS, Sevastopol, Russia

** e-mail: p_lomakin@mail.ru*

Abstract

Based on the oceanographic survey data taken by Marine Hydrophysical Institute in August 2019, the paper analyzes the structural features of the fields of temperature, salinity, concentration of total suspended organic matter and coloured dissolved organic matter in the area along the southwestern coast of the Heracleean Peninsula in the situation of wind upwelling. The structure of the fields of the studied quantities shows signs of ascending circulation and pollution due to offshore wind and the presence of two wastewater sources in the studied area. The numerical experiments performed using the 3D barotropic linear Felsenbaum model confirmed the observed upwelling and showed that the rise of anthropogenic waters from sewer sources to the sea surface was due to both alongshore and offshore winds oriented normally to the coastline. They also made it possible to trace the distribution of anthropogenic suspension in the upwelling situation. It is shown that suspension from sewer sources in the upper layer of water spread to the open sea, and in the intermediate and near-bottom layers it accumulated along the coastline. With a northerly wind, the effect of suspended matter accumulation in the coastal zone is more intense.

Keywords: water structure, upwelling, pollution, numerical modelling, Heracleean Peninsula, Crimea

Acknowledgements: The work was performed under state assignment on topic no. FN NN-2021-0005 “Complex interdisciplinary research of oceanologic processes, which determine functioning and evolution of the Black and Azov Sea coastal ecosystems”.

For citation: Lomakin, P.D. and Ryabtsev, Yu.N., 2023. Study of Wastewater Distribution near the Heracleean Peninsula (Crimea) in the Upwelling Situation Based on Expedition Data and Numerical Modelling. *Ecological Safety of Coastal and Shelf Zones of Sea*, (2), pp. 49–60. doi:10.29039/2413-5577-2023-2-49-60

© Lomakin P. D., Ryabtsev Yu. N., 2023



This work is licensed under a Creative Commons Attribution-Non Commercial 4.0 International (CC BY-NC 4.0) License

Исследование распространения сточных вод у Гераклейского полуострова (Крым) в ситуации апвеллинга на основе экспедицион- ных данных и численного моделирования

П. Д. Ломакин *, Ю. Н. Рябцев

Морской гидрофизический институт РАН, Севастополь, Россия

** e-mail: p_lomakin@mail.ru*

Аннотация

На основе данных океанологической съемки, проведенной Морским гидрофизическим институтом в августе 2019 г., проанализированы особенности структуры полей температуры, солености, концентрации общего взвешенного и окрашенного растворенного органического веществ на участке вдоль юго-западного берега Гераклейского полуострова в ситуации ветрового апвеллинга. В структуре полей рассматриваемых величин выявлены признаки восходящей циркуляции и загрязнения, обусловленные стгонным ветром и наличием на рассматриваемом участке двух источников сточных вод. Численные эксперименты, выполненные с использованием трехмерной баротропной линейной модели Фельзенбаума, подтвердили наблюдавшийся апвеллинг и показали, что подъем вод антропогенного происхождения из канализационных источников к поверхности моря обусловлен как вдольбереговым, так и ориентированным по нормали к береговой линии стгонным ветром. Модельные расчеты также позволили проследить распространение антропогенной взвеси в ситуации апвеллинга. Показано, что в верхнем слое вод взвесь из канализационных источников распространялась в открытое море, а в промежуточном и придонном слоях она накапливалась вдоль береговой линии. При северном ветре эффект аккумуляции взвеси в прибрежной зоне более интенсивный.

Ключевые слова: структура вод, апвеллинг, загрязнение, численное моделирование, Гераклейский полуостров, Крым

Благодарности: работа выполнена в рамках государственного задания по теме № FNNN-2021-0005 «Комплексные междисциплинарные исследования океанологических процессов, определяющих функционирование и эволюцию экосистем прибрежных зон Черного и Азовского морей».

Для цитирования: Ломакин П. Д., Рябцев Ю. Н. Исследование распространения сточных вод у Гераклейского полуострова (Крым) в ситуации апвеллинга на основе экспедиционных данных и численного моделирования // Экологическая безопасность прибрежной и шельфовой зон моря. 2023. № 2. С. 49–60. EDN UUGLBF. doi:10.29039/2413-5577-2023-2-49-60

Introduction

Over the past decade, the water area of the Sevastopol seashore near the Heracleon Peninsula has been actively studied both on the basis of actual observations and at the theoretical level. Such interest is caused by the increasing anthropogenic pressure on the aquatic environment of this section of the coast.

To date, a rather capacious literature has been formed [1–11] devoted to the analysis of the structure and dynamics of waters based on oceanographic data, sources of pollution and hydrochemical regime of the region, modelling of local systems of currents and transport of anthropogenic suspension, as well as satellite studies of pollutant distribution.

Among the indicated publications, the articles [8, 11] devoted to the water structure of the considered water area in the wind upwelling system are of particular interest. They show that in the summer months of the year, during upwelling, the wastewater from deep horizons penetrates through the seasonal thermocline and exits to the sea surface. This phenomenon confirms the conclusions about the distribution patterns of polluted bottom waters in the situation of local wind upwelling off the coast of Crimea, presented in monographs [12, 13]. According to the opinion of the authors of the cited books, in the warm half-year period, in the usual situation of a sharply stratified environment, wastewater spreads mainly in the horizontal direction under the seasonal thermocline layer. Whereas during upwelling, which contributes to the weakening of the water column stratification, wastewater plumes can reach the sea surface.

In August 2019, the employees of Marine Hydrophysical Institute conducted an expedition in the area located along the southwestern coast of the Heracleean Peninsula. According to the results of expeditionary studies in the observed situation of wind upwelling and the presence of a developed seasonal thermocline, the signs indicating penetration of polluted bottom waters into the surface layer of the sea and their spread to the beach zone were revealed in the structure of oceanological value fields [11].

Aims of this article:

- based on the data of this expedition and numerical modelling methods, to consider the features of water circulation and the spread of anthropogenic suspension from known sources of pollution in the sea area near the southwestern coast of the Heracleean Peninsula;
- to analyse the factors that form the coastal zone of upwelling, patterns of distribution and structure of the suspended matter concentration field;
- to compare the results of expeditionary research and numerical modelling.

The studied water area is a section of the Sevastopol seaside, located along the southwestern coast of the Heracleean Peninsula. There is a well-known source of pollution of the considered region – an underwater pipeline of domestic wastewater of the *Yuzhnye* Treatment Facilities in Sevastopol [10] (Fig. 1).

The outlet head of the treatment facilities pipeline is located at a distance of ~ 3 km from the shore at a depth of 88 m. At the time of the analyzed survey, there was a leak in the pipeline, which became an additional source of anthropogenic suspended matter. The first information about the leak appeared in 2014, and in 2017 it became known that it was located at a distance of ~ 700 m from the shore at a depth of 34–37 m [5].



Fig. 1. Geographical position of the studied water area and map of stations of the oceanological survey performed on 23 August 2019

Initial data and research methods

To analyze the structure of waters and select the parameters of the numerical experiment model, we used the data of the expedition conducted by Marine Hydrophysical Institute (Sevastopol) on August 23, 2019. Within the framework of this expedition, a complex of synchronous observations of temperature, salinity, total organic matter (TOM) and colored dissolved organic matter (CDOM) was carried out. The survey was performed according to a scheme that included 20 drift stations on five sections oriented approximately along the normal to the coastline (Fig. 1, a).

The station coordinates were determined using a GPS navigator. The observations were made from the board of a small vessel. The range of depths on the test site was 6–150 m. The limiting sounding horizon was 25–30 m. At each station, all four environmental parameters were synchronously recorded in the *in situ* probing mode with a depth step of 0.1 m using the Kondor measuring complex¹⁾.

¹⁾ HYDROoptics Ltd. *Complex Hydrobiophysical Multiparametric Submersible Autonomous "CONDOR"*. 2023. [online] Available at: <http://ecodevice.com.ru/ecodevice-catalogue/multiturbidimeter-kondor> [Accessed: 04 June 2023].

It should be noted that TOM and CDOM belong to the group of the best indicators of pollution (including bacterial one) of coastal marine areas, as well as other natural water bodies [14–16].

At present, there is no maximum allowable standard for TOM and CDOM as a numerical indicator of water pollution. Therefore, to assess the significance of the anthropogenic component in the concentration field of these substances, their actual content was compared with the concentration characteristic of the open waters of the Black Sea off the coast of Crimea, which, according to [11], is equal to 2 mg/L for CDOM and 0.8 mg/L for TOM.

These values are conditionally accepted by us as a natural norm for the concentration of these quantities in the Black Sea coastal waters near the Crimean Peninsula. They were used to identify areas with an anthropogenic component in the fields of TOM and CDOM concentrations and to assess the degree of contamination of the considered water area with these substances.

The atmospheric synoptic situation during the survey was determined by the southeastern periphery of the anticyclone with the centre over Belarus²⁾.

The survey was accompanied by a fresh and strong wind, the average daily velocity of which was 6 m/s, and the direction changed in the sector from north to northeast. At sea, the wind gusts reached 12–15 m/s. The excitement of the sea reached 3–4 points³⁾.

Numerical modelling methods were used to understand the origin of the identified features in the water structure and the distribution of pollutants in the water area near the Heracleean Peninsula.

Due to the comparative shallowness of the considered area, the currents here are mainly determined by the wind. We will assume that the impurity transfer is carried out by steady currents. To calculate them, we use the 3D barotropic linear Felsenbaum model [17, 18] generalized to the case when Rayleigh friction is taken into account.

The 3D character of suspension propagation was taken into account in this work. The process of passive suspension propagation due to currents and turbulent diffusion is described by an equation in a divergent form, which has the following form [19, 20]

$$C_t + (uC - \mu C_x)_x + (vC - \mu C_y)_y + ((w + w_c)C - \kappa C_z)_z = 0,$$

where $C(x, y, z, t)$ is suspension concentration; κ is vertical, μ is horizontal turbulent diffusion coefficient; w_c is own velocity of the suspension.

At the initial moment of time, the suspension concentration is equal to zero. We consider that at the given points the suspension is ejected. At the side boundaries and at the bottom, conditions are also set for the absence of suspended matter flows.

The problem of impurity transfer is solved numerically. A conservative scheme is used, which has the property of transportability and positive definiteness. This scheme is described in detail in [17].

²⁾ Wetterzentrale. *Top Karten: Archiv Reanalysis – Europa*. 2023. [online] Available at: <http://smtp.pilzevilze.de/topkarten/fsreaeur.html> [Accessed: 04 June 2023].

³⁾ Raspisanie Pogody, Ltd. *Weather Archive at the Chersonesos Lighthouse*. 2023. [online] Available at: https://rp5.ru/Архив_погоды_на_Херсонесском_маяке [Accessed: 04 June 2023].

A uniform grid with steps $\Delta x = \Delta y = 40$ m was used. An uneven grid was applied vertically $\Delta z_k = 1, 2, 4, 6, 14, 16, 27, H - 70$ m. The middle layers are at depths: 0.5, 2, 5, 10, 20, 35, 56.5 m. The kinematic coefficient of vertical viscosity is constant $A = 30$ cm²/s; Coriolis parameter $f = 10^{-4}$ s⁻¹, $\kappa = 0.1$ cm²/s, $\mu = 100$ cm²/s, $w_c = -2$ cm/s. The value of shear stresses at the upper boundary was assumed to be equal to 1 cm²/s², which corresponds to a wind speed of 8 m/s.

The integral water circulation is determined by the bottom topography and wind direction. The numerical experiments were carried out for two main wind directions that accompanied the survey, north and northeast, with real bottom topography and parameters of pollution sources.

Discussion of the results

Analysis of the results of expeditionary research showed the following. In the considered section, the direction of the actual wind changed in the sector from approximately 0° to 45°. Judging by the structure of the temperature, salinity, TOM and CDOM concentration fields, this wind situation was accompanied by the rise of water from near-bottom horizons to the sea surface in the ascending wind upwelling circulation system. Moreover, these waters had clear signs of pollution. This is evidenced by the following characteristic properties (Fig. 2).

The upwelling center was clearly distinguished in the temperature field in the form of a strip of coastal waters with a temperature lowered by ~ 1 °C against the ambient background. The temperature field was well stratified with a pronounced (vertical gradient ~ -1 °C/m) seasonal thermocline elevated near the coast, which was located between 10 and 15 m horizons and was clearly visible on the extreme southern section between stations 17–20 (Fig. 1; 2, *a*).

In the vertical structure of the salinity field, individual desalinated water lenses with salinity decreased by 0.05–0.17 PSU relative to the background were found. The vertical and horizontal dimensions of these formations were estimated to be about 10 and 300 m, respectively. The most significant inhomogeneities in the haline field were noted in the plane of the median section between stations 9–12 (Fig. 1; 2, *b*).

In the extreme southern area of the test site in the surface layer of the sea, against the background of a low-gradient field of TOM content, a lens with a vertical size of 5–7 m and a maximum concentration of 2.3–2.5 mg/L within the entire considered area was clearly distinguished, which was three times higher than the natural norm (extreme southern section, stations 17–20). In addition, smaller formations with the content of this substance of anthropogenic origin were noted (Fig. 1; 2, *c*).

In the northwestern part of the test site, a lens with a maximum CDOM concentration (up to 2.4 mg/L) was observed, and it was traced throughout the entire water column at the extreme northern section between stations 1–4. In the vertical structure of the CDOM concentration field, as well as in the structure of the fields of salinity and TOM content, smaller heterogeneities were recorded with an increase in the content of this substance by about 1.5 times relative to the natural norm (Fig. 1; 2, *d*).

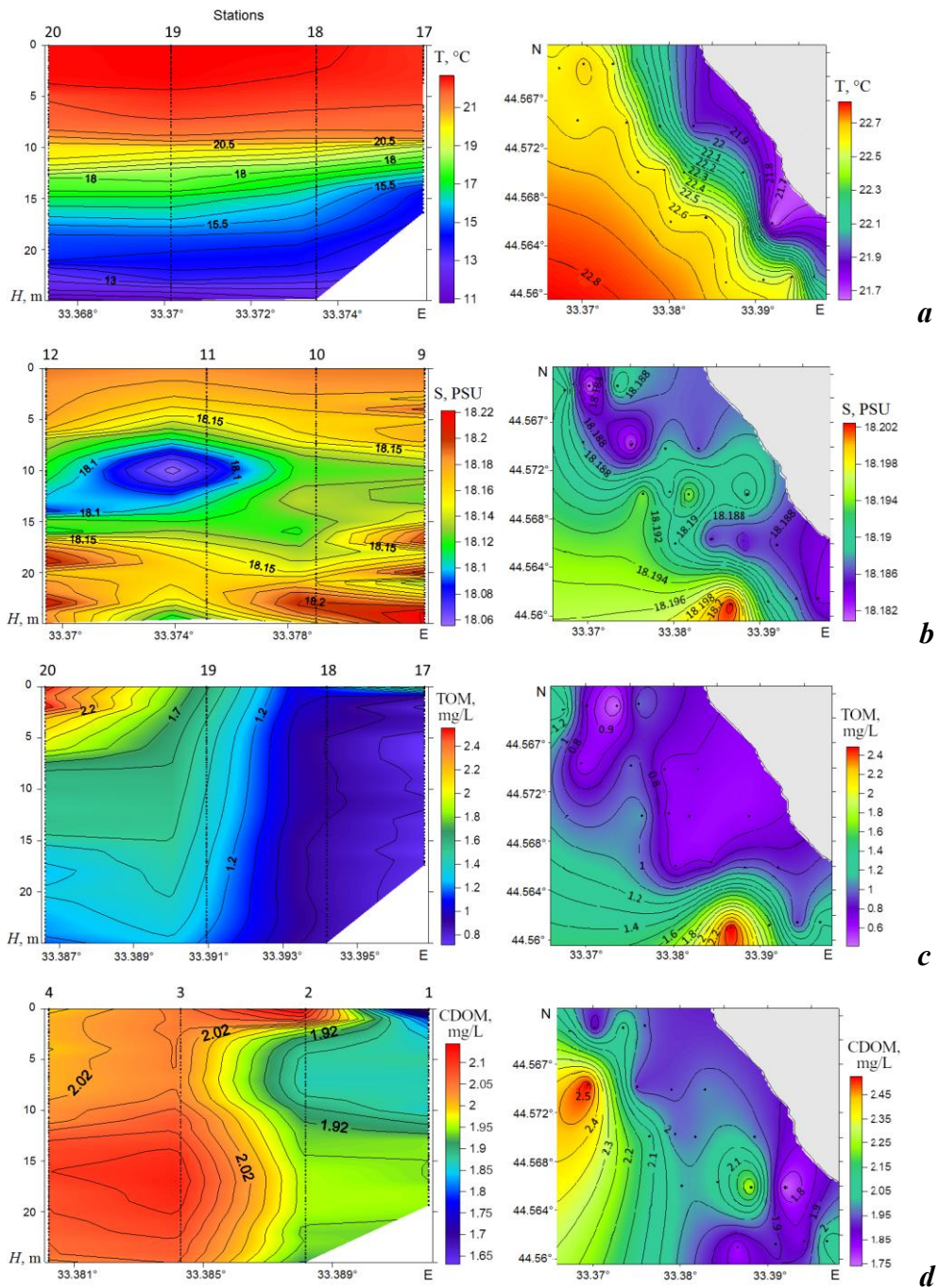


Fig. 2. Vertical (*left*) and horizontal in the surface layer (*right*) distribution of oceanological environmental parameters: *a* – temperature, °C; *b* – salinity, PSU; *c* – total organic matter concentration, mg/L; *d* – colored dissolved organic matter concentration, mg/L, near the wastewater outlet according to the data of the August 2019 expedition

Model experiments confirmed the wind upwelling observed during the oceanographic survey and the exit of anthropogenic waters to the sea surface. In addition, these experiments showed a number of interesting effects associated with water circulation and temporal dynamics of the spread of anthropogenic suspension, which can be applied in practice.

The calculated fields of current vectors along the given horizons for the north and northeast winds revealed a two-layer kinematic structure and a coastal cell of transverse water circulation typical of upwelling (Fig. 3).

The currents in the upper layer are directed downwind towards the sea, while the compensation current near the bottom is directed towards the shore. Near the shore on the sea surface, the current velocity was about 10 cm/s. The bottom layer was dominated by weak currents with a velocity of $1 \div 2$ cm/s.

With a northerly wind whose vector was directed at an obtuse angle to the coastline, and the eastward-oriented alongshore component was well pronounced (Fig. 3, *a, b*), the upwelling was determined by the Ekman effect. In the situation of the northeast wind, whose vector was directed approximately along the normal to the coastline, a typical upwelling was observed, caused by the wind surge (Fig. 3, *c, d*).

When modelling the distribution of suspended matter, the total volume of the pipeline outlet is assumed to be $Q = 43,800 \text{ m}^3/\text{year}$ (according to 1998 data [10]). Let us assume that $0.8 Q$ passes through the outlet head, and $0.2 Q$ passes through the emergency outlet (leakage). Positions of the sources are indicated by dots in Fig. 4.

The calculations were carried out on the second day. Fig. 4 shows the distribution of suspended matter concentration in isolines with a step of 10 % of

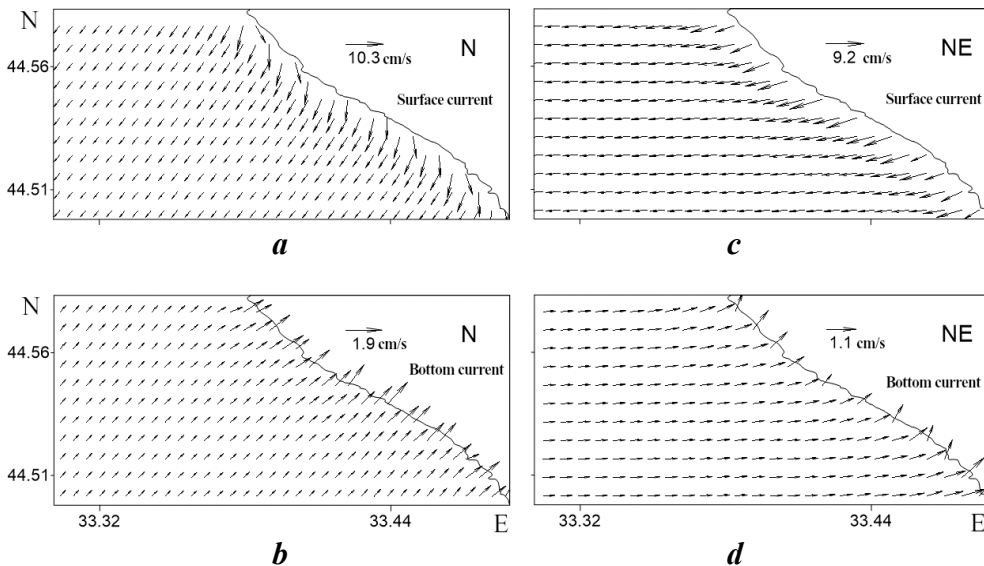


Fig. 3. Vectors of currents at the sea surface and near the bottom at north (*a, b*) and north-east (*c, d*) winds

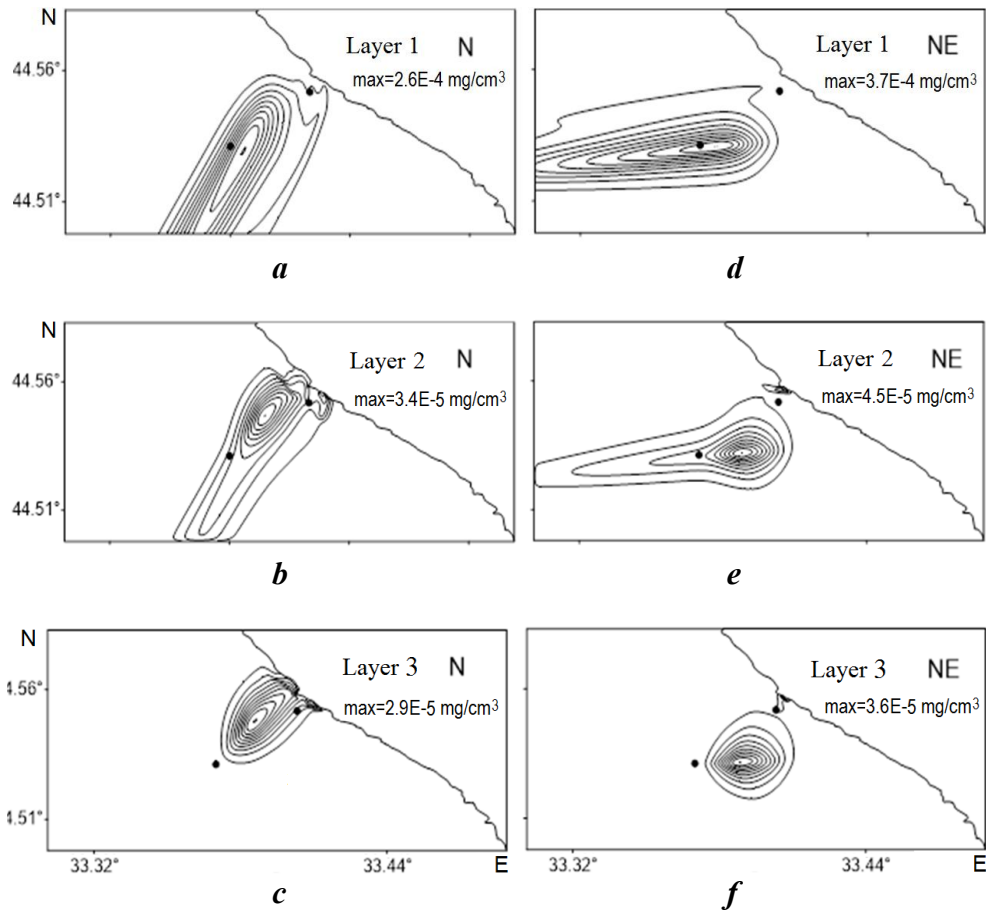


Fig. 4. Distribution of suspended matter concentration in two days in three sea layers (surface, intermediate and near-bottom) at north (*a, b, c*) and north-east (*d, e, f*) winds

the maximum value in each layer. This method of presentation was chosen to pay attention not to the quantitative characteristics of pollutants entering the water column, but to the features of the dynamics and transformation of suspension concentration distributions.

Analysis of the fields of the calculated content of suspended matter showed that from the moment of the “launch” of sources located at the bottom at given directions and wind speeds, a two-layer structure of the concentration field of the studied quantity with multidirectional currents is formed in the considered area. In the near-bottom horizons (layer 3), the suspension spread to the shore, while in the upper layers 1 and 2 it was carried out to the seaward side.

By the end of the second day, the maximum concentration of suspended matter appeared in the upper layer in the area of the main outlet, and its predominant current was directed to the sea and was traced at a distance of about 2.5 miles from the coast. In the lower layers, the maximum distribution of suspended matter shifted

towards the coast and spread to shallow water. Moreover, with the north wind, the concentration of suspended matter near the coast reached 40 % of the maximum, while with the northeast wind it was only 10 % (Fig. 4).

Off the coast of Crimea, in the warm half-year period during wind surges and upwelling, wastewater plumes from the near-bottom horizon penetrate through the thermocline to the sea surface. This property, first discovered and studied by the authors of the monograph [13], is confirmed by our results of numerical modelling (Fig. 4) and *in situ* observations (see Fig. 2).

Conclusion

Based on the structure analysis of the fields of temperature, salinity, concentration of total organic and colored dissolved organic matter, which were obtained from the materials of the MHI expedition conducted in August 2019, it was found that with north and northeast winds, waters of anthropogenic origin spread from the deep horizons to the sea surface. The rise of waters was associated with wind upwelling, and its source was represented by two outlets in the pipeline of the *Yuzhnye* Treatment Facilities.

The results of model experiments confirmed the upwelling observed during the oceanographic survey and the emergence of anthropogenic waters from the existing sources to the sea surface. They also made it possible to trace the spread of anthropogenic suspension coming from the sewer sources of the *Yuzhnye* Treatment Facilities.

The calculated fields of current vectors generated by north and northeast winds revealed a cell of transverse water circulation typical of coastal upwelling. It is also shown that upwelling in the coastal area under consideration is caused by both alongshore and offshore winds oriented along the normal to the coastline.

It has been established that near the southwestern coast of the Heracleean Peninsula, due to the special structure of the current field caused by the north and northeast winds, the suspension from sewer sources in the upper layer of water spreads into the open sea, and in the intermediate and near-bottom layers it accumulates along the coastline. With a northerly wind, the effect of anthropogenic suspension accumulation in the coastal zone is more intense.

REFERENCES

1. Ilyin, Yu.P., Repetin, L.N., Belokopytov, V.N., Goryachkin, Yu.N., Diakov, N.N., Kubryakov, A.A. and Stanichny, S.V., 2012. [*Hydrometeorological Conditions of the Ukrainian Seas. Vol. 2. The Black Sea*]. Sevastopol: ECOSI-Gidrofizika, 421 p. (in Russian).
2. Ivanov, V.A. and Belokopytov, V.N., 2013. *Oceanography of Black Sea*. Sevastopol: ECOSI-Gidrofizika, 210 p.
3. Dulov, B.A., Yurovskaya, M.V. and Kozlov, I.E., 2015. Coastal Zone of Sevastopol on High Resolution Satellite Images. *Physical Oceanography*, (6), pp. 39–54. doi:10.22449/1573-160X-2015-6-39-54
4. Bondur, V.G. and Grebenyuk, Yu.V., 2001. Remote Indication of Anthropogenic Influence on Marine Environment Caused by Depth Wastewater Plum: Modelling, Experiments. *Issledovanie Zemli iz Kosmosa*, (6), pp. 49–67 (in Russian).

5. Bondur, V.G., Ivanov, V.A., Dulov, V.A., Goryachkin, Yu.N., Zamshin, V.V., Kondratiev, S.I., Lee, M.E., Mukhanov, V.S., Sovga, E.E. and Chukharev, A.M., 2018. Structure and Origin of the Underwater Plume near Sevastopol. *Fundamentalnaya i Prikladnaya Gidrofizika*, 11(4), pp. 42–54. doi:10.7868/S2073667318040068 (in Russian).
6. Demyshev, S.G., Dymova, O.A., Kochergin, V.S. and Kochergin, S.V., 2020. Determination of Location of the Concentration Initial Field of a Possible Contamination Source in the Black Sea Water Area near the Gerakleisky Peninsula based on the Adjoint Equations Method. *Physical Oceanography*, 27(2), pp. 210–221. doi:10.22449/1573-160X-2020-2-210-221
7. Ivanov, V.A. and Fomin, V.V., 2016. Numerical Simulation of Underwater Runoff Propagation in the Heraklean Peninsula Coastal Zone. *Physical Oceanography*, (6), pp. 82–95. doi:10.22449/1573-160X-2016-6-82-95
8. Sovga, E.E., Kondrat'ev, S.I., Godin, E.A. and Slepchuk, K.A., 2017. Nutrient Content Seasonal Dynamics and Local Sources in the Heracleian Peninsula Coastal Waters. *Physical Oceanography*, (1), pp. 53–61. doi:10.22449/1573-160X-2017-1-53-61
9. Ivanov, V.A. and Ryabtsev, Ju.N., 2017. Modeling Transport Suspended Waste Outlet of the Cape Fiolent. *Processes in Geomedia*, (1), pp. 419–426 (in Russian).
10. Gruzinov, V.M., Dyakov, N.N., Mezenceva, I.V., Malchenko, Yu.A., Zhohova, N.V. and Korshenko A.N., 2019. Sources of Coastal Water Pollution near Sevastopol. *Oceanology*, 59(4), pp. 523–532. doi:10.1134/S0001437019040076
11. Lomakin, P.D. and Chepyzhenko, A.I., 2022. The Structure of Fields of Oceanological Quantities in the Upwelling Zone at the Herakleian Peninsula (Crimea) in August 2019. *Ecological Safety of Coastal and Shelf Zones of Sea*, (1), pp. 31–41. doi:10.22449/2413-5577-2022-1-31-41
12. Zats, V.I., Nemirovsky, M.S., Andryushchenko, B.F., Kandybko, V.V., Stepanov, V.N., Agarkov, A.K., Shulgina, E.F., Kiseleva, M.I., Senichkina, L.G. and Fedorenko, L.V., 1973. [The Experience of Theoretical and Experimental Research on Deep Wastewater Discharges (the Case of Yalta Area)]. Kiev: Naukova Dumka, 274 p. (in Russian).
13. Zats, V.I. and Goldberg, G.A., eds., 1991. *Modelling of Selfpurification Processes of the Shelf Zone Sea Water*. Leningrad: Gidrometeoizdat, 230 p. (in Russian).
14. Boss, E., Pegau, W.S., Zaneveld, J.R.V. and Barnard, A.H., 2001. Spatial and Temporal Variability of Absorption by Dissolved Material at a Continental Shelf. *Journal of Geophysical Research: Oceans*, 106(C5), pp. 9499–9507. doi:10.1029/2000JC900008
15. Tedetti, M., Longhitano, R., Garcia, N., Guigue, C., Ferretto, N. and Goutx, M., 2012. Fluorescence Properties of Dissolved Organic Matter in Coastal Mediterranean Waters Influenced by a Municipal Sewage Effluent (Bay of Marseilles, France). *Environmental Chemistry*, 9(5), pp. 438–449. doi:10.1071/EN12081
16. Karlsson, C.M.G., Cerro-Gálvez, E., Lundin, D., Karlsson, C., Vila-Costa, M. and Pinhassi, J., 2019. Direct Effects of Organic Pollutants on the Growth and Gene Expression of the Baltic Sea Model Bacterium *Rheinheimera* sp. BAL341. *Microbial Biotechnology*, 12(5), pp. 892–906. doi:10.1111/1751-7915.13441
17. Shapiro, N.B., 2006. Modeling of the Currents on the Seaside nearby Sevastopol City. In: MHI, 2006. *Ekologicheskaya Bezopasnost' Pribrezhnoy i Shel'fovoy Zon i Kompleksnoe Ispol'zovanie Resursov Shel'fa* [Ecological Safety of Coastal and Shelf Zones and Comprehensive Use of Shelf Resources]. Sevastopol, MHI. Iss. 14, pp. 119–134 (in Russian).

18. Shapiro, N.B. and Yushchenko, S.A., 1999. Simulation of Wind Currents in Sevastopol Bays. *Physical Oceanography*, 11(1), pp. 47–64. <https://doi.org/10.1007/BF02524495>
19. Astrakhantsev, G.P., Rukhovets, L.A. and Egorova, N.B., 1988. [Mathematical Modelling of Suspended Matter Distribution in Water Bodies]. *Meteorologiya i Gidrologiya*, (6), pp. 71–79 (in Russian).
20. Mikhailova, E.N., Shapiro, N.B. and Yushchenko, S.A., 1999. Modelling of the Propagation of Passive Impurities in Sevastopol Bays. *Physical Oceanography*, 11(3), pp. 233–247. <https://doi.org/10.1007/BF02508870>

Submitted 6.12.2022; accepted after review 21.03.2023;
revised 03.05.2023; published 26.06.2023

About the authors:

Pavel D. Lomakin, Leading Research Associate, Marine Hydrophysical Institute of RAS (2 Kapitanskaya St., Sevastopol, 299011, Russian Federation), Dr.Sci. (Geogr.), Professor, **ResearcherID: V-7761-2017**, **Scopus Author ID: 6701439810**, **IstinaResearcherID: 18321047**, *p_lomakin@mail.ru*

Yuri N. Ryabtsev, Research Associate, Marine Hydrophysical Institute of RAS (2 Kapitanskaya St., Sevastopol, 299011, Russian Federation), **ORCID ID: 0000-0002-9682-9969**, **SPIN-code: 7853-4597**, *ruab@mail.ru*

Contribution of the authors:

Pavel D. Lomakin – general supervision of the study, interpretation of expeditionary data, statement of the problem and objectives, interpretation of the overall result, writing the article

Yuri N. Ryabtsev – model parameter selection, model adaptation, performance of numerical experiments and their interpretation, revision of the article

All the authors have read and approved the final manuscript.

Variational Identification of the Initial Field of Chlorophyll A Concentration in the Transport Model according to Remote Sensing Data

V. S. Kochergin *, S. V. Kochergin

Marine Hydrophysical Institute of the Russian Academy of Sciences, Sevastopol, Russia

* *e-mail: vskocher@gmail.com*

Abstract

The work aims at construction of chlorophyll a fields based on variational assimilation of available satellite information for a few days in a transport model. Such information is the most real-time, but most often it has omissions (sometimes significant) in its structure due to the scattering effect of clouds, glares, etc. Therefore, obtaining reliable fields taking into account the available information for the Black Sea is an important and urgent task. In the numerical implementation of the transport model and variational method of measurement data assimilation, the results of calculations based on the MHI dynamic model for the Black Sea were used. In the numerical implementation of the variational assimilation algorithm, iterative gradient methods are used, and the solution of the adjoint problem is used to construct the gradient of the cost function in the parameter space. As a result of the calculations, a field of chlorophyll a concentration was obtained for almost the entire Black Sea area consistent with the measurement data. The paper implements a variational algorithm for the satellite information assimilation, which made it possible to obtain a chlorophyll a concentration field for the Black Sea area, taking into account incomplete coverage with observational data. The procedure can be used to determine concentration fields of various suspended substances in the sea based on data distributed over time and space.

Keywords: chlorophyll a concentration, variational algorithm, adjoint problem, measurement data assimilation, Black Sea, space-time interpolation

Acknowledgements: The work was carried out under state assignment on topic FNNN-2021-0005 “Complex interdisciplinary studies of oceanologic processes which determine functioning and evolution of ecosystems in the coastal zones of the Black Sea and the Sea of Azov” (code “Coastal research”).

For citation: Kochergin, V.S. and Kochergin, S.V., 2023. Variational Identification of the Initial Field of Chlorophyll A Concentration in the Transport Model according to Remote Sensing Data. *Ecological Safety of Coastal and Shelf Zones of Sea*, (2), pp. 61–70. doi:10.22449/2413-5577-2023-2-61-70

© Kochergin V. S., Kochergin S. V., 2023



This work is licensed under a Creative Commons Attribution-Non Commercial 4.0 International (CC BY-NC 4.0) License

Вариационная идентификация начального поля концентрации хлорофилла *a* в модели переноса по данным дистанционного зондирования

В. С. Кочергин *, С. В. Кочергин

Морской гидрофизический институт РАН, Севастополь, Россия

* e-mail: vskocher@gmail.com

Аннотация

Целью работы является построение полей хлорофилла *a* путем вариационной ассимиляции доступной спутниковой информации за несколько суток в модели переноса. Такая информация является наиболее оперативной, но чаще всего имеет в своей структуре пропуски, иногда существенные, вследствие рассеивающего эффекта облачности, бликов и т. д. Поэтому получение достоверных полей с учетом имеющейся информации для акватории Черного моря является важной и актуальной задачей. При численной реализации модели переноса и вариационного метода ассимиляции данных измерений использовались результаты расчетов по динамической модели МГИ для Черного моря. При численной реализации вариационного алгоритма ассимиляции применяются итерационные градиентные методы, а решение сопряженной задачи используется для построения градиента функционала качества в пространстве параметров. В результате проведенных расчетов получено поле концентрации хлорофилла *a*, согласованное с данными измерений, почти для всей акватории Черного моря. В работе реализован вариационный алгоритм усвоения спутниковой информации, который позволил получить поле концентрации хлорофилла *a* для акватории Черного моря с учетом неполного покрытия данными наблюдений. Процедура может быть использована для определения полей концентрации различных взвешенных веществ в море по данным, распределенным по времени и пространству.

Ключевые слова: концентрация хлорофилла *a*, вариационный алгоритм, сопряженная задача, ассимиляция данных измерений, Черное море, пространственно-временная интерполяция

Благодарности: работа выполнена в рамках государственного задания по теме FNNN-2021-0005 «Комплексные междисциплинарные исследования океанологических процессов, определяющих функционирование и эволюцию экосистем прибрежных зон Черного и Азовского морей» (шифр «Прибрежные исследования»).

Для цитирования: Кочергин В. С., Кочергин С. В. Вариационная идентификация начального поля концентрации хлорофилла *a* в модели переноса по данным дистанционного зондирования // Экологическая безопасность прибрежной и шельфовой моря. 2023. № 2. С. 61–70. EDN UHOSMC. doi: 10.29039/2413-5577-2023-2-61-70

Introduction

Solving the problem of environmental orientation for the Azov-Black Sea Basin requires the creation of systems that make it possible to receive real-time information about the state of the environmental situation. The main constituent elements of such systems are numerical dynamic models¹⁾ [1], models of transport

¹⁾ Marchuk, G.I. and Sarkisyan, A.S., 1988. *Mathematical Modelling of Ocean Circulation*. Berlin: Springer, 292 p.

and transformation of various components of suspended solids²⁾, as well as procedures concerning assimilation of available information³⁾ [2–7].

An extensive review of measurement data assimilation methods is presented in [8]. In this paper, a variational assimilation algorithm is implemented to assimilate satellite information on the concentration of chlorophyll a in the upper layer of the Black Sea. A characteristic feature of satellite information is that it often contains some omissions, for example due to clouds.

The use of surface values of chlorophyll concentration in the transport and diffusion model makes it possible to complete the missing information in the measurement data. In the algorithm, the applied model plays the role of a space-time interpolant, and the resulting solution of the problem on the time interval used is consistent not only with the model itself, but also with the measurement data. The initial field of chlorophyll concentration was chosen as a desired parameter. When implementing the search procedure for the extremum of the functional that characterizes the deviations of the model estimates from the measurement data, the solutions of the main, adjoint problems and the problem in variations are used to construct the gradient of the functional and organize the iterative process. With difference discretization of the above problems, TVD approximations are used [9]. As input information for the transport model, the results of calculations based on the MHI hydrothermodynamic model [1, 10] with a spatial step of 1.6 km and with realistic atmospheric action were used [11]. 27 horizons are used vertically with the time step of 1.5 min. To simulate the dynamics of chlorophyll a fields in the aquatic environment, the advection and diffusion equation is used.

Transport and diffusion model

Let us write the equation of the impurity transport model in the following form:

$$\frac{\partial C}{\partial t} + \frac{\partial(uC)}{\partial x} + \frac{\partial(vC)}{\partial y} + \frac{\partial(wC)}{\partial z} = A_H \nabla^2 C + \frac{\partial}{\partial z} A_V \frac{\partial C}{\partial z}, \quad (1)$$

where C – concentration; A_H , A_V – coefficients of horizontal and vertical turbulent diffusion, respectively.

On the sea surface ($z = 0$), the following condition is used:

$$A_V \frac{\partial C}{\partial z} = 0. \quad (2)$$

At the bottom and solid boundaries, the no-flow condition is taken. In the area of straits, the first type Dirichlet condition is used (homogeneous in this calculation). The concentration field $C^0(x, y, z)$ is set for the initial moment of time.

²⁾ Marchuk, G.I., 1986. *Mathematical Models in Environmental Problems*. Amsterdam: Elsevier Science Publishers B.V., 216 p.

³⁾ Penenko, V.V., 1981. *Methods of Numerical Modelling of Atmospheric Processes*. Leningrad: Gidrometeoizdat, 352 p. (in Russian).

The finite-different discretization of equation (1) is implemented on grid C [12]. TVD schemes [9] are used to approximate the advective terms. Vertical turbulent diffusion coefficient A_V is set in accordance with [13], with $A_H = 10^7 \text{ cm}^2/\text{s}$.

Variational algorithm of identification

Let us consider a functional of the following form:

$$I_0 = \frac{1}{2} \left(P \left(RC_{t_k} - C_{t_k}^{\text{meas}} \right), P \left(RC_{t_k} - C_{t_k}^{\text{meas}} \right) \right)_{S_t^0}, \quad (3)$$

which characterizes deviations of model concentration values from measurement data. In expression (3), R – operator of designing the model solution at the observation point; P – operator of zero expansion of the residuals of the forecast specified at the measurement points; t_k – time points at which the measurement data are received; the scalar product is defined in the standard way in $M_T = M \times [0, T]$; M – area in which the model is integrated on the time interval $[0, T]$; $S_t^0 = S^0 \times [0, T]$, S^0 – sea surface; $\Gamma_t = \Gamma \times [0, T]$, Γ – boundary of area M .

Minimization of expression (3) with the constraints of formulas (1)–(3) is reduced to finding the extremum of the functional of the following form:

$$I = I_0 + \left[\frac{\partial C}{\partial t} + \frac{\partial UC}{\partial x} + \frac{\partial VC}{\partial y} + \frac{\partial WC}{\partial z} - \frac{\partial}{\partial x} A_H \frac{\partial C}{\partial x} - \frac{\partial}{\partial y} A_H \frac{\partial C}{\partial y} - \frac{\partial}{\partial z} K \frac{\partial C}{\partial z}, C^* \right]_{M_t} + \left(\frac{\partial C}{\partial n}, C^* \right)_{\Gamma_t} + (C - C_0, C^*)_M, \quad (4)$$

where $\Gamma_t = \Gamma \times [0, T]$, Γ – boundary of area M .

By varying expression (4) and then integrating by parts, taking into account the boundary conditions and the continuity equation, the following expression can be obtained:

$$\delta I = (C - C_0, C^*)_M, \quad (5)$$

where C^* – Lagrange multipliers, which are chosen from the solution of the following adjoint problem:

$$\begin{aligned} -\frac{\partial C^*}{\partial t} - \frac{\partial UC^*}{\partial x} - \frac{\partial VC^*}{\partial y} - \frac{\partial WC^*}{\partial z} - \frac{\partial}{\partial x} A_H \frac{\partial C^*}{\partial x} - \frac{\partial}{\partial y} A_H \frac{\partial C^*}{\partial y} - \frac{\partial}{\partial z} K \frac{\partial C^*}{\partial z} = \\ = -P \left(RC_{t_k} - C_{t_k}^{\text{meas}} \right), \\ \Gamma : \frac{\partial C^*}{\partial n} = 0, \quad z = 0 : \frac{\partial C^*}{\partial z} = 0, \quad z = H : \frac{\partial C^*}{\partial z} = 0, \quad t = T : C^* = 0. \end{aligned}$$

The initial approximation is set to zero, and the next approximation can be found by the following formula:

$$C_0^{n+1} = C_0^n + \tau \nabla_{C_0} I,$$

where τ – iterative parameter.

Results and discussion

The flow rates for the period from 14 May 2016 to 17 May 2016 were calculated using the MHI model [1, 10] with a horizontal resolution of 1.6 km in latitude and longitude, taking into account the realistic atmospheric action for 2016 (according to ERA5 data with a spatial resolution of 0.25°) [10]. The reanalysis data [14] interpolated onto the model grid were used as initial fields. The obtained flow fields were used as input information.

The satellite data are often characterized by some omissions observed in their structure due to, for example, clouds or other factors that significantly affect the quality of incoming information processing. The presence of clouds over the Black Sea can be evaluated based on the information concerning pseudocolor composite MODIS-Aqua (URL: <https://earthdata.nasa.gov/labs/worldview/?p=geographic&l=MODIS>), which also characterizes the suspended matter concentration in the upper sea layer. As on 15 May 2016, the spatial structure of such fields is characterized by an increased concentration of chlorophyll a in the area of the Danube mouth and the area adjacent to the Dnieper-Bug Estuary. In addition, the composite contains areas of developed clouds in the eastern part of the sea. The increased concentration of impurities along the western coast is stipulated by the dynamics of the waters, namely the Main Black Sea Current. Figure 1 shows the composite as on 16 May 2016. Same as on May 15, the maximum concentration of chlorophyll a is located near the western coast of the Black Sea, and the eastern part of the sea along the Caucasian coast is covered with cloudy fields. On the contrary, clouds cover the central part of the sea on May 17.



Fig. 1. Pseudocolour composite MODIS-Aqua, 16 May 2016, the contrasts on the sea are determined by changes in the suspended matter concentration (<https://earthdata.nasa.gov/labs/worldview/?p=geographic&l=MODIS>)

Fig. 2 shows the chlorophyll a concentration field on 15 May 2016 according to the website <http://dvs.net.ru/mp/data/201507vw.shtml>.

The maximum values near the western coast reach 18–20 mg/m³. The values of the central part of the sea are 2–3 mg/m³. Figure 3 shows the chlorophyll a concentration field on May 16. Omissions in the data correspond to the clouds over the Black Sea in this period (see Fig. 1).

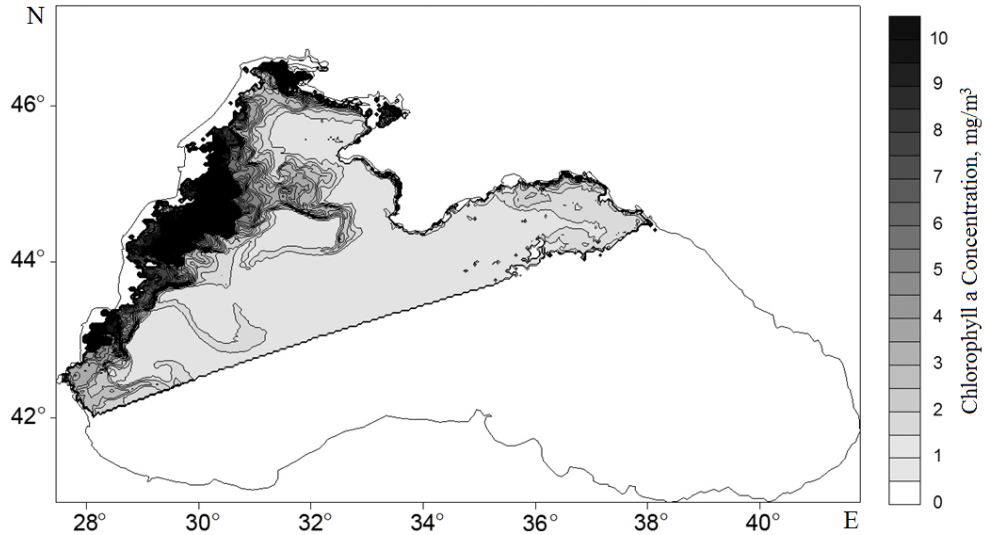


Fig. 2. Chlorophyll a concentration field on 15 May 2016 (available at: <http://dvs.net.ru/mp/data/201507vw.shtml>)

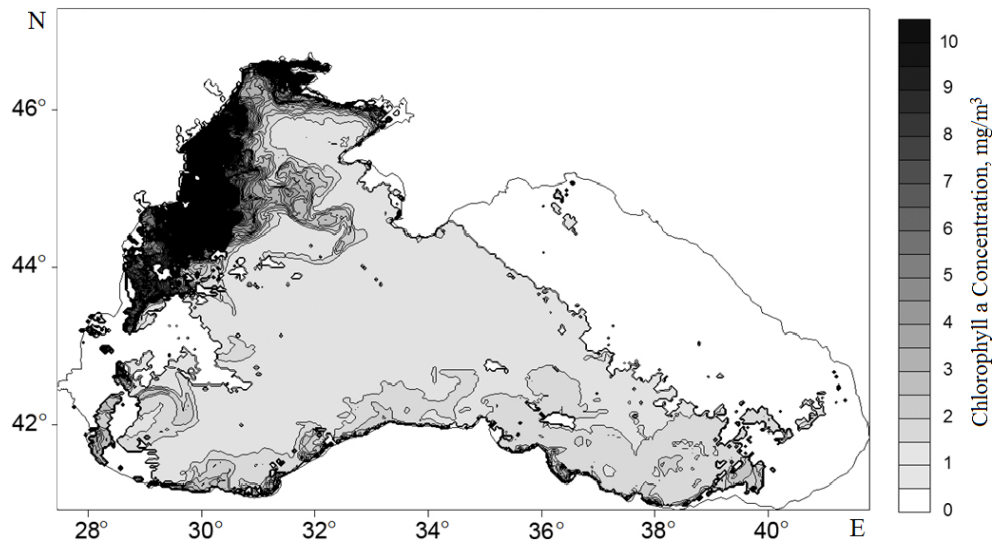


Fig. 3. Chlorophyll a concentration field on 16 May 2016

Fig. 4 similarly shows the data on May 17, which are available mainly for the eastern part of the sea.

Fig. 5 shows the result of the variational assimilation procedure.

In its structure, the presented field is in clear line with the image of the pseudocolor composite shown in Fig. 6. The remaining data omissions are determined by the assimilable information. Thus, zero concentration along

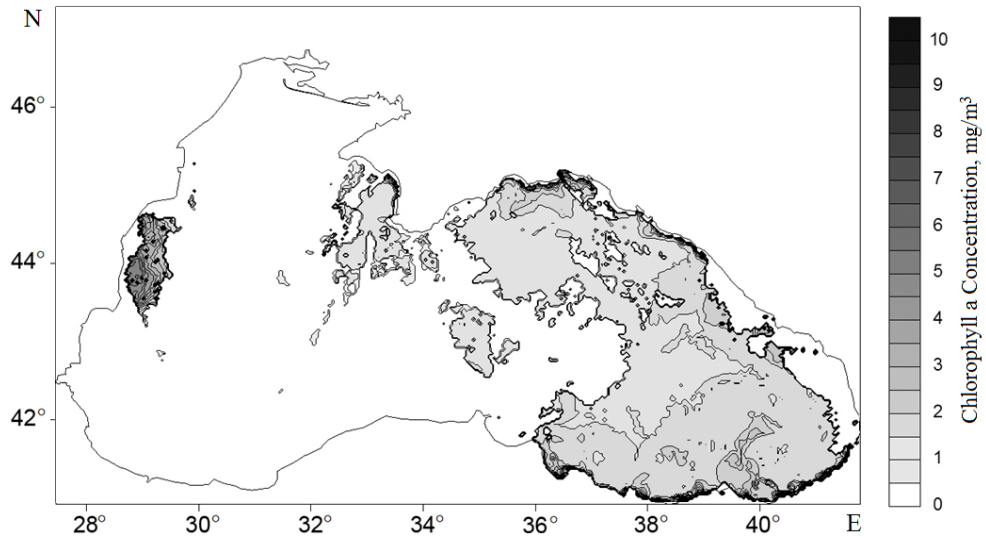


Fig. 4. Chlorophyll a concentration field on 17 May 2016

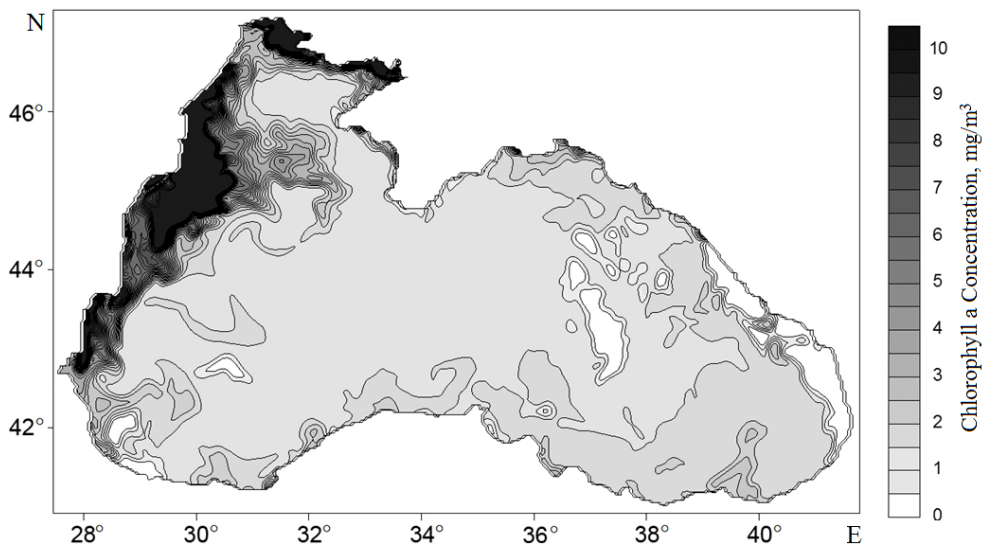


Fig. 5. Chlorophyll a initial concentration field on 14 May 2016



Fig. 6. Pseudocolour composite MODIS-Aqua, 14 May 2016

the Caucasian coast is stipulated by the lack of data for this area in assimilable fields. Most probably, the data omissions on May 17 are stipulated by the quality of the primary processing of satellite information, in which data with increased concentration were erroneously rejected.

As a result of the variational assimilation procedure, an initial field that is well consistent with the available information on the concentration of chlorophyll a and suspended matter in the upper sea layer, was obtained. The resulting field contains the main features of the spatial distribution of concentration with increased values in the area of the Danube and the Dnieper-Bug Estuary and along the western coast of the Black Sea. The spatial structure of the field is characterized by the influence of dynamic structures of a vortex nature on it. To the west of the Bosphorus, there is a mushroom-shaped structure, which is partially present in the data on May 15 and 16 and is clearly visible in the composite on May 14 (Fig. 6). The resulting chlorophyll a concentration field is consistent with the model and with the information used for subsequent time moments on the sea surface due to the minimization of the functional of expression (5). 3–4 iterations are sufficient to reach the extremum of the functional on a given time interval.

Conclusion

The performed calculations showed the effectiveness of the algorithm used in initializing the initial chlorophyll a concentration field in the Black Sea. The transport model is used as a space-time interpolant, and the solution of the adjoint problem is necessary to construct a gradient in the parameter space for iterative descent. The concentration fields obtained in this way are consistent with the measurement data distributed over time and space and the available information for the corresponding period of time. The results of the work can be used in order to solve environmental problems concerning the Azov-Black Sea Basin.

REFERENCES

1. Demyshev, S.G., 2012. A Numerical Model of Online Forecasting Black Sea Currents. *Izvestiya, Atmospheric and Oceanic Physics*, 48(1), pp. 120–132. <https://doi.org/10.1134/S0001433812010021>
2. Marchuk, G.I. and Penenko, V.V., 1979. Application of Optimization Methods to the Problem of Mathematical Simulation of Atmospheric Processes and Environment. In: G. I. Marchuk, ed., 2012. *Modelling and Optimization of Complex System*. Lecture Notes in Control and Information Sciences, vol. 18. Berlin, Heidelberg: Springer, pp. 240–252. <https://doi.org/10.1007/BFb0004167>
3. Semenov, E.V. and Mortikov, E.V., 2012. Problems of Operational Data Assimilation for Marginal Seas. *Izvestiya, Atmospheric and Oceanic Physics*, 48(1), pp. 74–85. <https://doi.org/10.1134/S0001433812010124>
4. Zalesny, V.B., Agoshkov, V.I., Shutyaev, V.P., Le Dimet, F. and Ivchenko, B.O., 2016. Numerical Modeling of Ocean Hydrodynamics with Variational Assimilation of Observational Data. *Izvestiya, Atmospheric and Oceanic Physics*, 52(4), pp. 431–442. <https://doi.org/10.1134/S0001433816040137>
5. Shutyaev, V.P., Le Dimet, F.-X. and Parmuzin, E., 2018. Sensitivity Analysis with Respect to Observations in Variational Data Assimilation for Parameter Estimation. *Nonlinear Processes in Geophysics*, 25(2), pp. 429–439. <https://doi.org/10.5194/npg-25-429-2018>
6. Kochergin, V.S., Kochergin, S.V. and Stanichny, S.V., 2020. Variational Assimilation of Satellite Data on Surface Concentration of Suspended Matter in the Azov Sea. *Sovremennye Problemy Distantionnogo Zondirovaniya Zemli iz Kosmosa*, 17(2), pp. 40–48. doi:10.21046/2070-7401-2020-17-2-40-48 (in Russian).
7. Demyshev, G.S., Dymova, O.A., Kochergin, V.S. and Kochergin, S.V., 2020. Determination of Location of the Concentration Initial Field of a Possible Contamination Source in the Black Sea Water Area near the Gerakleisky Peninsula Based on the Adjoint Equations Method. *Physical Oceanography*, 27(2), pp. 210–221. <https://doi.org/10.22449/1573-160X-2020-2-210-221>
8. Shutyaev, V.P., 2019. Methods for Observation Data Assimilation in Problems of Physics of Atmosphere and Ocean. *Izvestiya, Atmospheric and Oceanic Physics*, 55(1), pp. 17–31. doi:10.1134/S0001433819010080
9. Harten, A., 1984. On a Class of High Resolution Total-Variation-Stable Finite-Difference Schemes. *SIAM Journal on Numerical Analysis*, 21(1), pp. 1–23. <https://doi.org/10.1137/0721001>
10. Demyshev, S.G. and Dymova, O.A., 2013. Numerical Analysis of the Mesoscale Features of Circulation in the Black Sea Coastal Zone. *Izvestiya, Atmospheric and Oceanic Physics*, 49(6), pp. 603–610. <https://doi.org/10.1134/S0001433813060030>
11. Kallos, G., Nickovic, S., Papadopoulos, A., Jovic, D., Kakaliagou, O., Misirlis, N., Boukas, L., Mimikou, N.G.S.J.P., Sakellaridis, G., Papageorgiou, J., Anadranistakis, E. and Manousakis, M., 1997. The Regional Weather Forecasting System SKIRON: An Overview. In: University of Athens, 1997. *Proceedings of the Symposium on Regional Weather Prediction on Parallel Computer Environments*. Athens, Greece: University of Athens. Vol. 15, pp. 109–123.
12. Arakawa, A. and Lamb, V.R., 1981. A Potential Enstrophy and Energy Conserving Scheme for the Shallow Water Equations. *Monthly Weather Review*, 109(1), pp. 18–36. [https://doi.org/10.1175/1520-0493\(1981\)109<0018:APEAEC>2.0.CO;2](https://doi.org/10.1175/1520-0493(1981)109<0018:APEAEC>2.0.CO;2)

13. Demyshev, S.G., Zapevalov, A.S., Kubryakov, A.I. and Chudinovskikh, T.V., 2001. Evolution of the ^{137}Cs Concentration Field in the Black Sea after the Passage of the Chernobyl Cloud. *Russian Meteorology and Hydrology*, (1), pp. 37–46.
14. Korotaev, G.K., Ratner, Y.B., Ivanchik, M.V., Kholod, A.L. and Ivanchik, A.M., 2016. *Izvestiya, Atmospheric and Oceanic Physics*, 52(5), pp. 542–549. <https://doi.org/10.1134/S0001433816050078>

Submitted 19.01.2023; accepted after review 16.03.2023;
revised 03.05.2023; published 26.06.2023

About the authors:

Vladimir S. Kochergin, Junior Research Associate, Marine Hydrophysical Institute of RAS (2 Kapitanskaya St., Sevastopol, 299011, Russian Federation), **ORCID ID: 0000-0002-6767-1218**, **ResearcherID: AAG-4209-2020**, vskocher@gmail.com

Sergey V. Kochergin, Senior Research Associate, Marine Hydrophysical Institute of RAS (2 Kapitanskaya St., Sevastopol, 299011, Russian Federation), Ph.D. (Phys-Math.), **ORCID ID: 0000-0002-3583-8351**, **ResearcherID: AAG-4206-2020**, ko4ep@mail.ru

Contribution of the authors:

Vladimir S. Kochergin – problem statement, programme code writing and debugging, data preparation, analysis of calculation results, article text preparation

Sergey V. Kochergin – problem statement, analysis of calculation results, article text preparation

All the authors have read and approved the final manuscript.

Numerical Modelling of RedOx Condition Dynamics at the Water-Sediment Interface in Sevastopol Bay

Yu. S. Gurova^{1*}, E. V. Yakushev^{2,3}, A. V. Berezina^{2,3},
M. O. Novikov², K. I. Gurov¹, N. A. Orekhova¹

¹Marine Hydrophysical Institute of RAS, Sevastopol, Russia

²Shirshov Institute of Oceanology RAS, Moscow, Russia

³Norwegian Institute for Water Research, Oslo, Norway

* e-mail: kurinnaya-jul@yandex.ru

Abstract

The paper aims at assessing the variability of characteristics of redox conditions in the water column and the surface layer of sediments under changing anthropogenic load using *in situ* observational data and results of numerical modelling (the case of Sevastopol Bay). A comprehensive analysis is carried out of the chemical characteristics of the water column and pore water as well as geochemical characteristics of the bottom sediments. It is confirmed that there is the previously determined violation of the natural hydrochemical regime due to phytoplankton blooms in summer and the location of a large amount of stormwater and municipal wastewater in the bay. Despite the saturation of waters with oxygen in the bottom layer (94–113 % sat.), suboxic conditions are registered in the surface layer of bottom sediments. This is explained by predominance of the fine-grained fraction and high content of organic carbon. Mathematical calculations were performed using the one-dimensional benthic-pelagic Bottom RedOx Model (BROM). The numerical modelling results were validated using *in situ* observational data. The results showed that the model reproduces the natural seasonal variations of hydrochemical parameters associated with phytoplankton blooms, the occurrence of high concentrations of organic matter and its oxidation by the dissolved oxygen. Two numerical experiments with decreased and increased concentrations of organic matter were conducted to assess the effects of varying amounts of the organic matter entering the bay. It was found that the increased load on the bay results in a decrease in the oxygen concentration (up to 12 μM) and the development of anaerobic conditions in the bottom layer of water. Reduced organic matter input promotes aerobic conditions in the water column and in the bottom water layer. However, for bottom sediments, such a reduction in the load is not sufficient given the level of excess organic matter accumulated in them. The pore waters still consume oxygen and nitrates heavily and produce reduced forms of iron and manganese.

Keywords: bottom sediments, pore waters, oxygen, organic carbon, modelling, Black Sea, Sevastopol Bay, BROM model

© Gurova Yu. S., Yakushev E. V., Berezina A. V., Novikov M. O.,
Gurov K. I., Orekhova N. A., 2023



This work is licensed under a Creative Commons Attribution-Non Commercial 4.0 International (CC BY-NC 4.0) License

Acknowledgements: The work was carried out under state assignment no. FNNN-2021-0005 “Coastal research” of Marine Hydrophysical Institute and state assignment no. FMWE-2021-0001 of Shirshov Institute of Oceanology RAS; as well as funded by grants no. 20-35-90103 of the RFBR and no. 21-17-00191 of the RSF. The authors are grateful to A. I. Kubryakov, Dr.Sci. (Phys.-Math.), for the provision of calculation results obtained using the POM model.

For citation: Gurova, Yu.S., Yakushev, E.V., Berezina, A.V., Novikov, M.O., Gurov, K.I. and Orekhova, N.A., 2023. Numerical Modelling of RedOx Condition Dynamics at the Water-Sediment Interface in Sevastopol Bay. *Ecological Safety of Coastal and Shelf Zones of Sea*, (2), pp. 71–90. doi:10.29039/2413-5577-2023-2-71-90

Численное моделирование динамики окислительно-восстановительных условий на границе вода – донные отложения в Севастопольской бухте

**Ю. С. Гурова^{1*}, Е. В. Якушев^{2,3}, А. В. Березина^{2,3},
М. О. Новиков², К. И. Гуров¹, Н. А. Орехова¹**

¹ *Морской гидрофизический институт РАН, Севастополь, Россия,*

² *Институт океанологии им П.П. Ширшова РАН, Москва, Россия*

³ *Norwegian Institute for Water Research, Oslo, Norway*

* e-mail: kurinnaya-jul@yandex.ru

Аннотация

Цель работы – оценка изменчивости характеристик окислительно-восстановительных условий в водной толще и поверхностном слое отложений при изменяющейся антропогенной нагрузке с использованием данных натуральных наблюдений и результатов численного моделирования на примере Севастопольской бухты. Выполнен комплексный анализ химических характеристик водной толщи и поровых вод, а также геохимических характеристик донных отложений. Подтверждено, что происходит установленное ранее нарушение естественного гидрохимического режима, связанное с цветением фитопланктона в летнее время и расположением в акватории бухты большого количества ливневых и коммунальных стоков. Несмотря на насыщение придонного слоя вод кислородом (94–113 % нас.), в верхнем слое донных отложений зафиксированы субкислородные условия. Это объясняется преобладанием мелкозернистой фракции и высоким содержанием органического углерода. Математические расчеты выполнялись с помощью одномерной бентосно-пелагической модели Bottom RedOx Model (BROM). С использованием данных натуральных наблюдений проведена валидация результатов численного моделирования. Полученные результаты показали, что модель воспроизводит естественный сезонный ход гидрохимических параметров, связанный с цветением фитопланктона, появлением высоких концентраций органического вещества и его окислением растворенным кислородом. Для оценки последствий поступления различного количества органического вещества в акваторию бухты были проведены два численных эксперимента с уменьшением и увеличением его концентрации. Установлено, что увеличение нагрузки на акваторию бухты приводит к снижению концентрации кислорода (до 12 мкМ) и развитию анаэробных условий в придонном слое вод. Сокращение поступления органического вещества способствует формированию аэробных условий в водной

толще и придонном слое вод. Однако для донных отложений, с учетом уровня накопленного в них избыточного органического вещества, подобного снижения нагрузки недостаточно. В поровых водах все еще происходит интенсивное потребление кислорода и нитратов и образуются восстановленные формы железа и марганца.

Ключевые слова: донные отложения, поровые воды, кислород, органический углерод, моделирование, Черное море, Севастопольская бухта, модель *BROM*

Благодарности: работа выполнена в рамках государственного задания ФГБУН ФИЦ МГИ по теме № FNNN-2021-0005 «Прибрежные исследования» и государственного задания ФГБУН ИО РАН № FMWE-2021-0001, при финансовой поддержке Минобрнауки России в рамках Соглашения № 075-15-2021-946, а также при поддержке грантов РФФИ № 20-35-90103 и РНФ № 21-17-00191. Авторы выражают благодарность д-ру физ.-мат. наук А. И. Кубрякову за предоставленные результаты расчета гидрофизических характеристик, полученные с помощью модели POM.

Для цитирования: Численное моделирование динамики окислительно-восстановительных условий на границе вода – донные отложения в Севастопольской бухте / Ю. С. Гурова [и др.] // Экологическая безопасность прибрежной и шельфовой зон моря. 2023. № 2. С. xx–xx. doi:10.29039/2413-5577-2023-2-71-90

Introduction

Coastal ecosystems characterized by high biodiversity, play a significant role in the social and economic sphere. It is in the coastal water areas that the highest level of pollution is observed [1].

The anthropogenic load exerted on coastal water areas leads to the inflow of an additional amount of organic matter and nutrients into them. The consumption of oxygen for the oxidation of organic matter and other reduced compounds leads to a shift in the processes occurring due to the anaerobic oxidation of organic matter closer to the surface of bottom sediments. As a result, oxygen is exhausted in the upper layer of sediments, which results in the formation of anaerobic conditions [2]. An increase in the content of reduced compounds in the surface layer of sediments leads to an increase in their flow into the bottom layer of waters, due to which suboxic and anaerobic conditions are also registered in it [3].

The bays of the Sevastopol region are an example of the water areas of the Crimean shelf with the maximum anthropogenic load, in which the accumulation of organic matter in bottom sediments significantly prevails over its decomposition [4].

Of all the bays of the Sevastopol region, Sevastopol Bay stands out directly as the level of anthropogenic load on it has shown significant growth over the years [5–7]. This results in intensive silting of bottom sediments, accumulation of organic carbon in them, development of oxygen deficiency in bottom sediments and the bottom water layer, and further emergence of ecological risk zones.

Various systematic studies of the hydrological and hydrochemical parameters of waters [5, 6, 8–10], the spatial distribution of the geochemical characteristics of bottom sediments [11–13], and the level of their pollution [7, 14, 15] have been carried out for a long time in the bay water area. In addition to the characteristics of the solid phase of bottom sediments, the chemical composition of pore waters has also been actively studied [2, 13, 16].

Based on *in situ* measurements, important information about the current state of the water area was obtained. The use of the results of model calculations makes it possible to obtain a broader (in space and time) idea of possible changes in the characteristics of the ecosystem when the influencing factors change [17, 18].

Concerning Sevastopol Bay, both its hydrodynamic regime [19–21] and the distribution of pollutants in it [22, 23] are regularly modelled. However, no work has been carried out in the studied area to assess changes in redox conditions in bottom sediments and the bottom water layer on a space-time scale using mathematical modelling methods.

The paper aims at assessing the variability of characteristics of redox conditions in the water column and the surface layer of sediments under changing anthropogenic load using *in situ* observational data and numerical modelling (the case of Yuzhnaya Bay, which constitutes a part of Sevastopol Bay).

Area characteristics

Sevastopol Bay is a semi-enclosed water area with significantly limited water exchange between the bay and the open sea [24]. The water area of the bay is under constant anthropogenic pressure [10]. The average depth of the bay is 12.5 m. The formation of the hydrochemical structure of the Sevastopol Bay waters is significantly influenced by the river runoff in the eastern part and municipal wastewater, which transport an additional amount of organic matter into the water area (Fig. 1) [5, 13, 25]. For a long time, the bay was used for growing oysters, but now such use is impossible due to the depletion of bioresources and the increasing level of pollution [6]. Currently, the bay is one of the most polluted Black Sea coastal areas [4–7], with the maximum level of pollution in Yuzhnaya Bay. This bay is elongated in the meridional direction and is characterized by a large number of sources of municipal wastewater and stormwater and the location of ship repair facilities along its shores [7, 11, 26, 27] (Fig. 1).

According to [28], the hydrodynamic regime of the Yuzhnaya Bay ecosystem (Fig. 1) is characterized by difficult water exchange with the main water area of the bay and by water ventilation determined by the wind regime. With northerly and northeasterly winds, the waters are blocked in Yuzhnaya Bay. With southerly winds, waters polluted by municipal wastewater can be carried out of Yuzhnaya Bay and reach the northern shores of Sevastopol Bay [28].

Under certain conditions, bottom sediments also influence the characteristics of the bottom water layer of Yuzhnaya Bay [13]. The surface layer of bottom sediments (0–5 cm) in the bay is represented mainly by sandy silty and pelitic silts and, to a lesser extent, by silted shell rock [11–13]. Abrasion processes accumulate coarse-grained material at the outlet of the Sevastopol Bay and along the coastline.

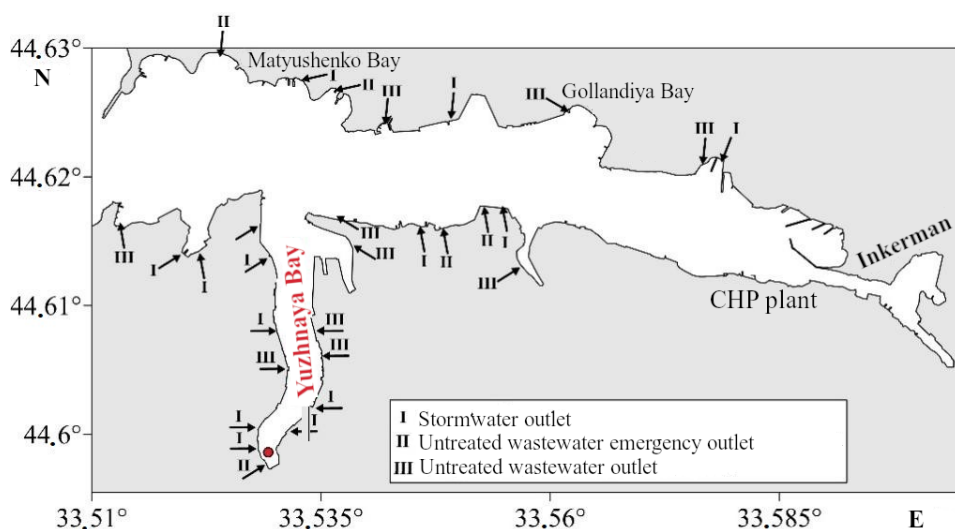


Fig. 1. Location of the bottom sediment column sampling station (red dot) as well as stormwater and emergency wastewater outlets [13]

In Yuzhnaya Bay, the rate of input of terrigenous material weakens, and fine-grained fractions accumulate here as a result of intensive input of organic matter (OM) and low water dynamics [11, 12]. In recent years, the proportion of the silt fraction in the surface layer of bottom sediments of the bay has been increasing, which can indicate silting of the bay [7]. The vertical distribution of C_{org} in Yuzhnaya Bay is heterogeneous and varies from 4.5 to 7 % dry weight [7].

In accordance with the hydrological and hydrochemical parameters of the waters of the bay and its physical and geographical characteristics, the seasonal distribution of hydrochemical components, in particular oxygen, is determined not only by the temperature regime and hydrodynamics of the waters, but also by a biological factor, namely, phytoplankton blooms [5]. At the same time, the saturation of the bottom layer of waters with oxygen, as a rule, does not reach 100 % during the year in the Yuzhnaya Bay apex. According to [5, 29], mass phytoplankton blooms both in the surface and in the bottom water layer are observed in July. The so-called summer maximum is typical for polluted water areas including Sevastopol Bay. The amount of phytoplankton decreases in the cold period of the year. Therefore, the Sevastopol Bay waters can be characterized in terms of phytoplankton biomass as conditionally clean in winter and polluted in summer [29].

Over the past 20 years, the supply of nutrients and organic matter to Sevastopol Bay has increased, which results in a decrease in oxygen concentration and pH, as well as acidification of the bay waters [6]. The results of the study [16] showed that the organic matter oxidation occurred mainly under anaerobic conditions.

Materials and methods

A comprehensive analysis of the hydrological and hydrochemical characteristics of the water column and the physical and chemical characteristics of bottom sediments was carried out in May 2018 under quarterly expeditions of the Marine Biogeochemistry Department of the Marine Hydrophysical Institute of RAS on-board the small vessel “Hydrograph-4”. Fig. 1 shows the location of the sea water and bottom sediment column sampling station in Yuzhnaya Bay.

Sea water samples from the surface and bottom horizons were taken with a bathometer.

The content of dissolved oxygen in water samples was determined by the method of Winkler volumetric titration modified by Carpenter [30]. This method makes it possible to obtain results with the accuracy of ± 0.01 ml/L (± 0.4 μ M). The degree of oxygen saturation (%) was calculated using Weiss formula [31]

$$\ln C = A_1 + A_2 (100/T) + A_3 \ln(T/100) + A_4 (T/100) + S [B_1 + B_2 (T/100) + B_3 (T/100)^2],$$

where C – solubility of oxygen at total pressure of 1 atmosphere, taking into account the pressure of saturated water vapor, ml/L; $A_{(1,2,3,4)}$ and $B_{(1,2,3)}$ – constants ($A_1 = -173.4292$; $A_2 = 249.6339$; $A_3 = 143.3483$; $A_4 = -21.8492$; $B_1 = -0.033096$; $B_2 = 0.014259$; $B_3 = -0.0017$); T – absolute temperature, K; S – salinity, PSU.

Mineral forms of biogenic substances (phosphates, silicic acid, ammonium nitrogen) were analyzed by the photometric method on a spectrophotometer KFK-3KM after seawater samples were filtered through a membrane filter with a pore size of 0.45 μ m (except for samples for determining the content of ammonium ions)¹⁾. When determining the concentration of silicic acid, a correction was made for salinity, calculated by the following formula

$$C_{\text{tru}} = C_{\text{obs}} \cdot (1 + 0.0045S),$$

where C_{tru} – true silicic acid concentration; C_{obs} – observed silicic acid concentration; S – final salinity of the analyzed sample, PSU¹⁾.

Ammonium nitrogen was determined using modified Sage-Solorzano method for sea water, which is based on a phenol-hypochlorite reaction using sodium nitroprusside and sodium citrate²⁾. To determine the amount of nitrates and nitrites on a flow autoanalyzer AutoAnalyzer AA II (*Bran+Luebbe*), the method of reducing nitrates to nitrites with copper-plated cadmium was used.

To determine the chemical composition of pore waters, bottom sediment columns were sampled using a Plexiglas tube, 6 cm in diameter, with a vacuum liquid trap.

¹⁾ Bordovsky, O.K. and Ivanenkov, V.N., eds., 1992. *Modern Methods of Ocean Hydrochemical Investigations*. Moscow: IO AS USSR, 201 p. (in Russian).

²⁾ UNESCO, 1987. *Thermodynamics of the Carbon Dioxide System in Seawater*. Paris: UNESCO, pp. 3–21.

When analyzing the chemical profile of the pore waters of bottom sediments, a polarographic method of analysis was used with a glass Au-Hg microelectrode [13, 32, 33]. An electrode saturated with silver chloride was used as a reference electrode, and a platinum electrode was used as an auxiliary one. Profiling of bottom sediment columns was carried out with a vertical resolution of 1 to 10 mm. The main advantage of the method is the ability to analyze the chemical composition of pore waters under conditions as close as possible to natural ones, without any sample destruction and additional sample preparation. For all the measurements, the determination error did not exceed 10 %.

The granulometric composition of bottom sediments was determined with the combined decantation and diffusion method. The separation of the silty and pelitic fraction (≤ 0.05 mm) was performed by wet sieving followed by gravimetric determination of the dry weight. Coarse-grained fractions (> 0.05 mm) were separated by the dry sieving method using standard sieves (GOST 12536-2014).

Carbon content (C_{org}) was determined coulometrically on an express analyzer AN 7529 according to the method adapted for marine bottom sediments. The standard deviation value for samples with C_{org} content less than 0.5 % was 0.03, and for samples with C_{org} more than 1.5 % it was 0.08 [34].

Mathematical model and input data

The one-dimensional benthic-pelagic Bottom RedOx Model (BROM) was used to calculate redox conditions and predict their possible changes in the water column and the surface layer of sediments of Yuzhnaya Bay [35].

BROM is integrated into the existing Framework for Aquatic Biogeochemical Modeling (FABM) and includes a 2D transport model 2DBP [36] and a biogeochemical module (BROM-biogeochemistry) [17, 37–41].

The biogeochemical module consists of several submodules that parameterize the processes in the ecosystem and the processes of transformation of the chemical elements considered in the model: nitrogen, phosphorus, carbon, silicon, iron, manganese, and sulfur. Within the framework of the model, OM is represented as particulate organic matter labile (POML) and dissolved organic matter labile (DOML), which can be oxidized by dissolved oxygen, being a part of various compounds.

The equations and parameters used in BROM are given in [35], and the block diagram of the model is shown in Fig. 2.

The temporal variability of the substance concentration is stipulated by its diffusion and sedimentation, taking into account the processes leading to the formation and consumption of this substance:

$$\frac{\partial \hat{C}}{\partial t} = \frac{\partial}{\partial z} D \frac{\partial \hat{C}_i}{\partial z} - \frac{\partial}{\partial z} (v_i \hat{C}_i) + \varepsilon_h (\hat{C}_{0i} - \hat{C}_i) + T_{birr(i)} + R_i,$$

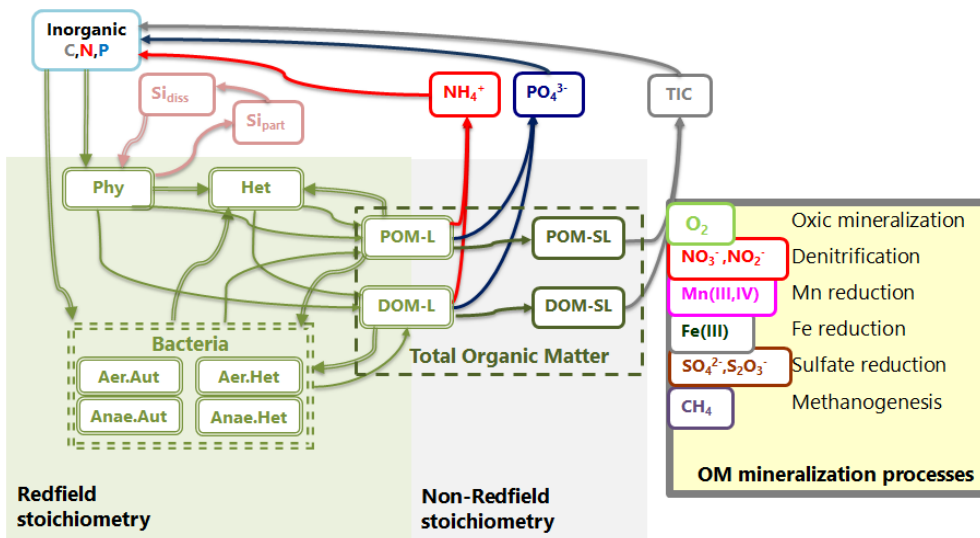


Fig. 2. Block diagram of the biogeochemical module provided in the Benthic RedOx Model (BROM)

where \hat{C}_i – concentration, $\text{mmol} \cdot \text{m}^{-3}$ total volume, i -th state variable; $D(z, t)$ – vertical diffusion coefficient; v_i – sedimentation rate; $\varepsilon_h(z, t)$ – specific rate of climatic concentration relaxation $\hat{C}_{0i}(z, t)$; $T_{birr(i)}$ – trend stipulated by bioirrigation (non-zero for solutes in the bottom water column only); R_i – sources minus wastewaters.

Sedimentation rate v_i is non-zero for weighted (undissolved) variables only and is determined at each time step by the biogeochemical module [36].

The vertical grid in the BROM transport is divided into the water column, the bottom boundary layer, and bottom sediments. The grid spacing in the water column is 2 m. For the bottom water layer (1 m above the sediment surface), the grid spacing decreases towards the water–bottom boundary from 20 cm to 17 mm for the fluffy layer. For the upper layer of deposits, the grid spacing increases geometrically downward from the boundary of the fluffy layer from 1.5 mm to 20 mm. The result is represented by a complete grid with non-uniform spacing and maximum resolution near the water–bottom boundary. In this vertical grid, temperature, salinity, and biogeochemical concentrations are determined at the centers of the layers, while diffusion coefficients, sedimentation rates, and net fluxes are determined at the boundaries between the layers [36].

The results of the calculation of the Princeton Ocean Model (POM) adapted for the bays of the Sevastopol region were used as input data in the BROM hydro-physical module [19].

Results and discussion

Chemical composition of bottom water layer

The concentrations of hydrochemical parameters in the surface and bottom water layers for the period from February 2017 to February 2022 are shown in Fig. 3.

For the surface water layer, high values of the degree of saturation of water with oxygen (98–102 %) are observed from April to September, while from November to February, these values decrease (87–94 %). Such a decrease in the oxygen content is explained by the fact that in cold weather, due to the absence of phytoplankton blooms, oxygen is probably consumed for the oxidation of organic substances entering the bay [5].

It is known from literary sources that the maximum values of ammonium ion concentrations and the sum of nitrates/nitrites are noted in the apex of Yuzhnaya Bay both in the surface and in the bottom water layer [5, 6]. This is explained by the presence of stormwater and municipal wastewater in the apex of the bay (Fig. 1). Analysis of the data obtained confirmed the change in the intra-annual course of hydrochemical parameters [5, 6], which takes place for the waters of

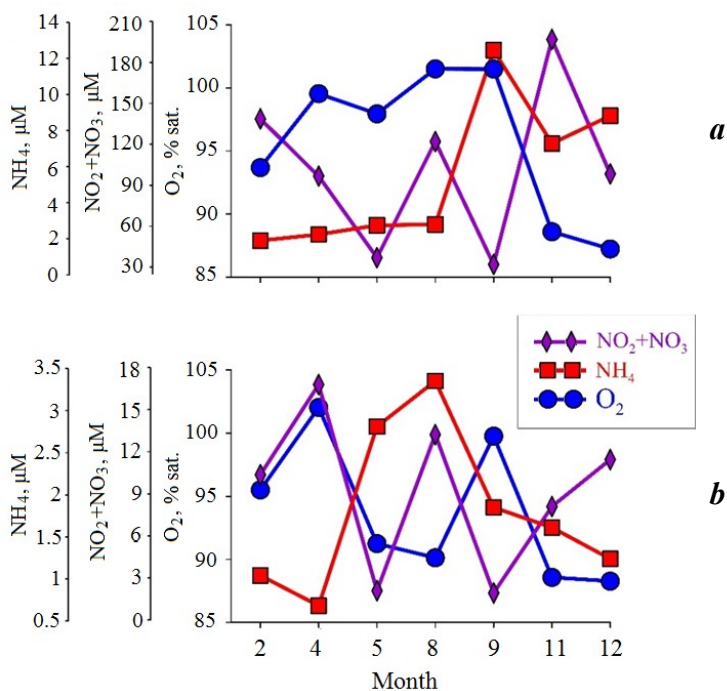


Fig 3. Temporal variability of hydrochemical characteristics in the surface (a) and bottom (b) water layers in Yuzhnaya Bay in 2017–2022

Sevastopol Bay, as well as significant difference in their concentration in the surface and bottom layers [6] (Fig. 3). The decrease in the concentration of the sum of nitrates/nitrites in the warm period of the year is explained by their consumption by phytoplankton, and in the autumn and winter seasons their concentrations increase.

The maximum concentrations of ammonium ions were determined in the warm period of the year: in the surface layer in September, and in the bottom layer from May to September. According to [5, 6], this is explained by the processes of bacterial destruction of organic matter, as well as the intensification of the processes of stormwater and municipal wastewater in the summer.

Geochemical composition of bottom sediments

The surface layer (0–5 cm) of bottom sediments in the apex of Yuzhnaya Bay is formed mainly by silty material (78 %), consisting of 51 % of the pelitic and aleurite fraction and 27 % of the aleurite and pelitic fraction. The proportion of fine-grained material increased with depth. The C_{org} content in the surface layer was 4.82 %, and its vertical distribution was distinguished by the presence of several concentration peaks at a depth of 30 and 90 mm (Fig. 4, a).

Chemical composition of pore waters

In the apex of Yuzhnaya Bay, oxygen penetrated into the bottom sediments to a depth of 4 mm, its average concentration was 132 μM (up to 79 % sat.). The characteristics of pore waters were determined by processes involving dissolved forms of iron (Fe(II, III)), with their maxima in the 40–60 mm and 130–140 mm layers (Fig. 4, b). The average Fe(II) concentration was 398 μM .

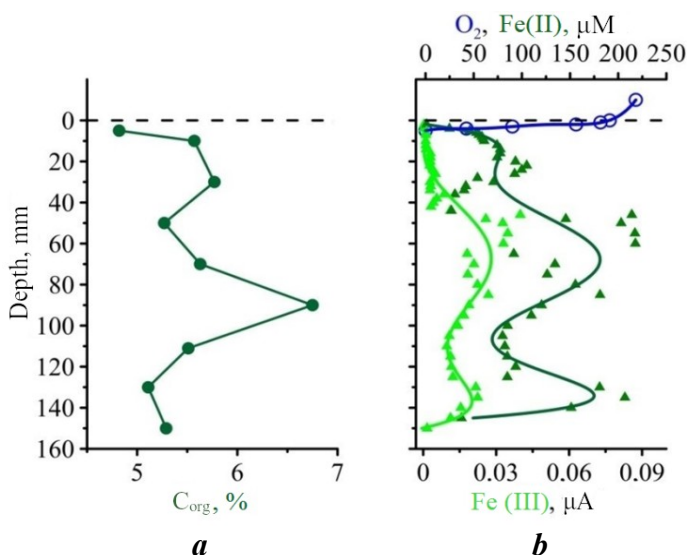


Fig. 4. Vertical distribution of C_{org} (a) and pore water components (b) in the bottom sediments of Yuzhnaya Bay

The analysis of the pore waters of bottom sediments showed that, despite sufficient saturation of the bottom water layer with oxygen (94–113 % sat.), suboxic conditions formed in the upper layer of bottom sediments. This is explained by the predominance of the fine-grained fraction (> 75 %) and high C_{org} content (> 4 %).

To predict the variability of the redox conditions in the bottom sediments and bottom water layer of Yuzhnaya Bay on a space-time scale, the numerical modelling results were validated and a series of model experiments was carried out, suggesting a change in the amount of OM in the water area of the bay.

Validation of numerical calculations

To validate the numerical modelling results, *in situ* observational data obtained for the water column (O_2 concentrations) and bottom sediments (concentrations of O_2 , Fe(II), Mn(II), H_2S , C_{org}) during expeditions along Sevastopol Bay (Yuzhnaya Bay) in 2017–2020, were used. To compare the numerical results with *in situ* observations, the BROM model was run with a vertically uniform initial distribution of parameters. After reaching a quasi-stationary state with seasonal fluctuations of the studied parameters, the results were compared with *in situ* observations. In order to adequately reproduce seasonal dynamics of biogeochemical characteristics and to adapt the model parameters to local conditions, the model was run several times. The validation results are shown in Fig. 5, 6.

The modelling took into account biogeochemical processes occurring under various redox conditions, which determine the mechanisms of OM mineralization (aerobic oxidation, denitrification, reduction of manganese and iron, and sulfate reduction). Most of the results of model calculations generally corresponded to the concentrations of the measured parameters in the water column, bottom sediments, and pore waters (points in Fig. 5).

Two numerical experiments were conducted to assess the effects of changes in the OM entering the bay for the distribution of hydrochemical characteristics in the water area of the bay. The first experiment assumed an increase in the OM concentration by a factor of two compared to the concentration observed in the water area of the bay. It was established that the seasonal course of biogeochemical processes was disturbed (Fig. 7). An increase in OM inflow can result from an increase in the impact of stormwater and emergency discharges of wastewater entering the water area of the bay (see Fig. 1).

A sharp increase in the amount of OM (DOML, DOMR) activates the process of oxygen consumption for its oxidation and disrupts the seasonal course of oxygen. If OM excessive supply occurs in February, then in June suboxic conditions are formed in the bottom water layer (the oxygen concentration decreases up to 12 μM) [42], and in August such conditions also arise in the water column. In September, hydrogen sulfide appears in the upper layer of sediments, and conditions in the bottom layer of waters change to anaerobic ones. The return to the original conditions of the bay ecosystem is slow and lasts for several months.

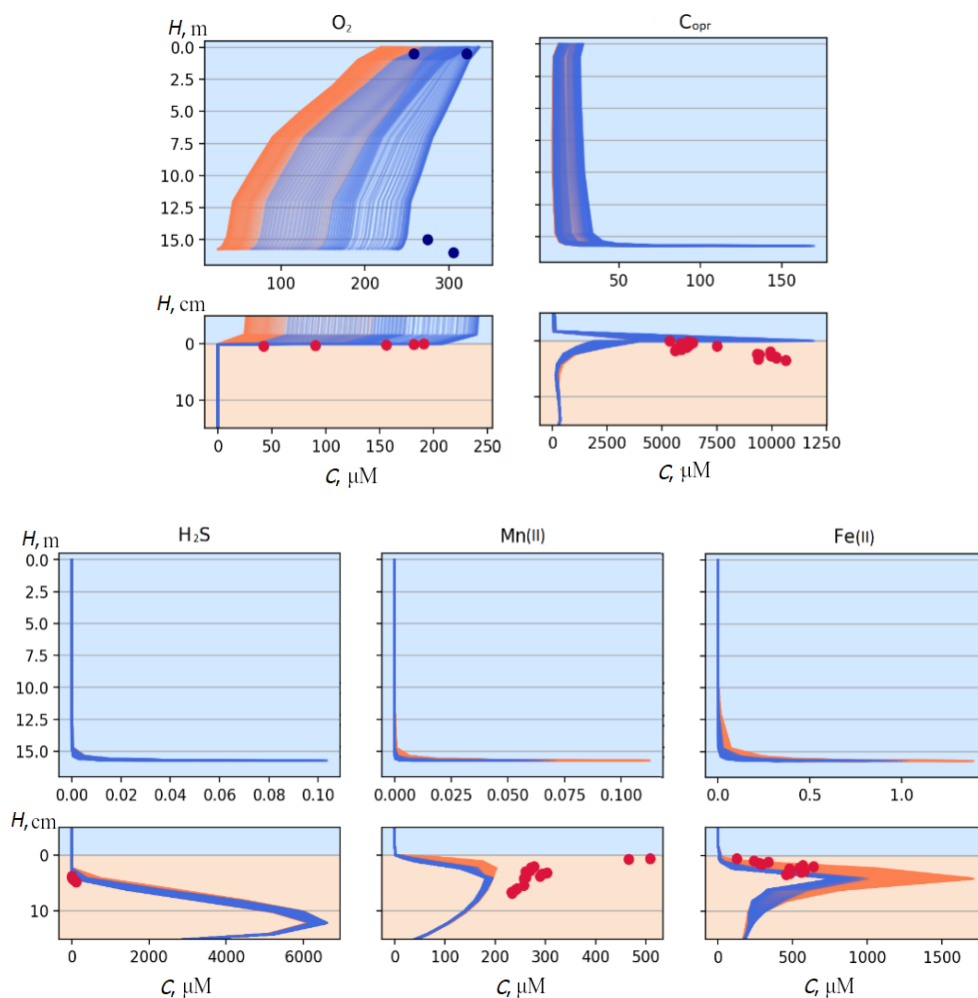


Fig. 5. Calculated seasonal changes of vertical profiles of the concentration of dissolved oxygen (O_2), organic carbon (C_{org}), hydrogen sulfide (H_2S), reduced iron ($Fe(II)$), reduced manganese ($Mn(II)$) and data from *in situ* observations in the water column (upper panels) and in the bottom layer of waters and bottom sediments (lower panels). The orange and blue lines are simulated warm and cold seasons, red and blue dots are *in situ* data in warm and cold seasons

For the second numerical experiment, the OM concentration was reduced by a factor of two compared to the observed concentration in the bay (Fig. 8).

It was found that with a decrease in the load on the bay, the seasonal course of biogeochemical parameters was preserved. The intensity of phytoplankton blooms decreases, and the period of blooms stretches out from March to October. When oxygen is consumed for OM oxidation, suboxic conditions do not arise either in the bottom water layer or in the water column. The minimum oxygen

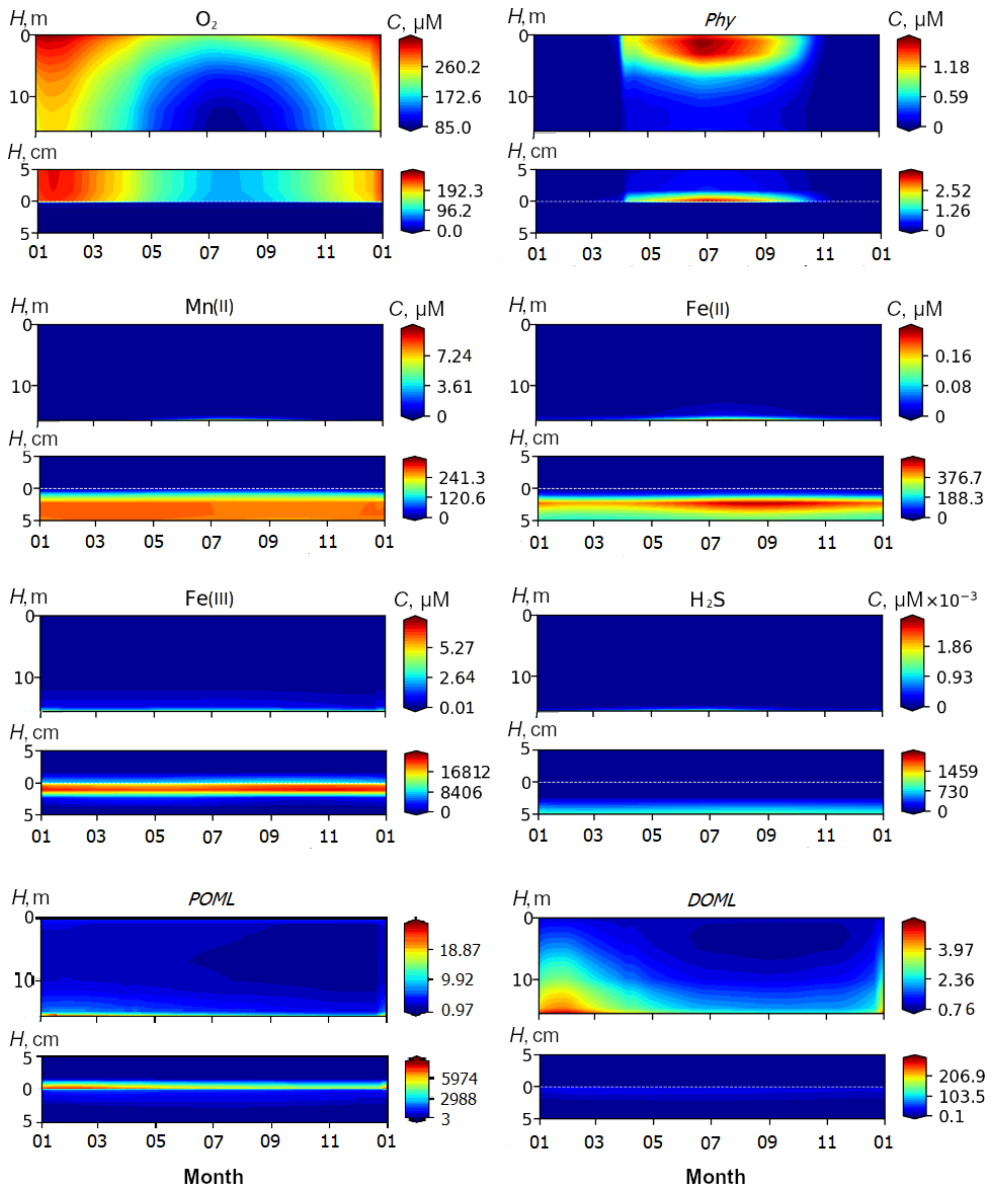


Fig. 6. The results of numerical calculations of seasonal dynamics of the BROM model variables in the water column (upper panels) and in the bottom layer of waters and bottom sediments (lower panels) when adapting the model to the waters of Yuzhnaya Bay. *Phy* – phytoplankton

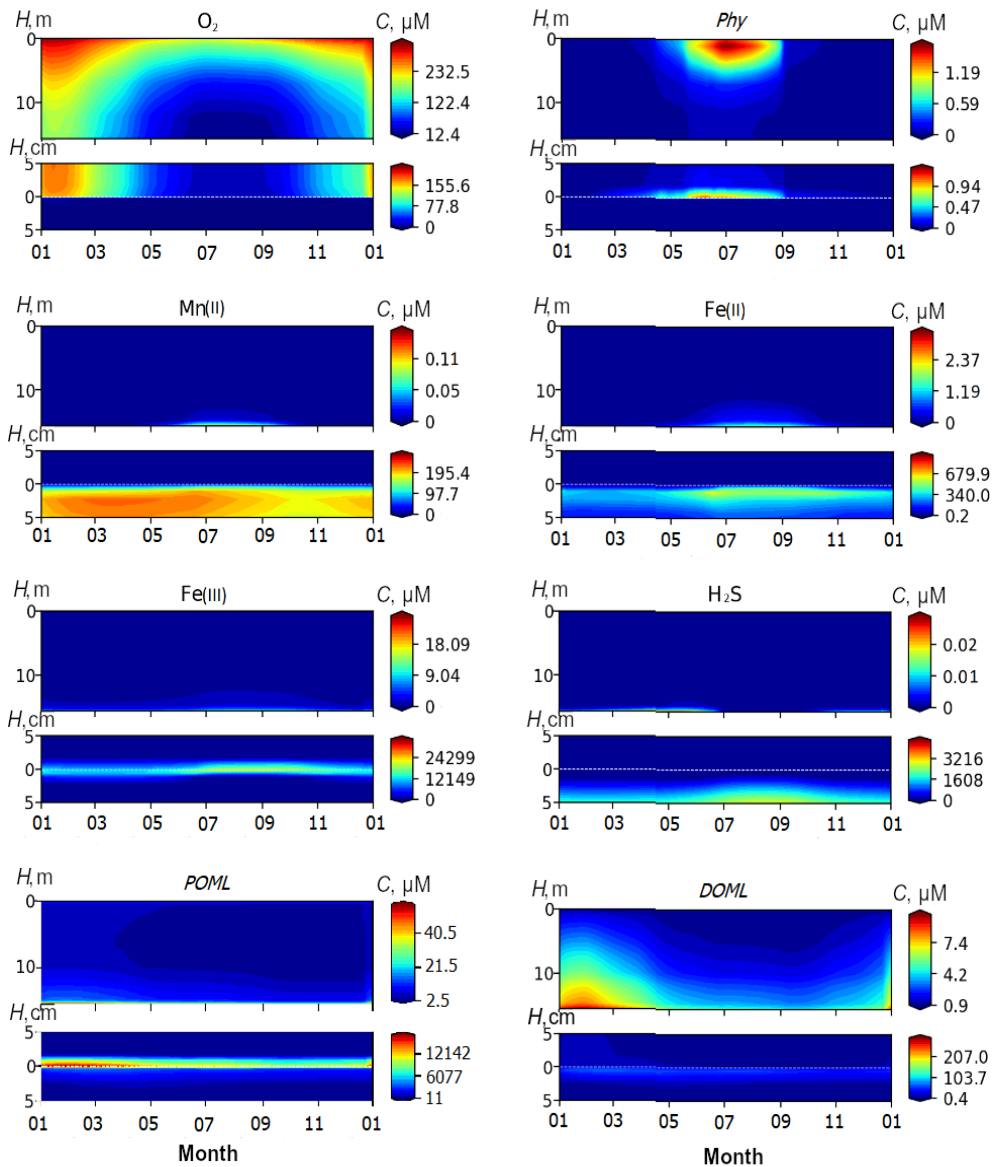


Fig 7. The results of numerical calculations of seasonal dynamics of the BROM model variables in the water column (upper panels) and in the bottom layer of water and bottom sediments (lower panels) with an increase in the content of organic matter. *Phy* – phytoplankton

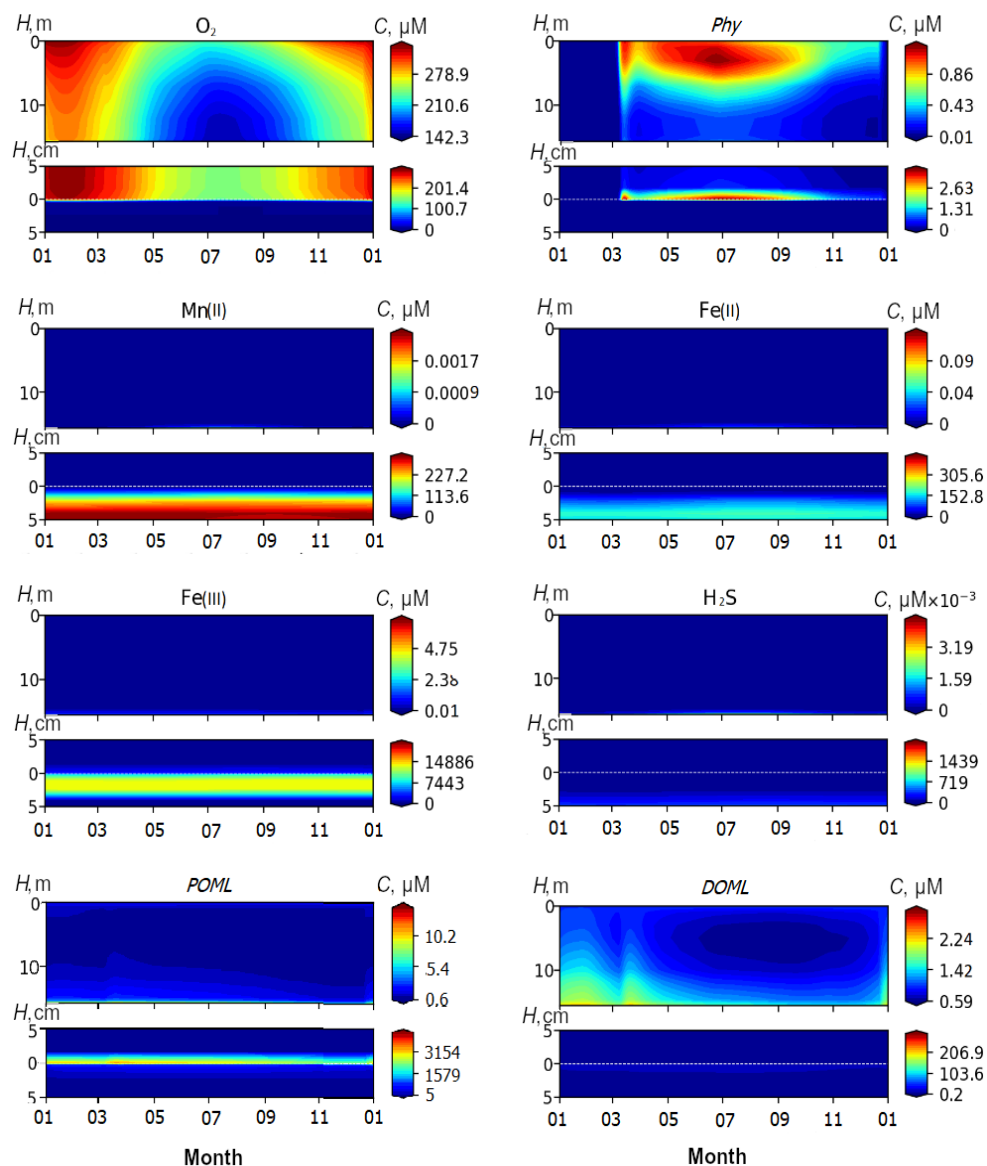


Fig. 8. Results of numerical calculations of seasonal dynamics of variables of the BROM model in the water column (upper panels) and in the bottom layer of waters and bottom sediments (lower panels) with a decrease in the content of organic matter. *Phy* – phytoplankton

concentration (142 μM) in the bottom water layer, which corresponds to aerobic conditions, is observed in July. However, in bottom sediments, despite the presence of oxygen in the bottom water layer, suboxic conditions are fixed, and this fact confirms the presence of reduced forms of iron and manganese in pore waters.

Conclusion

Based on observations and modelling, it is shown that the redox conditions in bottom sediments depend mostly on seasonal changes in the oxygen content in the bottom water layer, the particle size distribution of sediments, and the OM entering them. At the same time, bottom sediments, being a source of secondary water pollution, can also determine the hydrochemical characteristics and redox conditions in the bottom water layer.

It is shown that the BROM model used in the work to assess the redox conditions in the bottom sediments and the near-bottom water layer of Yuzhnaya Bay reproduces the seasonal course of hydrochemical parameters properly. The modelled increase in the load (a doubling of the OM concentration) on the bay water area leads to the OM accumulation and decrease in the oxygen concentration (up to 12 μM), as well as to the seasonal oxygen cycle violation in the bottom water layer. The results of numerical experiments showed that if the OM average annual concentration on the surface increased from 107 to 195 μM , anaerobic conditions developed in the bottom water layer.

The change in the load on the bay water area, which consisted in a twofold decrease in the OM entering the bay, contributed to the fact that the oxygen concentration did not fall below 142 μM throughout the year, and aerobic conditions were preserved in the water column and bottom water layer. However, such a load reduction is not sufficient for bottom sediments. Taking into account the level of accumulated pollutants determined by high concentrations of organic carbon in the surface layer of sediments (> 4 %), the oxygen is still insufficient for OM oxidation, and reduced forms of iron and manganese are still formed in the pore waters, which indicates the development of suboxic conditions in bottom sediments.

REFERENCES

1. Bryantsev, V.A., Litvinenko, N.M. and Sebakh, L.K., 1997. Anthropogenic Impacts on the Black Sea Ecosystem (Results of YugNIRO Nature Protective Studies for the Last Decade). In: YugNIRO, 1997. *Proceedings of the Southern Scientific Research Institute of Marine Fisheries & Oceanography*. Kerch: YugNIRO Publishers. Vol. 43, pp. 16–27 (in Russian).
2. Orekhova, N.A. and Konovalov, S.K., 2018. Oxygen and Sulfides in Bottom Sediments of the Coastal Sevastopol Region of Crimea. *Oceanology*, 58(5), pp. 679–688. <https://doi.org/10.1134/S0001437018050107>
3. Meysman, F.J.R., Middelburg, J.J., Herman, P.M.J. and Heip, C.H.R., 2003. Reactive Transport in Surface Sediments. II. Media: An Object-Oriented Problem-Solving Environment for Early Diagenesis. *Computers and Geosciences*. 2003. Vol. 29, iss. 3. P. 301–318. [https://doi.org/10.1016/S0098-3004\(03\)00007-4](https://doi.org/10.1016/S0098-3004(03)00007-4)
4. Ignat'eva, O.G., Ovsyanyi, E.I., Romanov, A.S., Konovalov, S.K. and Orekhova, N.A., 2008. Analysis of State of the Carbonate System of Waters and Variations of the Content of Organic Carbon in Bottom Sediments of the Sevastopol Bay in 1998–2005. *Physical Oceanography*, 18(2), pp. 96–105. doi:10.1007/s11110-008-9010-x

5. Ivanov, V.A., Ovsyany, E.I., Repetin, L.N., Romanov, A.S. and Ignatyeva, O.G., 2006. *Hydrological and Hydrochemical Regime of the Sebastopol Bay and Its Changing under Influence of Climatic and Anthropogenic Factors*. Sevastopol: MHI, 90 p. (in Russian).
6. Orekhova, N.A. and Varenik, A.V., 2018. Current Hydrochemical Regime of the Sevastopol Bay. *Physical Oceanography*, 25(2), pp. 124–135. doi:10.22449/1573-160X-2018-2-124-135
7. Gurov, K.I. and Kotelyanets, E.A., 2022. Distribution of Trace Metals (Cr, Cu, Ni, Pb, Zn, Sr, Ti, Mn and Fe) in the Vertical Section of Bottom Sediments in the Sevastopol Bay (Black Sea). *Physical Oceanography*, 29(5), pp. 491–507. doi:10.22449/1573-160X-2022-5-491-507
8. Svishchev, S.V., Kondrat'ev, S.I. and Konovalov, S.K., 2011. Regularities of Seasonal Variations in the Content and Distribution of Oxygen in Waters of the Sevastopol Bay. *Physical Oceanography*, 21(4), pp. 280–293. doi:10.1007/s11110-011-9122-6
9. Moiseenko, O.G. and Orekhova, N.A., 2011. Investigation of the Mechanism of the Long-Term Evolution of the Carbon Cycle in the Ecosystem of the Sevastopol Bay. *Physical Oceanography*, 21(2), pp. 142–152. doi:10.1007/s11110-011-9111-9
10. Orekhova, N.A., Medvedev, E.V. and Konovalov, S.K., 2016. Carbonate System Characteristics of the Sevastopol Bay Waters in 2009–2015. *Physical Oceanography*, (3), pp. 36–46. doi:10.22449/1573-160X-2016-3-36-46
11. Ovsyaniy, E.I., Romanov, A.S. and Ignatieva, O.G., 2003. Distribution of Heavy Metals in Superficial Layer of Bottom Sediments of Sevastopol Bay (the Black Sea). *Marine Ecological Journal*, 2(2), pp. 85–93 (in Russian).
12. Romanov, A.S., Orekhova, N.A., Ignatyeva, O.G., Konovalov, S.K. and Ovsyany, E.I., 2007. Influence of Physico-Chemical Characteristics of the Bottom Sediments on the Trace Elements' Distribution by the Example of Sevastopol Bays (Black Sea). *Ekologiya Morya = Ecology of the Sea*, 73, pp. 85–90 (in Russian).
13. Orekhova, N.A. and Konovalov, S.K., 2009. Polarography of the Bottom Sediments in the Sevastopol Bay. *Physical Oceanography*, 19(2), pp. 111–123. doi:10.1007/s11110-009-9038-6
14. Soloveva, O.V. and Tikhonova, E.A., 2018. The Organic Matter Content Dynamics in the Sea Bottom Sediments of the Sevastopol Harbor Water Area. *Scientific Notes of V.I. Vernadsky Crimean Federal University. Biology. Chemistry*, 4(4), pp. 196–206 (in Russian).
15. Malakhova, L.V., Egorov, V.N., Malakhova, T.V., Lobko, V.V., Murashova, A.I. and Bobko, N.I., 2020. Organochlorine Compounds Content in the Components of the Black River Ecosystem and Assessment of their Inflow to the Sevastopol Bay in the Winter Season 2020. *International Journal of Applied and Fundamental Research*, (5), pp. 7–14 (in Russian).
16. Orekhova, N.A., Konovalov, S.K. and Medvedev, E.V., 2019. Features of Inorganic Carbon Regional Balance in Marine Ecosystems under Anthropogenic Pressure. *Physical Oceanography*, 26(3), pp. 225–235. doi:10.22449/1573-160X-2019-3-225-235
17. Yakushev, E.V., Pollehne, F., Jost, G., Kuznetsov, I., Schneider, B. and Umlauf, L., 2007. Analysis of the Water Column Oxidic/Anoxic Interface in the Black and Baltic Seas with a Numerical Model. *Marine Chemistry*, 107(3), pp. 388–410. doi:10.1016/j.marchem.2007.06.003
18. Pakhomova, S., Vinogradova, E., Yakushev, E., Zatsepin, A., Shtereva, G., Chasovnikov, V. and Podymov, O., 2014. Interannual Variability of the Black Sea Proper Oxygen and Nutrients Regime: The Role of Climatic and Anthropogenic Forcing. *Estuarine, Coastal and Shelf Science*, 140, pp. 134–145. doi:10.1016/j.ecss.2013.10.006

19. Kubryakov, A.I., 2004. Application of the Nested Grids Method in Developing the System of Hydrophysical Fields Monitoring in the Coastal Regions of the Black Sea. In: MHI, 2004. *Ekologicheskaya Bezopasnost' Pribrezhnoy i Shel'fovoy Zon i Kompleksnoe Ispol'zovanie Resursov Shel'fa* [Ecological Safety of Coastal and Shelf Zones and Comprehensive Use of Shelf Resources]. Sevastopol: ECOSI-Gidrofizika. Iss. 11, pp. 31–50 (in Russian).
20. Mikhailova, E.N. and Shapiro, N.B., 2005. Simulation of the Circulation and Space Structure of Thermohaline Fields in the Sevastopol Bay with Regard for the Actual External Data (Winter, 1997). *Physical Oceanography*, 15(2), pp. 118–132. doi:10.1007/s11110-005-0035-0
21. Alekseev, D.V., Fomin, V.V., Ivancha, E.V., Kharitonova, L.V. and Cherkesov, L.V., 2012. Mathematical Simulation of Wind Waves in the Sevastopol Bay. *Morskoy Gidrofizicheskiy Zhurnal*, (1), pp. 75–84 (in Russian).
22. Belokopytov, V.N., Kubryakov, A.I. and Pryakhina, S.F., 2019. Modelling of Water Pollution Propagation in the Sevastopol Bay. *Physical Oceanography*, 26(1), pp. 3–12. doi:10.22449/1573-160X-2019-1-3-12
23. Ryabtsev, Yu.N. and Lemeshko, E.M., 2014. [Modelling of Sevastopol Bay Pollutant Distribution for Complex Ecological Monitoring]. In: MHI, 2014. *Ekologicheskaya Bezopasnost' Pribrezhnoy i Shel'fovoy Zon i Kompleksnoe Ispol'zovanie Resursov Shel'fa* [Ecological Safety of Coastal and Shelf Zones and Comprehensive Use of Shelf Resources]. Sevastopol: ECOSI-Gidrofizika. Iss. 28, pp. 165–171 (in Russian).
24. Pavlova, E.V., Ovsjany, E.I. Gordina, A.D., Romanov, A.S. and Kemp, R.B., 1999. Modern State and Tendencies of Change in Sevastopol Bay Ecosystem. In: E. V. Pavlova and N. V. Shadrin, eds., 1999. *Sevastopol Aquatory and Coast: Ecosystem Processes and Services for Human Society*. Sevastopol: Akvavita Publ., pp. 70–94 (in Russian).
25. Ovsyany, E.J., Romanov, A.S., Min'kovskaya, R.Ya., Krasnovid, I.I., Ozyumenko, B.A. and Zymbal, I.M., 2001. Basic Polluting Sources of Sea near Sevastopol. In: MHI, 2001. *Ekologicheskaya Bezopasnost' Pribrezhnoy i Shel'fovoy Zon i Kompleksnoe Ispol'zovanie Resursov Shel'fa* [Ecological Safety of Coastal and Shelf Zones and Comprehensive Use of Shelf Resources]. Sevastopol: ECOSI-Gidrofizika. Iss. 2, pp. 138–152 (in Russian).
26. Osadchaya, T.S., Alyomov, S.V. and Shadrina, T.V., 2004. Ecological Quality of Sevastopol Bay Bottom Sediments: Retrospective and Present-Day State. *Ekologiya Morya = Ecology of the Sea*, 66, pp. 82–87 (in Russian).
27. Minkina, N.I., Samyshev, E.Z. and Kopytov, Yu.P., 2015. Long-Term Changes of Level of Contamination and Development of Plankton in the Sevastopol Bay. *Monitoring Systems of Environment*, (1), pp. 82–93 (in Russian).
28. Sovga, E.E., Mezentseva, I.V. and Khmara, T.V., 2022. Simulation of Seasonal Hydrodynamic Regime in the Sevastopol Bay and of Assessment of the Self-Purification Capacity of its Ecosystem. *Fundamentalnaya i Prikladnaya Gidrofizika*, 15(2), pp. 110–123. doi:10.48612/fpg/92ge-ahz6-n2pt (in Russian).
29. Bersen'eva, G.P. and Gevoriz, N.S., 2003. Variability of Chlorophyll and Pheophytin Concentrations in the Phytoplankton of the Sevastopol Bay during 2000–2001. In: MHI, 2003. *Ekologicheskaya Bezopasnost' Pribrezhnoy i Shel'fovoy Zon i Kompleksnoe Ispol'zovanie Resursov Shel'fa* [Ecological Safety of Coastal and Shelf Zones and Comprehensive Use of Shelf Resources]. Sevastopol: ECOSI-Gidrofizika. Iss. 8, pp. 90–97 (in Russian).
30. Ereemeev, V.N., Konovalov, S.K. and Romanov, A.S., 1998. The Distribution of Oxygen and Hydrogen Sulfide in Black Sea Waters during Winter-Spring Period. *Physical Oceanography*, 9(4), pp. 259–272. doi:10.1007/BF02522712

31. Weiss, R.F., 1970. The Solubility of Nitrogen, Oxygen and Argon in Water and Seawater. *Deep Sea Research and Oceanographic Abstracts*, 17(4), pp. 721–735. doi:10.1016/0011-7471(70)90037-9
32. Brendel, P.J. and Luther III, G.W., 1995. Development of a Gold Amalgam Voltammetric Microelectrode for the Determination of Dissolved Fe, Mn, O₂, and S(-II) in Pore Waters of Marine and Freshwater Sediments. *Environmental Science and Technology*, 29(3), pp. 751–761. doi:10.1021/es00003a024
33. Luther III, G.W., Brendel, P.J., Lewis, B.L., Sundby, B., Lefrançois, L., Silverberg, N. and Nuzzio, D.B., 1998. Simultaneous Measurement of O₂, Mn, Fe, Γ, and S (-II) in Marine Pore Waters with a Solid-State Voltammetric Microelectrode. *Limnology and Oceanography*, 43(2), pp. 325–333. doi:10.4319/lo.1998.43.2.0325
34. Zabegaev, I.A., Shul'gin, V.F. and Orekhova, N.A., 2021. Application of Instrumental Methods for Analysis of Bottom Sediments for Ecological Monitoring of Marine Ecosystems. *Scientific Notes of V.I. Vernadsky Crimean Federal University. Biology. Chemistry*, 7(4), pp. 242–254 (in Russian).
35. Yakushev, E.V., Protsenko, E.A., Bruggeman, J., Wallhead, P., Pakhomova, S.V., Yakubov, Sh.Kh., Bellerby, R.G.J. and Couture, R.-M., 2017. Bottom RedOx Model (BROM v.1.1): a Coupled Benthic–Pelagic Model for Simulation of Water and Sediment Biogeochemistry. *Geoscientific Model Development*, 10(1), pp. 453–482. doi:10.5194/gmd-10-453-2017
36. Yakushev, E.V., Wallhead, P., Renaud, P.E., Illinskaya, A., Protsenko, E., Yakubov, Sh., Pakhomova, S., Sweetman, A.K., Dunlop, K., Berezina, A., Bellerby, R.G.J. and Dale, T., 2020. Understanding the Biogeochemical Impacts of Fish Farms Using a Benthic–Pelagic Model. *Water*, 12(9), 2384. doi:10.3390/w12092384
37. He, Y., Stanev, E.V., Yakushev, E.V. and Staneva, J., 2012. Black Sea Biogeochemistry: Response to Decadal Atmospheric Variability during 1960–2000 Inferred from Numerical Modeling. *Marine Environmental Research*, 77, pp. 90–102. doi:10.1016/j.marenvres.2012.02.007
38. Stanev, E.V., He, Y., Staneva, J. and Yakushev, E., 2014. Mixing in the Black Sea Detected from the Temporal and Spatial Variability of Oxygen and Sulfide – Argo Float Observations and Numerical Modelling. *Biogeosciences*, 11(20), pp. 5707–5732. doi:10.5194/bg-11-5707-2014
39. Yakushev, E., Pakhomova, S., Sørensen, K. and Skei, J., 2009. Importance of the Different Manganese Species in the Formation of Water Column Redox Zones: Observations and Modeling. *Marine Chemistry*, 117(1–4), pp. 59–70. doi:10.1016/j.marchem.2009.09.007
40. Yakushev, E.V., Pollehne, F., Günter, J., Kuznetsov, I., Schneider, B. and Umlauf, L., 2007. *Redox Layer Model (ROLM): A Tool for Analysis of the Water Column Oxidic/Anoxic Interface Processes*. *Meereswissenschaftliche Berichte*, no. 68. Warnemünde, 59 p. doi:10.12754/msr-2007-0068
41. Yakushev, E.V., Kuznetsov, I.S., Podymov, O.I., Burchard, H., Neumann, T. and Pollehne, F., 2011. Modeling the Influence of Oxygenated Inflows on the Biogeochemical Structure of the Gotland Sea, Central Baltic Sea: Changes in the Distribution of Manganese. *Computers and Geosciences*, 37(4), pp. 398–409. doi:10.1016/j.cageo.2011.01.001
42. Yakushev, E.V., ed., 2013. *Chemical Structure of Pelagic Redox Interfaces: Observation and Modeling*. Berlin: Springer, 290 p. doi:10.1007/978-3-642-32125-2

Submitted 18.02.2023; accepted after review 15.04.2023;
revised 03.05.2023; published 26.06.2023

About the authors:

Yulia S. Gurova, Junior Research Associate, Marine Hydrophysical Institute of RAS (2 Kapitanskaya St., Sevastopol, 299011, Russian Federation), **ORCID ID: 0000-0002-9826-4789**, **ResearcherID: AAB-5628-2019**, *kurinnaya-jul@yandex.ru*

Evgeniy V. Yakushev, Chief Research Associate, Shirshov Institute of Oceanology RAS (36 Nahimovskiy Ave., Moscow, 117997, Russian Federation), Dr.Sci. (Phys-Math.), **ORCID ID: 00000-0001-5008-9611**, **ResearcherID: M-5470-2019**, *evgeniy.yakushev@gmail.com*

Anfisa V. Berezina, Leading Engineer, Shirshov Institute of Oceanology RAS (36 Nahimovskiy Ave., Moscow, 117997, Russian Federation), **ORCID: 0000-0001-9356-8807**, **ResearcherID: AAK-7150-2021**, *fisa4247@gmail.com*

Matvey O. Novikov, Engineer, Shirshov Institute of Oceanology RAS (36 Nahimovskiy Ave., Moscow, 117997, Russian Federation), **ORCID ID: 0000-0003-3124-3702**, **ResearcherID: AGP-2782-2022**, *novikov.mo@ocean.ru*

Konstantin I. Gurov, Junior Research Associate, Marine Hydrophysical Institute of RAS (2 Kapitanskaya St., Sevastopol, 299011, Russian Federation), **ORCID ID: 0000-0003-3460-9650**, **ResearcherID: L-7895-2017**, *gurovki@gmail.com*

Natalia A. Orekhova, Head of Marine Biogeochemistry Department, Marine Hydrophysical Institute of RAS (2 Kapitanskaya St., Sevastopol, 299011, Russian Federation), Ph.D. (Geogr.), **ORCID ID: 0000-0002-1387-970X**, **ResearcherID: I-1755-2017**, *natalia.orekhova@mhi-ras.ru*

Contribution of the authors:

Yulia S. Gurova – problem statement, analysis of calculation results, article text and graphic material preparation

Evgeniy V. Yakushev – mathematical model development, performance of calculations, discussion of results, critical analysis and revision of the text

Anfisa V. Berezina – performance of calculations, graphic material preparation

Matvey O. Novikov – correction of the mathematical model

Konstantin I. Gurov – sampling, analysis of geochemical characteristics of bottom sediments, article text and graphic material preparation

Natalia A. Orekhova – analysis of pore water chemical composition, critical analysis and revision of the text

All the authors have read and approved the final manuscript.

Winter Peak of Phytoplankton Bloom in Sevastopol Bay according to Numerical Modeling

K. A. Slepchuk *, T. V. Khmara

Marine Hydrophysical Institute of RAS, Sevastopol, Russia

* e-mail: skira@mhi-ras.ru

Abstract

The winter peak of phytoplankton bloom in the Sevastopol Bay is reproduced using the 3D water quality model MECCA using meteorological data for January 2003. A detailed dynamic pattern of currents' variability, temperature, salinity, concentration of phytoplankton biomass and phosphate phosphorus is reproduced. The formation of an anticyclonic eddy in the central region of the bay is demonstrated, which led to an increase in the phosphorus phosphates concentration and phytoplankton bloom. The maximum of phytoplankton bloom (0.056 gC/m^3) was observed on the 23rd model day in the central part, then the maximum concentration of biomass decreased to 0.047 gC/m^3 in the central and eastern parts of the bay. There was also a decrease in phosphorus phosphates concentration from the maximum 0.0085 gP/m^3 on January, 10 to 0.0049 gP/m^3 on January, 23 in the central part of the bay. The concentration of phytoplankton biomass increased until January, 23, and then decreased, the phosphorus phosphates concentration decreased throughout the whole calculation period. The estimates obtained in the course of numerical modelling generally agree with the observational data. The performed study can serve as a basis for the development and application of a model approach to monitoring and managing of ecosystem processes on shallow water. Using this model, it is possible to calculate various scenarios for the bay eutrophication in case nutrients are discharged.

Keywords: phytoplankton biomass, phytoplankton bloom, biogeochemical simulation, hydrodynamic model, Sevastopol Bay

Acknowledgments: The authors are grateful to E. E. Sovga, Dr.Sci. (Geogr.), for discussion of the manuscript and valuable comments. The work was carried out under state assignment of Marine Hydrophysical Institute of RAS on topic no. FN NN-2021-0005 "Coastal research".

For citation: Slepchuk, K.A. and Khmara, T.V., 2023. Winter Peak of Phytoplankton Bloom in Sevastopol Bay according to Numerical Modeling. *Ecological Safety of Coastal and Shelf Zones of Sea*, (2), pp. 91–104. doi:10.29039/2413-5577-2023-2-91-104

© Slepchuk K. A., Khmara T. V., 2023



This work is licensed under a Creative Commons Attribution-Non Commercial 4.0 International (CC BY-NC 4.0) License

Зимний пик цветения фитопланктона в Севастопольской бухте по результатам численного моделирования

К. А. Слепчук*, Т. В. Хмара

Морской гидрофизический институт РАН, Севастополь, Россия

* e-mail: skira@mhi-ras.ru

Аннотация

В работе производится зимний пик цветения фитопланктона в Севастопольской бухте с помощью трехмерной модели качества вод *МЕССА* с использованием метеоданных за январь 2003 г. Воспроизведена детальная динамическая картина изменчивости течений, температуры, солёности, концентрации биомассы фитопланктона и фосфора фосфатов. Показано образование антициклонической вихревой ячейки в центральном районе бухты, которое привело к увеличению концентрации фосфора фосфатов и цветению фитопланктона в этом районе. Максимум цветения фитопланктона (0.056 гС/м^3) наблюдался 23 января в центральном районе, затем максимальная концентрация биомассы снизилась до 0.047 гС/м^3 в центральном и восточном районах бухты. Также прослеживается уменьшение концентрации фосфора фосфатов от максимальных 0.0085 гР/м^3 10 января до 0.0049 гР/м^3 23 января в центральном районе бухты. Концентрация биомассы фитопланктона растёт до 23 января, а затем снижается, концентрация фосфора фосфатов снижается на протяжении всего расчетного периода. Оценки, полученные в ходе численного моделирования, в целом соответствуют данным наблюдений. Выполненное исследование может служить основой для развития и применения модельного подхода к мониторингу и управлению экосистемными процессами в мелководных водоемах. С помощью данной модели можно рассчитать различные сценарии эвтрофирования бухты при сбросах в нее биогенных веществ.

Ключевые слова: биомасса фитопланктона, цветение фитопланктона, биогеохимическое моделирование, гидродинамическая модель, Севастопольская бухта

Благодарности: авторы выражают благодарность доктору географических наук Совге Елене Евгеньевне за обсуждение рукописи и ценные замечания. Работа выполнена в рамках государственного задания ФГБУН ФИЦ МГИ по теме № FNNN-2021-0005 «Прибрежные исследования».

Для цитирования: Слепчук К. А., Хмара Т. В. Зимний пик цветения фитопланктона в Севастопольской бухте по результатам численного моделирования // Экологическая безопасность прибрежной и шельфовой зон моря. 2023. № 2. С. 91–104. EDN PLLXAZ. doi:10.29039/2413-5577-2023-2-91-104

Introduction

The coastal areas of the sea, especially closed and semi-closed water areas, which include Sevastopol Bay, experience a significant man-caused load. Limited water exchange with the sea results in the pollution of the bay and prevents rapid self-purification. The stationary sources of pollution are economic and recreational facilities located on the shores of the bay, as well as ship moorings. More than thirty temporary and permanent wastewater and municipal sewage outlets, as well as

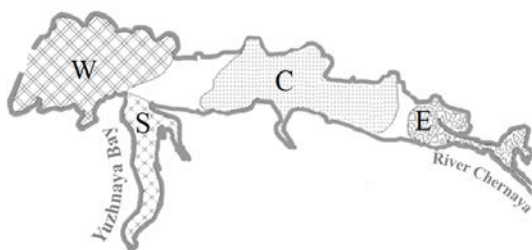


Fig. 1. Sevastopol Bay zoning according to the pollution level [2]: W – mild pollution zone; E – moderate pollution zone; C – strong pollution zone; S – very strong pollution zone

clean zones and zones of a stable high level of pollution (e.g., Yuzhnaya Bay) are formed in Sevastopol Bay [1]. According to the pollution level, the water area of Sevastopol Bay was divided into four zones (Fig. 1) [2].

When assessing the ecological state of the Sevastopol Bay ecosystems, it is also necessary to take into account the seasonality of biological processes (warm and cold periods), which determine the inclusion of nutrients in the composition of the waterbody primary production, their deposition in bottom sediments, and subsequent recycling resulted from the destruction of organic matter.

The winter period is one of the most important seasons for the shallow water ecosystems. The winter phytoplankton bloom in the bay is stipulated by an increase in the supply of nutrients resulted from the decomposition of organic matter in deeper layers with good vertical mixing throughout the entire water column of the bay.

An increase in the eutrophication level of a waterbody is one of the negative results of human impact on nature due to the saturation of the water area with nutrients, which is accompanied by an increase in phytoplankton biomass. Phytoplankton, being the initial element in the food chain of an aquatic ecosystem, produces organic matter with higher energy content from inorganic substances with low energy content. Phytoplankton can indicate the state of the ecosystem, because the state and development of zooplankton and fish depends on it.

Previously, the problem of the phytoplankton biomass modelling in Sevastopol Bay was solved using a 2D ecological model of the reaction-diffusion class [3]. In this model, the photosynthetic rate does not depend on the concentration of nutrients due to the fact that the bay is excessively enriched with them. Among other things, there is no dependence on water temperature. The only factor limiting the process in this model is light. Using a 3D physical and biochemical model [4], the concentration fields of phytoplankton biomass and nutrients in Sevastopol Bay were calculated for wind conditions prevailing in July, while in this work the photosynthetic rate depended on the concentration of nutrients and light.

runoff from the river Chernaya transport untreated or conditionally treated waters with pollutants of various nature to the bay. The consequences of such discharges depend on a number of physical, chemical and biological processes, the result of which is the response of phytoplankton.

Depending on the localization of pollution sources, morphometric characteristics and hydrometeorological conditions, both relatively

The aim of this work is to study the formation of the winter peak of phytoplankton bloom in the waters of Sevastopol Bay based on mathematical modelling, taking into account the variability of temperature and water dynamics in winter, as well as to assess the effect of phytoplankton bloom on changes in the eutrophication level of the bay.

Materials and methods

Using a numerical non-stationary 3D model MECCA¹⁾ (Model for Estuarine and Coastal Assessment) and chemical and biological module, the fields of variability of phytoplankton biomass, phosphate phosphorus, ammonium nitrogen, nitrates and nitrites, and oxygen in Sevastopol Bay in the period from January 1 to January 31 of the model year were calculated. Model days correspond to the days of the month. Previously, this model was standardized in a 1D version in order to obtain the specific rates of chemical and biological processes and coefficients reflecting the characteristics of the environment and external factors in empirical equations [5]. Using a standardized 1D version of the model, the annual variation of the phytoplankton biomass, the content of phosphorus phosphates, ammonium nitrogen, nitrite nitrogen and nitrate nitrogen, and oxygen in Sevastopol Bay was calculated. In addition, the annual variation of the E-TRIX eutrophication index was calculated both in the entire bay and in each of its zones [6, 7]. The results of calculations using the hydrodynamic module of the MECCA model 3D version are presented in [8].

The mathematical structure of the chemical and biological module of the MECCA model is based on the synthesis of known theoretical and applied water quality models [9]. When constructing the module, it is taken into account that the rates of phosphatization and ammonification of organic matter can be different. Inclusion of concentrations of nitrogen and phosphorus organic and inorganic forms in the structure of the model as variables makes it possible to automatically take into account possible differences in the ratios between nitrogen and phosphorus in the composition of autochthonous and allochthonous (including those coming from anthropogenic sources) organic matter. The combination of phosphorus and nitrogen cycles in the model is based on the equation of phytoplankton dynamics, which describes the primary production of organic matter by phytoplankton in the process of photosynthesis, as well as the replenishment of inert organic matter (in units of phosphorus and nitrogen) as a result of respiration, natural death rate, and phytoplankton grazing.

The following hydrochemical and hydrobiological characteristics are considered as model variables: phytoplankton biomass B_{ph} , constant P_{rpop} and labile P_{lpop} fractions of organic phosphorus in detritus, constant P_{rdop} and labile P_{ldop} fractions of dissolved organic phosphorus, mineral dissolved phosphorus P_{dip} , constant N_{rpon} and labile N_{lpon} fractions of organic nitrogen in detritus, constant N_{rdon} and labile N_{ldon} fractions of dissolved organic nitrogen, ammonium nitrogen N_{nh4} , nitrogen of

¹⁾ Hess, K.W., 1989. *MECCA Programs Documentation*. Washington, D.C.: U.S. Department of Commerce, 266 p. Available at: https://repository.library.noaa.gov/view/noaa/19301/noaa_19301_DS1.pdf [Accessed: 08 June 2023].

nitrites and nitrites $N_{\text{no3+no2}}$, constant C_{rdoc} and labile C_{lpoc} fractions organic carbon in detritus, constant C_{rdoc} and labile C_{ldoc} fractions of dissolved organic carbon, dissolved organic carbon emitted by algae C_{exdoc} , dissolved oxygen O_2 [10].

The model uses the assumption of the constancy of the organic matter chemical composition in accordance with its stoichiometric model $(\text{CH}_2\text{O})_{106}(\text{NH}_3)_{16}\text{H}_3\text{PO}_4$. Thus, the ratio between carbon, nitrogen and phosphorus in organic matter is C:N:P = 106:16:1 (μmol)². Since mineral phosphorus limits the phytoplankton bloom, we present the equations of phytoplankton biomass and phosphate phosphorus.

Phytoplankton biomass B_{ph} (gC/m³):

$$\frac{dB_{\text{ph}}}{dt} = [G_{\text{B}} - k_{\text{pr}}(T) - k_{\text{grz}}(T)]B_{\text{ph}},$$

where t – time, day; T – water temperature, °C; G_{B} – specific gross production, 1/day; k_{pr} – specific metabolic rate (respiration), 1/day; k_{grz} – specific rate of grazing of phytoplankton by zooplankton and natural death rate of phytoplankton, 1/day, which are written as the following functional dependencies:

$$G_{\text{B}} = G_{\text{Bmax}} G_T(T) G_I(T) G_{\text{NP}}(N_{\text{din}}, P_{\text{dip}}),$$

$$G(I) = \frac{1}{\Delta Z} \int_{Z_i}^{Z_{i+1}} f_Z(I_Z) dZ = \frac{2.718 f_d}{\Delta Z \alpha} [\exp(-R_{Z_i}) - \exp(-R_{Z_{i+1}})],$$

$$R_0 = \frac{I_a}{I_{\text{opt}}}, \quad R_{Z_i} = R_0 \exp(-\alpha Z_i), \quad \Delta z = z_{i+1} - z_i,$$

$$f_Z(I_Z) = \frac{I_Z}{I_{\text{opt}}} \exp\left(1 - \frac{I_Z}{I_{\text{opt}}}\right), \quad I_Z = I_a \exp(-\alpha z),$$

$$G_{\text{NP}}(N_{\text{din}}, P_{\text{dip}}) = \min\left\{\frac{N_{\text{din}}}{K_{\text{mn}} + N_{\text{din}}}, \frac{P_{\text{dip}}}{K_{\text{mp}} + P_{\text{dip}}}\right\},$$

where $N_{\text{din}} = N_{\text{nh4}} + N_{\text{no3+no2}}$;

$$G_T(T) = \begin{cases} e^{\varepsilon_1 (T-T_m)^2}, & \text{если } T \leq T_m, \\ e^{\varepsilon_2 (T_m-T)^2}, & \text{если } T > T_m, \end{cases}$$

$$k_{\text{pr}}(T) = r_g G_{\text{B}} + r_b \theta_{\text{pr}}^{(T-20)},$$

$$k_{\text{grz}}(T) = k_{\text{grz}}(20) \theta_{\text{grz}}^{(T-20)}.$$

Here, G_{Bmax} – maximum specific gross production, 1/day; I_a – average daylight flow of photosynthetically active radiation (PAR) that penetrates the sea surface, W/m²;

²) Alekin, O.A. and Lyakhin, Yu.I., 1984. *Chemistry of the Ocean*. Leningrad: Gidrometeoizdat, 343 p. (in Russian).

I_{opt} – optimal irradiance for photosynthesis, W/m^2 ; f_d – proportion of daylight hours per day and night period ($0 \leq f_d \leq 1$); I_z – irradiance at depth z , W/m^2 ; α – integral coefficient of PAR intensity attenuation with depth; K_{mn} , K_{mp} – half-saturation constants of the utilization rate of nitrogen and phosphorus mineral forms by phytoplankton, respectively, g/m^3 ; T_m – water temperature optimal for algae growth, $^{\circ}C$; ζ_1 , ζ_2 – coefficients that determine the nature of the temperature influence on the growth of algae in the ranges above and below T_m , $1/^{\circ}C^2$; r_g – proportion of algae production that is spent on the photosynthesis energy supply; r_b – specific algae metabolic rate at $20^{\circ}C$, 1/day; θ_{pr} – coefficient of temperature influence on metabolic rate; $k_{grz}(20)$ – specific rate of grazing and death of phytoplankton at $20^{\circ}C$, 1/day; θ_{grz} – coefficient of temperature effect on the rate of algae grazing and death.

Mineral dissolved phosphorus P_{dip} ($\Gamma P/M^3$):

$$\frac{dP_{dip}}{dt} = \alpha_{pc} f_{dip} (k_{pr}(T) + k_{grz}(T)) B_{ph} + (k_{mrdp} \theta_{mrdp}^{T-20} P_{rdop} + k_{mldp} \theta_{mldp}^{T-20} P_{ldop}) \frac{O_2}{K_{O_2} + O_2} - \alpha_{pc} (1 - f_{exB}) G_B B_{ph},$$

where α_{pc} – coefficient expressing the stoichiometric ratio between carbon and phosphorus in organic matter, gP/gC ; k_{mrdp} – specific rate of mineralization of dissolved organic phosphorus stable fraction at $20^{\circ}C$ water, 1/day; θ_{mrdp} – temperature coefficient; k_{mldp} – specific rate of mineralization of the dissolved organic phosphorus labile fraction at $20^{\circ}C$ water, 1/day; θ_{mldp} – temperature coefficient; K_{O_2} – process half-saturation constant in relation to available oxygen concentration, gO_2/m^3 ; f_{dip} – proportion of mineral phosphorus in the algae metabolic secretions, remains of dead and grazed algae; f_{exB} – proportion of algae primary production that is excreted as dissolved organic matter. The parameters and empirical coefficients used in the calculations are shown as follows:

G_{Bmax}	1.88 1/day	θ_{grz}	1.1
ζ_1	0.006 $1/^{\circ}C^2$	α_{pc}	0.022 gP/gC
ζ_2	0.006 $1/^{\circ}C^2$	f_{dip}	0.2
T_m	$9.5^{\circ}C$	k_{mrdp}	0.01
K_{mn}	$0.025 gN/m^3$	θ_{mrdp}	1.08
K_{mp}	$0.0025 gP/m^3$	k_{mldp}	0.1
r_g	0.2	θ_{mldp}	1.08
r_b	0.01	K_{O_2}	1 gC/m^3
θ_{pr}	1.067	f_{exB}	0.1
k_{gZr}	0.05 1/day		

During calculations, the water area of the bay was covered with a grid of 47×97 nodes with a step of 80 m and was divided into 10 model levels along

the vertical in the σ -coordinate system. Data on air temperature and wind impact were estimated from measurements at the hydrometeorological station at Cape Pavlovsky on the southern shore of Sevastopol Bay. Urgent data on wind speed and direction, air temperature for 2003 with a 6-hour interval, monthly average data on humidity and cloud cover for 2003 were used for modelling.

At the boundary between the bay and the open sea, average monthly values of temperature, salinity, phytoplankton biomass, phosphorus phosphates, nitrogen nitrates, nitrites and ammonium, oxygen on the surface and at the bottom were set. At the boundary between the bay and the river, daily values of temperature, salinity, phytoplankton biomass, phosphorus phosphates, nitrogen nitrates, nitrites and ammonium, oxygen on the surface and at the bottom of the river were set. The initial fields of temperature, salinity, phytoplankton biomass, content of nutrients and oxygen were set to be horizontally homogeneous.

Results

The cumulative effect of a number of factors, among which air and water temperature, waterbody hydrodynamic regime, and concentration of nutrients (mainly inorganic phosphorus), plays a significant role in the development of phytoplankton in shallow water areas.

The air temperature in January 2003 was characterized by strong fluctuations (from -5 to 15 °C) in the first half of the month and was relatively stable (about 5 °C) in the last third of January (Fig. 2). Such changes in air temperature affected the surface water temperature in the bay. *In situ* data analysis showed that the low air temperature in January 2003 led to the upper water layer cooling [11].

In January, low salinity was noted. The main reason for its change in the study area is a salinity decrease in the surface layer caused by rains during the survey period and just before [11].

The wind regime is the main factor determining the dynamics of waters in shallow water areas. Fig. 3 shows the windroses in Sevastopol Bay in January 2003: from 1 to 19 January, from 20 to 26 January, and from 27 to 31 January.

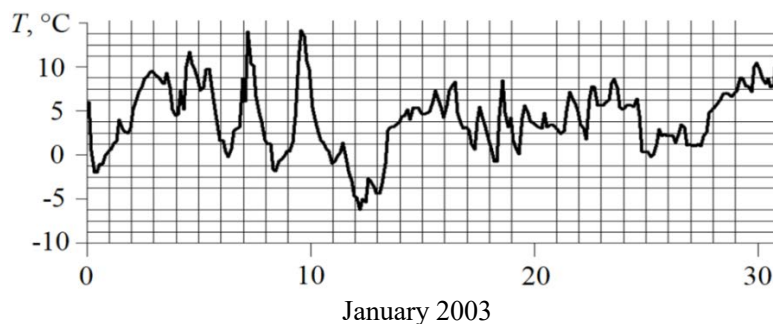


Fig. 2. Changes in air temperature in Sevastopol Bay area in January 2003

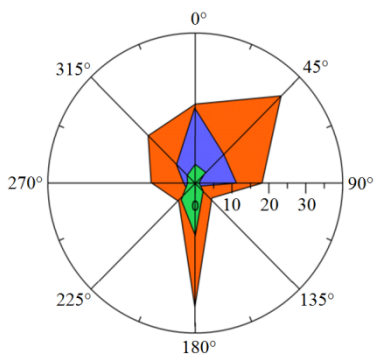


Fig. 3. Windroses from 1 to 19 January (red colour), from 20 to 26 January (blue colour) and from 27 to 31 January (green colour) 2003

In the first half of the month, the wind regime was very variable. Winds of all directions were observed with the predominance of southerly winds. From January 20, mainly northerly and northeasterly winds were observed, which from January 27 changed their direction to the south, southwest.

The structure and speed of currents in a reservoir affect production processes both directly and indirectly. The direct effect is manifested in the mechanical effect on the growth and development of phytoplankton, and the indirect effect is shown through the change in the physical and chemical conditions of algae vegetation.

The distribution of currents and water temperature in the Sevastopol Bay was obtained using a 3D hydrothermodynamic model. The pattern of currents in the bay is influenced by shallow depths, as well as by the large length and indentation of the coastline. The structure of the currents corresponds to the average climate for the winter period, obtained in [12] with an easterly wind. According to the calculation results, the current is directed from the bay to the open sea, while the highest vorticity is typical for the eastern part of the bay (Fig. 4).

Wind direction and bottom topography have the main effect on the formation of currents in the central region of the bay. In winter, there is almost no fresh water inflow from the river Chernaya. During the period of winter cooling, a sharp cooling of surface waters and activation of convective mixing lead to the appearance of many irregular structures in the overall flow pattern. One of the eddies is observed in the central region.

Figures 5 and 6 show the dynamics of phytoplankton biomass, phosphate phosphorus for the 10th, 17th, 23rd, and 29th model days. The table shows the values

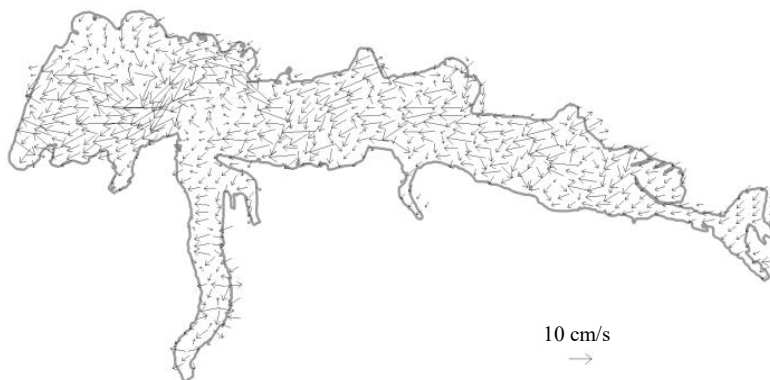


Fig. 4. Map of currents on the bay water surface on the 23rd model day

Variability range (above the line) and average values (under the line) of the phytoplankton biomass concentration B_{Ph} , gC/m^3 , and phosphate phosphorus PO_4 , gP/m^3 , in the Sevastopol Bay areas

Model day	Area	Concentration	
		B_{Ph}	PO_4
10	W	<u>0.0222–0.0355</u> 0.0307	<u>0.0011–0.0069</u> 0.0059
	S	<u>0.0272–0.0385</u> 0.0332	<u>0.0032–0.0078</u> 0.0064
	C	<u>0.0325–0.0444</u> 0.0404	<u>0.00590.0094</u> 0.0086
	E	<u>0.0238–0.0432</u> 0.0383	<u>0.0009–0.0094</u> 0.0085
17	W	<u>0.0235–0.035</u> 0.0306	<u>0.0014–0.0041</u> 0.0033
	S	<u>0.0306–0.0387</u> 0.0343	<u>0.0025–0.0048</u> 0.004
	C	<u>0.0401–0.0526</u> 0.047	<u>0.0053–0.0067</u> 0.0061
	E	<u>0.0282–0.0525</u> 0.0488	<u>0.0007–0.0068</u> 0.0061
23	W	<u>0.0242–0.0472</u> 0.0416	<u>0.0012–0.0038</u> 0.0032
	S	<u>0.0301–0.051</u> 0.0411	<u>0.0022–0.0042</u> 0.0034
	C	<u>0.0455–0.056</u> 0.0537	<u>0.0045–0.0053</u> 0.0049
	E	<u>0.0294–0.0553</u> 0.0504	<u>0.0006–0.0053</u> 0.0048
29	W	<u>0.0221–0.0343</u> 0.0291	<u>0.0009–0.0021</u> 0.0016
	S	<u>0.0294–0.036</u> 0.0332	<u>0.0009–0.0021</u> 0.0016
	C	<u>0.0377–0.0472</u> 0.0429	<u>0.0027–0.0041</u> 0.0033
	E	<u>0.029–0.0474</u> 0.0436	<u>0.0006–0.0043</u> 0.0039

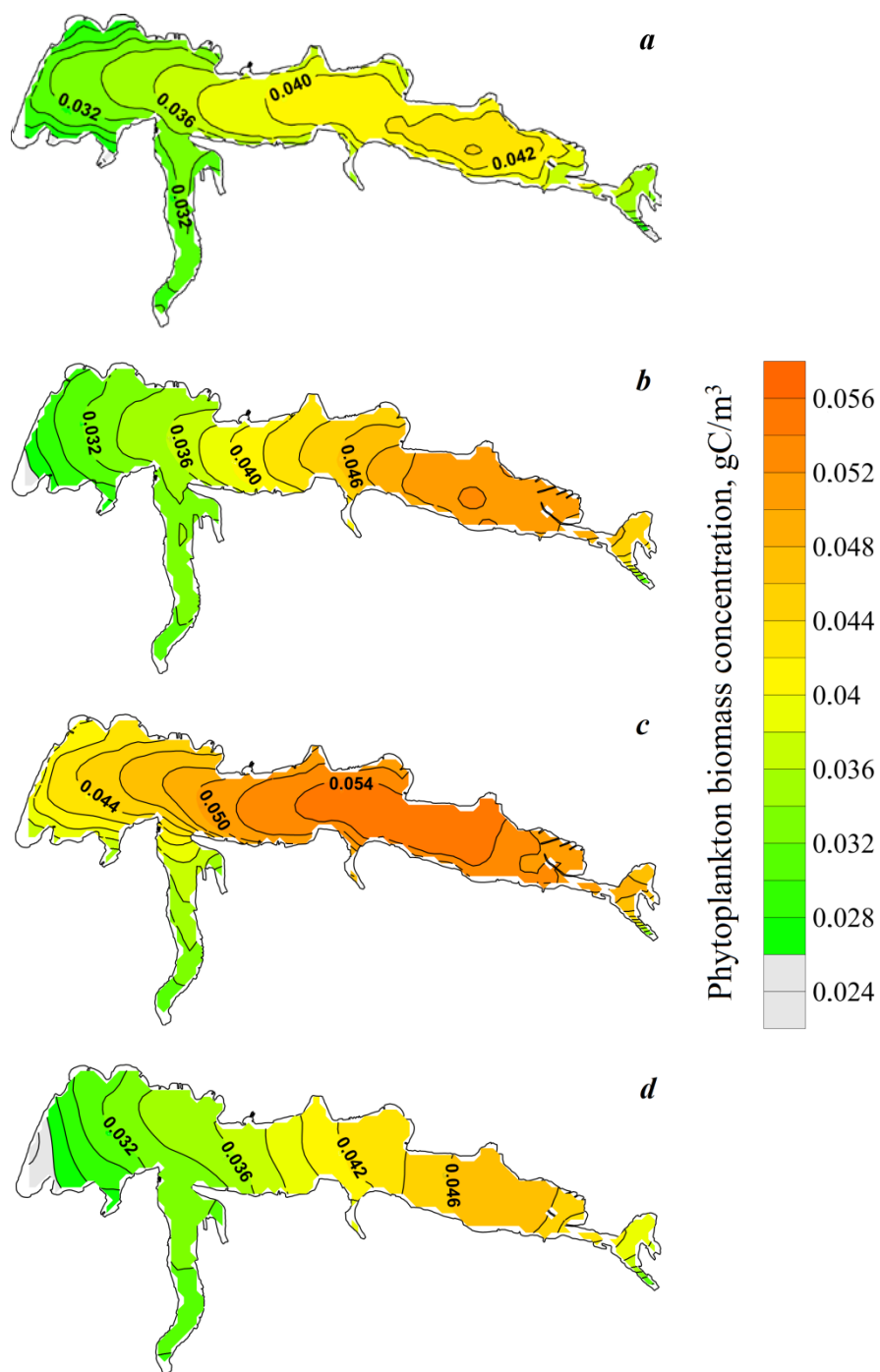


Fig. 5. Phytoplankton biomass concentration, gC/m^3 , on the 10th (*a*), 17th (*b*), 23rd (*c*) and 29th (*d*) model days in Sevastopol Bay

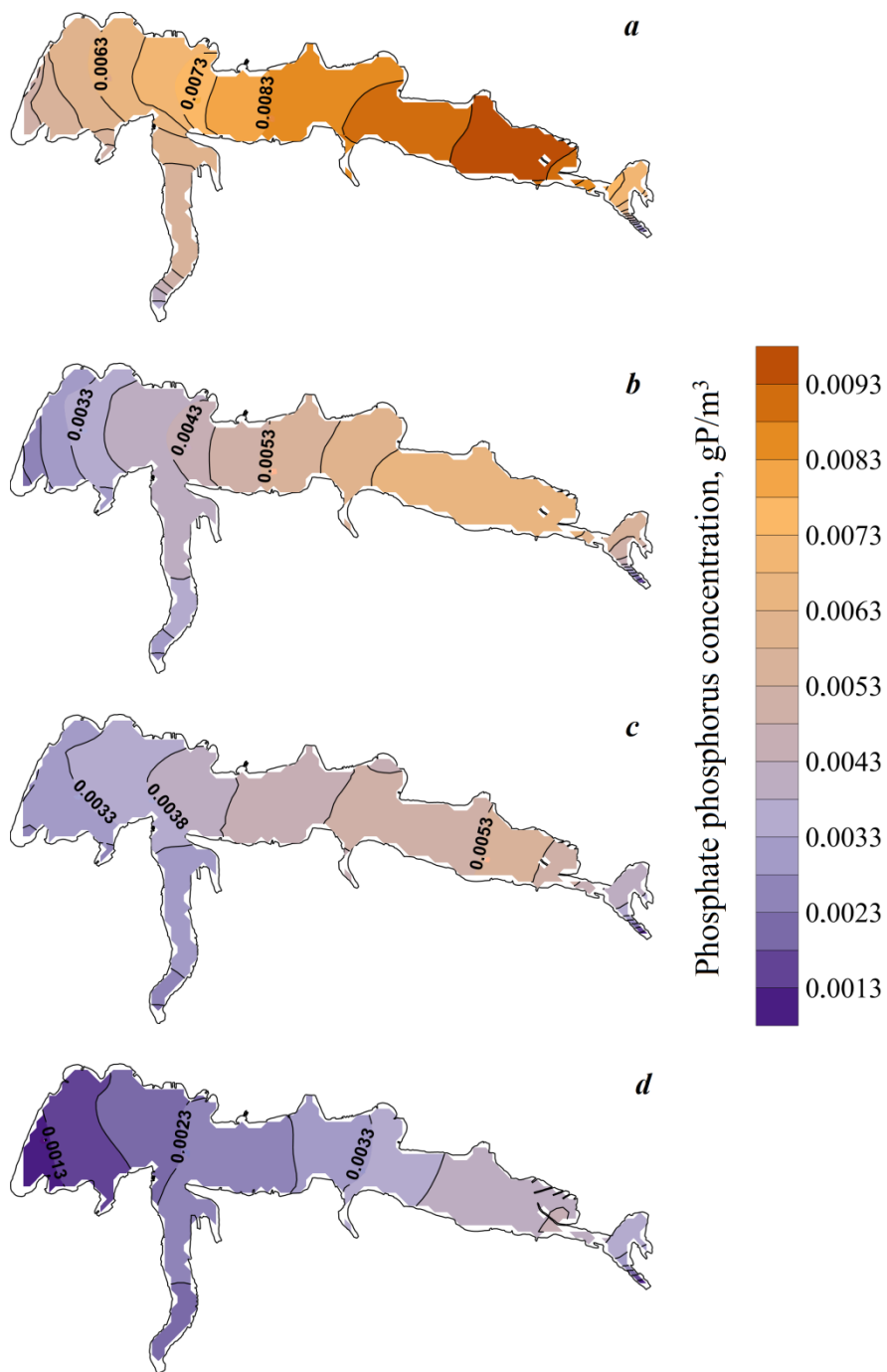


Fig. 6. Phosphate phosphorus concentration, gP/m^3 , on the 10th (*a*), 17th (*b*), 23rd (*c*) and 29th (*d*) model days in Sevastopol Bay

of these indicators on average, as well as their range of variability in the western (W), southern (S), central (C), eastern (E) areas of the bay according to zoning in [2] (see Fig. 1). The highest concentrations of phytoplankton biomass and phosphorus phosphates over the entire model period are observed in the eastern and central regions. The maximum phytoplankton bloom is observed on the 23rd model day – 0.056 gC/m^3 in the central region, then the maximum biomass concentration decreases to 0.047 gC/m^3 in the central and eastern regions. In addition, in the central region of the bay, a decrease in the concentration of phosphorus phosphates is observed from the maximum 0.0085 gP/m^3 on the 10th model day to 0.0049 gP/m^3 on the 23rd model day. This confirms the fact that phosphorus, being the limiting element, is consumed by phytoplankton.

The blooming area in the central region can be explained by the formed eddy, due to which an area with an increased concentration of phosphorus phosphates, as well as an increased temperature, compared to other areas of the bay, appeared, which is a favourable factor for the development of algae. If the phytoplankton biomass concentration increases on average in the bay from 0.0357 gC/m^3 on the 10th model day to 0.0467 gC/m^3 on the 23rd model day, and then decreases to 0.0372 gC/m^3 on the 29th model day, then the concentration of phosphorus phosphates during the entire model period decreases from 0.0074 gP/m^3 on the 10th model day to 0.0028 gP/m^3 on the 29th model day. This fact also indicates the consumption of phosphorus phosphates by phytoplankton and, due to its shortage by the end of the model period, a decrease in the concentration of phytoplankton biomass. The results obtained are in good agreement with the experimental data described in [11, 13, 14].

Conclusion

The performed numerical modelling of the winter phytoplankton bloom in the Sevastopol Bay under the meteorological conditions of January 2003 makes it possible to trace the dynamics of phytoplankton and phosphorus phosphates in different regions of the bay. The peak of phytoplankton bloom is observed on the 23rd model day in the central region of the bay, while the concentration of phosphorus phosphates decreases throughout the model period. The maximum values of the concentrations of these parameters in the central region of the bay are stipulated by the formed eddy and increased water temperature. The estimates obtained in the course of numerical simulation generally agree with the observational data.

Despite the fact that, in the absence of observational data, the results of modelling serve only as an indirect estimate, their use will help advance the understanding of the mechanisms of ecological processes and outline the direction of future clarifying studies. Through modelling, it is also possible to calculate various scenarios for the bay eutrophication with an increase in the volume of nutrients discharged into it.

The performed study can serve as a basis for further development of the model approach and its application to the monitoring and management of ecosystem processes in shallow waterbodies.

REFERENCES

1. Pavlova, E.V., Ovsjanyi, E.I., Gordina, A.D., Romanov, A.S. and Kemp, R.B., 1999. *Modern State and Tendencies of Change in Sevastopol Bay Ecosystem*. In: E. V. Pavlova and N. V. Shadrin, eds., 1999. Sevastopol Aquatory and Coast: Ecosystem Processes and Services for Human Society. Sevastopol: Aquavita Publ., pp. 70–94 (in Russian).
2. Ivanov, V.A., Ovsyany, E.I., Repetin, L.N., Romanov, A.S. and Ignatyeva, O.G., 2006. *Hydrological and Hydrochemical Regime of the Sevastopol Bay and its Changing under Influence of Climatic and Anthropogenic Factors*. Sevastopol: MHI, 90 p. (in Russian).
3. Lyubartsev, V.G. and Lyubartseva, S.P., 2008. Development of Two Dimensional Models of King of Reaction-Diffusion. In: MHI, 2008. *Ekologicheskaya Bezopasnost' Pribrezhnoy i Shel'fovoy Zon i Kompleksnoe Ispol'zovanie Resursov Shel'fa* [Ecological Safety of Coastal and Shelf Zones and Comprehensive Use of Shelf Resources]. Sevastopol: ECOSI-Gidrofizika. Iss. 16, pp. 314–322 (in Russian).
4. Filippova, T.A., Vasechkina, E.F. and Kubryakov, A.I., 2018. Numerical Simulation of Biochemical Processes in a Sea Coastal Zone. In: FSBSI “AzNIIRKH”, 2018. *Current Issues of Fisheries, Fish Breeding (Aquaculture), and Ecological Monitoring of Aquatic Ecosystems: Proceedings of the International Scientific and Practical Conference, dedicated to the 90th Anniversary of the Azov Sea Research Fisheries Institute. Rostov-on-Don, December 11–12, 2018*. Rostov-on-Don: FSBSI “AzNIIRKH” Publ., pp. 357–361 (in Russian).
5. Slepchuk, K.A. and Khmara, T.V., 2017. Usage of the Optimization Method during a Calibration of the Biogeochemical Model. *Ecological Safety of Coastal and Shelf Zones of Sea*, (2), pp. 90–97 (in Russian).
6. Slepchuk, K.A., Khmara, T.V. and Man'kovskaya, E.V., 2017. Comparative Assessment of the Trophic Level of the Sevastopol and Yuzhnaya Bays Using E-TRIX Index. *Physical Oceanography*, (5), pp. 60–70. <https://doi.org/10.22449/1573-160X-2017-5-60-70>
7. Slepchuk, K.A., 2020. Comparative Analysis of Eutrophication Level of the Sevastopol Bay Areas Based on the Results of E-TRIX Index Numerical Modeling. In: T. O. Chaplina, ed., 2020. *Processes in GeoMedia – Volume I*. Cham: Springer, pp. 101–107. https://doi.org/10.1007/978-3-030-38177-6_12
8. Sovga, E.E., Mezentseva, I.V. and Khmara, T.V., 2022. Simulation of Seasonal Hydrodynamic Regime in the Sevastopol Bay and of Assessment of the Self-Purification Capacity of its Ecosystem. *Fundamental and Applied Hydrophysics*, 15(2), pp. 110–123 (in Russian).
9. Ivanov, V.A. and Tuchkovenko, Yu.S., 2008. *Applied Mathematical Water-Quality Modeling of Shelf Marine Ecosystems*. Sevastopol: ECOSI-Gidrofizika, 311 p.
10. Tuchkovenko, Yu.S., Three-Dimensional Mathematical Model of Water Quality in Dneprovsko-Bugsky Estuary of the Northwestern Black Sea. In: MHI, 2005. *Ekologicheskaya Bezopasnost' Pribrezhnoy i Shel'fovoy Zon i Kompleksnoe Ispol'zovanie Resursov Shel'fa* [Ecological Safety of Coastal and Shelf Zones and Comprehensive Use of Shelf Resources]. Sevastopol: ECOSI-Gidrofizika. Iss. 12, pp. 374–391 (in Russian).
11. Kuftarkova, E.A., Gubanov, V.I., Kovrigina, N.P., Eremin, I.Y. and Senicheva M.I., 2006. Ecological Assessment of Modern State of Waters in the Region of Interaction of the Sevastopol Bay and Part of the Sea Contiguous to it. *Morskoy Ekologicheskij Zhurnal = Marine Ecological Journal*, 5(1), pp. 72–91 (in Russian).
12. Kubryakov, A.I., Belokopytov, V.N. and Pryakhina, S.F., 2019. Diagnostic Calculations of Climatic Winter and Summer Circulation in the Sevastopol Bay. In: V. M. Gruzinov,

- ed., 2019. *Proceedings of N.N. Zubov State Oceanographic Institute*. Moscow. Iss. 220, pp. 189–208 (in Russian).
13. Lopukhina, O.A. and Manzhos, L.A., 2005. Phytoplankton of the Sevastopol Bay (the Black Sea) in Warm and Cold Seasons 2001 – 2002. *Ekologiya Morya = Ecology of the Sea*, 63, pp. 25–31 (in Russian).
 14. Polikarpov, I.G., Saburova, M.A., Manzhos, L.A., Pavlovskaya, T.V. and Gavrilova, N.A., 2003. Microplankton Biological Diversity in the Black Sea Coastal Zone near Sevastopol (2001–2003). In: V. N. Eremeev and A. V. Gaevsкая, eds., 2003. *Modern Condition of Biological Diversity in Near-Shore Zone of Crimea (the Black Sea Sector)*. Sevastopol: ECOSI-Gidrofizika, pp. 16–42 (in Russian).

Submitted 10.02.2023; accepted after review 25.03.2023;
revised 03.05.2023; published 26.06.2023

About the authors:

Kira A. Slepchuk, Junior Research Associate, Marine Hydrophysical Institute of RAS (2 Kapitanskaya St., Sevastopol, 299011, Russian Federation), **ORCID ID: 0000-0001-5437-4866**, **ResearcherID: H-9366-2017**, skira@mhi-ras.ru

Tatyana V. Khmara, Research Associate, Marine Hydrophysical Institute of RAS (2 Kapitanskaya St., Sevastopol, 299011, Russian Federation), **Scopus Author ID: 6506060413**, **ResearcherID: C-2358-2016**, xmara@mhi-ras.ru

Contribution of the authors:

Kira A. Slepchuk – problem statement, performance of numerical calculations, processing and interpretation of modelling results, preparation of the article text and graphic materials

Tatyana V. Khmara – performance of numerical calculations, analysis and description of the study results, text preparation

All the authors have read and approved the final manuscript.

Lead contamination of water and sediments of the Taganrog Bay and the open part of the Sea of Azov in 1991–2020

M. V. Bufetova^{1*}, V. N. Egorov²

¹ *Federal State Budgetary Institution of Higher Education “Sergo Ordzhonikidze Russian State University for Geological Prospecting”, Moscow, Russia*

² *A.O. Kovalevsky Institute of Biology of the Southern Seas of RAS, Sevastopol, Russia*

*e-mail: mbufetova@mail.ru

Abstract

The paper analyzes the data on lead content in water and bottom sediments of the central part of the Sea of Azov and Taganrog Bay for 1991–2020. Studies have shown that in 1991–2009 the lead concentration in the water of the central part of the sea was below the maximum permissible concentration. Since 2010, the lead contamination in waters has been higher, but that in bottom sediments has been lower. It is shown that with an increase in the lead concentration in water its content in bottom sediments decreased, which is associated not only with saturation of the bottom sediment surface, but also with a decrease in the accumulation coefficient. Until 2006, in Taganrog Bay, except for small peaks in 1992–1998, the lead concentration in water was quite low. After 2006, its upward changes were noted, which generally did not exceed the maximum permissible concentration. The paper lists possible sources of increased lead concentration in the gulf and sea in 2010–2015. For 1991–2020, the lead concentration in the bottom sediments of Taganrog Bay varied in antiphase with changes in its content in the water and in all cases was below the permissible concentration normalized according to the Dutch Lists. The relationship between the accumulation coefficient and lead concentration in the bay water was characterized by a high coefficient of determination. The materials illustrate the sorption capacity of bottom sediments, which is an important component of their assimilation capacity for lead. The paper defines the maximum permissible flows of lead (59.6 t/year into the open part of the sea and 21.4 t/year into Taganrog Bay), which can be assimilated by water areas without affecting their biological and water resources. After analyzing the long-term data on the lead content in the water and bottom sediments of the central part of the sea and Taganrog Bay, the paper concludes that the bay can serve both as a lead pollution source and a barrier that either transports lead into the Sea of Azov or entraps it.

Keywords: Sea of Azov, lead, pollution, water, bottom sediments, marginal flows, rationing, assimilation capacity

Acknowledgements: The work was carried out under topic of A.O. Kovalevsky Institute of Biology of the Southern Seas of RAS «Seismological and biogeochemical bases of homeostasis of marine ecosystems» (121031500515-8). The authors are grateful to Azovmorinformcenter for the data provided. The authors also express their gratitude to the reviewers for useful comments and to the editorial staff of the journal for competent, high-quality and well-organized editorial work.

© Bufetova M. V., Egorov V. N., 2023



This work is licensed under a Creative Commons Attribution-Non Commercial 4.0 International (CC BY-NC 4.0) License

For citation: Bufetova, M.V. and Egorov, V.N., 2023. Lead Contamination of Water and Sediments of Taganrog Bay and the Open Part of the Sea of Azov in 1991–2020. *Ecological Safety of Coastal and Shelf Zones of Sea*, (2), pp. 105–119. doi:10.29039/2413-5577-2023-2-105-119

Загрязнение свинцом воды и донных отложений Таганрогского залива и открытой части Азовского моря в 1991–2020 годах

М. В. Буфетова¹*, В. Н. Егоров²

¹ *Российский государственный геологоразведочный университет
имени Серго Орджоникидзе (МГРИ), Москва, Россия*

² *Институт биологии южных морей им. А. О. Ковалевского РАН, Севастополь, Россия*

* e-mail: mbufetova@mail.ru

Аннотация

Проанализированы данные о содержании свинца в воде и в донных отложениях центральной части Азовского моря и Таганрогского залива за 1991–2020 гг. Исследования показали, что в 1991–2009 гг. концентрация свинца в воде центральной части моря была ниже предельно допустимой концентрации. С 2010 г. наблюдался более высокий уровень загрязнения свинцом вод, но более низкий уровень загрязнения им донных отложений. Показано, что с увеличением концентрации свинца в воде его содержание в донных отложениях снижалось, что связано не только с насыщением поверхности донных отложений, но и с уменьшением коэффициента накопления. В Таганрогском заливе до 2006 г., кроме небольших пиков в 1992–1998 гг., концентрация свинца в воде была достаточно низкой. После 2006 г. были отмечены ее изменения в сторону увеличения, которые в целом не превышали предельно допустимую концентрацию. Перечислены возможные источники повышения концентрации свинца в заливе и в море в 2010–2015 гг. За период 1991–2020 гг. концентрация свинца в донных отложениях Таганрогского залива изменялась в противофазе с изменением его содержания в воде и во всех случаях была ниже допустимой концентрации, нормируемой по «голландским листам». Зависимость между коэффициентом накопления и концентрацией свинца в воде залива характеризовалась высоким коэффициентом детерминации. Материалы иллюстрируют сорбционную способность донных отложений, которая является важным компонентом их ассимиляционной емкости в отношении свинца. Определены предельно допустимые потоки свинца (59.6 т/год – в открытую часть моря и 21.4 т/год – в Таганрогский залив), которые могут ассимилироваться акваториями без ущерба для их биологических и водных ресурсов. После анализа многолетних данных о содержании свинца в воде и в донных отложениях центральной части моря и Таганрогского залива делается вывод, что залив может выполнять функции как источника загрязнения свинцом, так и барьера, пропускающего свинец в Азовское море или задерживающего его.

Ключевые слова: Азовское море, свинец, загрязнение, вода, донные отложения, предельные потоки, нормирование, ассимиляционная емкость

Благодарности: работа выполнена в рамках темы ФИЦ ИнБЮМ «Молисмологические и биогеохимические основы гомеостаза морских экосистем» (121031500515-8). Авторы благодарны филиалу «Азовморинформцентр» ФГБВУ «Центррегионводхоз» за предоставленные данные.

Для цитирования: Буфетова М. В., Егоров В. Н. Загрязнение свинцом воды и донных отложений Таганрогского залива и открытой части Азовского моря в 1991–2020 годах // Экологическая безопасность прибрежной и шельфовой зон моря. 2023. № 2. С. 105–119. EDN PFVZIY. doi:10.29039/2413-5577-2023-2-105-119

Introduction

Radioactive and chemical contaminants of various nature entering the marine environment are exposed to many biotic and abiotic factors. First of all, they are carried by currents in water areas. Due to the vertical component of the current velocity, advection and diffusion, pollution penetrates into deep waters. Simultaneously with migration due to mixing of waters, they are absorbed by living and inert components of ecosystems, and abiotic and biotic transformation of physicochemical forms and transfer to water and geological depots take place [1, p. 150; 2].

According to modern concepts [2], the ecotoxicological situation of water areas is largely determined by the interaction of suspended matter with heavy metals (HMs). Under the influence of sorption and metabolic processes, HMs are extracted by suspended matter from the water solution, acquire a density that differs from the specific mass of water, and are involved in biogeochemical cycles that determine not only their migration over water areas, but also their sedimentation entry into bottom sediments. The intensity of biogeochemical cycles depends on the concentrating ability of suspended matter characterized by accumulation coefficients (Co_a) [1]. In the Black Sea, suspended matter can accumulate such HMs as Co, Ni, Cu, Zn, As, Mo, Cd, and Pb, with Co_a equal to $(0.02–180) \cdot 10^4$ units in terms of dry mass, and their pool can make 0.2–55.9 % of the total content in water [3]. The pool of mercury in the composition of the Black Sea suspended matter can exceed 98% of its content in the marine environment [4]. The pool of HMs (copper, zinc, mercury, lead) in the suspended matter of the Sea of Azov can reach 95.6% [5]. Hence it appears that the high concentrating ability of suspended matter is a significant factor in the biogeochemical self-purification of the aquatic environment.

It is commonly known that marine nature management is regulated by anthropocentric and ecocentric principles, which differ in the choice of the so-called weak link by which ecosystems are managed [6]. The anthropocentric approach is based on taking into account only the anthropogenic factor, while the ecocentric one proceeds from the objectivity of the existence of a single system within which the person and all living organisms interact with each other and with the environment. Therefore, not only the person can be the weak link in the ecosystem, but also its individual biotic components.

Consideration of this circumstance requires the development of new approaches in order to provide marine nature management activities. One of them is to implement the concept of sustainable development of water areas by maintaining a balance between consumption and natural reproduction. With regard to ecotoxicological problems, this concept is based on the consideration of the assimilation (ecological) capacity of the marine environment as a result of the impact of natural biogeochemical processes [1, 2, 7]. One of the promising ways to exploit this area is the development of biogeochemical criteria for the assessment of

the self-purification flows of waters with subsequent regulation of the maximum permissible anthropogenic impact on marine ecosystems by factors of radioactive and chemical pollution of the marine environment.

Currently, human health-related environmental criteria, which correspond to the maximum permissible concentrations (MPC) of pollutants in water or in hydrobionts, are used as the main indicators of the marine environment quality. The quality standards for water bodies of commercial fishing importance, which include the Sea of Azov, were established by Order No. 552 of the Minister of Agriculture of the Russian Federation of December 13, 2016 “On the Approval of Water Quality Standards for Water Bodies of Fishing Importance, Including Standards for the Maximum Permissible Concentrations of Harmful Substances in the Waters of Water-Based Fishing Objects”¹⁾. In accordance with this Order, lead belongs to the third hazard category with its MPC in sea water of 10 µg/L.

Concerning marine bottom sediments in the Russian territorial waters, there are currently no normatively fixed characteristics of their quality in terms of the level of pollutant concentration similar to MPC in the water column. However, it is possible to assess the degree of pollution of bottom sediments in a controlled area of the sea based on the compliance of the level of certain pollutants with the criteria for environmental assessment of soil pollution according to normative indicators adopted in other countries, e. g., the Dutch List²⁾. These indicators can be used for the simplified comparative characterization of different parts of the water area or for the assessment of interannual variability. Thus, in Russia, permissible concentrations according to the Dutch List are used in the *Marine Water Pollution Annual Reports*³⁾. According to the Dutch List, permissible concentration of lead in bottom sediments is 85 µg/g dry mass.

It should be noted that the ecotoxicological characteristics according to MPC and the Dutch List have the dimensions of the maximum permissible concentration of pollutants in water, hydrobionts and bottom sediments. These characteristics are diagnostic indicators only. On the other hand, biogeochemical criteria have the dimensions of self-purification flows of water [2]. Therefore, their use makes it possible to assess the maximum allowable water pollution flows based on the condition of maintaining the stationarity of the state of ecosystems due to the equality of flows of self-purification and pollution of the marine environment. At the same time, the fact should not be ignored that pollutants dissolved in water are

¹⁾ Ministry of Agriculture of the Russian Federation, 2016. *On the Approval of Water Quality Standards for Water Bodies of Fishing Importance, Including Standards for the Maximum Permissible Concentrations of Harmful Substances in the Waters of Water-Based Fishing Objects*. Order No. 552 of the Ministry of Agriculture of the Russian Federation of 13.12.2016 (in Russian).

²⁾ Ministerie van Volkshuisvesting, Ruimtelijke Ordening en Milieubeheer, 2000. *Dutch Target and Intervention Values (2000) (the New Dutch List). Annexes. Circular on Target Values and Intervention Values for Soil Remediation*. P. 8. Available at: <https://www.yumpu.com/en/document/read/44815398/dutch-target-and-intervention-values-2000-esdat/13> [Accessed: 26 June 2023].

³⁾ Korshenko, A.N., ed., 2022. *Marine Water Pollution. Annual Report 2021*. Moscow: Nauka, 230 p. (in Russian).

transported through water areas and in depth only in the direction of decreasing gradients in the fields of their distribution in water as a result of the impact of hydrodynamic processes, and pollutants as part of suspended matter can migrate through any water areas. These processes take place on different scales of space and time. Therefore, it is necessary to take into account the periods of averaging the characteristics of hydrodynamic and biogeochemical processes.

The purpose of the work was to study the lead content in water and bottom sediments of the central part of the Sea of Azov and Taganrog Bay for 1991–2020. In this work, the studies were carried out with the mid-annual averaging of the parameters. At the same time, the following problems were solved:

1) to determine the trends and level of lead pollution of the waters of Taganrog Bay and the open part of the Sea of Azov (the sea proper) based on the results of monitoring studies from 1991 to 2020;

2) to study the dependence of lead concentration in bottom sediments on its concentration in the water of the Sea of Azov;

3) to assess the assimilation capacity of bottom sediments in relation to lead in the open part of the Sea of Azov and Taganrog Bay;

4) to find out whether Taganrog Bay is a source of lead pollution of the open part of the Sea of Azov.

Materials and methods

The data on lead concentration in water and bottom sediments in 2010–2020 provided by the *Azovmorinformcenter* branch of *Centerregionvodkhoz* State Organization under cooperation with the Department of Ecology and Environment Management of the Federal State Budgetary Institution of Higher Education “Sergo Ordzhonikidze Russian State University for Geological Prospecting”, were used in this work. Water samples for analysis were taken by the PE-1220 sampling system in accordance with GOST 31861-2012 and RD 52.24.309-2016 from the surface horizon at 32 points (Fig. 1). The studies were carried out in the central and eastern parts of the Sea of Azov and in Taganrog Bay. Water samples were taken in spring (March–April), summer (June–July), autumn (September–October) and winter (December). Outboard works were performed according to standard methods. Chemical analysis of water samples concerning lead content was carried out in accordance with the method PND F 14.1:2:4.140-98, with the sensitivity lower limit of 0.0002 mg/dm³.

Samples of bottom sediments were taken for the analysis at the same stations as water samples using a bottom sampler DCh-0.034 according to GOST 17.1.5.01-80 in the surface layer of soils (0–2 cm). Samples of bottom sediments were taken annually in the summer. Chemical analysis of samples of bottom sediments for lead content was carried out in accordance with the M-MVI-80-2008 method, with the lead sensitivity lower limit of 0.0005 mg/g.

The lead content in water and in bottom sediments was measured with the AAS KVANT-Z.ETA device.

To determine interannual trends, retrospective data on the lead content in water and bottom sediments of the Sea of Azov from 1991 to 2006 were additionally used [8]. In this work, the studies were carried out in accordance with

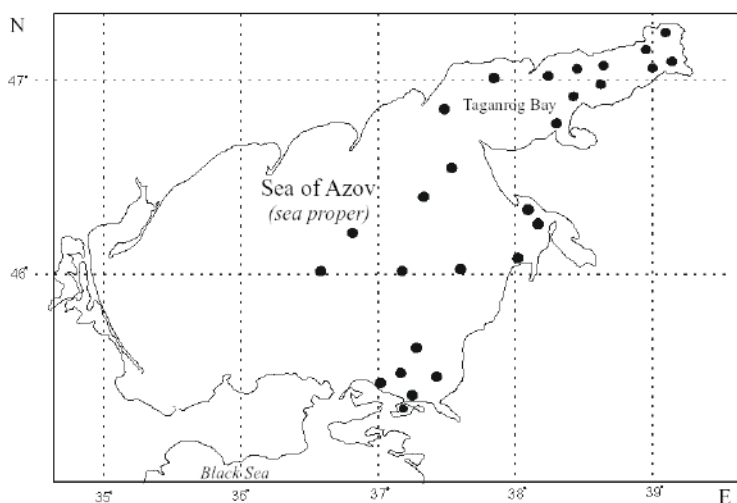


Fig. 1. Map of sampling of water and bottom sediments in 2010–2020

guideline FR.1.31.2005.01514 – this method preceded the method PND F 14.1:2:4.140-98, according to which lead concentrations were determined by the *Azovmorinformcenter* branch of *Centerregionvodkhoz* State Organization. With this consideration in mind, the data from monograph [8] were used in our work for comparison.

Mathematical processing of analytical data was carried out using the standard *Excel* package.

In the work, two areas were identified in the Sea of Azov: Taganrog Bay and the open part of the Sea of Azov (the sea proper), which is associated with their morphometric and hydrological features. The parameters of the districts used in the calculations are presented in the following table.

Parameters of the studied areas

Area	Total area, km ² [9]	Average sedimentation rate ⁴⁾ , g·m ⁻² ·year ⁻¹
Taganrog Bay	5600	700
Open part of Sea of Azov	33400	300

⁴⁾ Sorokina, V.V., 2006. [*Peculiarities of Terrigenous Sedimentation in the Sea of Azov in the Second Half of the 20th Century*]. Ph.D. Thesis. Rostov-on-Don, 216 p. (in Russian).

Key data

One of the objectives of the study was to determine the impact of Taganrog Bay on lead pollution of water and bottom sediments in the open part of the Sea of Azov. Its solution was carried out on the basis of a comparison of lead concentrations in water and bottom sediments of Taganrog Bay and the open part of the Sea of Azov (Fig. 2 and 3).

HMs, including lead, can enter the Sea of Azov from both natural and anthropogenic sources. One of the main ones is the flow of such large and small rivers as Don, Kuban, Mius, Yeya, Beisug, Kagalnik, etc. [10, 11]. An important role in sea pollution belongs to the cities located on the coast and in the delta of the Don River – Azov, Taganrog, Yeysk, Primorsko-Akhtarsk, Temryuk – as a result of the discharge of insufficiently treated wastewater. It is also worth noting the impact of ports, shipping, landfills, and soil dumping^{5), 6)}. Lead can come with atmospheric precipitation [8, 10–12] and also as a result of coastal abrasion.

The lead content in the water of the central part of the sea and Taganrog Bay increased in 2010–2015, which can have been associated with the development of industrial production in this region (thus, in 2010–2012, the following facts can be taken into account: the construction of a port complex near the city of Primorsko-Akhtarsk, of the Taman transshipment complex; the implementation of the Temryuk and Akhtarsk project for the extraction of oil and gas condensate; an increase in the capacity of the Taganrog Metallurgical Plant, the Taganrog Boiler Plant “Krasny Kotelschik” and the Taganrog Automobile Plant with an increase in emissions and discharges of pollutants).

According to the data presented in Fig. 2, *a*, it can be seen that in 1991–2009 the lead concentration in the water of the open part of the Sea of Azov was significantly below the MPC. Since 2010, there have been higher levels of lead pollution in waters, but lower levels of sediment pollution (Fig. 2, *b*). The dependence of lead concentration in bottom sediments on the change in the average annual values of its specific content in surface waters with a sufficient degree of probability ($R^2 = 0.6$) lay on a straight line on a logarithmic scale along the ordinate axes (Fig. 2, *c*), which allowed it to be described by the following exponential function:

$$C_{bs} = 14.14 \cdot C_w^{-0.39}, \quad (1)$$

where C_{bs} – concentration of lead contained in the upper layer of bottom sediments; C_w – lead concentration in the liquid phase.

Fig. 2, *d* shows the dependence of the change in Co_a on the value of C_w based on the results of observations in 1991–2020. Statistical analysis materials showed

⁵⁾ Bespalova, L.A., 2006. [Ecological Diagnostics and Assessment of Sustainability of the Landscape Structure of the Sea of Azov]. Ph.D. Thesis. Rostov-on-Don, 271 p. (in Russian).

⁶⁾ Latun, V.V., 2005. [Impact of the Operation of Shipping Channels on the Ecosystem of Taganrog Bay]. Ph.D. Thesis. Rostov-on-Don, 209 p. (in Russian).

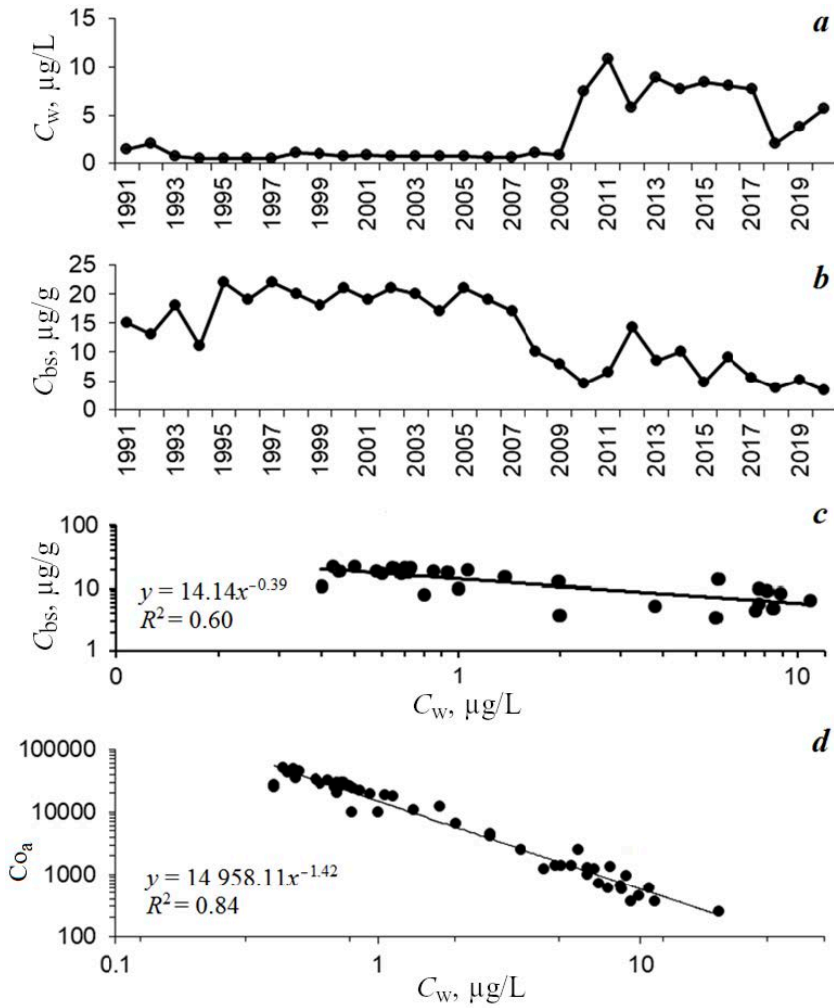


Fig. 2. Characteristics of lead distribution in the open part of the Sea of Azov: concentration in water, $\mu\text{g/L}$ (a); concentration in the surface layer of bottom sediments, $\mu\text{g/g}$ dry mass (b); dependence of the lead concentration in bottom sediments on its concentration in water (c); dependence of the change in the coefficient of accumulation of lead by bottom sediments on lead concentration in water (d)

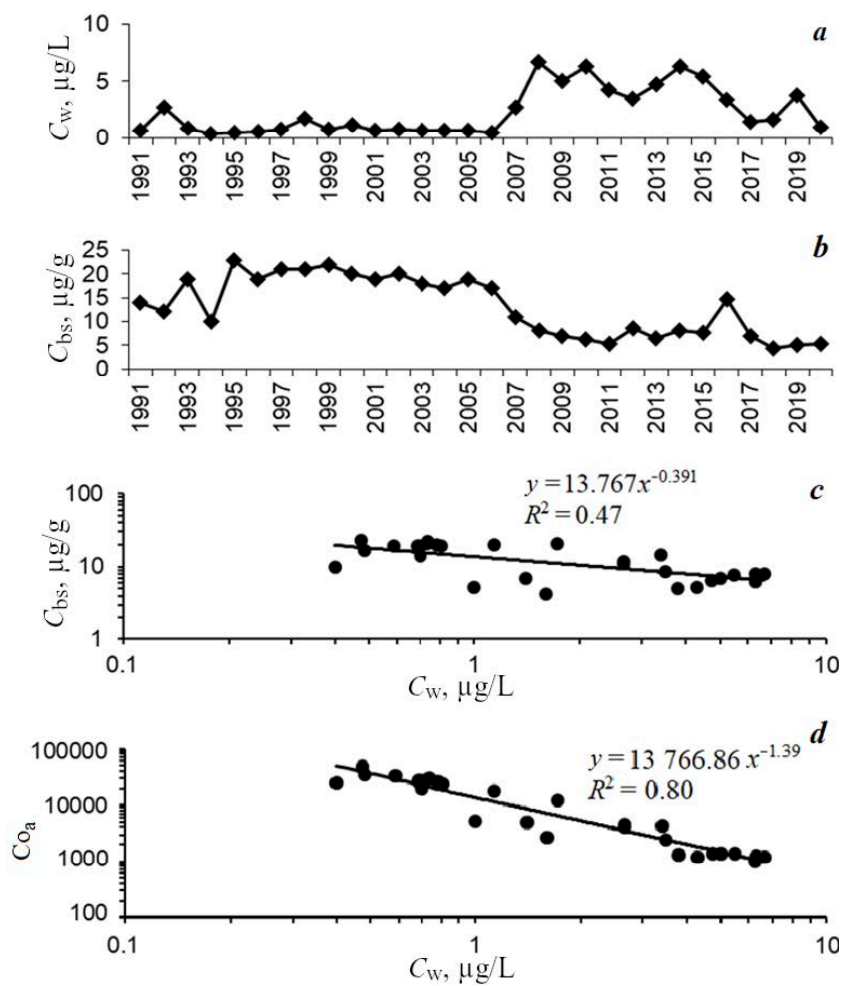


Fig. 3. Characteristics of lead distribution in Taganrog Bay: concentration in water, $\mu\text{g/L}$ (a); concentration in the surface layer of bottom sediments, $\mu\text{g/g}$ dry mass (b); dependence of the concentration in bottom sediments on the concentration in water (c); dependence of the change in the coefficient of accumulation of lead by bottom sediments on lead concentration in water (d)

that the correlation between Co_a and C_w with reliability characterized by the coefficient of determination $R^2 = 0.84$, could be described by the exponential function equation:

$$Co_a = 14958 C_w^{-1.42}. \quad (2)$$

Correlation (1) showed that with an increase in lead concentration in water (C_b), its concentration in bottom sediments (C_{bs}) decreased. The study of this effect showed that a decrease in the value of C_{bs} with an increase in C_w was associated not only with the saturation of the surface of bottom sediments, but also with a decrease in their Co_a , taking into account the dimensional matching $Co_a = 1000C_{bs}/C_w$.

Fig. 3, *a* shows that except for small peaks in 1992–1998, the lead concentration in the water of Taganrog Bay was quite low until 2006. After 2006, its oscillatory changes were noted with an increase of concentration in water, which in general did not exceed the MPC of 10 $\mu\text{g/L}$. In 1991–2020 (Fig. 3, *b*), the lead concentration in the bottom sediments of Taganrog Bay, as a rule, changed in antiphase with the change in its content in the water, and in all cases it was below the MPC rationed according to the Dutch List. The dependence between C_{bs} and C_w lay on a straight line with determination characterized by the corresponding coefficient $R^2 = 0.47$. The exponential function equation obtained according to Fig. 3, *c*, was as follows:

$$C_{bs} = 13.767 \cdot C_w^{-0.391}. \quad (3)$$

The dependence between Co_a and C_w on a logarithmic scale along the ordinate axes (Fig. 3, *d*) was also described by a straight line, characterized by the coefficient of determination $R^2 = 0.8$. When approximating these data by the exponential function equation, we obtained:

$$Co_a = 13766 \cdot C_w^{-1.39}. \quad (4)$$

Obviously, materials shown in Fig. 2, *c*, *d* and 3, *c*, *d*, illustrate the ability of bottom sediments to concentrate lead under the combined impact of biotic and abiotic factors of the marine environment. The determination of the biogeochemical mechanisms responsible for the formation of the types of exponential dependence between C_w and C_{bs} , as well as between C_w and Co_a , requires the study of sorption, metabolic, and trophic interactions of living and inert matter included in bottom sediments under conditions of changes in salinity, pH, temperature, and hydrodynamic characteristics of the water. The above mentioned parameters were not registered in 1991–2020 as a part of the monitoring carried out by *Centerregionvodkhoz* State Organization.

It should be noted that lead entering the Sea of Azov with river runoff, with slope runoff from the coast and from atmospheric precipitation, is carried by currents along the sea area and vertically. According to reference data³⁾, surge phenomena up to 4–6 m high, manifesting themselves on a time scale up to 12 h, and seiches up to 1 m with a period of some minutes to several hours, are observed

in the Sea of Azov. At an average current velocity of 60–80 cm/s, a relatively uniform distribution of impurities over the sea area is ensured on a weekly time scale and in depth on an hour scale. However, under strong winds, detachment of bottom sediments is observed. The frequency of waves with a height of over 2 m, causing detachment of the bottom sediment, is 13%. In general, the non-stationarity of the hydrodynamic characteristics of the Sea of Azov can be estimated on a time scale of no more than one month and a half. The size spectrum of suspended particles in the Sea of Azov ranges from 1 to 300 microns, and their sedimentation to the bottom proceeds on time scales from minute to week in accordance with the Stokes' Law and Bernoulli's Principle. A review of the hydrodynamic and sedimentation features of the Sea of Azov as a whole indicates that the average annual estimates of pollution of its waters and bottom sediments with lead are acceptably adequate.

According to modern concepts, bottom sediments can be considered as a sorbent interacting with lead dissolved in water. The degree of their sorption saturation is usually reflected by the Freundlich equation. In accordance with the designations adopted in this paper, the Freundlich equation has the following form:

$$C_{bs} = A \cdot C_w^n, \quad (5)$$

where A and n – parameters ($n < 1$).

Comparison of correlations (1) and (3) with expression (5) showed that with identical common notation of these equations, parameter n in equations (1) and (3) had a negative sign. This means that the Freundlich equation of form (5) does not reflect the sorption saturation of bottom sediments with lead or that the sorption saturation does not prevail over other factors not currently taken into account.

Consideration of relations (2) and (4) showed that a significant ($R^2 = 0.84$ and $R^2 = 80$) decrease in Co_a of lead has a significant effect on the concentrating ability of bottom sediments in accordance with a power function of form (5), but with a negative sign of exponent n . Comparison of correlations (1) and (3) showed that the relative error of parameter A incongruence in them was 7.9, and n – 2.1 %. With the variability of the data characterized by the coefficients of determination, respectively, $R^2 = 0.84$ and $R^2 = 80$, this indicates the identity of correlations (2) and (4). The former was obtained from the results of monitoring of the open part of the Sea of Azov with a sedimentation rate of $300 \text{ g}\cdot\text{m}^{-2}\cdot\text{year}^{-1}$, and the latter – according to the study of Taganrog Bay with a sedimentation rate of $700 \text{ g}\cdot\text{m}^{-2}\cdot\text{year}^{-1}$. Hence it appears that the regularities of changes in the concentrating capacity of bottom sediments with respect to lead do not depend on the intensity of sedimentation.

At the same time, it should be noted that materials shown in Fig. 2, c , d and 3, c , d , illustrate the regularities of change in the sorption (C_{bs}) and concentrating (Co_a) capacity of bottom sediments on the scale of the entire observation period. Therefore, these dependences are significant indicators of the assimilation capacity

of bottom sediments in relation to pollutants. The assimilation capacity of bottom sediments in water areas is determined from the correlation [2]:

$$Q_{as} = S \cdot V_{sed} \cdot C_{bs}, \quad (6)$$

where S – area of the water area under consideration, km^2 ; V_{sed} – specific sedimentation rate, $\text{g} \cdot \text{m}^{-2} \cdot \text{year}^{-1}$.

Formula (6) is applicable when rationing the maximum permissible flows of pollution of water areas with HMs according to the Dutch List (with $C_{bs} = \text{MPC}_{bs}$). Taking into account that $C_{bs} = C_w \cdot \text{Co}_a$, with due regard to formulas of forms (2) and (4), equation (6) is transformed into the following correlation:

$$Q_{as} = S \cdot V_{sed} \cdot C_w \cdot A \cdot C_w^{-n}, \quad (7)$$

which can be used for rationing according to ecotoxicological criteria (with $C_w = \text{MPC}$).

With $\text{MPC}_w = 10 \mu\text{g/L}$, the rationed maximum allowable flow of lead into the open part of the Sea of Azov calculated by correlation (7), was 59.6 t/year, and for Taganrog Bay, taking into account correlation (7), it was 21.4 t/year.

It can be seen from Fig. 4 that over the entire observation period from 1991 to 2020, except for 2007–2009, lead concentrations in the waters of Taganrog Bay and the open part of the Sea of Azov almost coincided. The same was noted for bottom sediments (Fig. 4, *b*). However, consideration of the dependences between the lead content in the water of the sea $C_{w(\text{sea})}$ and bay $C_{w(\text{bay})}$ revealed a weakly manifested relationship ($R^2 = 0.38$) between these two parameters. At the same time, the dependence between the lead content in the bottom sediments of the sea $C_{bs(\text{sea})}$ and bay $C_{bs(\text{bay})}$ was highly significant statistically ($R^2 = 0.87$). These data indicated that suspended matter with a higher lead content entering Taganrog Bay was transported as a result of hydrodynamic processes to the open part of the Sea of Azov and deposited in this water area as part of bottom sediments.

Calculations of the lead input resulted from water exchange through the Dolzhansky Strait (with average long-term values of the annual water outflow into the sea and the annual water inflow into the bay) performed in [13], showed that, e. g., in 2017, 302–1184 tons of lead could have arrived from the Sea of Azov to Taganrog Bay, and from Taganrog Bay to the sea proper – 131–827 tons. Thus, the sea proper acted as a source of pollution of Taganrog Bay. In 2007–2009, on the contrary, Taganrog Bay was a source of water pollution of the open part of the sea: lead concentrations in the bay were significantly higher than in the open part of the sea, e. g., in 2008, 6.67 $\mu\text{g/L}$ in the bay and 0.8 $\mu\text{g/L}$ in the open sea. Thus, Taganrog Bay can serve both as a source of pollution and a barrier that either transports HMs, including lead, into the Sea of Azov or entraps them [14].

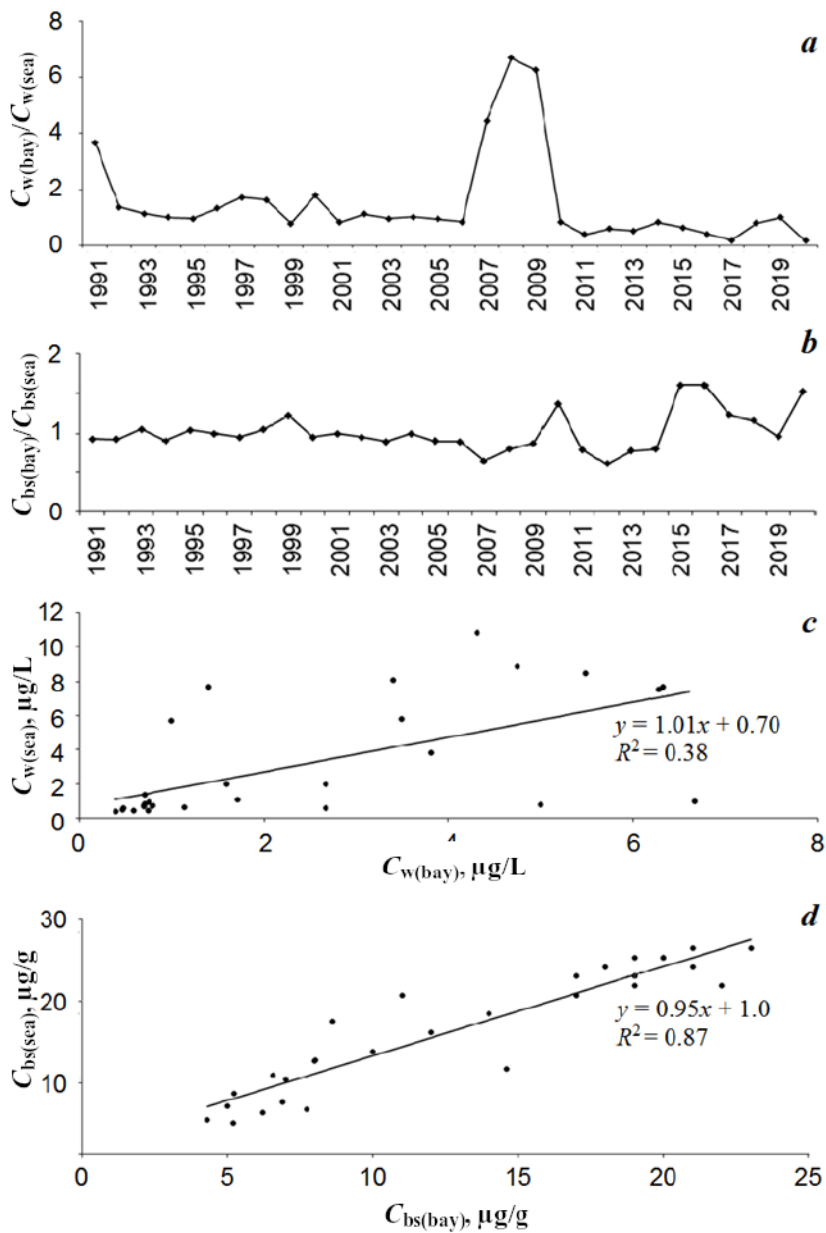


Fig. 4. Change in the ratio of lead concentrations in water of Taganrog Bay and in the open part of the Sea of Azov $C_{w(bay)}/C_{w(sea)}$ (a) and in bottom sediments of Taganrog Bay $C_{bs(bay)}/C_{bs(sea)}$ (b); dependence between lead concentrations in water of Taganrog Bay and the open part of the Sea of Azov (c) and in bottom sediments (d)

Conclusion

In general, for the period from 1991 to 2020, fluctuations in the average annual lead concentrations both in water and in bottom sediments of the open part of the sea and Taganrog Bay are not environmentally significant. The lead content in the water of the central part of the sea and Taganrog Bay increased in 2010–2015, which can have been associated with the development of industrial production in this region (thus, in 2010–2012, the following facts can be taken into account: the construction of a port complex near the city of Primorsko-Akhtarsk, of the Taman transshipment complex; the implementation of the Temryuk and Akhtarsk project for the extraction of oil and gas condensate; an increase in the capacity of the Taganrog Metallurgical Plant, the Taganrog Boiler Plant “Krasny Kotelschik” and the Taganrog Automobile Plant with an increase in emissions and discharges of pollutants).

It is determined that the dependences of the change in the concentration and coefficients of lead accumulation in bottom sediments on the change in its concentration in the water of Taganrog Bay and the open part of the Sea of Azov are described with a high degree of statistical significance by an exponential function equation. It is shown that the parameters of this equation represent the indicators of the assimilation capacity of bottom sediments in relation to lead. They can be used for the purposes of environmental regulation, taking into account sanitary and hygienic standards.

It is found that an increase in the lead concentration in the suspended matter of the Taganrog Bay led to an increase in its concentration in the suspended matter of the open part of the Sea of Azov.

Analysis of long-term data on the lead content in water and in bottom sediments of the central part of the sea and Taganrog Bay makes it possible to conclude that Taganrog Bay can serve both as a lead pollution source and a barrier that either transports lead into the Sea of Azov or entraps it.

REFERENCE

1. Polikarpov, G.G. and Egorov, V.N., 1986. [*Marine Dynamic Radiochemoecology*]. Moscow: Energoatomizdat, 176 p. (in Russian).
2. Egorov, V.N., 2019. *Theory of Radioisotope and Chemical Homeostasis of Marine Ecosystems*. Sevastopol: IBSS, 356 p. doi:10.21072/978-5-6042938-5-0 (in Russian).
3. Pospelova, N.V., Egorov, V.N., Proskurnin, V.Yu. and Priymak, A.S., 2022. Suspended Particulate Matter as a Biochemical Barrier to Heavy Metals in Marine Farm Areas (Sevastopol, the Black Sea). *Marine Biological Journal*, 7(4), pp. 55–69. doi:10.21072/mbj.2022.07.4.05
4. Stetsiuk, A.P. and Egorov, V.N., 2018. Marine Suspensions Ability to Concentrate Mercury Depending on its Contents in the Shelf Water Area. *Monitoring Systems of Environment*, 13, pp. 123–132. doi:10.33075/2220-5861-2018-3-123-132
5. Bufetova, M.V., 2022. Assessment of the Ability of Suspended Matter in the Sea of Azov to Concentrate Heavy Metals. *Ecological Safety of Coastal and Shelf Zones of Sea*, (1), pp. 55–65. doi:10.22449/2413-5577-2022-1-55-65
6. Alexakhin, R.M. and Fesenko, S.V., 2004. Radiation Protection of the Environment: Anthropogenic and Ecocentric Principles. *Radiation Biology. Radioecology*, 44(1), pp. 93–103 (in Russian).

7. Izrael, Yu.A. and Tsyban, A.V., 2009. *Anthropogenic Ecology of Ocean*. Moscow: Flinta; Nauka, 529 p. (in Russian).
8. Klenkin, A.A., Korpakova, I.G., Pavlenko, L.F. and Temerdashev, Z.A., 2007. [*Ecosystem of the Sea of Azov: Anthropogenic Pollution*]. Krasnodar: OOO “Prosveshcheniye-Yug”, 324 p. (in Russian).
9. Goptarev, N.P., Simonov, A.I., Zatuchnaya, B.M. and Gershanovich, D.E., eds., 1991. [*Hydrometeorology and Hydrochemistry of Seas of the USSR. Vol. 5. The Sea of Azov*]. St. Petersburg: Gidrometeoizdat, 236 p. (in Russian).
10. Khrustalev, Yu.P., 1999. *The Fundamental Problems of the Sedimentogenesis Geochemistry in the Azov Sea*. Apatity: Publishing house of the KSC RAS, 247 p. (in Russian).
11. Fedorov, Yu.A., Mikhaylenko, A.V. and Dotsenko, I.V., 2012. [Biogeochemical Conditions and their Role in Mass Transport of Heavy Metals in Aquatic Landscapes]. In: MSU, 2012. [*Landscape Geochemistry and Soil Geography: Proceedings of the All-Russian Scientific Conference (on the Occasion of Sentenary of the Birth of M. A. Glazovskaya)*. Moscow, 4–6 April 2012]. Moscow: MGU, pp. 332–334 (in Russian).
12. Mamykina, V.A. and Khrustalev, Yu.V., 1966. Abrasion and Accumulation Processes of Recent Sedimentation in the Azov Sea. *Okeanologiya*, 6(3), pp. 451–457 (in Russian).
13. Bufetova, M.V., 2019. Assessment of Income and Elimination of Heavy Metals in the Taganrog Bay of the Sea of Azov. *Ecological Safety of Coastal and Shelf Zones of Sea*, (2), pp. 78–85. doi:10.22449/2413-5577-2019-2-78-85 (in Russian).
14. Vishnevetskiy, V.Yu. and Ledyeva, V.S., 2012. Experimental Studies of the Dynamics of the Concentration of Heavy Metals in Surface Water in the Taganrog Bay. *Engineering Journal of Don*, (4–1), 5 p. (in Russian).

Submitted 7.02.2023; accepted after review 23.03.2023;
revised 03.05.2023; published 26.06.2023

About the authors:

Marina V. Bufetova, Associate Professor of the Department of Ecology and Nature Management, Faculty of Ecology, Sergo Ordzhonikidze Russian State Geological Exploration University (MGRI) (23 Miklukho-Maklaya St., Moscow, 117997, Russian Federation), Associate Professor, Ph.D. (Geogr.), **SPIN-code: 9133-4070**, **ORCID ID: 0000-0002-6247-1698**, mbufetova@mail.ru

Victor N. Egorov, Research Supervisor, A.O. Kovalevsky Institute of Biology of the Southern Seas of RAS (2 Nakhimov Av., Sevastopol, 299011, Russian Federation), Academician of RAS, Dr.Sci. (Biol.), Professor, **SPIN-code: 6595-6759**, **ORCID ID: 0000-0002-4233-3212**, egorov.ibss@yandex.ru

Contribution of the authors:

Marina V. Bufetova – problem statement, processing, analysis and description of the study results, discussion of the results, conclusion drawing, article text and graphic material preparation

Victor N. Egorov – qualitative analysis of the results and their interpretation, discussion of the results, article text preparation, conclusion drawing

All the authors have read and approved the final manuscript.

The First Data on the Hydrocarbon Composition of Water, Bottom Sediments of the North Crimean Canal and Soils Adjacent to Agricultural Land

O. V. Soloveva, E. A. Tikhonova *

A.O. Kovalevsky Institute of Biology of the Southern Seas of RAS, Sevastopol, Russia

* *e-mail: tihonoval@mail.ru*

Abstract

The paper presents the results of quantitative and qualitative indicators of the hydrocarbon composition of water, bottom sediments of the North Crimean Canal and soil from adjacent agricultural lands during filling the canal with water after an eight-year break. The material for the study was water, bottom sediments and soil samples taken in the spring of 2022. When planning sampling, the ways of hydrocarbon entry into the canal were taken into account: directly with the Dnieper water, with atmospheric precipitation, and with washout from nearby territories. The qualitative and quantitative composition of hydrocarbons in water, bottom sediments, and soil was determined by gas chromatography in the Scientific and Educational Center for Collective Use «Spectrometry and Chromatography» of IBSS. To identify probable sources of the studied class of substances, biogeochemical markers were used. The obtained concentrations of aliphatic hydrocarbons in water ($0.032 \pm 0.006 \text{ mg} \cdot \text{L}^{-1}$) of the studied section of the North Crimean Canal did not exceed the maximum permissible values ($0.05 \text{ mg} \cdot \text{L}^{-1}$) and were close to the values typical for unpolluted water areas. The hydrocarbon content in the bottom sediments of the canal ($30 \text{ mg} \cdot \text{kg}^{-1}$ air-dry bottom sediments) and in adjacent fields ($18.1 \text{ mg} \cdot \text{kg}^{-1}$ air-dry bottom sediments) also indicated the absence of high pollution levels. In the canal water, n-alkanes were identified in the C_{17} – C_{32} range; in the bottom sediments and soils of adjacent territories, the n-alkane range was C_{17} – C_{33} . The composition of n-alkanes and the values of biogeochemical markers in water indicated a mixed nature of hydrocarbons with a predominance of compounds of allochthonous origin washed away from the drainage basin of the lower Dnieper. The composition of n-alkanes and the markers calculated for the bottom sediments and soils were typical for the soils of the steppe regions and were significantly similar to them.

Key words: hydrocarbons, water, bottom sediments, soil, North Crimean canal

Acknowledgements: the authors are grateful to I. N. Moseichenko and D. B. Yevtushenko, the leading engineers of the Department of Radiation and Chemical Biology IBSS, for their assistance in sampling. The work was performed under RNF grant on topic no. 23-26-00128 “The role of the irrigation system of the North-Crimean Canal in processes of the transfer of long-lived radionuclides of the Chernobyl origin, heavy metals, and hydrocarbons with the Dnieper water to the irrigated farmlands of Crimea”.

© Soloveva O. V., Tikhonova E. A., 2023



This work is licensed under a Creative Commons Attribution-Non Commercial 4.0 International (CC BY-NC 4.0) License

For citation: Soloveva, O.V. and Tikhonova, E.A., 2023. The First Data on the Hydrocarbon Composition of Water, Bottom Sediments of the North Crimean Canal and Soils Adjacent to Agricultural Land. *Ecological Safety of Coastal and Shelf Zones of Sea*, (2), pp. 120–133. doi:10.29039/2413-5577-2023-2-120-133

Первые данные об углеводородном составе воды, донных отложений Северо-Крымского канала и почв прилегающих сельскохозяйственных угодий

О. В. Соловьёва, Е. А. Тихонова *

*ФГБУН ФИЦ Институт биологии южных морей
имени А. О. Ковалевского РАН, Севастополь, Россия*

** e-mail: tihonova@mail.ru*

Аннотация

Проведено исследование количественных и качественных показателей углеводородного состава воды, донных отложений Северо-Крымского канала и почвы прилегающих земель сельскохозяйственного назначения в период наполнения канала водой после восьмилетнего перерыва. Материалом для исследования послужили пробы воды, донных отложений и почвы, отобранные весной 2022 г. При планировании пробоотбора учитывались пути поступления углеводородов в канал: непосредственно с днепровской водой, выпадение с атмосферными осадками и поступление со смывом с близлежащих территорий. Качественный и количественный состав углеводородов в воде, донных отложениях и почве определяли методом газовой хроматографии на базе НОЦКП «Спектрометрия и хроматография» ФИЦ ИнБЮМ. Для идентификации вероятных источников исследуемого класса веществ использовали биогеохимические маркеры происхождения углеводородов. Полученные концентрации алифатических углеводородов в воде ($0.032 \pm 0.006 \text{ мг}\cdot\text{л}^{-1}$) исследуемого участка Северо-Крымского канала не превышают предельно допустимые значения ($0.05 \text{ мг}\cdot\text{л}^{-1}$) и близки к значениям, характерным для незагрязненных акваторий. Содержание углеводородов в донных отложениях канала ($30 \text{ мг}\cdot\text{кг}^{-1}$ воздушно-сухого донного осадка) и на прилегающих полях ($18.1 \text{ мг}\cdot\text{кг}^{-1}$ воздушно-сухого донного осадка) также подтверждало отсутствие высоких уровней загрязнения. В воде канала идентифицированы n-алканы в диапазоне C_{17} – C_{32} , в донных отложениях и грунтах прилегающих территорий диапазон n-алканов был C_{17} – C_{33} . Состав n-алканов и значения биогеохимических маркеров в воде указывают на смешанную природу углеводородов с преобладанием соединений аллохтонного происхождения, смываемых с территории водосборного бассейна нижнего течения Днепра. Состав n-алканов и маркеры, рассчитанные для донных отложений и почв, были характерными для грунтов степных районов и имели существенное сходство с ними.

Ключевые слова: углеводороды, вода, донные отложения, почва, Северо-Крымский канал

Благодарности: авторы выражают благодарность ведущим инженерам отдела радиационной и химической биологии ФИЦ ИнБЮМ И. Н. Мосейченко и Д. Б. Евтушенко за помощь в отборе проб. Работа выполнена в рамках гранта РНФ «Роль оросительной системы Северо-Крымского канала в процессах переноса долгоживущих радионуклидов черноморского происхождения, тяжелых металлов, а также углеводородов с днепровской водой на поливные сельхозугодья Крыма» № 23-26-00128.

Для цитирования: Соловьева О. В., Тихонова Е. А. Первые данные об углеводородном составе воды, донных отложений Северо-Крымского канала и почв прилегающих сельскохозяйственных угодий // Экологическая безопасность прибрежной и шельфовой зон моря. 2023. № 2. С. 120–133. EDN OTZUKF. doi:10.29039/2413-5577-2023-2-120-133

Introduction

The North Crimean Canal (NCC) and its branches, canals of melioration systems, water supply facilities of drinking water intakes of surface and groundwater sources, and water supply networks are used as water supply routes in the territory of the Republic of Crimea¹⁾.

The NCC was designed and built not only for land melioration, but also for public water supply. Now, it is an extensive network of main and inter-farm canals, reservoirs, hundreds of pumping stations and hydraulic engineering structures. The canal leaves the Kakhovka water reservoir and reaches Kerch through the Perekop Isthmus. Its length from Novaya Kakhovka (Kherson Region) to Kerch (Republic of Crimea) is 405 km, the length of the main canal and its branches exceeds 10,000 km¹⁾.

The canal width varies from 15 m to 150 m, with a depth of up to 7 m. The maximum discharge capacity is $300 \text{ m}^3 \cdot \text{s}^{-1}$, and on the border with the Republic of Crimea it is $1) 225 \text{ m}^3 \cdot \text{s}^{-1}$.

During its full operation, the NCC covered up to 85 % of the peninsula's total water consumption, of which almost 80 % was for agricultural production. Most of the irrigation water (about 60 %) was used for rice cultivation [1].

In the days of successful development of the melioration water management complex, the irrigated area reached almost 400,000 ha. In 2014, the supply of Dnieper water via the NCC was discontinued. From 2015 to 2022, the NCC route was used to supply water to fill off-stream reservoirs from Nezhin, Prostomoye and Novogrigoryevsk groundwater intakes, as well as from the Belogorsk and Taigan reservoirs supplied through the Biyuk-Karasu River bed to meet the drinking and domestic needs of the Feodosiya–Sudak and Kerch regions and some settlements of the Leninsky district. Since 2022, the supply of Dnieper water to the NCC has been resumed, which undoubtedly has a positive effect on the water supply of the peninsula. At the same time, the poor technical condition of the NCC led and still leads to significant water losses during transportation, to waterlogging of lands, and to salinization of soils in the nearby areas¹⁾ [1].

When running the Dnieper water through the canal, it is important to control not only the quality of the water in the canal itself but also that of the soil after irrigation. Hydrocarbons (HCs) in soils are a wide range of compounds, the study of which has recently received much attention due to their global distribution and impact on the condition of soils themselves, as well as the environment

¹⁾ Tkachuk, V.G., 1971. [*Hydrogeology of the USSR. Volume 8. Crimea*]. Moscow: Nedra, 364 p. (in Russian).

as a whole, including humans. Besides, HCs can serve as indicators of modern geochemical processes in landscapes, therefore it is essential to study the qualitative and quantitative composition of HCs in environments to increase the efficiency of ecological forecasts and ecological monitoring [2].

A group of authors performed a study [2] of soil samples taken from areas with different degrees of anthropogenic load and various soil formation processes and showed that the data on n-alkanes in soils have a certain indicative potential for identifying natural and anthropogenic processes affecting the hydrocarbon state of soils. Also, for aquatic ecosystems, n-alkanes are widely used as an indicator of biogeochemical processes of organic matter transformation [3]. Biogeochemical processes involving HCs occurring in such water bodies, particularly after a break in their functioning, are poorly studied.

Hence, a need arose to obtain information on the safety and quality of the Dnieper water that came through the canal bed and the possibility of using it for irrigated agriculture. Immediately after the filling of the NCC with water, studies were conducted to provide information on the current state of the environment and to become a basis for further observations.

The paper aims at studying quantitative and qualitative indicators of the HC composition of water, bottom sediments of the canal, and soil of the adjacent agricultural lands during the period of canal filling with water after an eight-year break.

Study material and methods

Water, sediment, and soil samples taken in spring 2022 were used as the material for the study. While planning sampling, we considered how HCs had entered the canal: directly from the Dnieper, with atmospheric precipitation, and with washout from nearby territories.

Therefore, water sampling was conducted along the course of the canal water flow from the transect related to a large industrial city of Crimea – Armyansk (Fig. 1). The transect included three water sampling stations, and we took into account the flush from both banks and the intense water flow in the canal: Station 1 – the left bank, Station 2 – the middle part, and Station 3 – the right bank. The bottom sediments were taken by a hand sampler directly in the canal, the soil was taken from the adjacent area. The material was transported on the day of sampling in special containers.

According to guideline FR.1.31.2010.08907 “Methodology for measurement of n-paraffin hydrocarbons mass fraction in samples of soil and bottom sediments of fresh and marine water bodies by gas-liquid chromatography”, soil and bottom sediments were dried in the laboratory in natural conditions, then pounded manually in a porcelain mortar and sieved through a 0.25 mm sieve. The dried and sieved sample in an amount of 1–2 g was extracted in 150 mL n-hexane in a Soxhlet extractor for one hour. The obtained extract was purified on a glass column filled with aluminium oxide to remove the polar compounds. The obtained extract was concentrated to 1 mL.

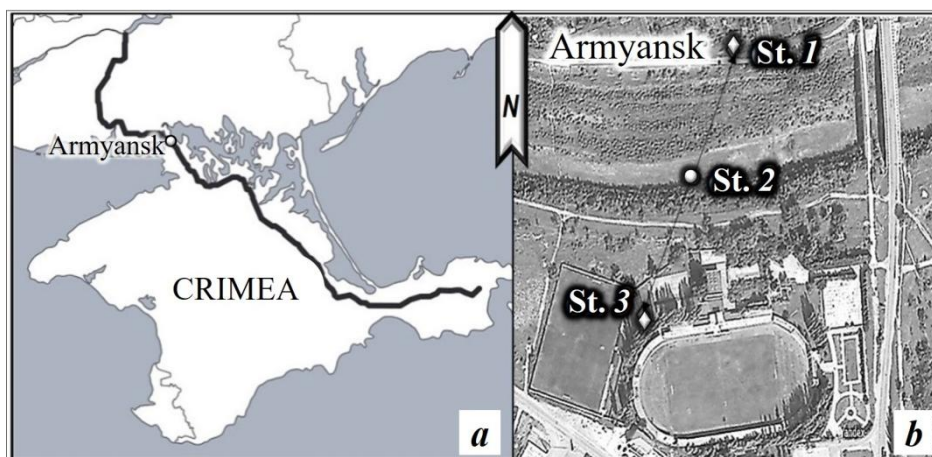


Fig. 1. Map of the North-Crimean Canal (a) and sampling stations for water, bottom sediments and adjacent soil, spring 2022 (b)

HCs were extracted with hexane under laboratory conditions from 1 L of water. An aliquot of the concentrated extract (1 μL) for all test objects was injected with a microsyringe into the evaporator of a Crystal 5000.2 gas chromatograph with a flame ionization detector heated to 250 $^{\circ}\text{C}$. HC separation was performed on a TR-1MS capillary column 30 m long, 0.32 mm in diameter, and with the stationary phase film thickness of 0.25 μm (Teramo Scientific). The column temperature was programmed from 70 to 280 $^{\circ}\text{C}$ (rate of temperature rise: 8 $^{\circ}\text{C}\cdot\text{min}^{-1}$). The carrier gas (nitrogen) flow in the column was 2.5 $\text{mL}\cdot\text{min}^{-1}$ without flow splitting. The detector temperature was 320 $^{\circ}\text{C}$.

Quantitation of HC content was performed by absolute calibration of the flame ionization detector with a mixture of HCs (ASTMD2887 Reference Gas Oil standard (SUPELCO, USA)), that of n-alkanes – by a reference sample of paraffin HCs in hexane with mass concentration of each component 200 $\mu\text{g}\cdot\text{mL}^{-1}$, pristane + phytane – 100 $\mu\text{g}\cdot\text{mL}^{-1}$ in hexane (SUPELCO, USA).

Determination of HCs and n-alkanes was carried out at the Scientific and Educational Center for Collective Use «Spectrometry and Chromatography» of IBSS. To process results during HC concentration determination, Chromatec Analytical 3.0 software (absolute calibration and percentage normalization method) was used.

HC markers were used to identify probable HC sources. In the course of work, a number of ratios were used allowing concluding about biogenic or petrogenic origin of n-alkanes and to some extent to differentiate their autochthonous or allochthonous origin. These ratios were calculated for each sample. The diagnostic indices used to determine the sources of organic compounds are shown in Table 1.

Table 1. Diagnostic molecular ratios and their value interpretation

Calculation formula	Index value	Entry source	Work
$LWH/HWH = \frac{\sum(C_{11} - C_{21})}{\sum(C_{22} - C_{35})}$	> 1	Oil	[4]
	< 1	Terrigenous, higher plant	
C_{31}/C_{19}	< 0.4	Autochthonous matter	[5]
	>0.4	Allochthonous matter	
$CPI_1 = (1/2)\{(C_{15} + C_{17} + C_{19} + C_{21}) / (C_{14} + C_{16} + C_{18} + C_{20}) + (C_{15} + C_{17} + C_{19} + C_{21}) / (C_{16} + C_{18} + C_{20} + C_{22})\}$	< 1	Intense microbial transformation of hydrocarbons	[6–8]
	near 1	Oil or biodegradation	
	< 1	Biogenic	
$CPI_2 = (1/2)\{(C_{25} + C_{27} + C_{29} + C_{31} + C_{33} + C_{35}) \cdot (C_{24} + C_{26} + C_{28} + C_{30} + C_{32} + C_{34}) + (C_{25} + C_{27} + C_{29} + C_{31} + C_{33} + C_{35}) \cdot (C_{26} + C_{28} + C_{30} + C_{32} + C_{34})\}$	5–10	Higher ground plant	[9]
	0.5–1	Mixed	
	> 1	Ground vegetation	
$TMD = \frac{(C_{25} + C_{27} + C_{29} + C_{31} + C_{33})}{(C_{15} + C_{17} + C_{19} + C_{21} + C_{23})}$	< 0.4	Tree vegetation predominance	[10–12]
	> 0.4	Herbaceous vegetation predominance	
Pr/Ph	> 1	Biogenic	[13–15]
	< 1	Oil	

Results and discussion

HCs in the NCC water. HC concentrations in the water of the studied area of the NCC averaged $0.032 \pm 0.006 \text{ mg}\cdot\text{L}^{-1}$. The obtained values are lower than the maximum permissible concentrations (MPC) for fishery water bodies ($0.05 \text{ mg}\cdot\text{L}^{-1}$), but slightly higher than those for low-polluted water areas [7]. The content of n-alkanes in the NCC water was in the range of 0.010–0.016 with average $0.013 \pm 0.003 \text{ mg}\cdot\text{L}^{-1}$.

All the samples recorded n-alkanes in the C_{17} – C_{29} range (Fig. 2, *a*). In two samples C_{30} was present. In one sample it was possible to identify C_{32} . In all three samples the dominant homologue was compound C_{25} (18–26 %). At the same time, the share of other n-alkanes did not exceed 11 %. N-alkane C_{25} is predominantly associated with bacterial and allochthonous production [6]. Along with the presence of C_{20} and C_{22} peaks, also typical of microbial production, we can speak of an active microbial community in the canal waters. Even-numbered n-alkanes with a high molecular weight (C_{28} , C_{30} , C_{32}) are often associated with sapropel matter formed from the organic matter of phyto- and zoobenthos, plankton, and lower plants and is autochthonous for aquatic ecosystems [6]. Such substances accumulate under reducing conditions. Light HCs (up to C_{17}) were not recorded, which indicates the absence of fresh oil inputs. The unresolved complex mixture was absent, which indicates the absence of chronic oil contamination of water (Fig. 2, *b*).

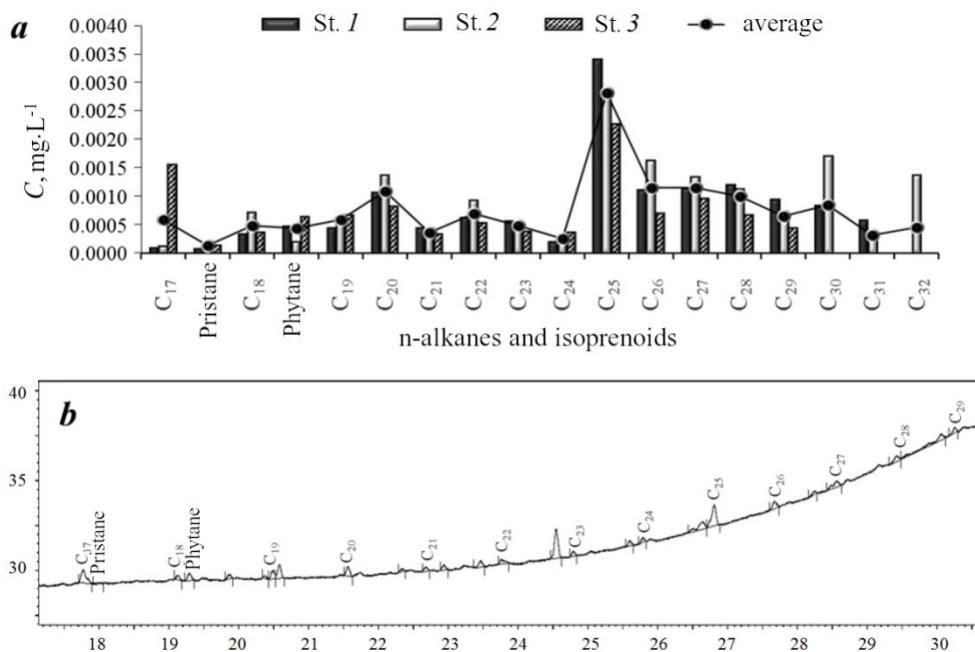


Fig. 2. Concentrations (*C*) of n-alkanes and isoprenoids (*a*) and a typical chromatogram of n-alkanes (*b*) in the water of the North Crimean Canal, spring 2022

A low weight to high weight HC ratio (LWH/HWH) of less than 1 demonstrates that the source of n-alkanes is higher plants, aquatic animals and bacteria [16]. When the values of this index are close to 1, we can speak of oil pollution, and when the values exceed 2, we can speak of fresh oil input [11]. The calculated LWH/HWH index, according to the received data, was on average 0.35, which indicates the biogenic nature of HCs.

The carbon preference index (CPI) reflects the ratio of odd-numbered to even-numbered n-alkanes. In the low-molecular ($C < 22$) and high-molecular ($C > 22$) spectral regions, the CPI_1 and CPI_2 indices have different interpretations, and therefore it is recommended to calculate them separately [17]. This index may indicate a biogenic or oil origin of hydrocarbons. The contribution of the bacterial community is not excluded. In our case, the average CPI_1 value is 0.62 and CPI_2 is 0.45, which is less than 1 and indicates the biogenic origin of hydrocarbons (Table 2).

The C_{31}/C_{19} ratio is an index showing the ratio of allochthonous to autochthonous components. Its value less than 0.4 indicates predominance of autochthonous substance and more than 0.4 – allochthonous. In our case, the average value of this index is 0.94, which indicates the allochthonous nature of hydrocarbons. The C_{31}/C_{29} ratio of 0.63 indicates the predominance of herbaceous vegetation [18].

The ratio of terrigenous to autochthonous matter is estimated by the TMD index [19]. A value of this diagnostic index of less than 0.5 indicates the predominance of autochthonous matter. The range 0.5–1 indicates a mixed input. In this study,

Table 2. Average values of diagnostic indices and the origin of hydrocarbons in the water of the North Crimean Canal, spring 2022

Index	Average	Hydrocarbon origin
<i>LWH/HWH</i>	0.35	Biogenic
<i>CPI₁</i>	0.62	Biogenic
<i>CPI₂</i>	0.45	Biogenic
<i>Pr/Ph</i>	0.40	Oil
C_{31}/C_{19}	0.94	Allochthonous
<i>TMD</i>	3.15	Terrigenous
C_{31}/C_{29}	0.63	Plant (herbaceous vegetation)

the mean value of this indicator was 3.15, which is more than 1 and indicates an intensive input of terrigenous matter produced by higher ground plants (Table 2). This fact is natural for river systems, as their filling with water occurs due to runoff from the river basin [18, 20].

An important diagnostic index²⁾ is the ratio of pristane, which is predominantly of natural origin, to phytane, which is present mostly in oil [21]. This ratio ranged from 0.22 to 0.82 with an average of 0.40, which most likely indicates the presence of oil products in the water. At the same time, other markers diagnose the biogenic nature of HCs.

HCs in the bottom sediments of the NCC and the soils of the adjacent areas. The sediments sampled from the canal bottom were not river sediments but rather soil that was in the canal bed and was flooded when the canal started working. It should be noted that soils in the area are dark brown³⁾, which are characterised by a neutral pH. In terms of mechanical composition, brown soils are mostly heavy. Due to deep (from 1 m) penetration of humus, a significant part of brown soils is highly fertile⁴⁾.

The HC concentration in bottom sediments of the NCC studied area was $30 \text{ mg}\cdot\text{kg}^{-1}$ air-dry bottom sediment (a.d.b.s.) (Fig. 3, a), which corresponds to naturally clean water areas [22]. The n-alkane content in the NCC bottom sediments was $18.7 \text{ mg}\cdot\text{kg}^{-1}$ a.d.b.s. In the soil sampled from the farmland adjacent to the canal, HC content was $18.1 \text{ mg}\cdot\text{kg}^{-1}$, n-alkanes accounted for $11.2 \text{ mg}\cdot\text{kg}^{-1}$ a.d.b.s., i. e. the proportion of n-alkanes in soil (62 %) was the same as in bottom sediments (62 %). The recorded HC content is low and characterizes the soils and bottom sediments as unexposed (in terms of oil contamination) [22].

In the samples of bottom sediments and soil, we identified n-alkanes in the range from C_{17} to C_{33} , which corresponded to the presence of these compounds in water at the sampling station and is also typical of the soil mantle of steppe areas [23]. The maximum concentrations of n-alkanes were in the high-molecular-weight range dominated by odd-numbered compounds indicating the predominance of compounds synthesized by land organisms. The even-numbered peaks in the C_{18} – C_{22} range were not pronounced indicating no active microbial degradation of organic matter in the bottom sediments of the canal and adjacent field areas. The autochthonous peaks corresponding to C_{17} , C_{19} etc. were also not pronounced. Active microbial processes were probably confined to the water column at the moment of sampling and were not characteristic of bottom sediments.

²⁾ AMAP, 2007. *AMAP (Arctic Monitoring and Assessment Programme). Chapter 4. Sources, inputs and concentrations of petroleum hydrocarbons, polycyclic aromatic hydrocarbons, and other contaminants related to oil and gas activities in the Arctic.* Oslo: AMAP, 87 p.

³⁾ Soboleva, E.V. and Guseva, A.N., 2010. [*Chemistry of Fossil Fuels*]. Moscow: Izd-vo Mosk-ovskogo Un-ta, 312 p. (in Russian).

⁴⁾ Shoba, S.A., ed., 2011. [*National Atlas of Soils of the Russian Federation*]. Moscow: Astrel, 632 p. (in Russian).

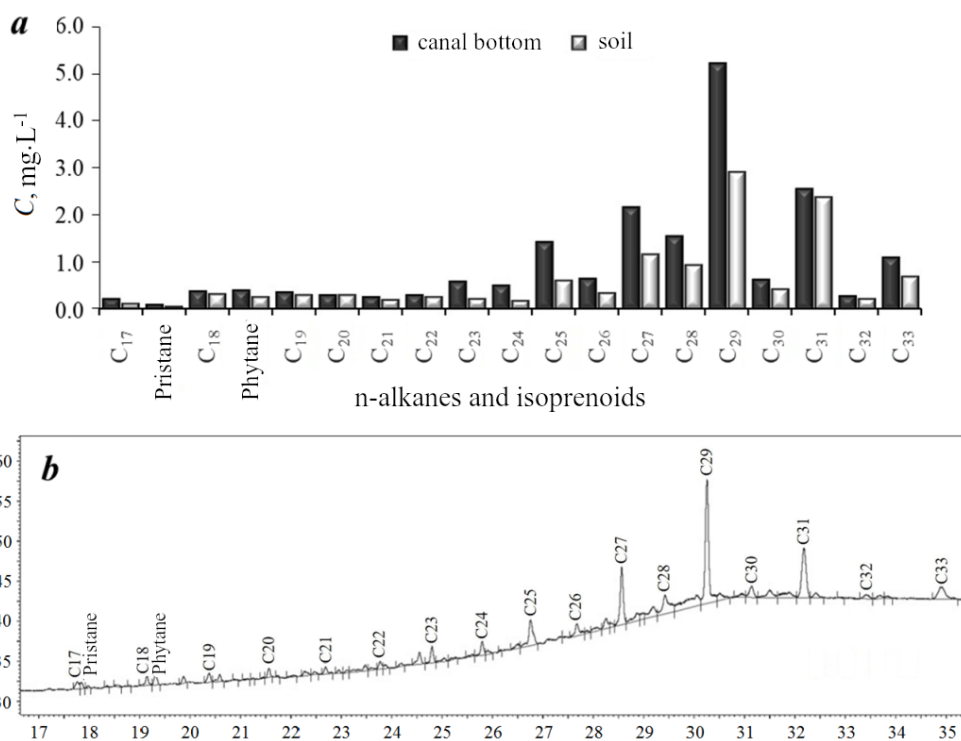


Fig. 3. Concentrations (C) of n-alkanes and isoprenoids (a) and typical chromatogram of n-alkanes (b) in bottom sediments of the North Crimean Canal and adjacent soil, spring 2022

The n-alkane C₂₉ (26–29 %) of plant origin (terrestrial herbaceous plants) was dominant in concentration both in soil and in bottom sediments [24]. This fact is consistent for soils in steppe areas. In addition, this, along with the lower proportion of C₂₉ (5 %) in the canal water, confirms the assumption that the large amount of allochthonous compounds in the canal bottom sediments may be associated with their accumulation in the canal bed during the eight-year period of no-runoff in the canal.

Today, it can be assumed that the canal bottom sediments can be a significant source of input of various compounds into the canal waters. The peaks from C₂₇ to C₃₁, which also indicate the presence of allochthonous compounds in the studied environment [5], are also sufficiently pronounced. It should be noted that separation of alkanes originating from aquatic and terrestrial plants is rather conventional. This is due to the fact that this approach is strictly applicable only to fresh organic matter [6], while in bottom sediments, transformed compounds are mostly presented.

The ratio of light to heavy n-alkanes in the mixture was low and averaged 0.10 (Table 3). These values are consistent with the biogenic nature of organic matter.

Table 3. Average values of diagnostic indices and the origin of hydrocarbons in the bottom sediments and adjacent soil of the North Crimean Canal, spring 2022

Index	Average		Hydrocarbon origin
	in bottom sediments	in soil	
<i>LWH/HWH</i>	0.09	0.11	Biogenic
<i>CPI₁</i>	1.06	0.81	Biogenic
<i>CPI₂</i>	7.64	8.42	Biogenic
<i>Pr/Ph</i>	0.18	0.14	Oil
<i>C₃₁/C₁₉</i>	7.26	8.56	Terrigenous
<i>TMD</i>	9.04	10.35	Terrigenous
<i>C₃₁/C₂₉</i>	0.49	0.81	Plant (herbaceous vegetation)

The CPI_1 marker for the low-molecular-weight region for both studied media is almost equal to 1 (Table 3), but one cannot conclude from this about the presence of petroleum products in the sediments. Similar CPI_1 values, along with a pronounced peak of C_{29} , are most likely indicative of natural ways of HC input and transformation [6]. In the high-molecular-weight region, where CPI_2 is more informative as a criterion of biogenicity, its value exceeded 7 indicating a large fraction of biogenic matter [13–15].

The ratio of the pristane (predominantly biogenic) to phytane (observed in oil) was low, suggesting the possible presence of traces of oil contamination in sediments and soil [25]. With a similar ratio of pristane to phytane, the transformation of organic matter in reducing condition³) can also be stated. This is a more likely explanation of this isoprenoid ratio, since the values of other markers indicate the biogenic nature of HCs.

The ratio of C_{31} and C_{19} n-alkanes in sediments from the canal bottom indicates a strong predominance of terrigenous matter in the composition of organic compounds in the bottom sediments [9]. The high TMD value (9.04) also indicates an active input of HC from land. In addition to direct outwash of substances from the land, their accumulation on the canal bottom during the period of water absence can also be assumed. On the whole, the predominantly terrigenous origin of HCs was indicated by the corresponding indices. The indices were higher in the soil than on the canal bottom. This fact seems to be expected, since organic matter is produced in the water column of the canal and is partially deposited on the bottom increasing the share of autochthonous n-alkanes of the bottom sediments.

The ratio of n-alkanes, which characterises the proportions of herbaceous and tree vegetation, averaged 0.49 for sediments and 0.81 for soil. This indicator shows the predominance of organic compounds associated with ground vegetation in soil rather than in canal bottom sediments. In the water column, the value of this index was 0.63, which was the average between its values in the two mentioned solid media.

Thus, the interpretation of the diagnostic relationships for the bottom sediments of the NCC and adjacent fields is generally consistent. A high correlation of soil organic compounds with ground vegetation was noted.

Conclusion

The obtained HC concentrations in the water ($0.032 \pm 0.006 \text{ mg}\cdot\text{L}^{-1}$) of the studied section of the NCC do not exceed the MPC and are close to the values characteristic of values typical of uncontaminated water areas. The HC content in the canal bottom sediments ($30 \text{ mg}\cdot\text{kg}^{-1}$ a.d.b.s.) and in the adjacent fields ($18.1 \text{ mg}\cdot\text{kg}^{-1}$ a.d.b.s.) also indicated the absence of high pollution levels.

In the NCC water, n-alkanes were identified in the C_{17} – C_{32} range with an average concentration of $0.013 \pm 0.003 \text{ mg}\cdot\text{L}^{-1}$. In the bottom sediments and soils of the adjacent areas, the range of n-alkanes was C_{17} – C_{33} and their concentrations were 18.7 and $11.2 \text{ mg}\cdot\text{kg}^{-1}$ a.d.b.s., respectively.

The composition of n-alkanes in water indicates the mixed nature of HCs, with the predominance of compounds of allochthonous origin, which are washed away from the river basin of the lower Dnieper. The compositions of n-alkanes of the bottom sediments and soils were significantly similar and were typical of soils of steppe areas. This is probably due to the accumulation of soil in the canal bed during the period of water absence in it.

Most of the markers for water, sediments and soil, which allow differentiating between oil and biogenic HCs (LWH/HWH, CPI_2 , Pr/Ph), indicate the predominance of natural components. The presence of oil HCs (Pr/Ph < 1) cannot be excluded, although this is unlikely due to the absence of other signs of oil contamination. At the same time, the markers which allow revealing predominance of autochthonous or allochthonous compounds (C_{31}/C_{19} , TMD) definitely indicate predominance of allochthonous ones. This fact is expected for river systems, as their filling with water occurs due to runoff from the river basin. The high amount of allochthonous compounds may also be due to their accumulation in the canal during the eight-year period of no-washout in it. The C_{31}/C_{29} ratio indicates the predominant formation of allochthonous organic matter by HCs originating from herbaceous plants. This fact is consistent with the fact that the NCC and adjacent parts of the Dnieper are located in steppe areas.

REFERENCES

1. Yurchenko, I.F., 2022. Water Supply for Irrigation in the Republic of Crimea. *International Agricultural Journal*, 65(6), pp. 1334–1352. doi:10.55186/25876740_2022_6_6_46
2. Gennadiyev, A.N., Pikovskii, Y.I., Tsibart, A.S. and Smimova, M.A., 2015. Hydrocarbons in Soils: Origin, Composition, and Behavior (Review). *Eurasian Soil Science*, 48(10), pp. 1076–1089. <https://doi.org/10.1134/S1064229315100026>

3. Kulkov, M.G., Artamonov, V.Yu., Korzhov, Yu.V. and Uglev, V.V., 2010. [Individual Organic Oil Compounds as Indicators of Anthropogenic Oil Pollution in the Aquatic Environment]. *Bulletin of the Tomsk Polytechnic University*, 317(1), pp. 195–200 (in Russian).
4. Wang, X.-C., Sun, S., Ma, H.-Q. and Liu, Y., 2006. Sources and Distribution of Aliphatic and Polyaromatic Hydrocarbons in Sediments of Jiaozhou Bay, Qingdao, China. *Marine Pollution Bulletin*, 52(2), pp. 129–138. doi:10.1016/j.marpolbul.2005.08.010
5. Fagbote, O.E. and Olanipekun, E.O., 2013. Characterization and Sources of Aliphatic Hydrocarbons of the Sediments of River Oluwa at Agbabu Bitumen Deposit Area, Western Nigeria. *Journal of Scientific Research and Reports*, 2(1), pp. 228–248. doi:10.9734/JSRR/2013/3063
6. Nemirovskaya, I.A., 2013. *Oil in the Ocean (Pollution and Natural Flow)*. Moscow: Nauchny Mir, 432 p. (in Russian).
7. Han, J. and Calvin, M., 1969. Hydrocarbon Distribution of Algae and Bacteria, and Microbiological Activity in Sediments. *Proceedings of the National Academy of Sciences of USA*, 64(2), pp. 436–443. doi:10.1073/pnas.64.2.436
8. Lü, X. and Zhai, S., 2008. The Distribution and Environmental Significance of n-Alkanes in the Changjiang River Estuary Sediment. *Acta Scientiae Circumstantiae*, 28(6), pp. 1221–1226.
9. Yusoff, H.B., Assim, Z.B. and Mohamad, S.B., 2012. Aliphatic Hydrocarbons in Surface Sediments from South China Sea off Kuching Division, Sarawak. *The Malaysian Journal of Analytical Science*, 16(1), pp. 1–11.
10. Zhao, M.-X., Zhang, Y.-Z., Xing, L., Liu, Y.-G., Tao, S.-Q. and Zhang, H.-L., 2011. The Composition and Distribution of n-Alkanes in Surface Sediments from the South Yellow Sea and their Potential as Organic Matter Source Indicators. *Periodical of Ocean University of China*, 41(4), pp. 90–96.
11. Zhang, S., Li, S., Dong, H., Zhao, Q. and Zhang, Z., 2013. Distribution and Molecular Composition of Organic Matter in Surface Sediments from the Central Part of South Yellow Sea. *Acta Sedimentologica Sinica*, 31(3), pp. 497–508. Available at: <http://www.cjxb.ac.cn/en/article/id/950> [Accessed: 10 May 2023].
12. Kai-Fa, W., Yu-Ian, Z., Hui, J., Jia-Sheng, X. and Youg-Ji, W., 1980. The Spore-Pollen and Algal Assemblages from the Surface Sediments of Yellow Sea. *Acta Botanica Sinica*, 22(2), pp. 182–190. Available at: <https://www.jipb.net/EN/abstract/abstract24546.shtml> [Accessed: 10 May 2023].
13. Cincinelli, A., Del Bubba, M., Martellini, T., Gambaro, A. and Lepri, L., 2007. Gas-Particle Concentration and Distribution of n-Alkanes and Polycyclic Aromatic Hydrocarbons in the Atmosphere of Prato (Italy). *Chemosphere*, 68(3), pp. 472–478. <https://doi.org/10.1016/j.chemosphere.2006.12.089>
14. Commendatore, M.G. and Esteves, J.L., 2004. Natural and Anthropogenic Hydrocarbons in Sediments from the Chubut River (Patagonia, Argentina). *Marine Pollution Bulletin*, 48(9–10), pp. 910–918. <https://doi.org/10.1016/j.marpolbul.2003.11.015>
15. Cripps, G., 1989. Problems in the Identification of Anthropogenic Hydrocarbons against Natural Background Levels in the Antarctic. *Antarctic Science*, 1(4), pp. 307–312. doi:10.1017/S0954102089000465
16. Wang, C., Wang, W., He, S., Du, J. and Sun, Z., 2011. Sources and Distribution of Aliphatic and Polycyclic Aromatic Hydrocarbons in Yellow River Delta Nature Reserve, China. *Applied Geochemistry*, 26(8), pp. 1330–1336. <https://doi.org/10.1016/j.apgeochem.2011.05.006>
17. Zhang, S., Li, S., Dong, H., Zhao, Q., Lu, X. and Shi, J., 2014. An Analysis of Organic Matter Sources for Surface Sediments in the Central South Yellow Sea, China: Evidence Based on Macroelements and n-Alkanes. *Marine Pollution Bulletin*, 88(1–2), pp. 389–397. <https://doi.org/10.1016/j.marpolbul.2014.07.064>

18. Soloveva, O.V., Tikhonova, E.A., Mironov, O.A. and Alyomova, T.E., 2021. Origin of Hydrocarbons in the Water of the River–Sea Mixing Zone: A Case Study from the Chernaya River – The Sevastopol Bay, Black Sea. *Regional Studies in Marine Science*, 45, 101870. doi:10.1016/j.rsma.2021.101870
19. Syakti, A.D., Hidayati, N.V., Hilmi, E., Piram, A. and Doumenq, P., 2013. Source Apportionment of Sedimentary Hydrocarbons in the Segara Anakan Nature Reserve, Indonesia. *Marine Pollution Bulletin*, 74(1), pp. 141–148. <https://doi.org/10.1016/j.marpolbul.2013.07.015>
20. Yunker, M.B., Backus, S.M., GrafPannatier, E., Jeffries, D.S. and Macdonald, R.W., 2002. Sources and Significance of Alkane and PAH Hydrocarbons in Canadian Arctic Rivers. *Estuarine, Coastal and Shelf Science*, 55(1), pp. 1–31. <https://doi.org/10.1006/ecss.2001.0880>
21. Nemirovskaya, I.A., 2020. Hydrocarbons in the Water and Bottom Sediments of the Barents Sea during Ice Cover Variability. *Geochemistry International*, 58(7), pp. 822–834. doi:10.1134/S0016702920070071
22. Mironov, O.G., Milovidova, N.Yu. and Kiryukhina, L.N., 1986. On Maximum Permissible Concentrations of Petroleum Products in Bottom Sediments of the Black Sea Littoral. *Gidrobiologicheskii Zhurnal*, 22(6), pp. 76–78 (in Russian).
23. Kuhn, T.K., Krull, E.S., Bowater, A., Grice, K. and Gleixner, G., 2010. The Occurrence of Short Chain n-Alkanes with an Even over Odd Predominance in Higher Plants and Soils. *Organic Geochemistry*, 41(2), pp. 88–95. doi:10.1016/j.orggeochem.2009.08.003
24. Ficken, K.J., Li, B., Swain, D.L. and Eglinton, G., 2000. An n-Alkane Proxy for the Sedimentary Input of Submerged/Floating Freshwater Aquatic Macrophytes. *Organic Geochemistry*, 31(7–8), pp. 745–749. doi:10.1016/S0146-6380(00)00081-4
25. Volkman, J.K., Holdsworth, D.G., Neill, G.P. and Bavor Jr., H.J., 1992. Identification of Natural, Anthropogenic and Petroleum Hydrocarbons in Aquatic Sediments. *Science of the Total Environment*, 112(2–3), pp. 203–219. doi:10.1016/0048-9697(92)90188-X

Submitted 10.04.2023; accepted after review 21.04.2023;
revised 03.05.2023; published 26.06.2023

About the authors:

Olga V. Soloveva, Leading Research Associate, A. O. Kovalevsky Institute of Biology of the Southern Seas of RAS (2 Nakhimova Ave, Sevastopol, 299011, Russian Federation), Ph.D. (Biol.), **ORCID ID: 0000-0002-1283-4593**, **Scopus Author ID: 57208499211**, **ResearcherID: X-4793-2019**, kozl_ya_oly@mail.ru

Elena A. Tikhonova, Leading Research Associate, A. O. Kovalevsky Institute of Biology of the Southern Seas of RAS (2 Nakhimova Ave, Sevastopol, 299011, Russian Federation), Ph.D. (Biol.), **ORCID ID: 0000-0002-9137-087X**, **Scopus Author ID: 57208495804**, **ResearcherID: X-8524-2019**, tihonoval@mail.ru

Contribution of the authors:

Olga V. Soloveva – problem statement, analysis of the obtained results, discussion of the results, writing and formatting of the article

Elena A. Tikhonova – sample preparation, determination of hydrocarbons in water, bottom sediments and soil, discussion of the results

All the authors have read and approved the final manuscript.

Autonomous Internal Wave Measurer based on Temperature Transmitters for Shelf Studies

A. N. Serebryany^{1,2} *, D. M. Denisov², E. E. Khimchenko¹

¹ Shirshov Institute of Oceanology, Russian Academy of Sciences, Moscow, Russia

² Andreyev Acoustics Institute JSC, Moscow, Russia

* e-mail: serebryany53@list.ru

Abstract

The paper describes a device for measuring internal waves, which is made on the basis of a line temperature sensor. This sensor measures the average temperature of the water layer it covers, which makes it possible to avoid registration of fine-structural distortions. The device works offline with the possibility of long-term accumulation of a large amount of information (with an interval of 1 minute – within 1 year). The measurement resolution is set from 1 to 1200 s. The average temperature measurement error is 0.1 °C, temperature resolution is not worse than 0.03 °C. The working depth is up to 200 m. The autonomous measurer is compact and easy to use. The device connects to a computer or smartphone via Bluetooth wireless technology. The paper presents the results of comparative simultaneous measurements carried out by the device and a chain of point temperature sensors on the Black Sea shelf in summer 2018 and autumn 2019. The paper gives examples of the use of an autonomous measurer for recording short-period and inertial internal waves. The comparison of the obtained series shows their close similarity. The conducted frequency spectral analysis also demonstrates a good match and identification of the main peaks of registered phenomena. The device proved to be a reliable and promising tool for measuring internal waves on the shelf.

Key words: internal wave measurer, measuring device, line temperature sensor, short-period internal waves, sensor chain, point temperature sensor, temperature sensor

Acknowledgements: The work was performed under state assignment no. FMWE-2021-0010 of the Ministry of Education and Science of the Russian Federation “Methods and means of oceanographic observations for the study of natural and technogenic underwater objects and ecology in the hydrosphere: development of technologies for multi-parameter scanning of underwater environment and objects by autonomous and tethered probes and profilers”.

For citation: Serebryany, A.N., Denisov, D.M. and Khimchenko, E.E., 2023. Autonomous Internal Wave Measurer based on Temperature Transmitters for Shelf Studies. *Ecological Safety of Coastal and Shelf Zones of Sea*, (2), pp. 134–144. doi:10.29039/2413-5577-2023-2-134-144

© Serebryany A. N., Denisov D. M., Khimchenko E. E., 2023



This work is licensed under a Creative Commons Attribution-Non Commercial 4.0 International (CC BY-NC 4.0) License

Автономный измеритель внутренних волн на базе измерительных преобразователей температуры для исследований на шельфе

А. Н. Серебряный^{1,2} *, Д. М. Денисов², Е. Е. Химченко¹

¹ Институт океанологии имени П. П. Ширшова РАН, Москва, Россия

² АО «Акустический институт имени академика Н.Н. Андреева», Москва, Россия

* e-mail: serebryany53@list.ru

Аннотация

Описывается устройство для измерений внутренних волн, выполненное на основе распределенного датчика температуры. Этот датчик измеряет среднюю температуру охватываемого им слоя водной толщи, что позволяет избежать регистрации тонкоструктурных искажений. Устройство работает в автономном режиме с возможностью долговременного накопления большого количества информации (при интервале 1 мин в течение 1 года). Дискретность измерений устанавливается от 1 до 1200 с. Погрешность измерения средней температуры составляет 0.1 °С, разрешение по температуре не хуже 0.03 °С. Рабочая глубина до 200 м. Автономный измеритель отличается компактностью и простотой использования. Устройство подключается к компьютеру или смартфону посредством беспроводной связи *Bluetooth*. Приводятся результаты сравнения одновременных измерений устройства с гирляндой точечных датчиков температуры. Измерения проведены на шельфе Черного моря летом 2018 г. и осенью 2019 г. Представлены примеры использования автономного измерителя для регистрации короткопериодных и инерционных внутренних волн. Сопоставление полученных рядов показывает их близкое сходство. Проведенный частотный спектральный анализ также демонстрирует хорошее совпадение данных распределенного датчика температуры с данными, полученными искусственным распределенным датчиком температуры на основе осреднения измерений гирляндой термодатчиков путем выявления основных пиков регистрируемых явлений. Устройство показало себя надежным и перспективным инструментом для проведения измерений внутренних волн на шельфе.

Ключевые слова: измеритель внутренних волн, измерительные приборы, распределенный датчик температуры, короткопериодные внутренние волны, гирлянда датчиков, точечные датчики температуры, датчик температуры

Благодарности: работа выполнена в рамках темы госзадания Минобрнауки РФ № FM WE-2021-0010 «Методы и средства океанологических наблюдений для исследования природных и техногенных подводных объектов и экологии в гидросфере: разработка технологий многопараметрического сканирования подводных сред и объектов автономными и привязными зондами и профилографами».

Для цитирования: Серебряный А. Н., Денисов Д. М., Химченко Е. Е. Автономный измеритель внутренних волн на базе измерительных преобразователей температуры для исследований на шельфе // Экологическая безопасность прибрежной и шельфовой зон моря. 2023. № 2. С. 134–144. EDN SOBKST. doi:10.29039/2413-5577-2023-2-134-144

Introduction

Measurement of internal waves in oceans and seas has always been a difficult task due to the complexity of this phenomenon and the inaccessibility of its observations in the water layer. To measure internal waves in the oceanic and marine environment, both contact and non-contact (remote) methods are used, which have recently become widespread. The most commonly used are contact measurement methods based on registering changes in the temperature of the water column by vertical chains of point temperature sensors. The widespread use of clusters of chains of point temperature sensors is typical for large-scale experiments conducted in recent decades to study internal waves on the shelves [1–3]. In these experiments, the chains are formed on the basis of a set of autonomous point temperature measurers of a proprietary design. Thermistor chains are also developed as a one-piece measuring tool [4].

An alternative to chains of temperature sensors for measuring internal waves is the line temperature sensor (LTS) proposed in [5]. The LTS measures the average temperature of the layer it covers, adequately tracking temperature fluctuations caused by internal waves. Its main advantage over a point sensor is that the LTS recording is free of the distortion introduced by the fine structure of the vertical temperature profile commonly found in real oceanic or marine conditions. LTS have proven themselves well in measurements on the shelves from stationary platforms [6, 7] and in measurements in the ocean from a vessel in the drift mode or on the move when towing [8].

The disadvantage of measurements based on LTS, which were placed in the aquatic environment, was the need to connect them with bonding wires to recorders located at a distance. The recently developed internal wave measurer [9] does not have this disadvantage, since the LTS is directly connected to a small-sized recording equipment (information storage device) made in a compact case, which, together with the sensor, is lowered into the aquatic environment for the time necessary for measurements. Here it is necessary to call back to the fact that 40 years ago, Marine Hydrophysical Institute developed an autonomous device MGI 1304 (RITM), which performed similar functions [10, 11]. The main difference between the device described in this paper and RITM is that the former is based on modern electronic technology, which makes it possible to reduce dimensions and improve data recording and reading.

This paper presents a modified version of such an autonomous internal wave measurer and presents comparative results of observations obtained when using it.

Technical details of internal wave measurer design

An autonomous internal wave measurer, the general view of which is shown in Fig. 1, structurally consists of a recording device (1) and a 20 m long line temperature sensor (2). The LTS is made of copper-covered steel wire protected from water by insulating coating. Resistance per unit length of wire is 5 Ohm/m, temperature coefficient of resistance is 0.36 Ohm/K, time constant is 20 s.



Fig. 1. Autonomous internal wave measurer: recording device – 1; line temperature sensor (LTS) 20 m long – 2

The recording device is designed for periodic recording of temperature values obtained from the LTS. The registration period can be set from 1 to 1200 s. The average temperature measurement error is 0.1 °C, temperature resolution is 0.03 °C. The working depth is up to 200 m.

The body of the device is a sealed cylinder made of a piece of polypropylene pipe with an outer diameter of 32 mm. The LTS is connected to the housing through a cable entry in the lower metal cover of the housing. The top cover is made of transparent organic glass, which makes it possible to observe the status of the device, displayed by the internal LED indicator flashes. Bluetooth radio communication is used to configure the device and read the temperature data archive. To enter the setup mode and read the data, it is necessary to bring a small permanent magnet to the top cover of the device for a short period of time. In this case, the device activates the Bluetooth module, which makes it possible for a computer or smartphone to connect to the device within 20 seconds. An AA-type 3.6 V lithium battery with a capacity of 2400 mAh ensures the operation of the device in the registration mode with an interval of 1 min within 1 year [9].

The recording device consists of a microcontroller with a real-time controller, a 16-bit analog-to-digital converter (ADC) microcircuit, a non-volatile Flash memory microcircuit, a Bluetooth wireless communication module, a proximity switch (a Hall sensor), and a lithium battery B (Fig. 2). The electronic circuit converts the sensor resistance into voltage, which is converted into an ADC code stored in memory.

Comparative results of measurements of internal waves by an autonomous measurer and a chain of temperature sensors

In June 2018, we carried out comparative measurements with an autonomous internal wave sensor (LTS) and a chain of five point temperature sensors in the Black Sea. The chain included autonomous DST centi-TD temperature measurers manufactured by *Star Oddi* company. The point measurers were located vertically with a spacing of 2 m, the time recording was carried out with an interval of 30 s. Both measurers were lowered from the service ramp of the Institute of Ecology of the Academy of Sciences of Abkhazia (IE of ASA) at the point where the sea depth is about 13 m. The horizontal distance between the measurers was about one meter, they were in almost the same conditions, covering a 10-meter water layer.

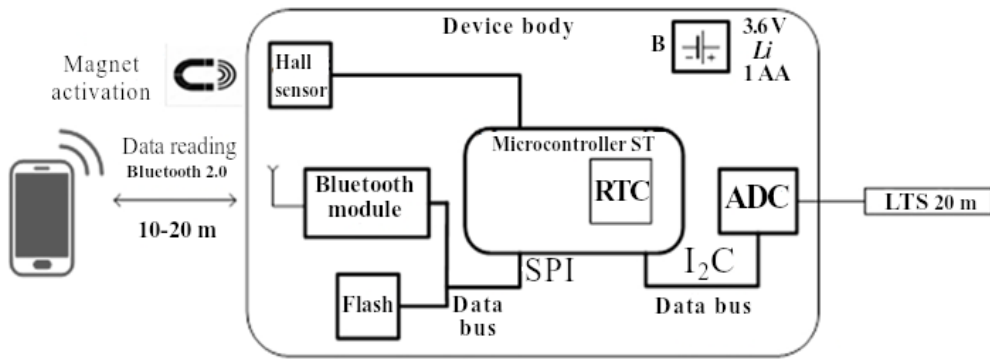


Fig. 2. Structural diagram of the internal wave measurer. RTC – real time controller; ADC – analog-to-digital converter; SPI – serial peripheral interface; I₂C – inter-integrated circuit

Fig. 3 shows the position of the LTS and temperature sensor chains at depth and vertical temperature profiles at the beginning of measurements. Temperature profiles were measured with a *Valeport* miniSVP probe.

The recording of the thermistor sensors at all five horizons for the entire observation time (45 h) are shown in Fig. 4. The entire water layer, with the exception of the near-surface area, is characterized by temperature fluctuations with a range

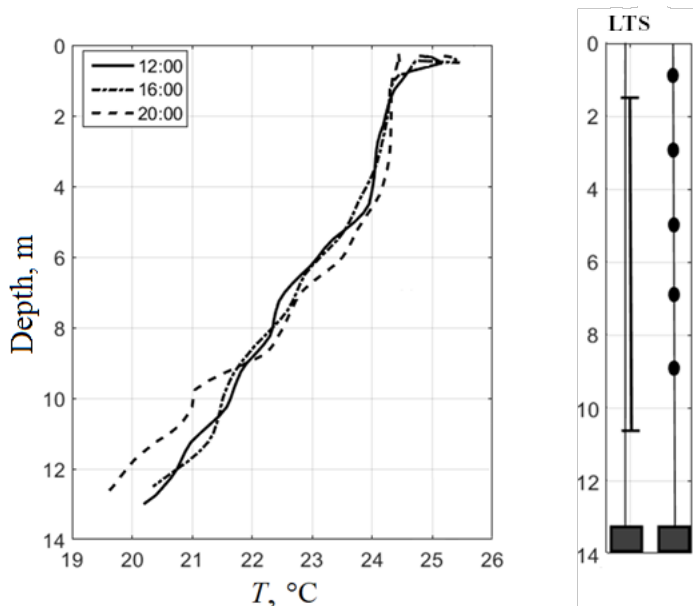


Fig. 3. Vertical temperature profile on June 15 at different time points (*left*); the position of the LTS and temperature sensor strings at depth (*right*)

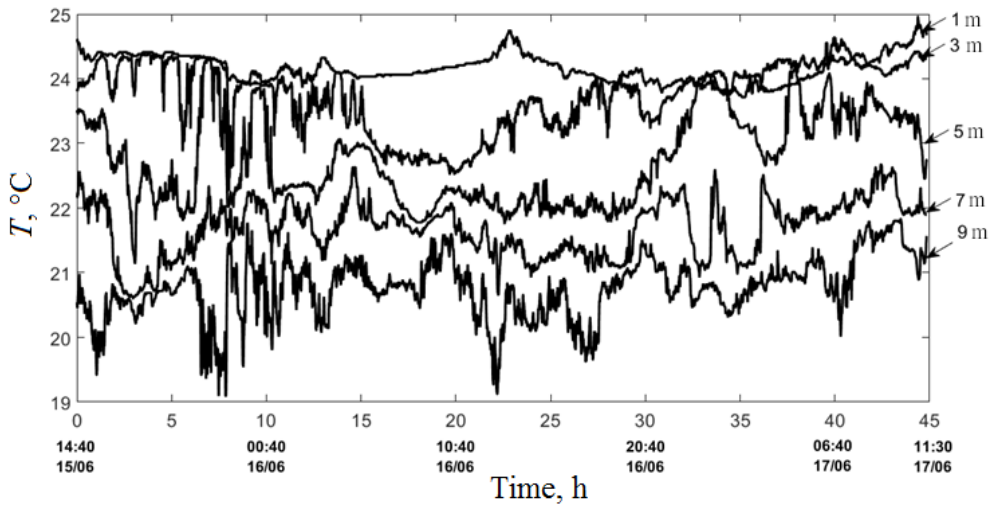


Fig. 4. Recording of thermistor sensors demonstrating temperature fluctuations at five horizons

of 1–2 °C with periods of several minutes or more. In the upper layer, temperature fluctuations are insignificant, but after 30 hours of observations, an inversion occurs.

Fig. 5 shows the implementation recorded by the LTS and the record of the thermistor sensors averaged over five horizons where the sensors were located. To convert the recording of the thermistor sensors into vertical displacements, it was normalized to the measured vertical temperature gradient within the length of the chain. The resulting series represented an artificially modeled LTS based

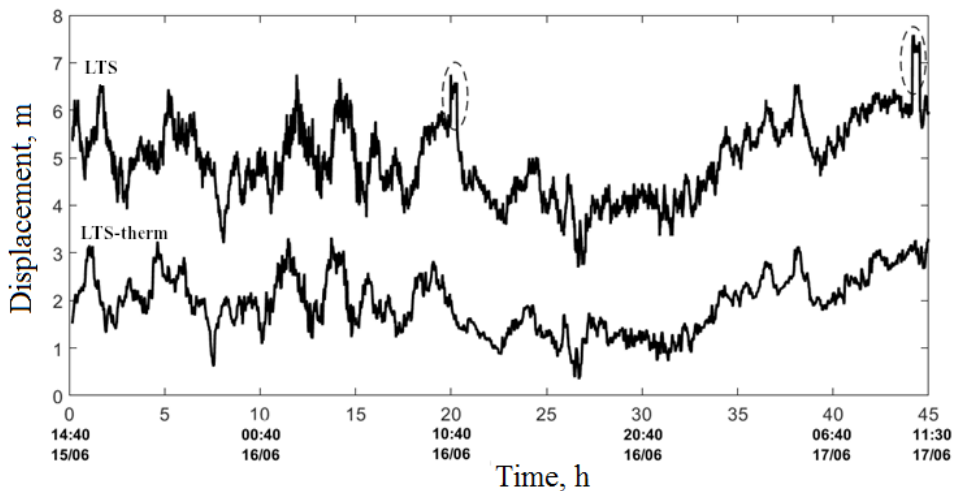


Fig. 5. Comparison of the LTS recording (*top*) and the averaged signal of the five point temperature sensors (*bottom*). The ellipses indicate the moments of measurement of the response of the LTS to a vertical displacement of 1 m

on a chain of point temperature sensors. The LTS recording was converted into vertical displacements of the water column using the measured responses obtained with a short-term (20-minute) vertical displacement of the sensor by 1 m. The conversion of the LTS average temperature recording into vertical thermocline displacements in meters by measuring the sensor response to a given vertical displacement is a well-known method when working with LTS [12, 13].

Simple visual comparison of two obtained series shows their close similarity. Both series demonstrate synchronous thermocline fluctuations with a vertical range of 2–3 m (Fig. 5). To further compare the data and to determine the period of prevailing fluctuations, the spectra of the obtained series were calculated (Fig. 6). The frequency spectra of thermocline fluctuations calculated within the measured series show peaks corresponding to the periods of 2–2.4 h, 30–40 min, 18 min, and 4 min. The spectral tilt, which is close to the Garrett–Munk model spectrum [14], and the spectral energy level, which is underestimated compared to the model one, can also be noted. The Garrett–Munk spectrum developed for internal waves in the ocean, is used here for comparison with waves in shallow water. All the above features are characteristic of the tideless Black Sea spectra [15, 16], and the thermocline fluctuations with such parameters are typical for short-period internal waves in the Black Sea.

Registration of inertial internal waves using autonomous LTS

In addition to short-period internal waves, long-period inertial internal waves, which play an important role in water dynamics, often occur in the sea shelf zone.

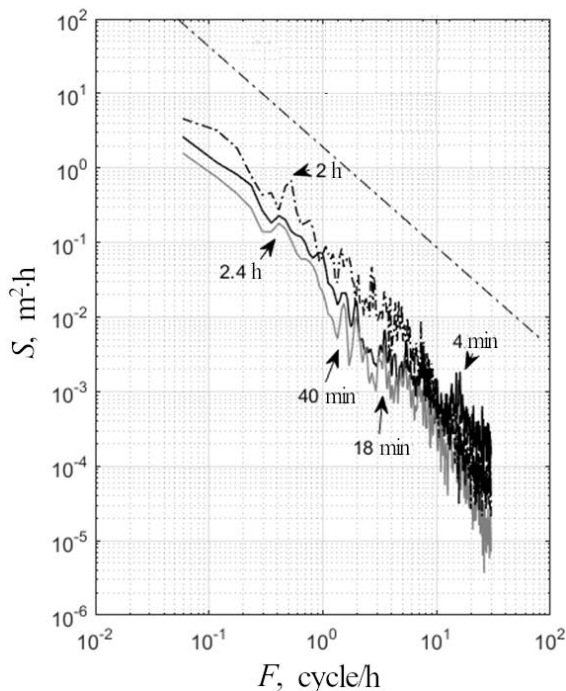


Fig. 6. Frequency spectra calculated from records of the LTS (black curve), temperature sensors chain (grey curve), and point sensor (dashed-dotted curve) at a depth of 9 m. The dash-dotted straight line shows the Garrett–Munk spectrum

They are reliably recorded using current measurers [17, 18], but LTS also makes it possible to track them reliably by the thermocline vertical displacements.

In the autumn of 2019, we conducted studies of internal waves in the Black Sea near the city of Sukhum, the area of which is characterized by a narrow shelf edge. In these measurements, we used an autonomous LTS described in this paper. An experimental batch of sensors was manufactured by Acoustics Institute. The results of this work are published in [19], but here we want to give a clear example of internal wave registration with a period close to the inertial one, registered by this autonomous LTS located on the Abkhazian shelf at a depth of about 50 m, at a distance of about 150 m from the coast.

An inertial internal wave with a period close to 17 h (see Fig. 7) causes the thermocline shear 2.5 m upwards and then, after passing through the crest, on which there are packets of short-period internal waves, it descends almost to its original position. Most probably, the vertical gradient of the shear flow increases in the region of the wave crest causing the formation of a set of short-period internal waves. The packets of short-period internal waves are shown in the inset of Fig. 7.

The inertial internal wave shown in Fig. 7 refers to the lowest (first) mode. In this case, the entire water layer synchronously shifts up and down in turn. This is the most common type of inertial motion in the marine environment. But there are also inertial internal waves of the second mode. They were also registered in the Black Sea [16, 20], and the second mode internal waves have also recently been recorded on the ocean shelf [21]. In order to detect internal waves

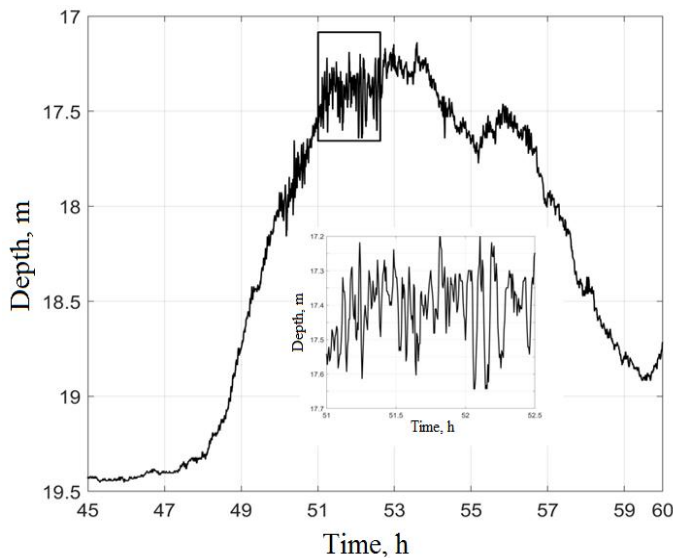


Fig. 7. Record of an inertial internal wave made by an autonomous LTS on the Black Sea shelf

above the first mode, it is necessary to design sensors in stages consisting of a set of several LTS located vertically, by analogy with the point thermistor sensors.

Conclusion

Both the proposed autonomous LTS-based measurer and chain of point temperature sensors are necessary means of contact measurements of internal waves in the marine environment with their own advantages. As for LTS, this is the ability to better transmit the thermocline wave fluctuations, its relative ease of fabrication and calibration. LTS-based records make it possible to reveal the nonlinear nature of internal waves, as well as to compare the profiles of the recorded waves with theoretical models. In addition, the use of several spatially separated LTS forming antennas makes it possible to measure reliably the spatial spectra of internal waves, which is hardly achievable by other contact means. The only drawback of the LTS is its filtering of wave fluctuations above the first mode. This drawback can be overcome by designing sensors in stage consisting of a set of several LTS located vertically.

The tests of the developed autonomous internal wave LTS-based measurer demonstrated its applicability for marine experiments. The use of several corresponding measurers in the shelf zone of the seas will make it possible to design spatial antennas and measure spatial spectra of internal waves, as well as to determine the wavelength, direction, and speed of their propagation.

REFERENCES

1. Lynch, J.F., Ramp, S.R., Chiu, Ch.-S., Tang, T.Y., Yang, Y.-J. and Simmen, J.A., 2004. Research Highlights from the Asian Seas International Acoustics Experiment in the South China Sea. *IEEE Journal of Oceanic Engineering*, 29(4), pp. 1067–1074. doi:10.1109/JOE.2005.843162
2. Tang, D., Moum, J.N., Lynch, J.F., Abbot, P., Chapman, R., Dahl, P.H., Duda, T.F., Gawarkiewicz, G., Glenn, G. [et al.], 2007. Shallow Water '06: A Joint Acoustic Propagation/Nonlinear Internal Wave Physics Experiment. *Oceanography*, 20(4), pp. 156–167. <https://doi.org/10.5670/oceanog.2007.16>
3. Yang, Y.J., Fang, Y.C., Tang, T.Y. and Ramp, S.R., 2010. Convex and Concave Types of Second Baroclinic Mode Internal Solitary Waves. *Nonlinear Processes in Geophysics*, 17(6), pp. 605–614. <https://doi.org/10.5194/npg-17-605-2010>
4. Ocherednik, V.V., Baranov, V.I., Zatsepin, A.G. and Kyklev, S.B., 2018. Thermochains of the Southern Branch, Shirshov Institute of Oceanology, Russian Academy of Sciences: Design, Methods, and Results of Metrological Investigations of Sensors. *Oceanology*, 58(5), pp. 661–671. doi:10.1134/S0001437018050090
5. Konjaev, K.V. and Sabinin, K.D., 1973. New Data Concerning Internal Waves in the Sea Obtained Using Distributed Temperature Sensors. *Doklady Akademii Nauk SSSR*, 209(1), pp. 86–89 (in Russian).
6. Serebryany, A.N. and Ivanov, V.A., 2013. Study of Internal Waves in the Black Sea from Oceanography Platform of Marine Hydrophysical Institute. *Fundamentalnaya i Prikladnaya Gidrofizika*, 6(3), pp. 34–45 (in Russian).

7. Gaisky, V.A. and Gaisky, P.V., 1999. Distributed Thermoprofilemeters and their Possibilities in Oceanographic Investigations. *Morskoy Gidrofizicheskiy Zhurnal*, (6), pp. 46–76 (in Russian).
8. Sabinin, K.D., Nazarov, A.A. and Serebryany, A.N., 1990. Short Period Internal Waves and Currents in the Ocean. *Izvestiya, Atmospheric and Oceanic Physics*, 26(8), pp. 621–625.
9. Denisov, D.M. and Serebryany, A.N., 2019. [Autonomous Internal Wave Measurer Based on a Line Temperature Sensor]. *Pribory i Tehnika Eksperimenta*, (2), pp. 159–160 (in Russian).
10. Kuznetsov, A.S. and Paramonov, A.N., 1980. An Autonomous System of Distributed Temperature Sensors. In: MHI, 1980. *Marine Hydrophysical Research*. Sevastopol: MHI AS USSR. No. 1, pp. 147–151 (in Russian).
11. Paramonov, A.N. and Kuznetsov, A.S., 1985. Aspects of Experimental Investigations of the Single Internal Waves. *Okeanologiya*, 25(2), pp. 312–318 (in Russian).
12. Sabinin, K.D., 1978. [Use of Line Temperature Sensors for Internal Waves Measurements]. In: MHI, 1978. [*Surface and Internal Waves*]. Sevastopol: MHI, pp. 134–145 (in Russian).
13. Konyaev, K.V., 1990. *Spectral Analysis of Physical Oceanographic Data*. Rotterdam: A.A. Balkema, 200 p.
14. Garrett, C. and Munk, W., 1975. Space-Time Scales of Internal Waves: A Progress Report. *Journal of Geophysical Research*, 80(3), pp. 291–297. doi:10.1029/JC080i003p00291
15. Ivanov, V.A. and Serebryanyy, A.N., 1982. Frequency Spectra of Short-Period Internal Waves in a Nontidal Sea. *Izvestiya, Atmospheric and Oceanic Physics*, 18(6), pp. 527–529.
16. Khimchenko, E.E. and Serebryany, A.N., 2018. Internal Waves on the Caucasian and Crimean Shelves of the Black Sea (According to Summer-Autumn Observations 2011–2016). *Journal of Oceanological Research*, 46(2), pp. 69–87. doi:10.29006/1564-2291.JOR-2018.46(2).7 (in Russian).
17. Kuznetsov, A.S., 2020. Structure of the Coastal Current Direction Bimodality at the Southern Coast of Crimea in 2002–2008. *Ecological Safety of Coastal and Shelf Zones of Sea*, (4), pp. 78–88. doi:10.22449/2413-5577-2020-4-78-88 (in Russian).
18. Kuznetsov, A.S., Zima, V.V. and Shcherbachenko, S.V., 2020. Variability of Characteristics of the Coastal Current at the Southern Coast of Crimea in 2017–2019. *Ecological Safety of Coastal and Shelf Zones of Sea*, (3), pp. 5–16. doi:10.22449/2413-5577-2020-3-5-16 (in Russian).
19. Serebryany, A., Khimchenko, E., Popov, O., Denisov, D. and Kenigsberger, G., 2020. Internal Waves Study on a Narrow Steep Shelf of the Black Sea Using the Spatial Antenna of Line Temperature Sensors. *Journal of Marine Science and Engineering*, 8(11), 833. doi:10.3390/jmse8110833
20. Serebryany, A.N. and Khimchenko, E.E., 2019. Internal Waves of Mode 2 in the Black Sea. *Doklady Earth Sciences*, 488(2), pp. 1227–1230. doi:10.1134/S1028334X19100180
21. Rayson, M.D., Jones, N.L. and Ivey, G.N., 2019. Observations of Large-Amplitude Mode-2 Nonlinear Internal Waves on the Australian North West Shelf. *Journal of Physical Oceanography*, 49(1), pp. 309–328. doi:10.1175/JPO-D-18-0097.1

Submitted 23.03.2023; accepted after review 05.04.2023;
revised 03.05.2023; published 26.06.2023

About the authors:

Andrey N. Serebryany, Chief Research Associate, Shirshov Institute of Oceanology, RAS (36 Nakhimov Av., Moscow, 117997, Russian Federation), Dr.Sci. (Phys-Math.), **ORCID 0000-0001-6449-8002**, **ResearcherID: F-9009-2014**, **Scopus Author ID: 6604015592**, *serebryany53@list.ru*

Dmitriy M. Denisov, Senior Research Associate, Andreyev Acoustics Institute (4 Shvernika St., Moscow, 117036, Russian Federation), *denisov.dimitry@gmail.com*

Elizaveta E. Khimchenko, Research Associate, Shirshov Institute of Oceanology, RAS (36 Nakhimov Av., Moscow, 117997, Russian Federation), Ph.D. (Geogr.), *ekhym@ocean.ru*

Contribution of the authors:

Andrey N. Serebryany – problem statement, participation in the construction of the internal wave measurer, analysis and description of the study results, preparation of the graphic materials, preparation of the article text

Dmitriy M. Denisov – design and development of the autonomous internal wave measurer, software development, analysis of the measurement data, preparation of the graphic materials, revision of the article text

Elizaveta E. Khimchenko – performance of *in situ* measurements, data processing, discussion of the results, preparation of the graphic materials, revision of the article text

All the authors have read and approved the final manuscript.